



UNIVERSITÀ DEGLI STUDI DI TORINO

UNIVERSITY OF COPENHAGEN
FACULTY OF HEALTH AND MEDICAL SCIENCES



PhD Thesis

Alessandro Giraudò

Development of innovative GABA_A receptor ligands using a bioisosteric approach

Supervisors: Prof. Bente Frølund

Prof. Marco L. Lolli

This thesis has been submitted to the Graduate School of Health and Medical Sciences, University of Copenhagen and to the University of Turin on 1st February 2018.

Thesis title: Development of innovative GABA_A receptor ligands using a bioisosteric approach

Author: Alessandro Giraudo

Supervisors: Professor Bente Frølund
Assistant Professor Marco L. Lolli

PhD Schools: Doctoral School of Sciences and Innovative Technologies (University of Turin, UNITO)
Graduate School of Health and Medical Sciences (University of Copenhagen, UCPH)

PhD Programs: Pharmaceutical and Biomolecular Sciences (UNITO, XXX cycle)
Drug Research Academy (UCPH)

Departments: Department of Drug Science and Technology (UNITO)
Department of Drug Design and Pharmacology (UCPH)

Academic Discipline: Pharmaceutical and technological applications of chemistry (*Chimica Farmaceutica*, CHIM/09)

Submitted on: 1st February 2018

Assessment committee: Associate Professor Anders Bach, Department of Drug design and Pharmacology, University of Copenhagen
Full Professor Filippo Minutolo, Università degli Studi di Pisa
Associate Professor Francesca Spyraakis, Università degli Studi di Torino
Associate Professor Tracey Pirali, Università degli Studi del Piemonte Orientale "Amedeo Avogadro"
Ulrik Sørensen, PhD, COO at Acesion Pharma

Preface

The work reported in this thesis is the result of a research project carried out in a double PhD degree program between the Department of Drug Science and Technology at the University of Turin (UNITO) and the Department of Drug Design and Pharmacology at the University of Copenhagen (UCPH). During the PhD program, a common main project was followed aiming to synthesize small ligands for the GABA_ARs using a bioisosteric replacement approach.

The first chapter of the thesis describes the structure, function and pharmacology of the GABA_ARs. On the other hand, the second and third chapters are focussed on the research carried out during the three years project (November 2014–October 2017), where a bioisosteric approach has been directed to replace either the carboxylic acid or the amino moieties of GABA. The work reported in the second chapter has been performed at UNITO, while the project reported in the third chapter has been performed at UCPH. All the work has been supervised by Prof. Bente Frølund (UCPH) and Prof. Marco Lolli (UNITO).

Two research articles are in preparation and will describe some of the results reported in this dissertation. A manuscript describing the bioisosteric replacement of the carboxylic acid moiety of GABA will be soon submitted to *Organic and Biomolecular Chemistry* (please refer to Supplementary Information), while a second manuscript focussing on amino bioisosteres will be submitted to *Journal of Medicinal Chemistry*.

- Giraud, A.; Krall, J.; Nielsen, B.; Sørensen, T. E.; Kongstad, K. T.; Rolando, B.; Boschi, D.; Frølund, B.; Lolli, M. L. 5-(Piperidin-4-yl)-4-hydroxy-1,2,3-triazole: A novel scaffold to probe the orthosteric γ -aminobutyric acid receptor binding site.
- Giraud, A.; Krall, J.; Nielsen, B.; Kongstad, K. T.; Rolando, B.; De Blasio, R.; Löffler, R.; Frydenvang, K.; Boschi, D.; Wellendorph, P.; Lolli, M. L.; Jensen, A. A.; Frølund, B. Synthesis and pharmacological evaluation of novel heterocyclic amino bioisosteres of GABA.

The following research article describing a research project in the bioisosteres field has been published by the author during the PhD program:

- Pippione, A. C.; Giraud, A.; Bonanni, D.; Carnovale, I. M.; Marini, E.; Cena, C.; Costale, A.; Zonari, D.; Pors, K.; Sadiq, M.; Boschi, D.; Oliaro-Bosso, S.; Lolli, M. L. Hydroxytriazole derivatives as potent and selective aldo-keto reductase 1C3 (AKR1C3) inhibitors discovered by bioisosteric scaffold hopping approach. *Eur. J. Med. Chem.* **2017**, 139, 936-946.

A research article concerning the hydroxy-1,2,3-triazole moiety, which has been used in this PhD research project as carboxylic acid bioisostere, has been recently submitted to *Tetrahedron*:

- Sainas, S.; Pippione, A.; Giraud, A.; Martina, K.; Bosca, F.; Rolando, B.; Barge, A.; Ducime, A.; Federico, A.; Grosset, S.; White, R.; Boschi, D.; Lolli, M. Regioselective N alkylation of ethyl 4-benzyloxy-1,2,3-triazolecarboxylate: a useful tool for the synthesis of carboxylic acids bioisosteres. Submitted, **2018**.

Acknowledgements

The first acknowledgements are for my supervisors Prof. Bente Frølund and Prof. Marco Lolli. Three years ago you have started this double degree and I'm glad to be part of this. I think it was not easy to begin the bureaucracy and, set the rules, but you made it real and you also made a great effort in term of funding. You have given to me a great opportunity and, now, I can say it was a remarkable experience and a pleasure to be part of two research environments. You gave me the opportunity to do what I really like for three years. Thank you for your time, explanations, corrections and for creating such a good environment.

Thank to Prof. Donatella Boschi who was unofficially co-supervisor. You have always been available for practical advice regarding the chemistry lab, and precious suggestions about literature. You helped me a lot, especially when the synthesis became challenging.

I want to acknowledge PhD Jacob Krall. You have supported me all the way while I was in Copenhagen. Thank you for your advices about chemistry, papers, lab work, NMR and thank you also for every meeting we had.

Thank to PhD Agnese Chiara Pippione and PhD Antonella Federico. Both of you have helped me a lot in the lab. Agnese, you taught me how to be a chemist, back during my master thesis, and then you gave me many advices during the PhD. I will be always grateful to you for this. Antonella, beside the chemical advices, you remind me many time to calm down and take it easy and I would have listen to you more somehow. Thank also to PhD Stefano Sainas for useful chemistry discussions, ideas and some intermediates. Thanks to all the other current members of MeDSynth lab but also who left during the years. In this respect, I would like to mention the master student I had the privilege to supervise: M. Sc. Federica Banin, M. Sc. Valeria Anglani, M. Sc. Piermichele Kobaouri, M. Sc. Rossella De Blasio, and M. Sc. students Giulia Valpreda and Alessandra Valle. It was really nice to work with you. I really hope that I was able to teach you something. I can certainly say that for me: I learn from all of you and I apologize with the first couple of you, maybe I still had to learn my way of teaching.

I would like to acknowledge Prof. Alessandro Barge for teaching me a bit of NMR and HPLC and for your willingness. Thank to Prof. Katia Martina for the intense collaboration in the project regarding the N alkylation of ethyl 4-benzyloxy-1,2,3-triazolecarboxylate. Thanks to Livio Stevanato for the NMR analyses and to M. Sc. Annalisa Costale for the MS analyses.

Then I would like to acknowledge all the people in Bente's group who make a special work environment and they help me sometimes to forget about the chemical frustrations. Thanks to the people (M. Sc. and PhD students) who were with me in the last period (Ahmed, Benjamin, Carolina, Christian, Francesco, Henriette, Julie, Lucill, Signe, Sophie, Yong-Son, Yue) and to all

the previous members who left. Thank to Kirsten Iskov who was so helpful from day 1, back in my Erasmus placement. You also made me laughing a lot with amazing stories.

Thanks to M. Sc. Birgitte Nielsen who was so helpful with HPLC during the last period of my PhD project. You taught me lot of thing, I really appreciate that. Thank you also for carrying out the muscimol binding affinity test.

Regarding other precious collaborations, a lot of people contributed to this PhD project. I would like to acknowledge Prof. Anders A. Jensen for performing the FMP assay and for data analysis, Prof. Kenneth T. Kongstaad for helping with structure elucidations and for HRMS analyses, Prof. Karla Frydenvang for X-ray data analysis, Prof. Jesper Bendix for collecting the X-ray data, Prof. Barbara Rolando for the determination of ionization constants, PhD student M. Sc. Troels E. Sørensen and PhD student M. Sc. Francesco Bavo for the modelling experiments and Prof. Petrine Wellendorph for the GATs experiment.

Grazie ai miei amici di sempre per le belle serate che abbiamo passato insieme nonostante non ci si veda più spesso come una volta. Grazie agli amici di università per le reunion (anche quelle latino-americane). Grazie a Galle e Fede per la compagnia e le serate danesi.

Grazie a te Ire per quanto mi sei stata vicino in questo dottorato che ci ha fatto vivere un po' part-time. Sei anche stata una collega eccezionale: grazie per le discussioni chimiche, l'aiuto con i tesisti, i bei momenti in laboratorio e, infine, per aver letto la tesi e avermi dato preziosi consigli. È stato bello condividere questo dottorato, su e giù dall'aereo.

Infine grazie ai miei genitori che hanno sempre appoggiato le mie scelte, sopportato e supportato durante questo periodo.

Abstract

γ -Aminobutyric acid (GABA) is a widespread neurotransmitter in the central nervous system (CNS). GABA exerts its actions by activating two groups of receptors, the ionotropic GABA_A receptors (GABA_ARs) and metabotropic GABA_B receptors (GABA_BRs) and is responsible of the main inhibition functions in the CNS. GABA_ARs are ligand gated ion channels permeable to chloride ions. These receptors are membrane spanning proteins composed of five subunits, which assemble together in pentameric complexes building the chloride ions conducting pore. The existence of different genes encoding for 19 different subunits (α_{1-6} , β_{1-3} , γ_{1-3} , δ , ϵ , θ , π , ρ_{1-3}) makes the GABA_ARs a complex target because these subunits assemble together to build 26 different GABA_ARs.

Cellular or subcellular specific localization together with peculiar pharmacological properties possessed by the different GABA_AR subtypes, make them attractable drug target for several pathological conditions. In addition, more has to be revealed about the physiological role of specific GABA_AR subtypes. For these reasons, the development of selective ligands for GABA_AR subtypes has been extensively targeted, even if, the high sequence similarity between GABA_AR subtypes makes the objective challenging.

In this work, the bioisosteric replacement tool is employed to synthesize novel GABA_AR ligands aiming to achieve functional subtype selectivity and to expand already elaborated SAR. Moreover, the synthesis of novel bioisosteres in the GABA_ARs area is developed, and the physicochemical properties of them determined.

Pharmacological characterization of these new GABA_AR ligands has revealed interesting pharmacodynamic properties. In particular, the successful replacement of the carboxylic acid moiety of GABA and 4-PIOL using the hydroxy-1,2,3-triazole heterocycle leads to a small series of novel ligands that expanded knowledge about SAR study. Moreover, the strict structural limitations imposed by the GABA_AR to the ligands were confirmed.

On the other hand, the amino moiety of GABA and IAA has been replaced and the structural requirements of the orthosteric binding site of GABA_AR were challenged introducing stereochemistry in order to explore novel areas in the binding pocket. A small series of ligands was developed using the partly saturated heterocycles dihydroimidazole, and 2-amino analogues of dihydroimidazole and dihydrothiazole. A preliminary SAR study showed interesting pharmacological results and further investigation will be performed.

Abbreviations

δ	Chemical shift in parts per million	CAMP	2-(Aminomethyl)cyclopropane carboxylic acid
μ	Micro	cat	Catalytic
Å	Angstrom(s)	Cbz	Benzyloxycarbonyl
°C	Degrees Celsius	CI	Chemical ionization
2D	Two-dimensional	cm	Centimetre(s)
4-PHP	4-(Piperidin-4-yl)-1H-pyrazol-1-ol	CNS	Central nervous system
4-PIOL	5-(Piperidin-4-yl)isoxazol-3-ol	Cys	Cysteine
5-HT ₃ R	Serotonin type 3 receptor	d	Day(s); doublet (spectral); deci
aa	Amino acid	DCM	Dichloromethane
Ach	Acetylcholine	dec	Decomposition
AEMI	4-(2-Aminoethyl)-5-methylisoxazol-3-ol	DMF	<i>N,N</i> -dimethylformamide
AIBN	2,2'-Azobisisobutyronitrile	DMSO	Dimethyl sulfoxide
Anal.	Combustion elemental analysis	e.g.	For example (exempli gratia)
aq	Aqueous	EC ₅₀	Half maximal effective concentration
Arg	Arginine	ee	Enantiomeric excess
Aza-4-PHP	5-(Piperidin-4-yl)-1H-pyrazol-3-ol	ESI	Electrospray ionization
B3LYP	3-Parameter hybrid Becke exchange/Lee–Yang–Parr correlation functional	Et	Ethyl
Bn	Benzyl	<i>et al.</i>	And others
Boc	<i>tert</i> -Butoxycarbonyl	etc.	And so forth
bp	Boiling point	FLIPR	Fluorescent Imaging Plate Reader
CACA	(<i>Z</i>)-4-Aminobut-2-enoic acid	FMP	FLIPR membrane potential assay
calcd	Calculated	Fmoc	9-Fluorenylmethoxycarbonyl

g	Gram(s)	K	Kelvin(s) (absolute temperature)
GABA	γ -Aminobutyric acid	kcal	Kilocalorie
GABA _A R	γ -Aminobutyric acid type A receptor	K_i	Inhibition constant
GABA _B R	γ -Aminobutyric acid type B receptor	L	Litre(s)
GABA-T	GABA transaminase	LC-HRMS	Liquid chromatography-high-resolution mass spectrometry
GAD	Glutamic acid decarboxylase	LC-MS	Liquid chromatography-mass spectrometry
GATs	GABA transporters	Leu	Leucine
Glu	Glutamic acid	LGIC	Ligand gated ion channel
Gly	Glycine	lit.	Literature value
GlyR	Glycine receptor	M	Molar (moles per litre); mega
h	Hour(s)	m	Multiplet (spectral); meter(s); milli
<i>h</i>	Human	m/z	Mass-to-charge ratio (not m/e)
HMBC	Heteronuclear multiple bond correlation	max	Maximum
HPLC	High-performance liquid chromatography; high-pressure liquid chromatography	Me	Methyl
HRMS	High-resolution mass spectrometry	MHz	Megahertz
HSQC	Heteronuclear single quantum correlation	min	Minute(s)
Hz	Hertz	mL	Millilitre
IAA	Imidazole-4-acetic acid	mmol	Milli mole
IC ₅₀	Half-maximum inhibitory concentration	mol	Mole(s)
ⁱ Pr	Isopropyl	mp	Melting point
<i>J</i>	Coupling constant (in NMR spectrometry)	MS	Mass spectrometry

Mw	Molecular weight	SEM	Standard error of mean
nAChR	Nicotinic ACh receptor	Ser	Serine
NBS	<i>N</i> -bromosuccinimide	t	Triplet (spectral)
nm	Nanometre(s)	T	Temperature in units of degrees Celsius (°C)
NMR	Nuclear magnetic resonance	TFA	Trifluoroacetic acid
obsd	Observed	THF	Tetrahydrofuran
Pg	Protecting group	Thio-4-PIOL	5-(Piperidin-4-yl)isothiazol-3-ol
Ph	Phenyl	Thio-THIP	4,5,6,7-Tetrahydroisothiazolo[5,4-c]pyridin-3-ol
Phe	Phenylalanine	THIP	4,5,6,7-Tetrahydroisoxazolo[5,4-c]pyridin-3-ol
pK _a	Negative logarithm (base 10) of the acid dissociation constant	THPO	4,5,6,7-Tetrahydroisoxazolo[4,5-c]pyridin-3-ol
ppm	Part(s) per million	Thr	Threonine
Pr	Propyl	TLC	Thin-layer chromatography
psi	Pounds per square inch	TM	Transmembrane domain
q	Quartet (spectral)	TMS	Tetramethylsilane
R _f	Retention factor (in chromatography)	TPMPA	Methyl(1,2,3,6-tetrahydropyridin-4-yl)phosphinic acid
R _{max}	Maximal response	t _R	Retention time (in chromatography)
ROE	Rotating frame Overhauser effect	Trp	Tryptophan
ROESY	Rotating frame Overhauser effect Spectroscopy	Tyr	Tyrosine
R _s	Resolution	UHPLC	Ultra-high pressure liquid chromatography
rt	Room temperature	UV	Ultraviolet
s	Singlet (spectral); second(s)	v/v	Volume per unit volume (volume to volume ratio)
SAR	Structure–activity relationship	w/w	Weight to weight ratio

Table of contents

1	Introduction	1
1.1	GABAergic neurotransmission: an overall view	1
1.2	GATs: a brief overview	2
1.3	GABA _A Rs: structure, classification and pharmacology	2
1.3.1	Subcellular localization and activation of GABA _A R subtypes	4
1.3.2	Pharmacology and functional properties of GABA _A Rs	4
1.4	Structural information of the GABA _A Rs	6
1.4.1	The orthosteric binding site of the GABA _A Rs	7
1.5	Orthosteric ligands for the GABA _A Rs	8
1.6	The bioisosteric replacement tool	11
1.7	General objectives	11
2	4-Hydroxy-1,2,3-triazole and 3-hydroxy-1,2,5-thiadiazole as novel carboxylic acid bioisosteres for the GABA _A Rs	13
2.1	Background and rationale	13
2.2	Results and discussion	16
2.2.1	Chemistry	16
2.2.2	Characterization	22
2.2.3	Pharmacology	25
2.3	Conclusions	29
2.4	Experimental section	30
3	Synthesis and pharmacological evaluation of novel amino bioisosteres for the GABA _A Rs	47
3.1	Background and rationale	47
3.2	Results and discussion	50
3.2.1	Chemistry	50
3.2.2	Stereochemistry	55
3.2.3	Characterization	57
3.2.4	Pharmacology	58

3.3	Conclusions	63
3.4	Experimental section	64
	References	77
	Supplementary Information.....	85

1 Introduction

1.1 GABAergic neurotransmission: an overall view

γ -Aminobutyric acid (GABA) is a widespread inhibitory neurotransmitter in the central nervous system (CNS). It is synthesized in the synapses from glutamate through an enzymatic catalysed reaction which involves glutamic acid decarboxylase (GAD) and the pyridoxal phosphate as cofactor.¹⁻³ Neurons do not possess all the enzymes necessary for the *de novo* synthesis of GABA from glucose. Hence, the astrocytes provide the precursor glutamine that is converted to glutamate by the enzyme glutaminase.^{4, 5} GABA is then incorporated in vesicles by vesicular neurotransmitter transporters (VGAT) and released in response to electrostatic potentials or directly from the cytoplasm by non-conventional mechanisms (e.g. by reverse action of GABA transporters).^{6, 7} Upon release in the synaptic cleft, GABA exerts its actions by activating two groups of receptors, the ionotropic GABA_A receptors (GABA_ARs) and metabotropic GABA_B receptors (GABA_BRs) and it is responsible of the main inhibition functions in the CNS.^{8, 9} The termination of the neurotransmission is facilitated by transport protein (GABA transporters, GATs), which mediate either the re-uptake of the neurotransmitter in the presynaptic neurons, and consequent re-cycle, or the uptake by the astrocytes in which the metabolism mediated by GABA transaminase (GABA-T) takes place (Figure 1.1).¹⁰

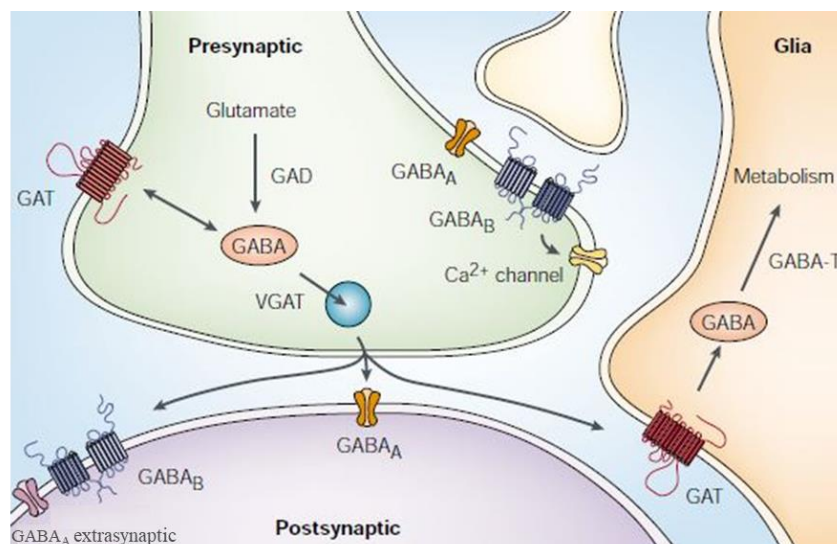


Figure 1.1 Schematic representation of the GABAergic neurotransmission with focus on the biosynthesis, action, re-uptake and metabolism of GABA. The figure is adapted and modified from Owens *et al.*¹¹

In this chapter, the GABA_ARs will be described as the main topic of this PhD thesis. A brief overview on GATs will also be reported as background of results presented in chapter 3.

In addition, insights on medicinal chemistry used to develop pharmacological tools will be elucidated with a specific focus on the orthosteric ligands for the GABA_ARs.

1.2 GATs: a brief overview

GABA transporters (GATs) are important membrane protein implicated in the clearance of GABA from the synaptic cleft where it cannot be metabolised due to the lack of enzymes. GATs can be expressed in pre-synaptic neurons that mediate the re-uptake of the neurotransmitter and, hence, the re-cycle. On the other hand, GATs are also expressed in astrocytes and mediate the re-uptake of GABA which is subsequently metabolised.¹⁰

Four different GATs have been cloned in the mammals namely GAT1, GAT2, GAT3 and BGT1. These Na⁺/Cl⁻ dependent GABA transporters are member of a class of transport proteins named SLC6, which also comprises transporters for monoamine, amino acid and others.¹²

The crystal structure of a member of the family (i.e. leucine transporter from *Aquifex aeolicus*, LeuT_{Aa}), which share a 20–25% sequence identity with GATs, shed light on the structure and mechanism of transport of neurotransmitters. The transporters are composed by 12 transmembrane domains with N- and C- terminals in the intracellular space.¹²

It is assumed that GABA and co-transported ions enter in the substrate binding site which recognises the neurotransmitter, inducing conformational change of the protein. These rearrangements promote the release of GABA in the intracellular space due to a change of affinity for the binding site.^{12, 13}

GATs have been extensively studied from the 1960 as possible drug target. In particular, they have been extensively studied as therapeutic target for epilepsy and the discovery of Tiagabine (i.e. selective GAT1 inhibitor) proved the therapeutic relevance of the target.¹⁴

Nowadays, research projects focus on the development of selective inhibitors for the other subtypes to avoid the side effect induced by Tiagabine.^{13, 15}

1.3 GABA_ARs: structure, classification and pharmacology

GABA_ARs are ligand gated ion channels (LGIC) permeable to chloride ions. The activation of the receptors mediated by GABA induces inhibitory response by hyperpolarization. These receptors are membrane spanning proteins composed of five subunits which assemble together and encircle the chloride ions conducting pore. Each subunit is constituted of a long extracellular N-terminal domain consisting mainly of β-sheets (200-250 amino acids), followed by four α-helical transmembrane domains (TM1–TM4) and a short extracellular C-terminal domain (Figure 1.2). The TM3 and TM4 are connected by a relatively long intracellular loop which is site of phosphorylation and interactions with specific proteins involved in trafficking and anchoring of the formed receptors in the membranes. Once the GABA_ARs is formed, the TM2 of the five subunits line the ion conducting pore.¹⁶

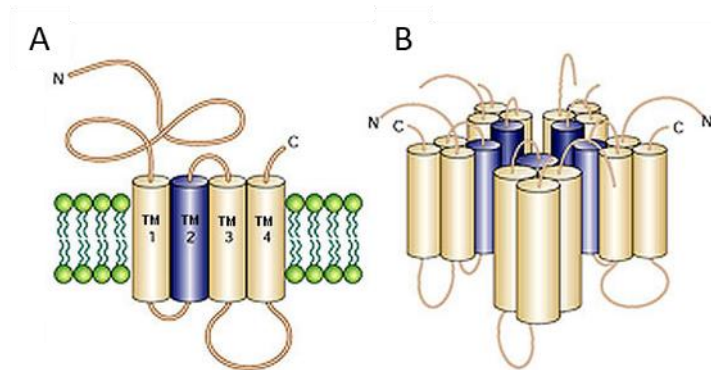


Figure 1.2 Schematic view of a single subunit (A), and lateral view of a general structure of GABA_AR (B). The figure is adapted and modified from Moss *et al.*¹⁷

The existence of different genes for the GABA_ARs has been discovered by decoding the human genome. These genes encode 19 different subunits (α_{1-6} , β_{1-3} , γ_{1-3} , δ , ϵ , θ , π , ρ_{1-3}) which assemble together in pentameric complexes to build GABA_ARs.¹⁸ Theoretically, all these subunits can produce homo- or heteromeric complexes, so more than 150000 different subtypes of GABA_AR can be potentially built. However, specialized pharmacological studies have shown that different subunits have different cellular and regional distribution which make not all the subtypes *in vivo* relevant.¹⁹ To date, the existence of 26 GABA_AR subtypes has been proposed and these subtypes have been divided in three classes depending on the available proof of relevance. In accordance with the latter classification, the GABA_AR subtypes are divided in a) identified, b) existence with high probability and c) tentative, as described by Olsen and Sieghart (Figure 1.3).²⁰

The most abundant GABA_AR subtype in the brain is the $\alpha_1\beta_2\gamma_2$ where two α_1 , two β_2 and one γ_2 subunits assemble around the ion conducting pore with a defined order ($\gamma_2\beta_2\alpha_1\beta_2\alpha_1$, Figure 1.4).²¹ In general, the majority of GABA_ARs are built by different classes of α , β and γ subunits which are assembled in a 2:2:1 stoichiometry respectively. Other subunits (i.e. δ , ϵ , θ , π) can replace the γ subunit in these heteromeric complexes and form specific receptors with different pharmacological properties as outlined later (e.g. $\alpha_4\beta_2\delta$ and $\alpha_6\beta_3\delta$) or receptors which the existence has been proposed tentatively (i.e. $\alpha\beta\epsilon$, $\alpha\beta\theta$ and $\alpha\beta\pi$).²²⁻²⁴ In addition, homomeric or pseudohomomeric assemblies of ρ_{1-3} subunits form a distinct class of GABA_ARs called GABA_CRs, characterised by specific pharmacological properties and specific distribution. In particular, these receptors are highly expressed in the retina, but it is recommended to consider them as part of GABA_ARs despite their specific localization and pharmacological properties.²⁰

The specific localization in the retina of ρ subunits is not the only reported example. In this respect, other subunits composing GABA_ARs have been localized specifically in certain regions or in specific cells, as the α_6 subunits exclusively expressed in the cerebellar granule cells.¹⁶

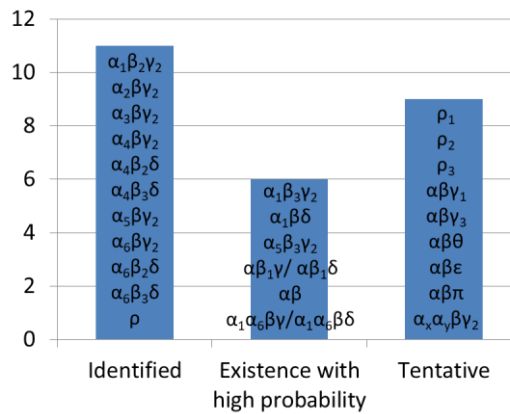


Figure 1.3 Classification of GABA_AR subtypes based on proof of existence of proposed subtypes according to the classification proposed by Olsen and Sieghart.²⁰

1.3.1 Subcellular localization and activation of GABA_AR subtypes

Some GABA_AR subtypes have peculiar subcellular localization and these receptors also express characteristic pharmacological properties. For example, GABA_AR subtypes expressing δ subunits ($\alpha_4\beta_2\delta$ and $\alpha_6\beta_3\delta$) or α_5 subunits ($\alpha_5\beta\gamma_2$) are located in extrasynaptic regions.²⁵

Synaptic GABA_AR subtypes (in general $\alpha\beta\gamma$) are activated by high concentration of released neurotransmitter (GABA) from the presynaptic nerve terminal which bind and activate the receptors. Therefore, the chloride ion pore opens and induces transient hyperpolarization (few milliseconds). The generated response is fast and induces the so-called phasic current. On the other hand, extrasynaptic receptors are usually activated by low concentration of GABA for longer time, generating the so-called tonic current.^{25, 26}

1.3.2 Pharmacology and functional properties of GABA_AR subtypes

The majority of GABA_AR subtypes are constituted by α , β and γ subunits and the most abundant subtype in the CNS is the $\alpha_1\beta_2\gamma_2$ as previously described. This section will focus on this class of subtypes, as they have been widely characterized than the others because of their higher expression.

GABA_AR subtypes are activated by two molecules of GABA which bind two distinct binding sites (i.e. orthosteric binding sites) located at each α/β subunits interface (Figure 1.4).¹⁹ Many other ligands activate the GABA_AR subtypes through the orthosteric binding site and some of them will be described later (please refer to section 1.5). In fact, GABA_AR subtypes are also modulated by diverse substances (Figure 1.4) including steroids and ethanol, and several drugs approved for clinical use including benzodiazepines, barbiturates and anaesthetics.²⁷ In general, these substances are positive allosteric modulators able to bind allosteric binding sites and modulate the action of GABA by increasing the conductance of the chloride ions through the ion conducting pore.¹⁹ Furthermore GABA_AR subtypes are blocked by the action of bicuculline, gabazine, other orthosteric antagonists and the channel blocker picrotoxinin.²⁸

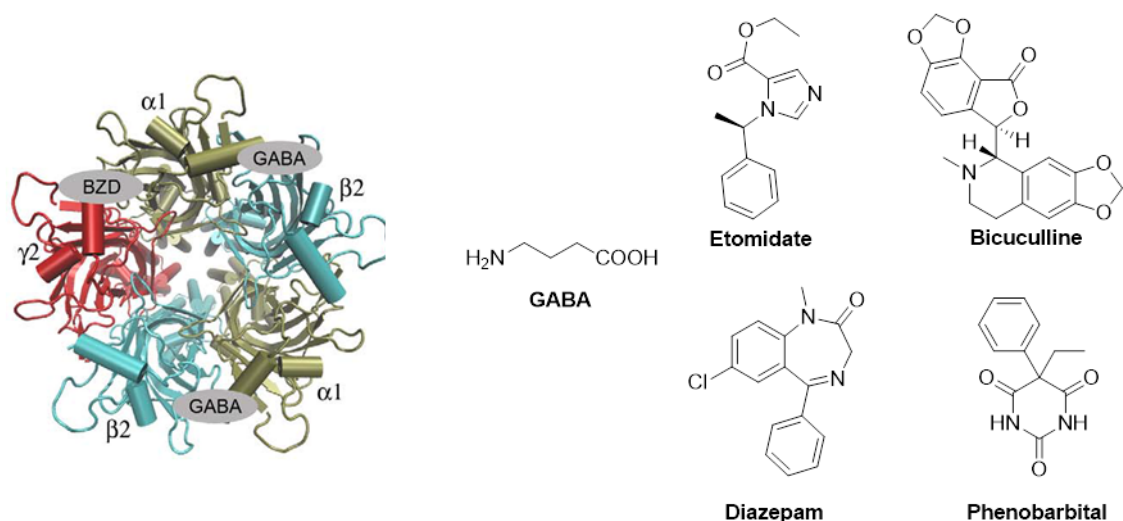


Figure 1.4 Left: Schematic top view of the most abundant GABA_ARs subtype. Right: structures of the endogenous orthosteric ligand GABA, positive allosteric modulators etomidate (anaesthetic), diazepam (benzodiazepine), phenobarbital (barbiturate) and antagonist bicuculline. The figure is adapted and modified from Bergmann *et al.*²⁹

The benzodiazepines are widely used drugs with anticonvulsant, sedative, hypnotic and anxiolytic effects. They are positive allosteric modulators and increase the conductance of chloride ions by increasing the frequency of channel opening induced by GABA. They interact with the so-called benzodiazepine binding site situated at α/γ_2 subunit interface. The widespread use in clinical practice of benzodiazepines can be justified by their high safety profile, as they cannot directly activate the GABA_ARs.^{30, 31}

The combined use of benzodiazepines with molecular genetics allowed to discover that GABA_ARs containing different α subunits mediate different pharmacological effects of diazepam, one of the oldest commercially available benzodiazepines. The study consisted on the introduction of point mutation in the α subunits of engineered animals, that make specific GABA_AR subtypes insensitive to diazepam. By comparison of the effects of diazepam in wild- and engineered- animals, it was possible to distinguish between the sedative, anticonvulsant, anxiolytic, muscle relaxant, hypnotic and memory impairing effects.^{19, 32} The GABA_ARs containing α_1 subunits were proved to mediate sedative and anticonvulsant effects.³³ Moreover, the anxiolytic, muscle relaxant and hypnotic effects are mediated by GABA_ARs containing α_2 subunits, whereas the GABA_ARs containing α_3 subunits also contribute to the anxiolytic effect.³⁴ Lastly, the memory impairing effect of diazepam has been proved to be mediated by α_5 containing GABA_ARs.³⁵

A similar approach using the intravenous anaesthetic etomidate allowed to distinguish between the effects mediated by the GABA_ARs containing β_2 subunits (sedative, hypothermic effects etc.) and effects mediated by the GABA_ARs containing β_3 subunits (anaesthetic effect etc.).^{36, 37}

The knowledge reported in this section outline some diverse role of GABA_ARs subtypes which are limited to some therapeutic effects. More have still to be revealed on the contribution of

GABA_ARs subtypes in physiological or pathophysiological conditions, but it is already known that dysfunctions in the GABA_AR system is implicated in a variety of pathologies as generalized anxiety disorders, depression, schizophrenia etc.³⁸ Beside the classical non-selective benzodiazepines which are clinically used for treatment of sleep and anxiety disorders, general anaesthetics and barbiturates,³⁹ other more selective compounds have recently been studied. For example, a selective partial inverse agonist for the α_5 containing GABA_ARs (i.e. RG1662) is currently being evaluated in clinical trials for down syndrome patients with the aim of reducing cognitive deficits.^{38, 40} Selective drugs may also be potential therapeutic solutions for other diseases including depression, schizophrenia and autism, as well as neurodevelopmental disorders as fragile X syndrome and Dravet syndrome.^{38, 41}

1.4 Structural information of the GABA_ARs

GABA_ARs are part of a superfamily of pentameric LGIC called cys-loop receptors which also comprises receptors activated by acetylcholine (nicotinic acetylcholine receptors, nAChRs), glycine (glycine receptors, GlyRs) and serotonin (serotonin type 3 receptors, 5-HT₃Rs). The cys-loop name derives from a highly conserved residue of 13 amino acids which is terminated by two cysteine residues that form a disulphide bridge. The named cys-loop is not the only conserved residue in the family: a high homology exists between members of the receptor superfamily due to the evolution from a common ancestral gene.^{42, 43}

In the last years, the first crystal structures of GABA_ARs began to appear in literature.⁴⁴⁻⁴⁶ Even if the *in vivo* relevance of the described homomeric β_3 GABA_AR has been discussed,⁴⁴ the new crystal structure shed light on molecular details which can better describe the gating process, signal transduction mechanisms and was the first proof of already available information.⁴⁴ However, before the first crystal structures of the GABA_AR appeared,⁴⁴⁻⁴⁶ a lot of information were already available, deriving from structural information of other type of receptors of the cys-loop family.⁴⁷ The first structural information derives from the electric organs of *Torpedo* ray, which are rich in nAChRs.⁴⁸ Later, the soluble acetylcholine binding protein derived from garden snails was discovered being the first high resolution image of a cys-loop receptor extracellular domain.⁴⁹ The latter structure has a 15–20% sequence identity with other receptors in the cys-loop family. Some other structures followed these results, enlarging the amount of available structural information, such as the bacterial homologues ELIC⁵⁰ and GLIC⁵¹ and the first anion selective cys-loop receptor (i.e. glutamate gated chloride channel of *Caenorhabditis elegans*, GluCl α).⁵² Moreover, the structure of GluCl α provided a great advance in the structural knowledge of GABA_ARs because the homology between the two receptors was 36% for the entire receptor and up to 48% considering the orthosteric binding site.²⁹ All these structures were

used by medicinal chemists to build homology models for drug design purpose and resulted in useful and reliable models of GABA_AR for agonists and antagonists based on multiple templates.^{29, 53} In this respect, a homology model of GABA_CR based on multiple template has also been developed and is currently being evaluated at the Department of Drug Design and Pharmacology of the University of Copenhagen.

Moreover, other templates of GABA_ARs and GABA_CRs based on single templates also exists,^{54, 55} but it has to be said that the reliability of these models is limited due to the sparse homology between different receptor of the same superfamily.²⁹

All the available models can be used by medicinal chemists to predict binding modes of available ligands, as well as design new orthosteric ligands for the GABA_ARs. However, the design of subtype selective GABA_AR ligands based on available structural information is still a challenge. Moreover, a high sequence identity in the orthosteric binding site of different GABA_AR subtypes exist and might compromise the possibility to develop subtype selective ligands based on affinity. It is instead possible, as later elaborated, to develop functional subtype selective GABA_AR ligands.⁵⁶

1.4.1 The orthosteric binding site of the GABA_ARs

The orthosteric binding sites of $\alpha_1\beta_2\gamma_2$ GABA_ARs (Figure 1.4) are located in the extracellular domain at each α/β subunits interface. The cavity of the binding site is formed by 6 so-called loops (Figure 1.5) from the principle β subunit (loops A–C) and the complementary α subunit (loops D–F). The defined binding pocket interacts with different orthosteric ligands, such as the physiological agonist GABA and other orthosteric agonists and antagonists (please refer to section 1.5).^{29, 53}

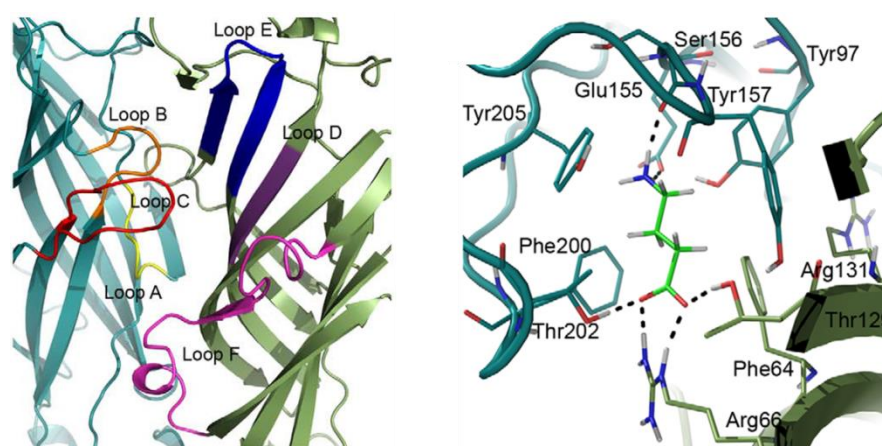


Figure 1.5 Left: GABA_ARs binding site formed by loops A–F at the α/β interface in the extracellular domain. Right: predicted key interactions of GABA in the orthosteric binding site of GABA_AR. The figure is adapted and modified from Bergmann *et al.*²⁹

Key interactions between GABA and the orthosteric binding site were discovered by mutational studies and docking studies on homology models (Figure 1.5). According to these studies, the γ -

amino moiety forms a salt bridge with Glu155, a hydrogen bond with Ser156 and a cation- π interaction with Tyr205. All these residues are part of the principle β subunit. On the other hand, the carboxylic acid moiety of GABA interacts with Arg66 of the complementary α subunit by salt bridge and with Thr129 (α subunit) and Thr202 (β subunit) by hydrogen bonds. Other residues (e.g. β_2 Phe200 and α_1 Phe64) compose the so-called aromatic box which is important for the charge shielding inside the binding site.^{29,53}

1.5 Orthosteric ligands for the GABA_ARs

As outlined in section 1.4, structural information derived from other receptors types and, during the last years, the report on crystal structures of GABA_ARs have largely contributed to enrich the knowledge about the structure of GABA_ARs.^{29, 44-46} Nevertheless, 50-years of medicinal chemistry efforts have contributed substantially at the available knowledge on the orthosteric binding site and the structural requirements and restrictions of the orthosteric ligands imposed by the structure of GABA_ARs.⁵⁷ Considering what is known so far, GABA_AR agonists and partial agonists are, in general, relatively small molecules with a fixed distance (4-5 Å in the putative bioactive conformation of agonists) between the amino and acidic moiety, while GABA_ARs antagonists are larger molecules with less structural requirements.^{56, 58}

The use of powerful medicinal chemistry tools such as conformational restrictions and bioisosteric replacements permitted to distinguish between different GABA_AR subtypes (e.g. distinguish orthosteric ligands for GABA_AR and GABA_CR),⁵⁹ to modulate selectively the GABA_ARs over the GATs and *vice versa*,⁶⁰ and to perform structure-activity relationship (SAR) studies which were then used to develop a pharmacophore model.⁶¹

GABA is the natural occurring neurotransmitter which activates GABA_ARs. It is known to be antagonized by bicuculline (or bicuculline methochloride) and gabazine (please refer to Figure 1.6 for these structures and the following reported in this section).²⁸

Modification of the structure of GABA resulted in the conformational restricted analogues isonipecotic acid and isoguvacine that are GABA_AR agonists, and CACA and (+)-CAMP which are selective GABA_CR agonists. On the other hand, the replacement of the carboxylic moiety of isoguvacine with a methylphosphinic acid moiety resulted in TPMPA, a potent antagonist for the GABA_CRs.⁶²

The bioisosteric replacement of the carboxylic moiety of GABA has been used extensively starting from the natural occurring GABA_ARs ligand muscimol. The 3-hydroxyisoxazol moiety of muscimol replaced the carboxylic acid moiety of GABA and resulted in a potent but unselective GABA_AR agonist. However, the conformational restricted analogue of muscimol THIP, characterized by the amino moiety enclosed in a piperidine ring, was shown to be an

interesting ligand with peculiar pharmacological properties.⁶³ In particular, THIP has been characterized as functionally selective agonist with high efficacy at the $\alpha_4\beta_3\delta$ GABA_ARs, a receptor subtype with extrasynaptic expression.⁶³ In contrast, the isomeric compound THPO is a selective GABA uptake inhibitor.⁶⁴ THIP (Gaboxadol) entered in clinical trials for sleep disorders (i.e. primary insomnia) but failed phase III and is again in phase II clinical trials for Angelman syndrome.⁴⁰

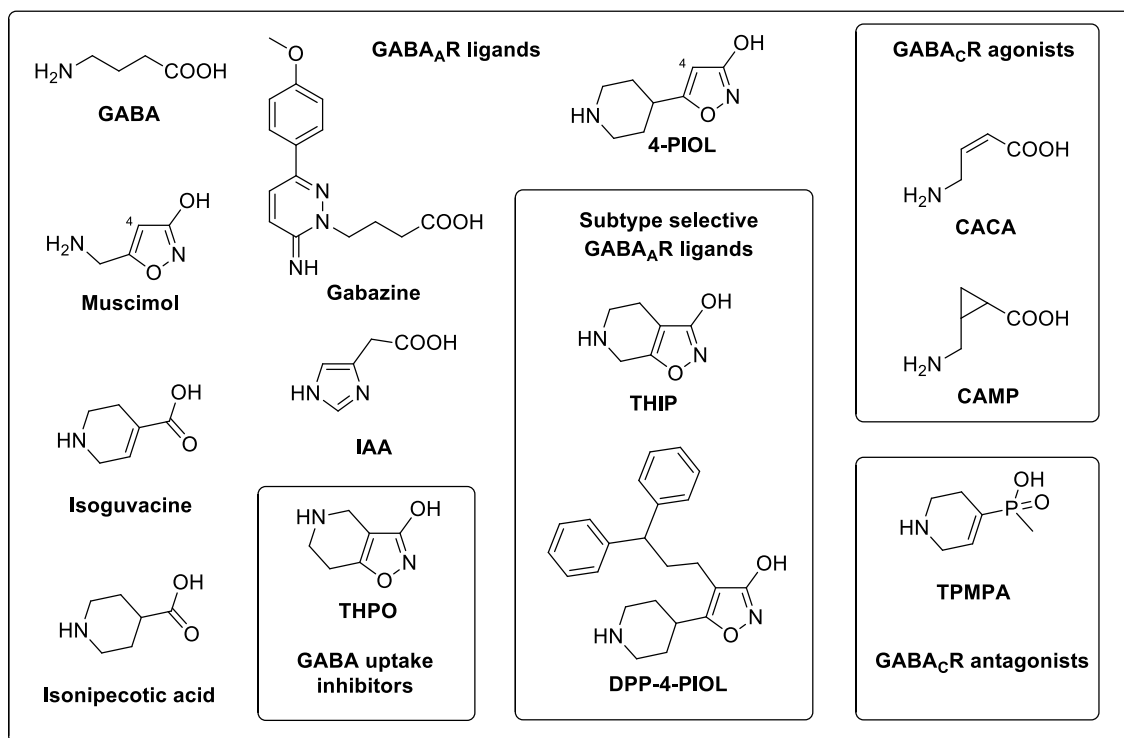


Figure 1.6 Structure of selective and unselective GABA_AR agonists, partial agonists, antagonists and GABA uptake inhibitors.

The non-fused analogue of THIP named 4-PIOL is a low efficacy partial agonist for GABA_ARs. The different SAR of muscimol and 4-PIOL and in particular the different response to the introduction of substituent in the 4-position led to the conclusion that the two molecules adopt two different binding modes in the orthosteric site of the GABA_ARs.^{56, 58} As better elaborated in chapter 2, the introduction of substituents in the 4-position of muscimol (e.g. methyl group) led to analogues with impaired affinity for the GABA_ARs. However, introduction of small substituents in the 4-position of 4-PIOL (e.g. methyl group) is tolerated, whereas larger substituents (e.g. diphenylpropyl moiety of DPP-4-PIOL) enhance binding affinities and leads to potent antagonists. To explain the latter results, the presence of a cavity above the core scaffold of 4-PIOL was postulated to enable the accommodation of bulky substituents.⁶¹

The different binding mode of muscimol and 4-PIOL derivatives was supposed to be mediated by a flexible arginine residue (Arg66 of the complementary α subunit) that interacts with the 3-hydroxyisoxazole moiety of the two ligands (Figure 1.7).⁶¹

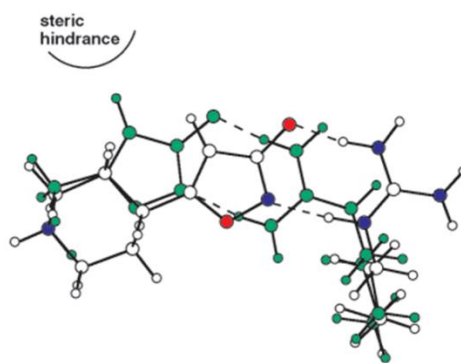


Figure 1.7 Superimposition of muscimol and 4-PIOL displaying the different binding mode mediated by a flexible arginine residue (Arg66).⁶¹

Another important insight in the architecture of the orthosteric binding site of the GABA_AR was given by the bioisosteric replacement of the 3-hydroxyisoxazol moiety of 4-PIOL with 1-hydroxypyrazole, which resulted in the synthesis of 4-PHP (Figure 1.8).⁶⁵ This novel bioisostere has two different positions suitable for the introduction of bulky substituents. This modification led to discover that the core scaffold of 4-PHP is actually surrounded by two cavities: one corresponding to the already defined “above” cavity and the other named “below” cavity (e.g. compound 1.1, Figure 1.8).⁶⁵

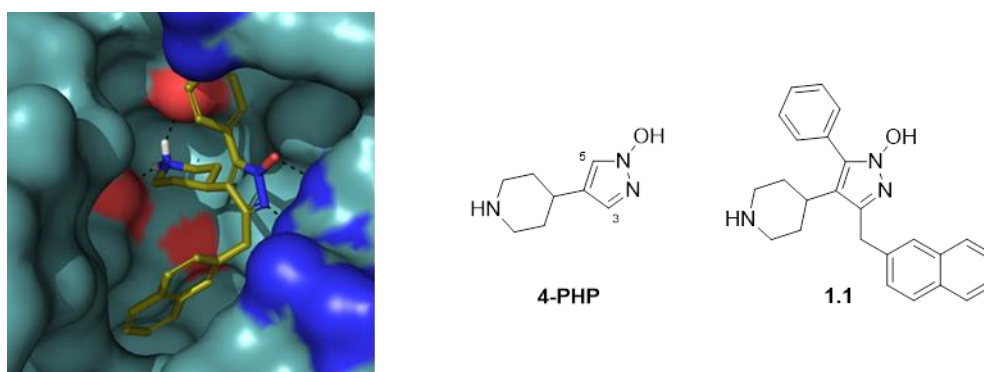


Figure 1.8 Proposed binding mode of compound 1.1 in the orthosteric binding site of GABA_AR. The cavities above and below the core scaffold of 4-PHP accommodate the phenyl and naphthyl substituents.

To a less extent, the bioisosteric replacement was also directed to replace the amino moiety of GABA.^{59, 66} An example is given by IAA (Figure 1.6) which is non-selective GABA_AR partial agonist. SAR study of IAA and in particular the introduction of a methyl group in the 5- or α -position of the scaffold produced selective analogues for the GABA_CRs as better explained in chapter 3.⁶⁷

The reported examples together with recent publication regarding Thio-THIP,⁶⁸ Thio-4-PIOL,⁶⁹ DPP-4-PIOL⁷⁰ prove that bioisosteric replacement and SAR study can play an important role not only on the identification of GABA_AR subtype selective ligands, but also functional selectivity. The latter concept means that, even if the ligand is not definable subtype selective based on affinity, it exploits certain subtype selectivity in terms of efficacy. In conclusion, all this

knowledge shed light on structural requirements for GABA_AR ligands and structural information of the orthosteric binding site.

1.6 The bioisosteric replacement tool

The term bioisosteres was firstly introduced in 1950 and it is important to point out the difference between this and the isosteric concept. Isosteres are traditionally defined as chemical groups or atoms with similar physicochemical properties. On the other hand, bioisosteres are similar chemical groups and the replacement of one with another results in similar biological properties on a given biological target. That is to say that two compounds can be isosteric but not bioisosteric if they do not possess similar biological effect.⁷¹

Bioisosteres are generally used in medicinal chemistry as a tool not only to mimic groups, but also to change some properties including size of the group, electrostatic properties, ionization constants and lipophilicity. For this reason, the bioisosteric replacement can then play an essential role in modulating different properties of the final molecule, such as pharmacokinetic properties (e.g. distribution, metabolism etc.) and pharmacodynamic properties (e.g. efficacy, potency or selectivity).^{72, 73}

Considering the GABA_ARs, the bioisosteric replacement approach has been extensively used and either the carboxylic acid or the amino moieties of GABA have been substituted by a variety of heterocycles.^{56, 66} The changes produced structural knowledge in the fields and permitted to explore chemical space in the orthosteric binding site of GABA_ARs. Moreover, pharmacological properties have been modulated and some interesting results in terms of selectivity between GABA_ARs and GABA_CRs were obtained.⁶⁷

1.7 General objectives

So far, the more interesting results in terms of selectivity or functional selectivity of orthosteric ligands have been obtained with compounds capable to distinguish between GABA_ARs and GABA_CRs or between synaptic and extrasynaptic currents modulated by different GABA_AR subtypes. However, there is still a need of selective or functional selective ligands for GABA_AR subtypes. In this work, the use of the bioisosteric replacement tool is widely employed to synthesize novel GABA_AR ligands with modulated pharmacological properties.

The overall aim of the project is the discovery of functional subtype selective ligands and the introduction of novel structural details to already elaborated SAR. Moreover, this project can address specific questions related to unclear structural requirements of GABA_AR ligands. Furthermore, the novel bioisosteres here synthesized and characterized could be used as starting point for other studies in the GABA_AR area or for other medicinal chemistry application.

2 4-Hydroxy-1,2,3-triazole and 3-hydroxy-1,2,5-thiadiazole as novel carboxylic acid bioisosteres for the GABA_ARs

2.1 Background and rationale

Muscimol, 4,5,6,7-tetrahydroisoxazolo[5,4-c]-pyridine-3-ol (THIP, Gaboxadol) and 5-(4-piperidyl)-3-isoxazolol (4-PIOL) are important examples of bioisosteric replacement in the GABA_ARs area using a 3-hydroxyisoxazole ring as carboxylic acid mimic (Figure 2.1). Muscimol is a natural product derived from *Amanita Muscaria* and is a well-known and potent agonist for the GABA_ARs.^{74, 75} THIP is a synthetic product which was characterized as a selective GABA_AR agonist,^{76, 77} while 4-PIOL is a synthetic product which behaves as partial GABA_AR agonist.^{78, 79}

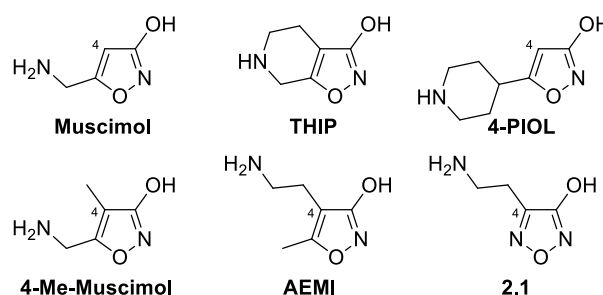


Figure 2.1. Structure of lead compounds Muscimol, THIP, 4-PIOL, 4-Me-muscimol, AEMI and **2.1**.

Structure activity relationship (SAR) studies proved that substitution in the 4-position of muscimol impaired activity for the GABA_ARs. 4-Me-muscimol,⁸⁰ AEMI^{81, 82} and **2.1**⁸³ are structurally derived from muscimol where a methyl group (4-Me-muscimol) or a 2-aminoethyl chain (AEMI and **2.1**) were introduced in the 4-position. The binding affinities are shown in Table 2.1.

Table 2.1 Pharmacological data for reference compounds GABA, Muscimol, THIP, 4-Me-muscimol, AEMI and **2.1**.^a

Compound	[³ H] Muscimol <i>K_i</i> (μM)
GABA	0.049 ^b
Muscimol	0.007 ^c
THIP	0.16 ^d
4-Me-muscimol	54 ^e
AEMI	>100 ^d
2.1	13 ^b

^aGABA_A receptor binding affinities at rat synaptic membranes. ^bData from Lolli *et al.*⁸³ ^cData from Krosggaard-Larsen *et al.*⁷⁷ ^dData from Krehan *et al.*⁸² ^eData from Petersen *et al.*⁸⁰

However, whether AEMI was completely devoid of affinity, the hydroxy-1,2,5-oxadiazolyl derivative (**2.1**) showed binding affinity for GABA_ARs in the micromolar range, comparable with 4-Me-muscimol.^{82, 83}

The difference in binding affinities for AEMI and **2.1** could be explained by an accessible conformation of **2.1** which is similar to the crystallographic conformation of THIP, where the 4-substitution is instead allowed because of the conformational restriction (Figure 2.2). The THIP-like conformation is indeed less probable for AEMI.⁸⁴

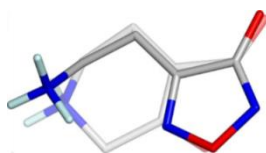


Figure 2.2 Superimposition between **2.1** in the supposed bioactive conformation and the crystallographic conformation of THIP. Oxygen is displayed in red and nitrogen in blue. The figure is adapted and modified from Tosco *et al.*⁸⁴

To support the assumption and alter or modulate the pharmacological properties of **2.1**, a bioisosteric replacement of the 3-hydroxy-1,2,5-oxadiazolyl (furazanyl) moiety was designed. Among others, 3-hydroxy-1,2,5-thiadiazole and 4-hydroxy-1,2,3-triazole have been recently studied by our research group at the Department of Drug Science and Technology of the University of Turin and, thanks to their marked acidic properties, they have been successfully applied as carboxylic acid bioisosteres in medicinal chemistry studies.^{85, 86} For this reason, two analogues of **2.1** were designed (**2.2** and **2.3**, Figure 2.3), where the 3-hydroxy-1,2,5-oxadiazolyl moiety has been replaced by 3-hydroxy-1,2,5-thiadiazole and 4-hydroxy-1,2,3-triazole respectively.

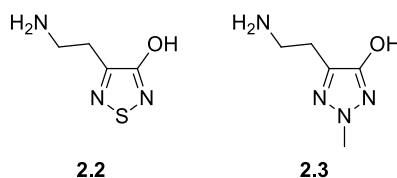


Figure 2.3 Structure of target compounds **2.2** and **2.3**.

In contrast, SAR studies performed on 4-PIOL revealed that insertion of small substituents (e.g. Me-4-PIOL, Et-4-PIOL) in the 4-position of 4-PIOL is tolerated. In addition, the introduction of larger substituents (e.g. NaphMe-4-PIOL and DPP-4-PIOL) was proved to not only enhance binding affinities, but also lead to potent antagonists (Table 2.2).^{61, 87}

More recently, a variety of carboxylic acid bioisosteres have been employed to replace the 3-hydroxyisoxazole moiety of 4-PIOL affording a range of ligands.⁵⁸ Of particular interest, 4-PHP and Aza-4-PIOL were reported as new analogues of 4-PIOL where the 3-hydroxyisoxazole moiety has been replaced by 1- or 3-hydroxypyrazole respectively.^{65, 88} SAR study for 4-PHP indicated the 3- and 5- position as possible sites of structure modification since the insertion of

bulky substituents is tolerated (e.g. 3-NaphMe-4-PHP and 5-NaphMe-4-PHP).⁶⁵ 3,5-disubstituted 4-PHP analogues were also shown to have affinity in the nanomolar or micromolar range (compounds **1.1** and **1.2** respectively) indicating the existence of a cavity above and below the core scaffold of 4-PHP (Table 2.2).⁶⁵

Table 2.2 Pharmacological data for reference compounds GABA, 4-PIOL, 4-PHP, Aza-4-PHP and other derivatives.^a

Compound	R ₁	R ₂	[³ H] Muscimol K _i (μM)
GABA			0.049 ^b
4-PIOL	H		9.1 ^c
4-PHP	H	H	10 ^c
Aza-4-PIOL			>100 ^c
Me-4-PIOL	Me		10 ^d
Et-4-PIOL	Et		6.3 ^d
NaphMe-4-PIOL	2-Naphtylmethyl		0.049 ^c
DPP-4-PIOL	3,3-diphenylpropyl		0.068 ^c
3-NaphMe-4-PHP		2-Naphtylmethyl	0.0030 ^e
5-NaphMe-4-PHP	2-Naphtylmethyl		0.033 ^e
1.1	Phenyl	2-Naphtylmethyl	0.022 ^e
1.2	2-Naphtylmethyl	Phenyl	1.5 ^e

^aGABA_A receptor binding affinities at rat synaptic membranes. ^bData from Lolli *et al.*⁸³ ^cData from Krall *et al.*⁵⁸ ^dData from Frølund *et al.*⁶¹ ^eData from Møller *et al.*⁶⁵

As second aim of the project, the above mentioned 4-hydroxy-1,2,3-triazole was used as the core scaffold in the design of 4-PIOL analogues in order to modulate the pharmacological properties of the already known partial agonists and antagonists for the GABA_AR. In particular, two different isomers were designed as potential GABA_AR partial agonists (**2.4a** and **2.5a**) and four new analogues as potential GABA_AR antagonists (**2.4b–c** and **2.5b–c**, Figure 2.4).

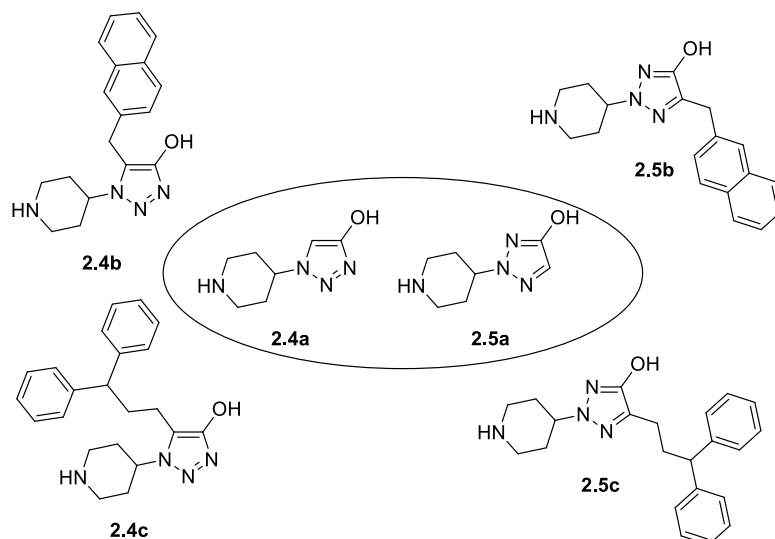


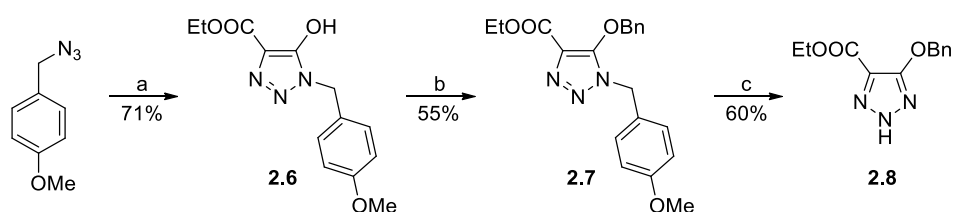
Figure 2.4 Target compounds **2.4a–c** and **2.5a–c**.

In conclusion, the novel target molecules reported in this chapter permit to evaluate the 4-hydroxy-1,2,3-triazole and 3-hydroxy-1,2,5-thiadiazole as potential bioisosteres in the GABA_ARs context, vary the chemical and pharmacodynamic properties of GABA_ARs pharmacological tools and expand the knowledge on available ligands targeting the orthosteric binding site of the GABA_ARs.

2.2 Results and discussion

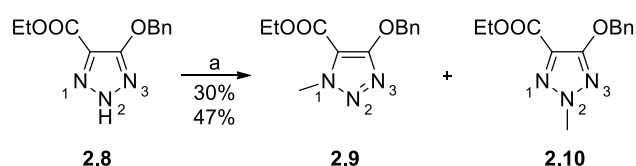
2.2.1 Chemistry

4-Hydroxy-1,2,3-triazole is an acidic hydroxylated azole which has been recently studied in bioisosteric applications by our research group at the University of Turin.^{85, 86, 89} In 2015, Pippione *et al.* reported a synthetic pathway for the synthesis of **2.8** (Scheme 2.1),⁸⁵ which was used as key intermediate in this project for the synthesis of **2.3**, **2.4a–c** and **2.5a–c**.



Scheme 2.1 Reagents and conditions: (a) diethylmalonate, NaOEt, EtOH, reflux, (b) BnBr, K₂CO₃, DMF, rt, (c) CAN, CH₃CN/H₂O (1:1, v/v), rt.⁸⁵

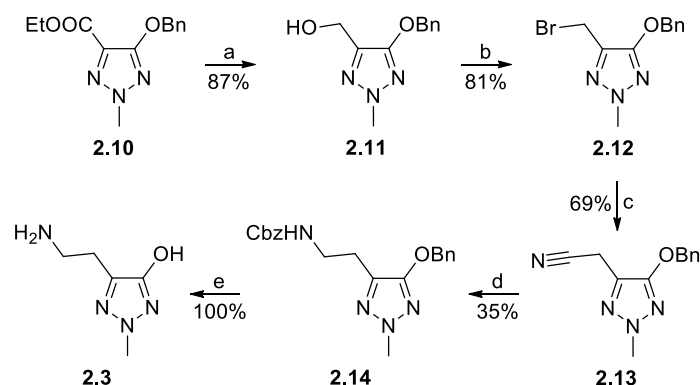
Alkylation reactions between **2.8** and alkyl or benzyl halides in acetonitrile using potassium carbonate as base always afford an isomeric mixture of two different products, where the nitrogen atom called *N*₁ or the nitrogen atom called *N*₂ bear the substituent (Scheme 2.2). The obtained regioisomers are usually resolved using flash chromatography with consistent eluting order and the structure determined using 2D-NMR analyses (please refer to section 2.2.2). In this project, the strategy to obtain **2.9** and **2.10** involved methyl iodide as alkylating agent.⁸⁵



Scheme 2.2 Reagents and conditions: (a) MeI, K₂CO₃, CH₃CN, rt. Please note: the given nomenclature to nitrogen atoms (i.e. *N*₁, *N*₂ and *N*₃) do not follow IUPAC recommendations. However, the given nomenclature is used consistently as here reported.

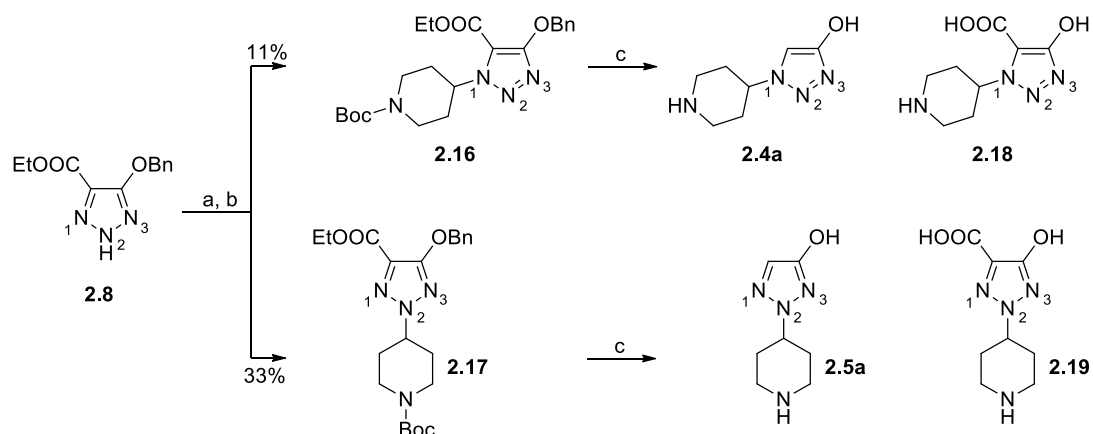
The synthetic scheme used for the synthesis of **2.3** starting from **2.10** is depicted in Scheme 2.3. The synthesis of the alcohol derivative **2.11** was achieved using lithium aluminium hydride as reducing agent. The following treatment of **2.11** with *N*-bromosuccinimide and triphenylphosphine led to **2.12** which was subsequently treated with sodium cyanide affording **2.13**. Using a one-pot method previously described,^{80, 90} the nitrile group of **2.13** was reduced to amino group and protected in order to optimize the purification procedure. The protecting groups

of **2.14** (*Cbz*- and *Bn*-) were subsequently removed under acidic conditions affording the target compound **2.3**.



Scheme 2.3 Reagents and conditions: (a) LiAlH₄, dry THF, 0 °C to rt, (b) PPh₃, NBS, dry CH₂Cl₂, -10 °C, (c) NaCN, EtOH/H₂O, rt, (d) BnOCOCl, NaBH₄, NiCl₂, MeOH, 0 °C to rt, (e) 2M HCl, reflux.

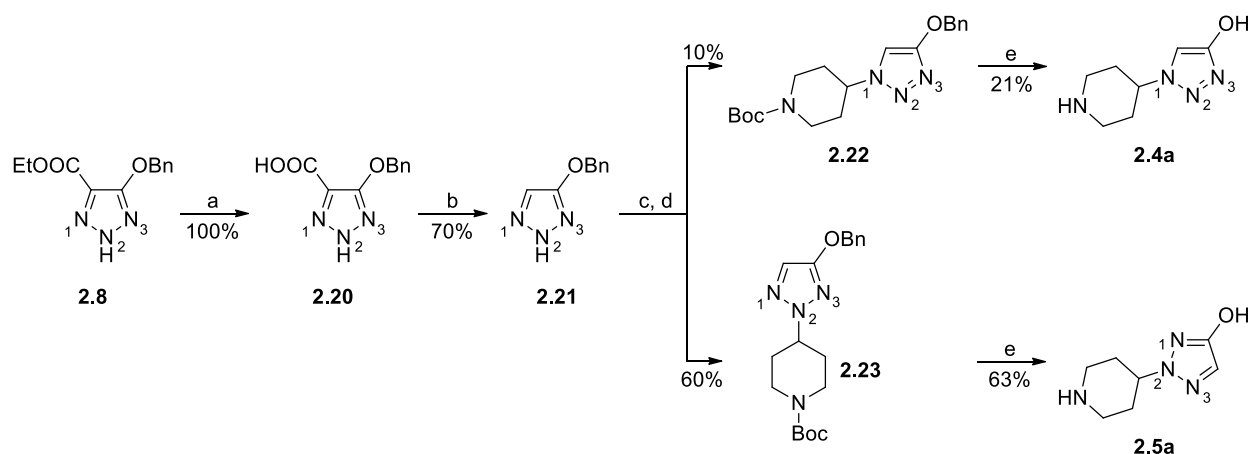
Compound **2.8** was also used as starting material for the synthesis of **2.4a** and **2.5a** (Schemes 2.4 and 2.5). **2.8** was made reacted with *tert*-butyl 4-bromopiperidine-1-carboxylate (**2.15**) and potassium carbonate in acetonitrile at reflux (condition a, Scheme 2.4). Lower temperature did not allow the formation of the products. However, at 80 °C a competition between elimination and substitution reaction occurs and more than one equivalent of alkyl bromide (**2.15**) was required to complete the reaction. As expected, two regioisomers (**2.16** and **2.17**) were obtained and separated using flash chromatography. The deprotection of the two isomers was attempted using 6M HCl at reflux, 48% HBr at reflux and 6M HCl in microwave reactor. However, a mixture of **2.4a** (or **2.5a**) and **2.18** (or **2.19**) was obtained with all these experimental conditions.



Scheme 2.4 Reagents and conditions: (a) *tert*-butyl 4-bromopiperidine-1-carboxylate (**2.15**), K₂CO₃, CH₃CN, reflux, (b) flash chromatography (petroleum ether/EtOAc 70:30 v/v), (c) 6M HCl reflux or 6M HCl reflux microwave assisted or 48% HBr reflux.

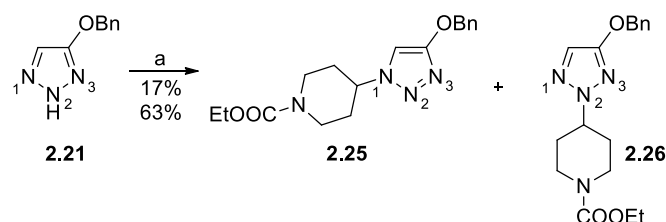
For this reason, another synthetic pathway was developed (Scheme 2.5). **2.21** was obtained in two steps starting from basic catalysed hydrolysis of **2.8** and consequent decarboxylation at high temperature of the formed carboxylic acid (**2.20**). Compounds **2.22** and **2.23** were obtained by the following alkylation reaction between **2.21** and *tert*-butyl 4-bromopiperidine-1-carboxylate (**2.15**). Also in this case, the two regioisomers were separated using flash chromatography and

distinguished by 2D-NMR experiments (see section 2.2.2). Differently from previously described 5-(ethoxycarbonyl)-1*H*-1,2,3-triazoles, the *N*₂ isomer **2.23** was the first eluted product (60% yield, major product), while the *N*₁ isomer **2.22** was the second eluted (10% yield, minor product). The subsequent deprotection under acidic conditions afforded **2.4a** and **2.5a**.



Scheme 2.5 Reagents and conditions: (a) 6M NaOH, EtOH, 50 °C, (b) DMF, 130 °C, 6h, (c) *tert*-butyl 4-bromopiperidine-1-carboxylate (**2.15**), K₂CO₃, CH₃CN, reflux, (d) flash chromatography (petroleum ether/EtOAc from 10% to 40% EtOAc), (e) 6M HCl reflux.

The same alkylation conditions applied for the synthesis of **2.22** and **2.23** were employed using ethyl 4-bromopiperidine-1-carboxylate (**2.24**) for the synthesis of **2.25** and **2.26** (Scheme 2.6).



Scheme 2.6 Reagents and conditions: (a) ethyl 4-bromopiperidine-1-carboxylate (**2.24**), Cs₂CO₃, CH₃CN, reflux.

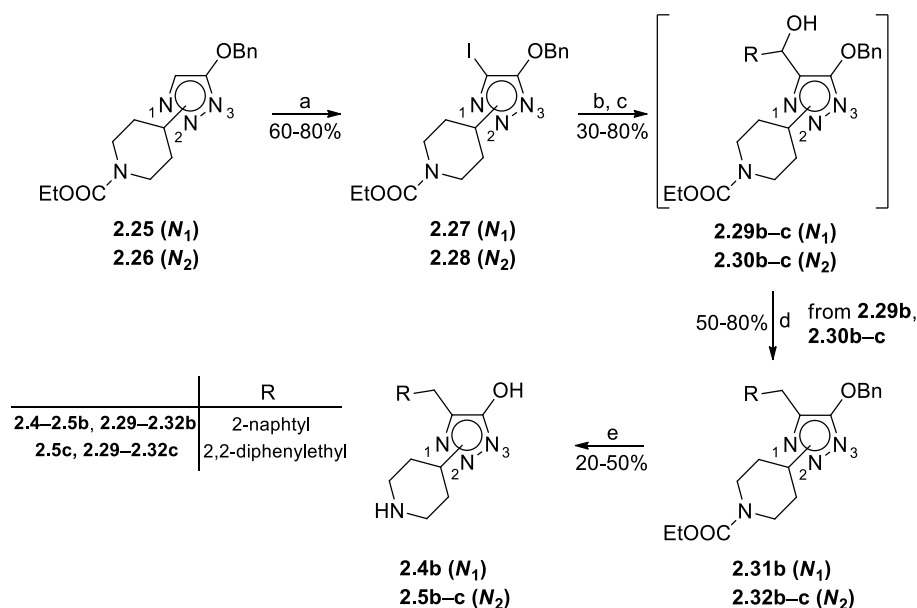
Analogously to the reaction described before, the *N*₂ isomer **2.26** was obtained as major product in 63% yield and the *N*₁ isomer **2.25** in 17% yield. Since both regioisomers were interesting in our synthetic scheme, a preliminary study of the alkylation reaction between **2.21** and **2.24** was performed (Table 2.3) aiming to optimize the synthesis of the *N*₁ isomer.

Table 2.3 Optimization of the alkylation reaction between **2.21** and ethyl-4-bromopiperidine-1-carboxylate (**2.24**). The relative areas reported are based on HPLC analysis at 254 nm. Reagents and side products are not considered in the given values.

Entry	Solvent, T	bp (°C)	Dielectric constant	Base	Relative area <i>N</i> ₁	Relative area <i>N</i> ₂
1	CH ₃ CN, reflux	81.6	37.5	Cs ₂ CO ₃	12%	88%
2	CH ₃ CN, reflux	81.6	37.5	KOH	11%	89%
3	DMF, 90 °C	153	36.7	Cs ₂ CO ₃	8%	92%
4	DMF, 150 °C	153	36.7	Cs ₂ CO ₃	8%	92%
5	EtOH, reflux	78.5	24.5	Cs ₂ CO ₃	9%	91%
6	1,2-dimethoxyethane, reflux	85	7.2	Cs ₂ CO ₃	25%	75%
7	1,4-dioxane, reflux	101.1	2.25	Cs ₂ CO ₃	33%	67%
8	Toluene, reflux	110.6	2.38	Cs ₂ CO ₃	27%	73%

Only one experiment using a different base was attempted without any significant improvement (entry 2). The temperature was increased in DMF from the starting point of 90 °C to 150 °C using caesium carbonate as base, and this parameter did not affect the N_1/N_2 ratio in the investigated experimental conditions (entries 3 and 4). The solvent of the reaction was varied choosing between aprotic or protic solvents with different dielectric constants. Even if only a limited set of reaction has been attempted, aprotic solvents with low dielectric constant seem to increase the N_1/N_2 ratio, being caesium carbonate in anhydrous 1,4-dioxane at reflux the best condition found. The reaction was repeated affording **2.25** and **2.26** in 1:1 ratio (41% and 39% isolated yields respectively). The N_1/N_2 ratio in Table 2.3 differs from isolated yields because the wavelength selected for the analysis do not probably correspond to the isosbestic point.

The synthesized products were then used in the following synthetic pathway for the synthesis of **2.4b–c** and **2.5b–c** (Scheme 2.7). Iodination of **2.25** and **2.26** using iodine monochloride afforded **2.27** and **2.28** respectively. The latter were converted in the corresponding Grignard reagents, which were then quenched with 2-naphthaldehyde (b series) or 3,3-diphenylpropanal (c series) affording the corresponding alcohol derivatives **2.29b–c** and **2.30b–c**. Ionic hydrogenation⁹¹ of **2.29b** and **2.30b–c** afforded **2.31b** and **2.32b–c**.



Scheme 2.7 Reagents and conditions: (a) ICl, AcOH, H₂O, 80 °C, (b) ⁱPrMgCl, dry THF, -10 °C, (c) 2-naphthaldehyde or 3,3-diphenylpropanal (**2.33**), dry THF, 0 °C to rt, (d) Et₃SiH, TFA, CH₂Cl₂, 0 °C to rt, (e) 35% HCl, EtOH, reflux.

Usually, ionic hydrogenation (step d, Scheme 2.7) is performed using triethylsilane (1.6 equivalents) and large excess of trifluoroacetic acid (26 equivalents) for one day at room temperature. However, ionic hydrogenation of **2.30c** in the mentioned condition afforded a mixture of **2.32c** and probably the trifluoromethyl ester intermediate **2.34c** which was proposed by NMR analysis (proposed mechanism depicted in Figure 2.5). Longer reaction times (3 days) and larger excess of triethylsilane (6 equivalents) were required to afford **2.32c** without traces of

the above mentioned impurity. Subsequent deprotection of **2.31b** and **2.32b–c** (Scheme 2.7) under acidic condition afforded final compounds **2.4b** and **2.5b–c**.

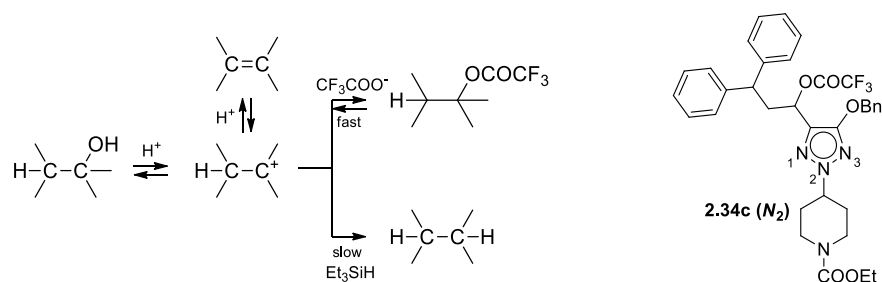
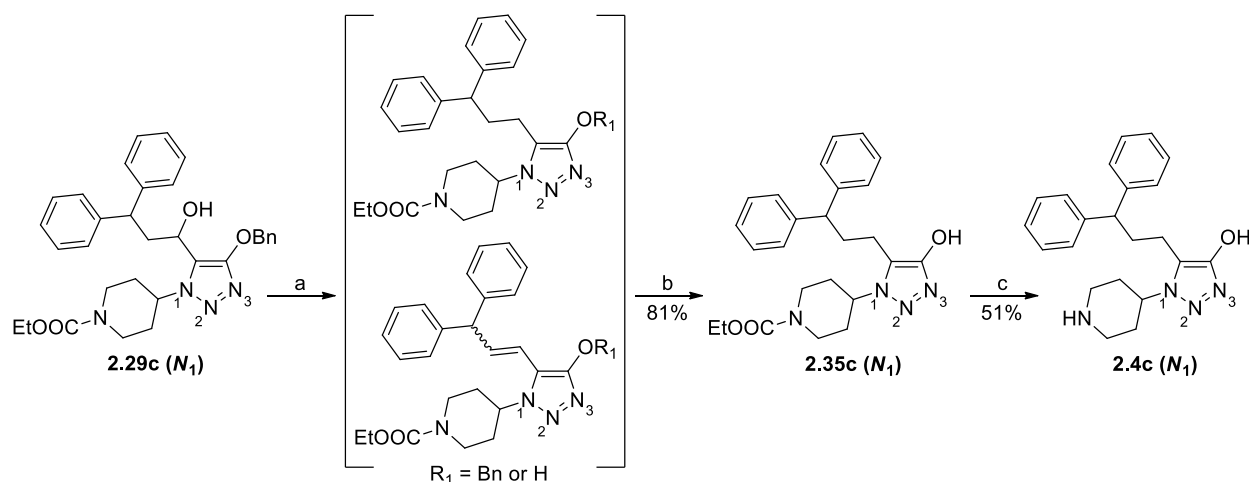


Figure 2.5 Proposed mechanism⁹¹ for ionic hydrogenation (left) and probable side product **2.34c**.

A modification of the synthetic strategy reported before was needed to afford compound **2.4c**. Standard ionic hydrogenation of **2.29c** afforded a complex mixture and also longer reaction time and more equivalent of triethylsilane did not allow the synthesis of **2.31c** (Scheme 2.7). The reaction was then performed at 50 °C in a sealed tube affording a mixture of saturated and unsaturated products in comparable amount as outlined in Scheme 2.8 (determined using LC-MS analysis). The complex mixture was hydrogenated to **2.35c** and the following acid catalysed hydrolysis afforded the target compound **2.4c**.



Scheme 2.8 Reagents and conditions: (a) Et_3SiH , TFA, CH_2Cl_2 , 50 °C, sealed tube, (b) H_2 , Pd/C, MeOH, rt, (c) 35% HCl, EtOH, reflux.

The synthesis of the last target compound **2.2** was attempted using two different strategies (Figure 2.6). On one hand the synthesis of the lateral amino ethyl chain was tried by homologation reactions on the formed 3-hydroxy-1,2,5-thiadiazole ring (left, Figure 2.6). On the other hand the synthesis of the heterocycle was tried at the last stage of the synthesis (right).

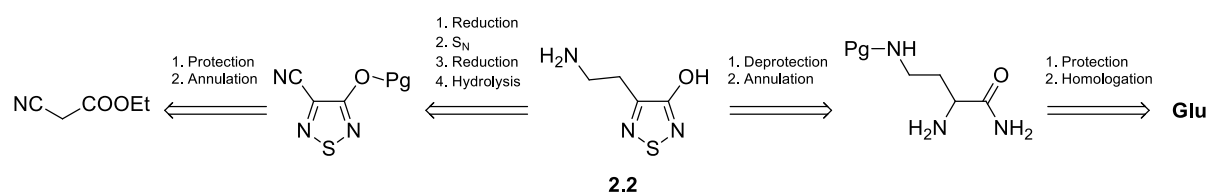
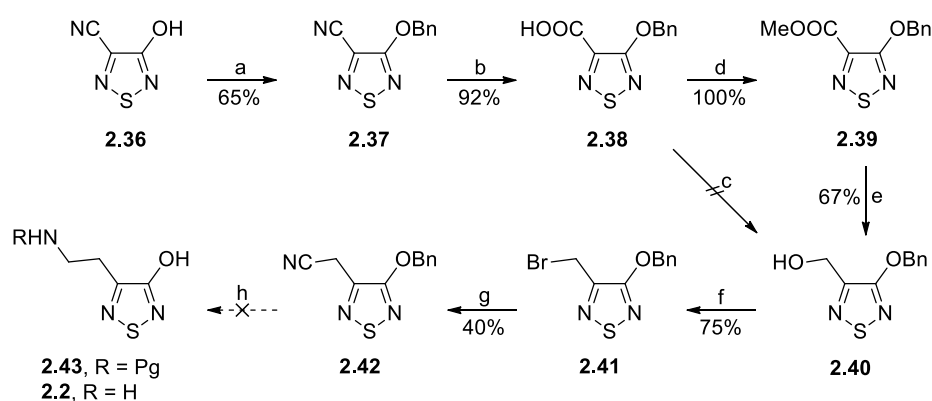


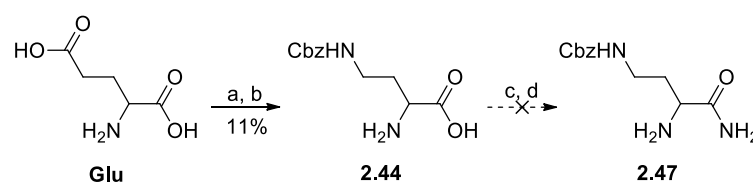
Figure 2.6 Retrosynthetic strategies for the synthesis of **2.2**.

The first synthetic strategy for the synthesis of **2.2** (Scheme 2.9) started from **2.36**, which was synthesized in our group at the University of Turin as previously described.⁹² Then, **2.37**⁸⁶ was obtained by protection of the hydroxy group using benzyl bromide. The nitrile group of **2.37** was hydrolysed to **2.38**⁸⁶ in basic conditions and consequent reduction of the resulting carboxylate using borane dimethyl sulphide complex afforded a mixture of **2.40** and benzyl alcohol (determined using NMR analysis). Consequently, the alcohol derivative **2.40** was obtained by first converting **2.38** to the ester **2.39** and subsequent reduction of this latter using NaBH₄. Treatment of the alcohol derivative **2.40** with triphenylphosphine and *N*-bromosuccinimide gave **2.41**, which was made reacted with sodium cyanide affording **2.42**. Reduction of the nitrile group was tried using the method described by Petersen *et al.*^{80, 90} which consists of reduction using sodium borohydride catalysed by nickel (II) chloride and consequent protection of the produced amine in one-pot. However, the procedure tried did not allow the synthesis of the last intermediate **2.43** and the synthetic scheme was not further investigated. The unsuccessful procedure is probably due to sulphur containing heterocycle which could poison the catalyst.⁸⁶



Scheme 2.9 Reagents and conditions: (a) BnBr, K₂CO₃, dry DMF, rt, (b) 6M NaOH, EtOH, 55 °C, (c) (CH₃)₂S·BH₃, THF, rt, (d) 1st step: ClCOCOCl, dry DMF, dry THF, 0 °C, 2nd step: dry MeOH, 0 °C to rt, (e) NaBH₄, dry THF, 0 °C to rt, (f) PPh₃, NBS, dry CH₂Cl₂, -10 °C. (g) NaCN, EtOH/H₂O, rt, (h) BnOCOCl, NaBH₄, NiCl₂, MeOH, 0 °C to rt.

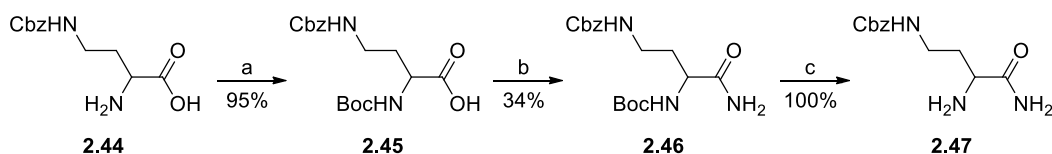
Compound **2.2** was finally synthesized (Scheme 2.12) starting from **2.47**, a known compound previously described by Treder *et al.* which was obtained as reported in Scheme 2.10.⁹³ The synthesis of **2.44** from glutamic acid was reproduced with lower yield in our group. However, the simple procedure reported for **2.47** was not reproducible in our hand.



Scheme 2.10 Reagents and conditions: (a) NaN₃, H₂SO₄, CHCl₃, 50-60 °C, (b) Cu(OAc)₂, CbzCl, H₂O/dioxane, rt, (c) MeOH/HCl, (d) MeOH/NH₃.

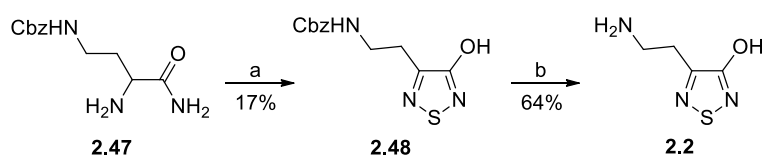
Therefore, the synthesis of **2.47** was achieved through three steps (Scheme 2.11). The α-amino group of **2.44** was protected with di-*tert*-butyl dicarbonate affording **2.45**. Following a modified

procedure described by Pozdnev *et al.*,⁹⁴ **2.45** was converted to **2.46** and subsequently deprotected to afford the α -amino amide **2.47**.



Scheme 2.11 Reagents and conditions: (a) Boc_2O , NaHCO_3 , Dioxane, rt, (b) NH_4HCO_3 , Boc_2O , Pyridine, CH_3CN , rt, (c) TFA, dry CH_2Cl_2 , rt.

Annulation of **2.47** and sulphur monochloride (Scheme 2.12), using a method previously described by Weinstock *et al.*,⁹² and subsequent deprotection under acidic condition afforded the target compound **2.2**.



Scheme 2.12 Reagents and conditions: (a) S_2Cl_2 , DMF, rt, (b) 2M HCl, reflux.

2.2.2 Characterization

^{13}C chemical shift and heteronuclear ^1H - ^{13}C HMBC correlations has been proved to be diagnostic analyses for the characterization of N_1 , N_2 and N_3 regiosubstituted ethyl 4-hydroxy-1,2,3-triazolecarboxylate.⁹⁵ Previously, the three isomers of compound **2.49** ($N_{1,2,3}$ -**2.49**) were characterized using the ^1H , ^{13}C , HSQC and HMBC experiments. The analyses were used to unequivocally assign all the chemical shifts of the molecules and to determine the structure of the analysed isomers. All the isomers show a $^3J_{\text{H,C}}$ correlation between $\text{H}_{(\text{f})}$ and $\text{C}_{(\text{e})}$ as proof of the correct $\text{C}_{(\text{e})}$ chemical shift. The analysis of HMBC spectra of N_3 -**2.49** shows a $^3J_{\text{H,C}}$ correlation between $\text{H}_{(\text{g})}$ and $\text{C}_{(\text{e})}$, as expected for N_3 substituted isomer (Figure 2.7). N_1 substituted regioisomers (e.g. N_1 -**2.49**) show diagnostic $^3J_{\text{H,C}}$ correlation between $\text{H}_{(\text{g})}$ and $\text{C}_{(\text{d})}$ (Figure 2.7). However, N_2 substituted regioisomers (e.g. N_2 -**2.49**) do not show any $^3J_{\text{H,C}}$ correlation between $\text{H}_{(\text{g})}$ and neither $\text{C}_{(\text{e})}$ or $\text{C}_{(\text{d})}$ (Figure 2.8).

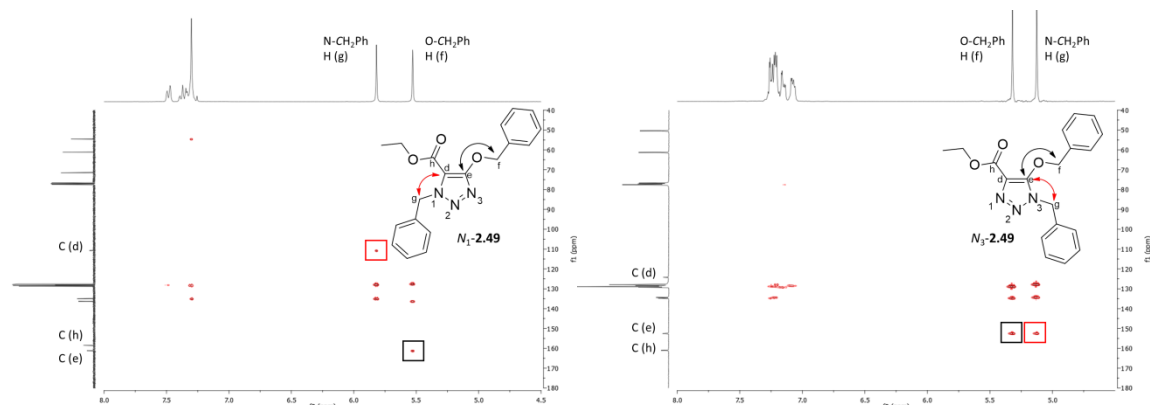


Figure 2.7 HMBC analyses of $N_{1,3}$ -**2.49**: $^3J_{\text{H,C}}$ correlation between $\text{H}_{(\text{f})}$ and $\text{C}_{(\text{e})}$ in black and $^3J_{\text{H,C}}$ correlation between $\text{H}_{(\text{g})}$ and $\text{C}_{(\text{e})/(\text{d})}$ in red.

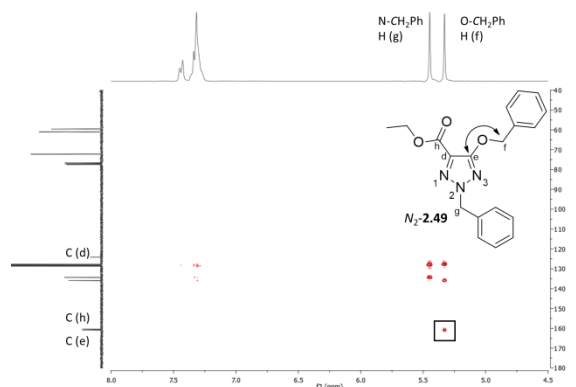
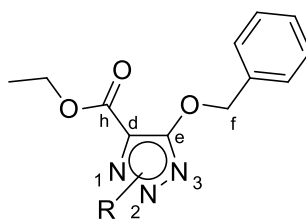


Figure 2.8 HMBC analyses of N_2 -**2.49**: $^3J_{H,C}$ correlation between $H_{(f)}$ and $C_{(e)}$ in black.

$C_{(d)}$ and $C_{(e)}$ chemical shift are also diagnostic for the three regioisomers. In particular, the signal of $C_{(d)}$ occurs at 120 ppm for N_2 -**2.49** and N_3 -**2.49**, while it is observed at higher field for N_1 -**2.49** (110 ppm). On the other hand, the $C_{(e)}$ chemical shift is similar for N_1 -**2.49** and N_2 -**2.49** and at higher field for N_3 -**2.49**. The trend observed for $C_{(d)}$ and $C_{(e)}$ chemical shift is retained for a number of analogues of **2.49**⁹⁵ (representative analogues reported in Table 2.4).

Table 2.4 $^{13}C_{(d)}$ and $^{13}C_{(e)}$ chemical shift of representative compounds **2.9**, **2.10** and **2.49**: NMR experiment were recorded using a Bruker Avance 300 MHz.



Cpd.	R	N_1		N_2		N_3	
		$C_{(d)}$	$C_{(e)}$	$C_{(d)}$	$C_{(e)}$	$C_{(d)}$	$C_{(e)}$
2.9 (N_1), 2.10 (N_2), 2.53 (N_3) ^a	CH ₃	112.4	161.6	124.3	161.6	124.6	152.7
2.49 ^a	CH ₂ Ph	110.8	161.3	124.2	161.0	124.2	152.5

^aNMR recorded in CDCl₃.

Analogously to N_1 , N_2 and N_3 regioisomers of compound **2.49**, the structure of compounds **2.22** and **2.23** (N_1 and N_2 regioisomers respectively) were studied and determined using 2D NMR analyses. 1H , ^{13}C and HSQC were used to assign the chemical shifts and then HMBC was used to determine the isomer identity.

A $^3J_{H,C}$ correlation between $H_{(g)}$ and $C_{(d)}$ was observed in **2.22**, whilst HMBC of **2.23** did not show any $^3J_{H,C}$ correlation between $H_{(g)}$ and neither $C_{(e)}$ or $C_{(d)}$ confirming the structure of the compounds (Figure 2.9). The same study was also performed for compounds **2.25** and **2.26** leading to the final structural assignments (Figure 2.10).

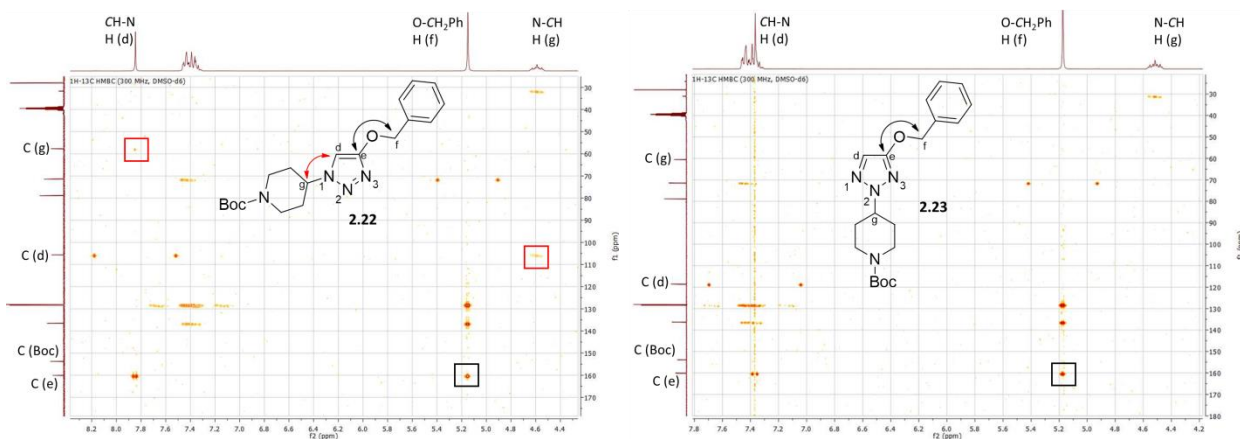


Figure 2.9 HMBC analyses of **2.22** and **2.23**: $^3J_{\text{H,C}}$ correlation between $\text{H}_{(\text{f})}$ and $\text{C}_{(\text{e})}$ in black and $^3J_{\text{H,C}}$ correlation between $\text{H}_{(\text{f})}$ and $\text{C}_{(\text{d})}$ and *vice versa* in red.

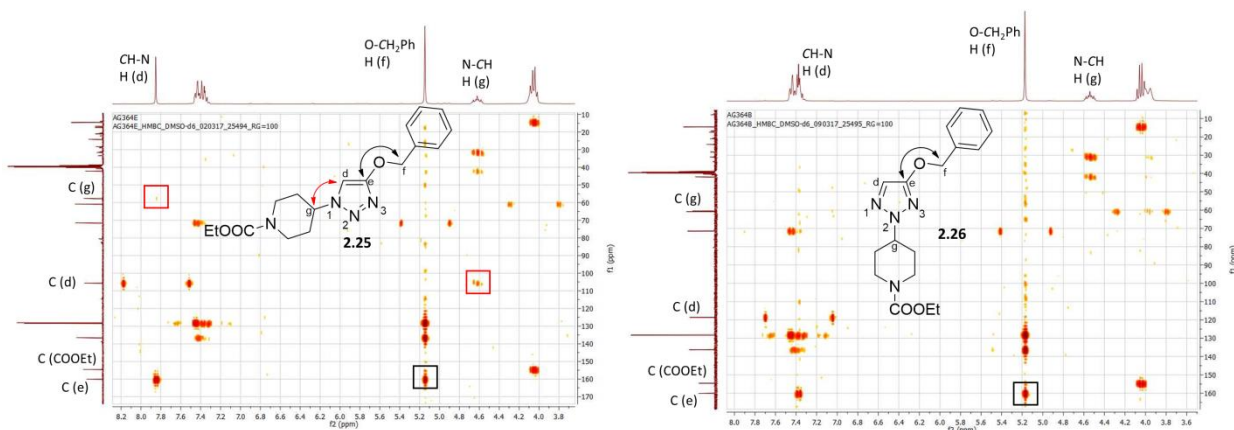
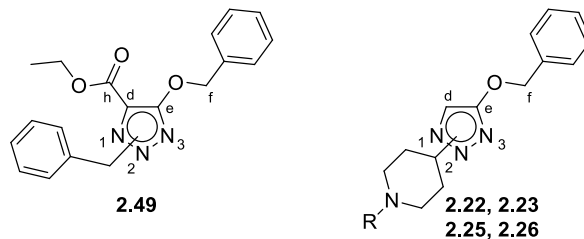


Figure 2.10 HMBC analyses of **2.25** and **2.26**: $^3J_{\text{H,C}}$ correlation between $\text{H}_{(\text{f})}$ and $\text{C}_{(\text{e})}$ in black and $^3J_{\text{H,C}}$ correlation between $\text{H}_{(\text{f})}$ and $\text{C}_{(\text{d})}$ and *vice versa* in red.

Even if compounds **2.22**, **2.23**, **2.25** and **2.26** differ from the compounds previously described in the chapter (**2.9**, **2.10** and **2.49**) for the missing carboxyethyl moiety on $\text{C}_{(\text{d})}$, the characteristic difference in chemical shift of $^{13}\text{C}_{(\text{d})}$ and $^{13}\text{C}_{(\text{e})}$ between different regioisomers (Table 2.5) were observed and were coherent with the values previously reported.

Table 2.5 $^{13}\text{C}_{(\text{d})}$ and $^{13}\text{C}_{(\text{e})}$ chemical shift of representative compound **2.49** and compounds of the study **2.22–2.23** and **2.25–2.26**: NMR experiment were recorded using a Bruker Avance 300 MHz.



Cpd.	R	N_1		N_2		N_3	
		$\text{C}_{(\text{d})}$	$\text{C}_{(\text{e})}$	$\text{C}_{(\text{d})}$	$\text{C}_{(\text{e})}$	$\text{C}_{(\text{d})}$	$\text{C}_{(\text{e})}$
2.49 ^a	-	110.8	161.3	124.2	161.0	124.2	152.5
2.22 (N_1), 2.23 (N_2) ^b	Boc	105.6	160.1	118.6	160.1	-	-
2.25 (N_1), 2.26 (N_2) ^b	EtOCO	105.6	160.1	118.6	160.1	-	-

^aNMR recorded in CDCl_3 ; ^bNMR recorded in $\text{DMSO}-d_6$.

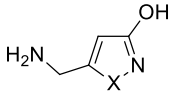
2.2.3 Pharmacology

The binding affinities of the synthesized compounds (**2.2–2.5**) at native GABA_ARs were measured by displacement of [³H]muscimol in rat brain membrane preparations.

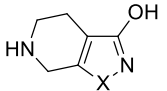
Compounds **2.2** and **2.3** were shown to have lower affinity than lead compound **2.1**, resulting in a six fold decrease in affinity and inactive compound respectively (Table 2.6). Steric hindrance of sulphur atom of compound **2.2** and *N*-methyl of compound **2.3** were supposed to be the reason for the impaired affinity. This trend is also clear considering activities of muscimol and THIP versus the sulphur containing analogue thiomuscimol and thio-THIP, which resulted in three fold and 300 fold decrease in affinity respectively.^{77, 82} These results are in accordance with the literature suggesting that the binding site is sensible to steric hindrance in the explored position. Ionization constants of the novel analogues has also been determined and resulted comparable with those of muscimol and thiomuscimol. Consequently, the effects of this property may play a minor role in determining affinity of these ligands.

Considering the obtained results, it was not possible to obtain further proof of the hypothesized bioactive conformation of **2.1**, even if the hypothesis could still explain the affinity of **2.1** and **2.2**. The new compounds were not further pharmacologically characterized due to low affinity for the native GABA_ARs, but it is not possible to exclude that these derivatives could be evaluated again in the future showing some interesting pharmacological properties.

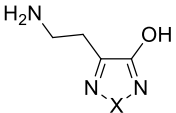
Table 2.6 Pharmacological data of reference compounds GABA, muscimol, thiomuscimol, THIP, thio-THIP and compounds **2.1–2.3**.^a



(thio)-muscimol



(thio)-THIP



2.1–2.3

Compound	X	[³ H] Muscimol <i>K_i</i> (μM) ^b	p <i>K_{a1}</i> ^c
GABA	-	0.049 ^d	4.04 ^g
Muscimol	O	0.007 ^e	4.8 ^h
Thiomuscimol	S	0.019 ^e	6.1 ^h
THIP	O	0.16 ^f	4.4 ^d
Thio-THIP	S	52 ^f	6.1 ^d
2.1	O	13 ^d	3.12 ^b
2.2	S	75 [4.13±0.04]	4.54±0.03
2.3	NMe	>100	5.92±0.02

^aGABA_A receptor binding affinities at rat synaptic membranes. ^bIC₅₀ values were calculated from inhibition curves and converted to *K_i* values. Data is given as the mean [mean p*K_i* ± SEM] of three to five independent experiments. ^cThe ionization constants of compounds **2.2** and **2.3** were determined by potentiometric titration using a GLp*K_a* apparatus (Sirius Analytical Instruments Ltd., Forest Row, East Sussex, UK). ^dData from Lolli *et al.*⁸³ ^eData from Krosggaard-Larsen *et al.*⁷⁷ ^fData from Krehan *et al.*⁸² ^gData from Albert *et al.*⁹⁶ ^hData from Petersen *et al.*⁵⁶

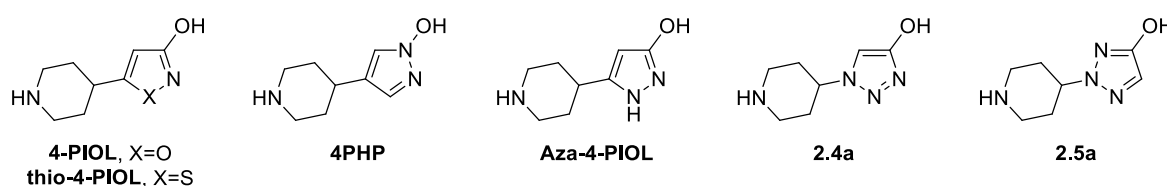
The binding affinity of **2.4a** resulted lower, but in the same magnitude order, than 4-PIOL and compound **2.5a** resulted devoid of affinity to the native GABA_ARs (Table 2.7). Considering

these results, the bioisosteric replacement of the 3-hydroxyisoxazole moiety of 4-PIOL using the N_1 regioisomer of 3-hydroxytriazole was successful whilst, at this stage, the N_2 regioisomer could not be considered a suitable bioisostere in the GABA_ARs area. The two regioisomers **2.4a** and **2.5a** were also evaluated in terms of ionization constants (6.51 and 6.36 respectively). The reported experimental values were comparable each other and similar with reference compound thio-4-PIOL (6.9), meaning that the difference in binding affinity is probably not related to difference in protolytic properties.

On the other hand, the difference in binding affinity could be explained by a different charge distribution in the two heterocycles or by a high desolvation energy as postulated for Aza-4-PIOL, which is devoid of affinity for the GABA_ARs.⁸⁸ Using the program Jaguar,⁹⁷ the free energies of solvation for the zwitterionic forms of 4-PHP (-77.9 kcal/mol), aza-4-PIOL (-101.2 kcal/mol), **2.4a** (-97.2 kcal/mol) and **2.5a** (-88.5 kcal/mol) were calculated, indicating a significantly higher desolvation energy penalty for **2.4a** and **2.5a** than for 4-PHP.

In general, the heterocyclic carboxylic acid bioisosteres interacting with the GABA_AR resemble the electrostatic properties of the carboxylic acid in GABA.⁵⁶ The electronegative charge is usually delocalized in the area around the hydroxy group and the neighbouring nitrogen, allowing the ligands to interact in a bidentate manner with the conserved Arg66 residue of the GABA binding site (e.g. 4-PHP and Aza-4-PIOL, Figure 2.11). In contrast, the electrostatic potential maps of the heterocyclic carboxylic acid bioisosteres of **2.4a** and **2.5a** showed a slightly different charge distribution (Figure 2.11) which might compromise the bidentate interaction between the ligand and the Arg66 leading to a decrease in term of binding affinity.

Table 2.7 Pharmacological data for reference compounds GABA, 4-PIOL, Thio-4-PIOL, 4-PHP, Aza-4-PHP and compounds **2.4–2.5a**.^a



Compound	[³ H] Muscimol K_i (μ M) ^b	pK_{a1} ^c
GABA	0.049 ^d	4.04 ^g
4-PIOL	9.1 ^e	5.3 ^f
thio-4-PIOL	1.3 ^f	6.9 ^f
4-PHP	10 ^e	5.4 ^e
Aza-4-PIOL	>100 ^e	6.7 ^h
2.4a	55 [4.26±0.05]	6.51±0.03
2.5a	>100	6.36±0.01

^aGABA_A receptor binding affinities at rat synaptic membranes. ^b IC_{50} values were calculated from inhibition curves and converted to K_i values. Data is given as the mean [mean $pK_i \pm$ SEM] of three to five independent experiments. ^cThe ionization constants of compounds **2.4a** and **2.5a** were determined by potentiometric titration using a GLpK₃ apparatus (Sirius Analytical Instruments Ltd., Forest Row, East Sussex, UK). ^dData from Lolli *et al.*⁸³ ^eData from Krall *et al.*⁵⁸ ^fData from Frølund *et al.*⁹⁸ ^gData from Albert *et al.*⁹⁶ ^hData from Krall *et al.*⁸⁸

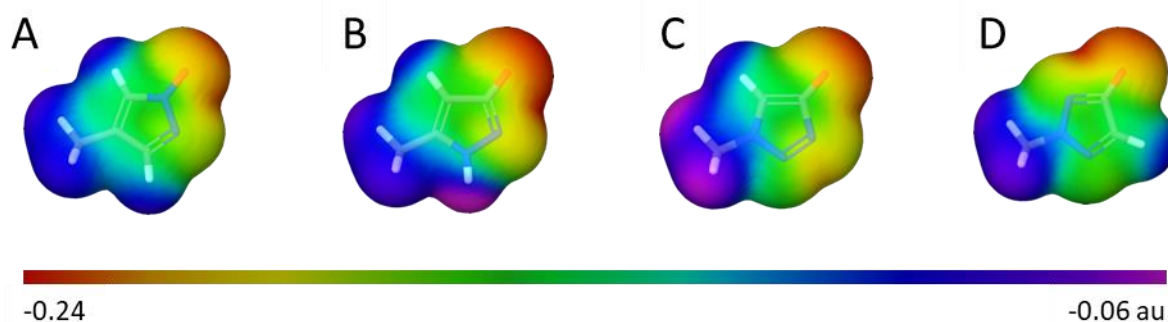


Figure 2.11 Electrostatic potential maps on the surface of the molecular electron density for the anionic form of the heterocyclic carboxylic acid bioisosteres of (A) 4-PHP, (B) Aza-4-PIOL, (C) **2.4a** and (D) **2.5a**. Calculations were carried out with Jaguar using the cc-PVDZS basis set and the B3LYP hybrid potential. au, atomic units.

In general, introduction of aryl or arylalkyl substituents in the 5-position of **2.4a** and **2.5a** led to improved GABA_AR binding affinities (Table 2.8). The introduction of 2-naphtylmethyl in 5-position of **2.5a** (**2.5b**) led to an improvement of binding affinity greater than 30 fold. The corresponding *N*₁ regioisomer **2.4b** resulted in comparable binding affinity with **2.5b**, with an enhancement of 20 fold when compared to the non-substituted analogue **2.4a**. Moreover, derivative **2.4c**, which is substituted in 5-position with a 3,3-diphenylpropyl moiety, showed binding affinity in the same range of **2.4b**. On the other hand, introduction of 3,3-diphenylpropyl in the 5-position of **2.5a** led to impaired affinity for the GABA_ARs.

Table 2.8 Pharmacological data for reference compounds GABA, **2.50–2.52** (Figure 2.15) and compounds **2.4a–c**, **2.5a–c**.^a

R1c1c(O)nnc1N2CCCCN2

R2c1c(O)nn1N2CCCCN2

Compound	R ₁	R ₂	[³ H] Muscimol K _i (μM) ^b
GABA			0.049 ^c
2.50			0.005 ^d
2.51			0.58 ^e
2.52			0.94 ^e
2.4a	H		55 [4.26±0.05]
2.4b	2-naphtylmethyl		2.4 [5.62±0.04]
2.4c	3,3-diphenylpropyl		1.6 [5.80±0.03]
2.5a		H	>100
2.5b		2-naphtylmethyl	3.3 [5.49±0.04]
2.5c		3,3-diphenylpropyl	>100

^aGABA_A receptor binding affinities at rat synaptic membranes. ^bIC₅₀ values were calculated from inhibition curves and converted to K_i values. Data is given as the mean [mean pK_i ± SEM] of three to five independent experiments. ^cData from Lolli *et al.*⁸³ ^dData from Krehan *et al.*⁹⁹ ^eData from Krall *et al.*⁸⁸

To further assess the obtained pharmacological data the binding modes of the synthesized compounds were evaluated using the reported homology model of the α₁β₂γ₂ GABA_AR in the antagonist bound state.⁵³ The obtained docking poses for the non-substituted ligands (**2.4a** and **2.5a**) were comparable with the binding mode previously reported. The amino moiety formed

salt bridge with β_2 Glu155 and hydrogen bonds with β_2 Ser156 and the backbone carbonyl of β_2 Tyr157. On the other hand, the 4-hydroxy-1,2,3-triazole moiety formed a bidentate interaction to α_1 Arg66 mimicking the binding interactions of GABA (Figure 2.12).

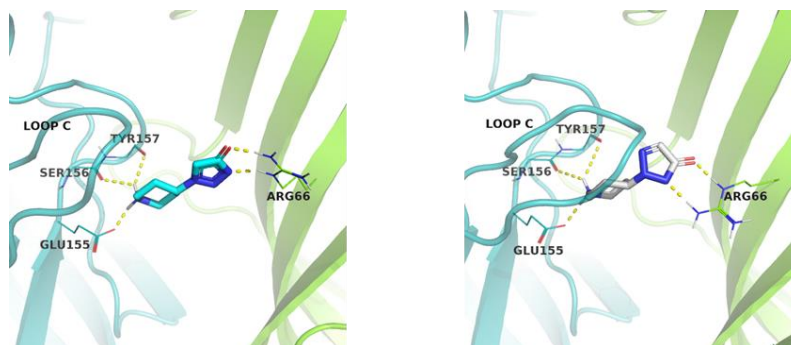


Figure 2.12 Predicted binding poses of **2.4a** (left) and **2.5a** (right) in the homology model of the $\alpha_1\beta_2\gamma_2$ GABA_AR in the antagonist bound state.⁵³

As previously reported for 4-PHP,^{65, 100} compound **2.4b** is able to bind in two different orientations maintaining the bidentate interaction described above (Figure 2.13). Therefore, the naphthylmethyl substituent could be accommodated in the cavity above the core scaffold (Figure 2.13, left), or in the cavity below by a 180° flip of the core scaffold (Figure 2.13, centre). On the other hand, the diphenylpropyl substituted analogue (i.e. **2.4c**) adopts a binding pose where the substituent is accommodated in the more spacious cavity below the core scaffold.



Figure 2.13 Predicted binding poses of **2.4b** (left and centre) and **2.4c** (right) in the homology model of the $\alpha_1\beta_2\gamma_2$ GABA_AR in the antagonist bound state.⁵³

The binding site optimized for **2.5a** (Figure 2.12) showed a marked difference in the conformation of α_1 Arg66, allowing the bidentate interaction with the 4-hydroxy-1,2,3-triazole. Analogously, **2.5b** is supposed to form a bidentate interaction with α_1 Arg66 and to accommodate the hydrophobic substituent into the previously reported cavity above the core scaffold (Figure 2.14). The more bulky diphenylpropyl substituted analogue, **2.5c**, is not able to interact with α_1 Arg66 in this conformation, probably due to limited space in the aforementioned cavity. Furthermore, the suggested 180° flip described for **2.4b** and **2.4c** is not optimal for this series of compounds.

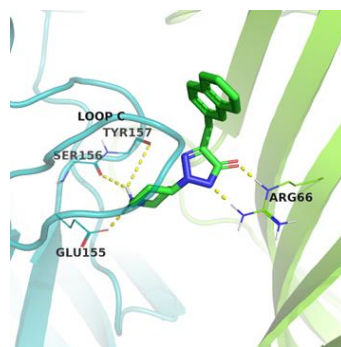


Figure 2.14 Predicted binding pose of **2.5b** in the homology model of the $\alpha_1\beta_2\gamma_2$ GABA_AR in the antagonist bound state.⁵³

The reported pharmacological results and molecular modelling analyses are coherent with previously reported SAR studies of 4-PIOL, 4-PHP and Aza-4-PIOL and with pharmacophore and homology models that hypothesised the accommodation of bulky substituents in cavities above or below the core scaffolds. However, the functional properties of this series were not evaluated and could be part of upcoming research projects.

The new analogues showed binding affinities comparable to aza-4-PIOL analogues (e.g. compounds **2.51** and **2.52**, Figure 2.15 and Table 2.8),⁸⁸ but lower than thio-4-PIOL analogues (e.g. compound **2.50**, Figure 2.15 and Table 2.8). As shown before, the difference in binding affinities between the latter compound and the synthesized analogues (**2.4b–c** and **2.5b–c**) does not seem to be related to protolytic properties. However, the electrostatic potential properties of the substituted hydroxytriazoles could explain the lower affinities for the GABA_ARs.

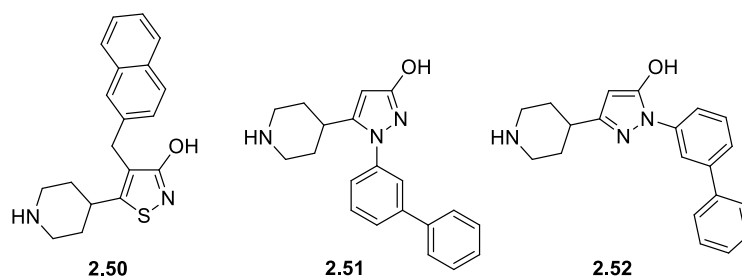


Figure 2.15 Substituted analogues of Thio-4-PIOL and Aza-4-PIOL compounds **2.50**, **2.51** and **2.52**.

2.3 Conclusions

In this study a bioisosteric replacement of 3-hydroxy-1,2,5-oxadiazole of **2.1** was evaluated using two different bioisosteres, the 3-hydroxy-1,2,5-thiadiazole and 4-hydroxy-1,2,3-triazole. Moreover, a bioisosteric replacement of 3-hydroxyisoxazole of 4-PIOL was performed using two regioisomers of 4-hydroxy-1,2,3-triazole. In addition, a preliminary SAR study was performed by introducing substituents in the 5-position of the new analogues **2.4a** and **2.5a**. The synthesis of the new compounds has been designed and successfully performed, and the pharmacological evaluation at native GABA_ARs using rat brain membranes has also been performed and reported. The monocyclic analogues **2.2** and **2.3** resulted in lower binding affinities for the GABA_ARs when compared to the lead compound **2.1**, meaning that the binding site is sensible to steric

hindrance in the explored position. Moreover, it was not possible to support the hypothesis of the bioactive conformation of compound **2.1** whereas it could also explain the residue activity of **2.2**. On the other hand, the synthesized analogues of 4-PIOL led to a new small series of compounds where the non-substituted **2.4a** was proved to bind the GABA_ARs. The introduction of bulky substituents in 5-position of **2.4a** and **2.5a** generally leads to enhance the binding affinities in accordance with previous studies. The bulky substituents are supposed to be accommodated in the cavities above or below the core scaffold by molecular modelling studies. The results of modelling studies also give possible explanation for the inactivity of compound **2.5c**. Lastly, the reported results proved the 4-hydroxy-1,2,3-triazole as suitable bioisostere in the GABA_AR area. Moreover, as already outlined in the chapter, the possible substitution on different nitrogen atoms of the hydroxytriazole ring facilitates the synthesis of different regioisomers with different properties. In this project, this strategy led to two different regioisomers (*N*₁ and *N*₂ substituted) which behave as two distinct bioisosteres.

2.4 Experimental section

Chemistry

Compounds **2.8**, **2.36** and **2.44** were prepared as described in the literature.^{85, 92, 93} All chemical reagents and solvents (analytical grade) were obtained from commercial sources (Sigma Aldrich, Alfa Aesar, or TCI) and used without further purification. Air- and/or moisture sensitive reactions were performed under a nitrogen atmosphere using syringe-septum techniques and dried glass-ware. Anhydrous solvents were dried over 4 Å molecular sieves or by distillation (i.e. THF) prior to use from Na and benzophenone under N₂. ⁱPrMgCl (in THF) was titrated using *sec*-BuOH and 1,10-phenanthroline as indicator.¹⁰¹ Thin layer chromatography (TLC) on silica gel was carried out using 5 × 20 cm plates with a silica layer of 0.25 mm in thickness. Purification of synthesized compounds were performed using flash column chromatography on silica gel (Merck Kieselgel 60, 230-400 mesh ASTM) or by CombiFlash Rf 200 apparatus (Teledyne Isco) with 5–200 mLmin⁻¹, 200 psi (with automatic injection valve) using RediSep Rf Silica columns (Teledyne Isco). Melting points (mp) were measured on a Büchi 540 apparatus in open capillary tubes and are uncorrected. Analytical high performance liquid chromatography (HPLC) analysis were performed on a Perkin Elmer Flexar UHPLC system equipped with an UHPLC Acquity BEH C₁₈ column (1.7 μm, 2.1 x 50 mm, Waters) and a 20 μL loop. Elution of analysed samples was performed using mixtures of eluent A (H₂O/TFA, 100/0.1) and eluent B (CH₃CN/TFA, 100/0.1) at a flow rate of 0.5 mLmin⁻¹. For HPLC control, data collection, and data handling Chromera Software ver. 4.1.0 was used. Alternatively, analytical HPLC analyses were performed on an Ultimate 3000 HPLC system with an Ultimate 3000 pump (Dionex,

Thermo Scientific), an Ultimate WPS-3000SL autosampler (Dionex, Thermo Scientific), an Ultimate Photodiode Array Detector (Dionex, Thermo Scientific) and 100 μL loop using a Gemini® NX-C₁₈ column (3 μm , 110 \AA , 4.6 \times 250 mm) and eluents A (H₂O/TFA, 100/0.1) and B (CH₃CN/H₂O/TFA, 90/10/0.1) at a flow rate of 1 mLmin⁻¹. For HPLC control, data collection, and data handling, Chromeleon Software ver. 6.80 was used. The purity of the analysed compounds is $\geq 95\%$, unless otherwise stated. The purity of compound **2.4c** was analysed using combustion analysis and calculated elementary analyses are within 0.4% of found values. Elementary analyses were performed by Mr. J. Theiner, Department of Physical Chemistry, University of Vienna, Austria. Preparative reversed phase HPLC was carried out on an Ultimate 3000 HPLC system (Dionex) with a multi-wavelength UV detector (200, 210, 225, and 254 nm) and 10 mL loop using a preparative RP Phenomenex Gemini NX-C₁₈ column (5 μm , 21.2 \times 250 mm) and eluents A (H₂O/TFA, 100/0.1) and B (CH₃CN/H₂O/TFA, 90/10/0.1) at a flow rate of 20 mLmin⁻¹. For HPLC control, data collection, and data handling, Chromeleon Software ver. 6.80 was used. ¹H and ¹³C NMR were recorded on either a Bruker Avance 300 MHz, a Jeol JNM-ECZR 600 MHz, or a Bruker Avance 600 MHz spectrometer equipped with a cryogenically cooled 5 mm CPDCH ¹³C[¹H] Z-GRD probe, at 300 K. Data are tabulated in the following order: chemical shift (δ) [multiplicity (b, broad; s, singlet; d, doublet; t, triplet; q, quartet; m, multiplet), coupling constant(s) *J* (Hz), number of protons]. The solvent residual peak or TMS were used as internal reference.¹⁰² Mass spectra were recorded on a Finnigan-Mat TSQ-700, 70 eV, direct inlet using chemical ionization (CI) or on a Micromass ZQ spectrometer (Waters) using electrospray ionization (ESI) in positive ion mode. HPLC-HRMS analyses were performed on a system comprised of an Agilent 1200 HPLC system comprising of a G1311B quaternary pump with a built-in degasser, a G1316A thermostated column compartment, a G1329B autosampler, and a G1315D photodiode array detector, coupled with a Bruker microOTOF-Q II mass spectrometer equipped with an electrospray ionization (ESI) source and operated via a 1:99 flow splitter. Mass spectra were acquired in positive ionization modes, using drying temperature of 200 °C, a capillary voltage of -4100 and +4000 V for positive and negative ion modes, respectively, nebulizer pressure of 2.0 bar, and drying gas flow of 7 Lmin⁻¹. A solution of sodium formate clusters was injected in the beginning of each run to enable internal mass calibration. Chromatographic separation was acquired on a Phenomenex Luna C₁₈(2) column (150 mm \times 4.6 mm, 3 μm , 100 \AA) maintained at 40 °C, using a flow rate of 0.5 mLmin⁻¹ and a linear gradient of the binary solvent system water-acetonitrile-formic acid (eluent A: 95/5/0.1, and eluent B: 5/95/0.1) rising from 0% to 100% of eluent B over 20 minutes. Data was acquired using Compass HyStar Ver. 3.2 (Bruker Daltonic GmbH, Germany) and processed using Compass DataAnalysis Ver. 4.0 (Bruker Daltonic GmbH, Germany).

Ethyl 4-(benzyloxy)-1-methyl-1H-1,2,3-triazole-5-carboxylate (2.9) and **ethyl 5-(benzyloxy)-2-methyl-2H-1,2,3-triazole-4-carboxylate (2.10)**.⁸⁵ To a solution of **2.8**⁸⁵ (5.5 g, 22.3 mmol) in CH₃CN (100 mL), K₂CO₃ (6.1 g, 44.5 mmol) and methyl iodide (1.4 mL, 22.3 mmol) were added. The resulting mixture was stirred at rt. When the reaction was complete, the mixture was concentrated under reduced pressure, the crude product was taken up with EtOAc (50 mL) and the resulting suspension washed with 1M HCl (30 mL), 1M NaOH (30 mL) and brine. The organic phase was dried over anhydrous Na₂SO₄ and evaporated *in vacuo* affording colourless oil. The mixture of the two regioisomers was separated using flash chromatography (petroleum ether 40–60 °C/EtOAc 90:10 v/v) affording **2.9** (first eluted, N₁ isomer) and **2.10** (second eluted, N₂ isomer) as white solids. **2.9** (1.7 g, 29%): mp 76–80 °C. ¹H NMR (300 MHz, (CD₃)₂CO): δ 7.54–7.32 (m, 5H), 5.48 (s, 2H), 4.34 (q, *J* = 7.2 Hz, 2H), 4.21 (s, 3H), 1.35 (t, *J* = 7.2 Hz, 3H). ¹³C NMR (75 MHz, (CD₃)₂CO): δ 161.6, 159.2, 137.8, 129.2, 129.2, 128.8, 128.4, 112.4, 71.9, 61.6, 39.1, 14.5. MS (CI) 262 [M+H]⁺. **2.10** (3.15 g, 54%): mp 52–56 °C. ¹H NMR (300 MHz, (CD₃)₂CO): δ 7.52–7.34 (m, 5H), 5.33 (s, 2H), 4.30 (q, *J* = 7.2 Hz, 2H), 4.09 (s, 3H), 1.32 (t, *J* = 7.2 Hz, 3H). ¹³C NMR (75 MHz, (CD₃)₂CO): δ 161.6, 160.6, 137.4, 129.2, 128.9, 128.5, 124.3, 72.7, 60.9, 42.9, 14.6. MS (CI) 262 [M+H]⁺.

(5-(Benzyloxy)-2-methyl-2H-1,2,3-triazol-4-yl)methanol (2.11).⁸⁵ LiAlH₄ (0.36 g, 9.6 mmol) was added to a cooled (0 °C) solution of compound **2.10**⁸⁵ (2.50 g, 9.6 mmol) in anhydrous THF (125 ml). The reaction mixture was stirred for 2 h at 0 °C before it was quenched with first water (0.37 mL) and then 15% w/w NaOH (0.37 mL) and water (0.37 mL). The volatiles were evaporated *in vacuo* and the residue was taken up in water. The resulting mixture was extracted with Et₂O (3 × 100 mL) and the combined organic phase was washed with brine (150 mL), dried over anhydrous Na₂SO₄, and evaporated *in vacuo* to afford compound **2.11** as colourless oil (1.82 g, 87%). ¹H NMR (300 MHz, DMSO-*d*₆): δ 7.50–7.28 (m, 5H), 5.22 (s, 2H), 5.05 (t, *J* = 5.5 Hz, 1H), 4.36 (d, *J* = 5.5 Hz, 2H), 3.95 (s, 3H). ¹³C NMR (75 MHz, DMSO-*d*₆): δ 157.4, 136.5, 131.8, 128.3, 128.0, 127.8, 71.4, 52.2, 41.3. HRMS (ESI-TOF): *m/z* calculated for C₁₁H₁₂N₃O [M+H]⁺, 202.0975. Found, 202.0974 (ΔM=0.3 ppm).

4-(Benzyloxy)-5-(bromomethyl)-2-methyl-2H-1,2,3-triazole (2.12).⁸⁵ PPh₃ (1.58 g, 6.0 mmol) was added to a stirred solution of **2.11**⁸⁵ (1.10 g, 5.0 mmol) in anhydrous CH₂Cl₂ (30 mL) at –10 °C. To the resulting mixture, NBS (1.07 g, 6.03 mmol) was added in small portions over 30 min. The reaction mixture was stirred for 1 h at –10 °C before the solvent was evaporated *in vacuo*. Purification of the resulting residue by flash chromatography (CH₂Cl₂) afforded compound **2.12** as colourless oil (1.13 g, 81%), which was used immediately upon purification in the synthesis of compound **2.13** due to stability issues of **2.12**. ¹H NMR (300 MHz, CDCl₃): δ 7.43–7.22 (m,

5H), 5.18 (s, 2H), 4.38 (s, 2H), 3.93 (s, 3H). ^{13}C NMR (75 MHz, CDCl_3): δ 158.0, 136.2, 128.7, 128.6, 128.4, 128.0, 72.2, 42.0, 20.4. MS (CI) 282, 284 $[\text{M}+\text{H}]^+$.

2-(5-(Benzyloxy)-2-methyl-2H-1,2,3-triazol-4-yl)acetonitrile (2.13). A solution of **2.12**⁸⁵ (1.13 g, 4.0 mmol) in EtOH (20 mL) was added dropwise to a solution of NaCN (0.39 g, 8.0 mmol) in EtOH/water (9:1 v/v, 25 mL). The reaction mixture was stirred for 48 h at rt before the volatiles were evaporated *in vacuo*. The resulting residue was taken up in water and extracted with EtOAc (3 \times 100 mL). The combined organic phase was washed with water (1 \times 100 mL), brine (1 \times 100 mL), dried over anhydrous Na_2SO_4 , and evaporated *in vacuo*. Purification by flash chromatography (petroleum ether 40–60 °C/EtOAc, gradient 0%–20% EtOAc) afforded **2.13** as colourless oil (0.63 g, 69%). ^1H NMR (300 MHz, $\text{DMSO}-d_6$): δ 7.50–7.30 (m, 5H), 5.24 (s, 2H), 4.05–3.90 (m, 5H). ^{13}C NMR (75 MHz, $\text{DMSO}-d_6$): δ 156.8, 136.1, 128.3, 128.1, 127.8, 121.8, 117.0, 71.7, 41.7, 12.3. HRMS (ESI-TOF): m/z calculated for $\text{C}_{12}\text{H}_{13}\text{N}_4\text{O}$ $[\text{M}+\text{H}]^+$, 229.1084. Found, 229.1085 ($\Delta\text{M}=0.5$ ppm).

Benzyl (2-(5-(benzyloxy)-2-methyl-2H-1,2,3-triazol-4-yl)ethyl)carbamate (2.14). Benzyl chloroformate (0.65 mL, 4.6 mmol) and $\text{NiCl}_2\cdot 6\text{H}_2\text{O}$ (54 mg, 0.23 mmol) were added to a stirred solution of **2.13** (0.52 g, 2.3 mmol) in MeOH (20 mL) at 0 °C. NaBH_4 (0.69 g, 18 mmol) was then added in small portions over 1 h while keeping the temperature at 0 °C, whereupon the reaction mixture was allowed to reach rt and stirred for 24 h before water was added (300 mL). The resulting mixture was extracted with CH_2Cl_2 (6 \times 100 mL) and the combined organic phase was washed with brine (200 mL), dried over anhydrous Na_2SO_4 , and evaporated *in vacuo*. Purification by column chromatography (petroleum ether 40–60 °C/EtOAc, gradient 0%–70% EtOAc) afforded **2.14** (0.28 g, 35%) as white solid: mp 44–46 °C. ^1H NMR (300 MHz, $\text{DMSO}-d_6$): δ 7.51–7.23 (m, 10H), 5.19 (s, 2H), 4.99 (s, 2H), 3.92 (s, 3H), 3.21 (q, $J = 6.9$ Hz, 2H), 2.64 (t, $J = 7.5$ Hz, 2H). ^{13}C NMR (75 MHz, $\text{DMSO}-d_6$): δ 157.4, 155.9, 137.1, 136.5, 128.9, 128.3, 128.2, 127.9, 127.7, 127.65, 127.6, 71.4, 65.1, 41.2, 39.2, 23.8. HRMS (ESI-TOF): m/z calculated for $\text{C}_{20}\text{H}_{23}\text{N}_4\text{O}_3$ $[\text{M}+\text{H}]^+$, 367.1765. Found, 367.1760 ($\Delta\text{M}=1.3$ ppm).

5-(2-Aminoethyl)-2-methyl-2H-1,2,3-triazol-4-ol hydrochloride (2.3). A solution of **2.14** (0.18 g, 0.50 mmol) in MeOH/2M HCl (1:4 v/v, 25 mL) was refluxed for 72 hours. The resulting solution was washed with EtOAc (3 \times 15 mL) and evaporated *in vacuo*. Recrystallization from i -PrOH/Et₂O afforded **2.3** (40 mg, 45%) as white solid: mp 191–192 °C. ^1H NMR (300 MHz, D_2O): δ 3.94 (s, 3H), 3.29 (t, $J = 7.0$ Hz, 2H), 2.96 (t, $J = 7.0$ Hz, 2H). ^{13}C NMR (75 MHz, D_2O , int. std. MeOH): δ 156.1, 128.2, 41.5, 38.8, 21.7. HRMS (ESI-TOF): m/z calculated for $\text{C}_5\text{H}_{11}\text{N}_4\text{O}$ $[\text{M}+\text{H}]^+$, 143.0927. Found, 143.0927 ($\Delta\text{M}=0.5$ ppm).

***tert*-Butyl 4-bromopiperidine-1-carboxylate (2.15).** Triethylamine (2.3 mL, 16.3 mmol) and di-*tert*-butyl dicarbonate (1.9 g, 8.6 mmol) were added to a stirred suspension of 4-bromopiperidine hydrobromide (2.0 g, 8.2 mmol) in THF (40 mL). The reaction mixture was stirred for 48 h at rt. The suspension was filtered and the filter was washed with THF. The combined filtrate was evaporated *in vacuo*. Purification by flash chromatography (petroleum ether 40–60 °C/EtOAc 95:5 *v/v*) afforded **2.15** (2.11 g, 98%) as colourless oil. ¹H NMR (600 MHz, DMSO-*d*₆): δ 4.53 (tt, *J* = 8.2, 3.8 Hz, 1H), 3.62–3.50 (m, 2H), 3.19 (ddd, *J* = 13.2, 8.6, 3.4 Hz, 2H), 2.06 (ddt, *J* = 13.6, 6.9, 3.7 Hz, 2H), 1.76 (dtd, *J* = 12.6, 8.3, 3.8 Hz, 2H), 1.39 (s, 9H). ¹³C NMR (150 MHz, DMSO-*d*₆) δ 153.8, 78.9, 50.9, 42.2, 35.5, 28.0. HRMS (ESI-TOF): *m/z* calculated for C₆H₁₁NO₂Br [M+⁺C₄H₈+H]⁺, 207.9968. Found, 207.9968 (ΔM=0.1 ppm).

***tert*-Butyl 4-(4-(benzyloxy)-5-(ethoxycarbonyl)-1*H*-1,2,3-triazol-1-yl)piperidine-1-carboxylate (2.16)** and ***tert*-butyl 4-(4-(benzyloxy)-5-(ethoxycarbonyl)-2*H*-1,2,3-triazol-2-yl)piperidine-1-carboxylate (2.17).** To a solution of **2.8**⁸⁵ (0.20 g, 0.81 mmol) in CH₃CN (10 mL), K₂CO₃ (0.22 g, 1.6 mmol) and *tert*-butyl 4-bromopiperidine-1-carboxylate (**2.15**, 0.21 g, 0.81 mmol) were added. The resulting mixture was stirred at 80 °C for 48 h. The reaction mixture was cooled at rt and the solvent was evaporated *in vacuo*. The resulting residue was taken up in water (50 mL) and extracted with EtOAc (3 × 25 mL). The combined organic phase was washed with brine (25 mL), dried over anhydrous Na₂SO₄, and evaporated *in vacuo*. Purification by flash chromatography (petroleum ether 40–60 °C/EtOAc, 70:30 *v/v*) afforded **2.16** (first eluting, *N*₁ isomer) and **2.17** (second eluting, *N*₂ isomer) as amorphous solids. The assignment was accomplished by the eluting order which is always consistent for (4-(benzyloxy)-5-(ethoxycarbonyl)-1*H*-1,2,3-triazoles. **2.16** (37 mg, 11%). ¹H NMR (300 MHz, DMSO-*d*₆): δ 7.54–7.29 (m, 5H), 5.45 (s, 2H), 5.15 (tt, *J* = 11.1, 3.6 Hz, 1H), 4.30 (q, *J* = 7.1 Hz, 2H), 4.16–3.96 (m, 2H), 3.08–2.78 (m, 2H), 2.12–1.99 (m, 2H), 1.87 (qd, *J* = 12.2, 3.9 Hz, 2H), 1.42 (s, 9H), 1.29 (q, *J* = 7.1 Hz, 3H). **2.17** (0.12 g, 33%). ¹H NMR (300 MHz, DMSO-*d*₆): δ 7.54–7.31 (m, 5H), 5.31 (s, 2H), 4.65 (tt, *J* = 10.9, 4.0 Hz, 1H), 4.26 (q, *J* = 7.1 Hz, 2H), 4.06–3.88 (m, 2H), 3.10–2.87 (m, 2H), 2.15–2.01 (m, 2H), 1.79 (qd, *J* = 12.2, 4.3 Hz, 2H), 1.41 (s, 9H), 1.26 (q, *J* = 7.1 Hz, 3H).

5-(Benzyloxy)-2*H*-1,2,3-triazole-4-carboxylic acid (2.20). 6M NaOH (14.2 mL, 85.0 mmol) was added to a solution of **2.8**⁸⁵ (3.5 g, 14.2 mmol) in EtOH (100 mL). The reaction mixture was heated at 50 °C for 24 h. Upon cooling to rt, the reaction mixture was neutralized with 6M HCl and the solvents were evaporated. The residue was taken in up in water and 1M HCl was added until pH 1. The resulting suspension was filtered and the solid was washed with hexane to give **2.20** (3.1 g, quant.) as white solid: mp 172 °C dec. ¹H NMR (600 MHz, DMSO-*d*₆): δ 14.05 (br

s, 1H), 7.54–7.27 (m, 5H), 5.32 (s, 2H). ¹³C NMR (75 MHz, DMSO-*d*₆): δ 161.2, 159.8, 136.5, 128.4, 128.1, 128.0, 121.6, 71.5. HRMS (ESI-TOF): *m/z* calculated for C₁₀H₁₀N₃O₃ [M+H]⁺, 220.0717. Found, 220.0712 (ΔM=2.3 ppm).

4-(Benzyloxy)-2H-1,2,3-triazole (2.21). **2.20** (3.5 g, 16.0 mmol) was dissolved in anhydrous DMF (50 mL) and the resulting solution heated at 130 °C for 6 h. Upon cooling to rt, water (500 mL) was added and the mixture was extracted with Et₂O (5 × 100 mL). The combined organic phase was washed with water (2 × 100 mL), brine (2 × 100 mL), dried over anhydrous Na₂SO₄, and evaporated *in vacuo*. Purification by flash chromatography (CH₂Cl₂/EtOAc, 95:5 *v/v*) afforded **2.21** (2.25 g, 70%) as white solid: mp 100–102 °C. ¹H NMR (600 MHz, DMSO-*d*₆): δ 14.1 (br s, 1H), 7.29–7.49 (m, 6H), 5.19 (s, 2H). ¹³C NMR (75 MHz, DMSO-*d*₆): δ 160.5, 136.6, 128.4, 128.1, 128.0, 118.7, 71.4. HRMS (ESI-TOF): *m/z* calculated for C₉H₁₀N₃O [M+H]⁺, 176.0818. Found, 176.0812 (ΔM=3.6 ppm).

tert-Butyl 4-(4-(benzyloxy)-1H-1,2,3-triazol-1-yl)piperidine-1-carboxylate (2.22) and **tert-butyl 4-(4-(benzyloxy)-2H-1,2,3-triazol-2-yl)piperidine-1-carboxylate (2.23).** K₂CO₃ (1.7 g, 12.6 mmol) was added to a solution of **2.21** (1.1 g, 6.3 mmol) in CH₃CN (35 mL). The reaction mixture was heated at reflux and *tert*-butyl 4-bromopiperidine-1-carboxylate (**2.15**, 2.2 g, 8.2 mmol) was added in portions over 48 h. The reaction mixture was cooled at rt and the solvent was evaporated *in vacuo*. The resulting residue was taken up in water (200 mL) and extracted with EtOAc (3 × 100 mL). The combined organic phase was washed with brine (50 mL), dried over anhydrous Na₂SO₄, and evaporated *in vacuo*. Purification by flash chromatography (petroleum ether 40–60 °C/EtOAc, gradient 10%–40% EtOAc) afforded **2.23** (first eluting, *N*₂ isomer) and **2.22** (second eluting, *N*₁ isomer) as white solids. **2.23** (1.36 g, 60%): mp 87–88 °C. ¹H NMR (300 MHz, DMSO-*d*₆): δ 7.48–7.30 (m, 6H), 5.17 (s, 2H), 4.52 (tt, *J* = 10.8, 4.0 Hz, 1H), 3.94 (d, *J* = 13.3 Hz, 2H), 3.08–2.86 (m, 2H), 2.09–1.96 (m, 2H), 1.78 (qd, *J* = 4.3, 11.6 Hz, 2H), 1.41 (s, 9H). ¹³C NMR (75 MHz, DMSO-*d*₆): δ 160.1, 153.9, 136.3, 128.4, 128.2, 128.1, 118.6, 78.9, 71.5, 60.6, 41.8, 31.0, 28.0. HRMS (ESI-TOF): *m/z* calculated for C₁₉H₂₆N₄O₃Na [M+Na]⁺, 381.1897. Found, 381.1895 (ΔM=0.6 ppm). **2.22** (0.21 g, 10%): mp 106–107 °C. ¹H NMR (300 MHz, DMSO-*d*₆): δ 7.85 (s, 1H), 7.49–7.29 (m, 5H), 5.15 (s, 2H), 4.59 (tt, *J* = 11.3, 3.8 Hz, 1H), 4.03 (d, *J* = 12.9 Hz, 2H), 3.05–2.80 (m, 2H), 2.08–1.96 (m, 2H), 1.79 (qd, *J* = 12.2, 4.3 Hz, 2H), 1.41 (s, 9H). ¹³C NMR (75 MHz, DMSO-*d*₆): δ 160.1, 153.7, 136.5, 128.4, 128.1, 128.0, 105.6, 78.9, 71.5, 57.7, 42.1, 31.7, 28.1. HRMS (ESI-TOF): *m/z* calculated for C₁₉H₂₇N₄O₃ [M+H]⁺, 359.2078. Found, 359.2068 (ΔM=2.7 ppm).

1-(Piperidine-4-yl)-1H-1,2,3-triazol-4-ol hydrochloride (2.4a). **2.22** (0.17 g, 0.47 mmol) was suspended in 6M HCl (10 mL) and the suspension heated at reflux for 48 h. Upon cooling to rt,

the reaction mixture was washed with EtOAc (2 × 10 mL) and the aqueous phase evaporated *in vacuo*. Recrystallization from EtOH/Et₂O afforded **2.4a** (20 mg, 21%) as white crystals: mp 243 °C dec. ¹H NMR (300 MHz, D₂O): δ 7.36 (s, 1H), 4.73 (m, 1H), 3.57 (dt, *J* = 6.9, 3.2 Hz, 2H), 3.22 (td, *J* = 13.2, 3.2 Hz, 2H), 2.49–2.36 (m, 2H), 2.34–2.16 (m, 2H). ¹³C NMR (75 MHz, D₂O): δ 157.5, 107.8, 56.3, 42.9, 28.3. HRMS (ESI-TOF): *m/z* calculated for C₇H₁₃N₄O [M+H]⁺, 169.1084. Found, 169.1085 (Δ*M*=0.9 ppm).

2-(Piperidine-4-yl)-2*H*-1,2,3-triazol-4-ol hydrochloride (2.5a). **2.23** (0.25 g, 0.70 mmol) was suspended in 6M HCl (10 mL) and the suspension was heated at reflux for 48 h. Upon cooling to rt, the reaction mixture was washed with EtOAc (2 × 10 mL) and the aqueous phase evaporated *in vacuo*. Recrystallization from EtOH/Et₂O afforded **2.5a** (90 mg, 63%) as white crystals: mp 259–263 °C. ¹H NMR (300 MHz, D₂O): δ 7.17 (s, 1H), 4.65 (tt, *J* = 10.3, 4.3 Hz, 1H), 3.52 (dt, *J* = 13.3, 3.9 Hz, 2H), 3.28–3.13 (m, 2H), 2.42–2.14 (m, 4H). ¹³C NMR (75 MHz, D₂O): δ 158.4, 120.1, 58.1, 42.7, 27.9. HRMS (ESI-TOF): *m/z* calculated for C₇H₁₃N₄O [M+H]⁺, 169.1084. Found, 169.1083 (Δ*M*=0.6 ppm).

Ethyl 4-bromopiperidine-1-carboxylate (2.24). K₂CO₃ (30.0 g, 0.22 mol) and ethyl chloroformate (20.7 mL, 0.22 mol) were added to a stirred suspension of 4-bromopiperidine hydrobromide (10.6 g, 0.043 mol) in THF (150 mL) at 40 °C. After 48 h at this temperature, the solvent was removed *in vacuo* and the residue taken in water (200 mL) and extracted with CH₂Cl₂ (3 × 75 mL). The combined organic phase was washed with 0.5M HCl (50 mL), brine (100 mL), dried over anhydrous Na₂SO₄, and evaporated *in vacuo*. Purification by flash chromatography (petroleum ether 40–60 °C/EtOAc 90:10 *v/v*) afforded **2.24** (9.7 g, 95%) as colourless oil. ¹H NMR (600 MHz, DMSO-*d*₆): δ 4.55 (tt, *J* = 8.0, 3.7 Hz, 1H), 4.03 (q, *J* = 7.1 Hz, 2H), 3.62–3.55 (m, 2H), 3.31–3.20 (m, 2H), 2.12–2.04 (m, 2H), 1.79 (dtd, *J* = 13.7, 8.3, 3.8 Hz, 2H), 1.17 (t, *J* = 7.2 Hz, 3H). ¹³C NMR (150 MHz, DMSO-*d*₆) δ 154.5, 60.8, 50.9, 42.1, 35.4, 14.6. HRMS (ESI-TOF): *m/z* calculated for C₈H₁₅NO₂Br [M+H]⁺, 236.0281. Found, 236.0277 (Δ*M*=1.6 ppm).

Ethyl 4-(4-(benzyloxy)-1*H*-1,2,3-triazol-1-yl)piperidine-1-carboxylate (2.25) and **ethyl 4-(4-(benzyloxy)-2*H*-1,2,3-triazol-2-yl)piperidine-1-carboxylate (2.26).** Cs₂CO₃ (17.3 g, 53 mmol) was added to a solution of **2.21** (4.6 g, 26.5 mmol) in anhydrous 1,4-dioxane (100 mL). The reaction mixture was heated at reflux and ethyl 4-bromopiperidine-1-carboxylate (**2.24**, 18.8 g, 80 mmol) was added in small portions over 72 h. The reaction mixture was cooled to rt, neutralized by adding 1M HCl, and the volatiles were removed *in vacuo*. The resulting residue was taken up in water (100 mL) and extracted with EtOAc (3 × 100 mL). The combined organic phase was washed with brine (50 mL), dried over anhydrous Na₂SO₄, and evaporated *in vacuo*.

Purification by flash chromatography (petroleum ether 40–60 °C/EtOAc, gradient 15%–40% EtOAc) afforded **2.26** (first eluting, N_2 isomer) and **2.25** (second eluting, N_1 isomer) as colourless oil and white solid, respectively. **2.26** (3.45 g, 39%): ^1H NMR (300 MHz, $\text{DMSO-}d_6$): δ 7.50–7.30 (m, 6H), 5.17 (s, 2H), 4.54 (tt, $J = 10.7, 4.0$ Hz, 1H), 4.05 (q, $J = 7.1$ Hz, 2H), 4.03–3.89 (m, 2H), 3.18–2.90 (m, 2H), 2.05 (dd, $J = 12.8, 3.0$ Hz, 2H), 1.79 (ddd, $J = 15.9, 12.1, 4.3$ Hz, 2H), 1.19 (t, $J = 7.1$ Hz, 3H). ^{13}C NMR (75 MHz, $\text{DMSO-}d_6$) δ 160.1, 154.6, 136.3, 128.4, 128.2, 128.1, 118.6, 71.5, 60.8, 60.4, 41.9, 31.0, 14.6. HRMS (ESI-TOF): m/z calculated for $\text{C}_{17}\text{H}_{23}\text{N}_4\text{O}_3$ $[\text{M}+\text{H}]^+$, 331.1765. Found, 331.1760 ($\Delta\text{M}=1.5$ ppm). **2.25** (3.6 g, 41%): mp 98–100 °C. ^1H NMR (600 MHz, $\text{DMSO-}d_6$): δ 7.85 (s, 1H), 7.48–7.31 (m, 5H), 5.15 (s, 2H), 4.62 (tt, $J = 11.3, 4.0$ Hz, 1H), 4.14–4.01 (m, 4H), 3.09–2.89 (m, 2H), 2.06–1.99 (m, 2H), 1.82 (qd, $J = 12.3, 4.4$ Hz, 2H), 1.19 (t, $J = 7.1$ Hz, 3H). ^{13}C NMR (150 MHz, $\text{DMSO-}d_6$) δ 160.1, 154.5, 136.5, 128.4, 128.1, 128.0, 105.6, 71.5, 60.9, 57.6, 42.2, 31.6, 14.6. HRMS (ESI-TOF): m/z calculated for $\text{C}_{17}\text{H}_{23}\text{N}_4\text{O}_3$ $[\text{M}+\text{H}]^+$, 331.1765. Found, 331.1761 ($\Delta\text{M}=1.0$ ppm).

Ethyl 4-(4-(benzyloxy)-5-iodo-1H-1,2,3-triazol-1-yl)piperidine-1-carboxylate (2.27). A solution of ICl (0.14 g, 0.88 mmol) in AcOH (4 mL) were added to a solution of **2.25** (0.22 g, 0.68 mmol) in AcOH (6 mL). Water (14 mL) was added and the resulting mixture was heated at 80 °C for 24 h. A solution of sodium thiosulfate 15-20% w/w was added and the reaction mixture was concentrated *in vacuo*. Water (50 mL) was added and the mixture was extracted with Et_2O (3×50 mL). The combined organic phase was washed with brine (50 mL), dried over anhydrous Na_2SO_4 , and evaporated *in vacuo*. Purification by flash chromatography (petroleum ether 40–60 °C/EtOAc, gradient 0%–30% EtOAc) afforded **2.27** as white solid (0.19 g, 60%): mp 103–107 °C. ^1H NMR (600 MHz, $\text{DMSO-}d_6$): δ 7.48–7.31 (m, 5H), 5.31 (s, 2H), 4.54 (tt, $J = 11.4, 4.1$ Hz, 1H), 4.14–4.07 (m, 2H), 4.06 (q, $J = 7.1$ Hz, 2H), 3.15–2.94 (m, 2H), 2.04–1.96 (m, 2H), 1.89 (qd, $J = 12.1, 4.4$ Hz, 2H), 1.19 (t, $J = 7.1$ Hz, 3H). ^{13}C NMR (150 MHz, $\text{DMSO-}d_6$) δ 161.9, 154.6, 136.6, 128.5, 128.2, 128.1, 71.4, 65.0, 60.9, 57.9, 42.2, 31.1, 14.6. HRMS (ESI-TOF): m/z calculated for $\text{C}_{17}\text{H}_{21}\text{N}_4\text{O}_3\text{INa}$ $[\text{M}+\text{Na}]^+$, 479.0551. Found, 479.0556 ($\Delta\text{M}=1.2$ ppm).

Ethyl 4-(4-(benzyloxy)-5-iodo-2H-1,2,3-triazol-2-yl)piperidine-1-carboxylate (2.28). A solution of ICl (0.12 g, 0.73 mmol) in AcOH (2 mL) were added to a solution of **2.26** (0.20 g, 0.61 mmol) in AcOH (3 mL). Water (7 mL) was added and the resulting mixture was heated at 80 °C for 24 h. A solution of sodium thiosulfate 15-20% w/w was added and the reaction mixture was concentrated *in vacuo*. Water (50 mL) was added and the mixture was extracted with Et_2O (3×50 mL). The combined organic phase was washed with brine (50 mL), dried over anhydrous Na_2SO_4 , and evaporated *in vacuo*. Purification by flash chromatography (petroleum ether 40–60 °C/EtOAc, gradient 0%–25% EtOAc) afforded **2.28** as colourless oil (0.21 g, 76%). ^1H NMR

(300 MHz, DMSO- d_6): δ 7.54–7.28 (m, 5H), 5.23 (s, 2H), 4.67–4.50 (m, 1H), 4.05 (q, J = 7.1 Hz, 2H), 4.02–3.88 (m, 2H), 3.14–2.90 (m, 2H), 2.12–1.97 (m, 2H), 1.78 (qd, J = 12.2, 4.1 Hz, 2H), 1.19 (t, J = 7.1 Hz, 3H). ^{13}C NMR (75 MHz, DMSO- d_6) δ 161.3, 154.6, 136.0, 128.5, 128.3, 128.2, 77.2, 72.0, 61.3, 60.8, 41.8, 30.9, 14.6. HRMS (ESI-TOF): m/z calculated for $\text{C}_{17}\text{H}_{22}\text{N}_4\text{O}_3\text{I} [\text{M}+\text{H}]^+$, 457.0731. Found, 457.0732 (ΔM =0.3 ppm).

3,3-diphenylpropanal (2.33). 3,3-diphenylpropanol (2.5 g, 11.8 mmol) was dissolved in CH_2Cl_2 (50 mL) under a nitrogen atmosphere. The solution was cooled to 0 °C and Dess-Martin periodinane (5.2 g, 12.4 mmol) was added. The reaction mixture was stirred 1 h at 0 °C and then diluted with dichloromethane up to 100 mL. The organic phase was washed with 2M NaOH (2 \times 50 mL), water (50 mL), brine (50 mL), dried over anhydrous Na_2SO_4 , and evaporated *in vacuo*. Purification by flash chromatography (gradient petroleum ether 40–60 °C/EtOAc, gradient 0%–5% EtOAc) afforded **2.33** (1.6 g, 65%) as white amorphous solid. ^1H NMR (600 MHz, DMSO- d_6): δ 9.64 (s, 1H), 7.36–7.23 (m, 8H), 7.20–7.12 (m, 2H), 4.61 (t, J = 7.8 Hz, 1H), 3.24 (dd, J = 7.8, 1.9 Hz, 3H). ^{13}C NMR (150 MHz, DMSO- d_6) δ 202.1, 144.0, 128.5, 127.6, 126.3, 48.2, 44.2. MS (ESI) 233 $[\text{M}+\text{Na}]^+$.

Ethyl 4-(4-(benzyloxy)-5-(1-hydroxy-3,3-diphenylpropyl)-1H-1,2,3-triazol-1-yl)piperidine-1-carboxylate (2.29c). A 1.7M solution of $^i\text{PrMgCl}$ in THF (0.67 mL, 1.1 mmol) was added dropwise to a cooled (–10 °C) solution of **2.27** (0.48 g, 1.0 mmol) in anhydrous THF (7 mL). The resulting mixture was stirred at the same temperature for 2 h. A solution of 3,3-diphenylpropanal (**2.33**, 0.24 g, 1.1 mmol) in anhydrous THF (3 mL) was added and the mixture was allowed to reach rt. After 48 h, saturated aqueous NH_4Cl (7 mL) was added and the mixture stirred for 30 min before it was evaporated *in vacuo*. The residue was taken up in water (50 mL) and extracted with Et_2O (3 \times 50 mL). The combined organic phase was washed with brine (50 mL), dried over anhydrous Na_2SO_4 , and evaporated *in vacuo*. Purification by flash chromatography ($\text{CH}_2\text{Cl}_2/\text{EtOAc}$ 85:15 v/v) afforded **2.29c** (0.26 g, 46%) as white solid: mp 62–66 °C. ^1H NMR (600 MHz, DMSO- d_6): δ 7.38–7.31 (m, 5H), 7.29–7.21 (m, 8H), 7.20–7.14 (m, 2H), 5.62 (d, J = 5.3 Hz, 1H), 5.27 (s, 2H), 4.47 (dt, J = 8.2, 5.9 Hz, 1H), 4.38 (tt, J = 10.6, 4.6 Hz, 1H), 4.05 (q, J = 7.1 Hz, 2H), 4.01 (t, J = 8.0 Hz, 1H), 4.01–3.95 (m, 2H), 2.96–2.71 (m, 2H), 2.64–2.53 (m, 2H), 1.96–1.87 (m, 2H), 1.80–1.67 (m, 2H), 1.19 (t, J = 7.1 Hz, 3H). ^{13}C NMR (150 MHz, DMSO- d_6) δ 155.8, 154.5, 144.5, 144.1, 136.9, 128.5, 128.4, 128.2, 127.8, 127.7, 127.65, 127.6, 126.2, 126.1, 120.8, 71.1, 60.8, 60.3, 55.7, 47.0, 42.4, 42.3, 31.9, 31.3, 14.6. HRMS (ESI-TOF): m/z calculated for $\text{C}_{32}\text{H}_{37}\text{N}_4\text{O}_4 [\text{M}+\text{H}]^+$, 541.2809. Found, 541.2804 (ΔM =1.0 ppm).

Ethyl 4-(5-(3,3-diphenylpropyl)-4-hydroxy-1H-1,2,3-triazol-1-yl)piperidine-1-carboxylate (2.35c). Et₃SiH (0.3 mL, 1.8 mmol) and TFA (0.67 mL, 8.7 mmol) were added to a solution of **2.29c** (0.17 g, 0.31 mmol) in CH₂Cl₂ (6 mL). The reaction mixture was heated at 50 °C in a sealed tube for 48 h. After cooling, CH₂Cl₂ was added up to 50 mL and the resulting mixture washed with 2M NaOH (50 mL). The aqueous phase was extracted with CH₂Cl₂ (2 × 50 mL). The combined organic phase was washed with brine (50 mL), dried over anhydrous MgSO₄, and evaporated. The crude product was dissolved in MeOH (20 mL) and Pd/C (15 mg) added. The reaction mixture was stirred under a hydrogen atmosphere for 16 h. The reaction mixture was filtered through a PVDF filter (0.45 μm) and the volatiles were evaporated *in vacuo*. Purification by preparative HPLC (gradient 50%–70% solvent B over 10 min) afforded **2.35c** (0.11 g, 81%) as colourless oil. ¹H NMR (600 MHz, DMSO-*d*₆): δ 7.37–7.25 (m, 8H), 7.21–7.15 (m, 2H), 4.05 (q, *J* = 7.0 Hz, 2H), 4.05–3.98 (m, 2H), 3.95 (t, *J* = 7.8 Hz, 1H), 2.90–2.72 (m, 2H), 2.49–2.44 (m, 2H), 2.30–2.23 (m, 2H), 1.84–1.74 (m, 4H), 1.19 (t, *J* = 7.1 Hz, 3H). ¹³C NMR (150 MHz, DMSO-*d*₆) δ 155.4, 154.5, 144.5, 128.5, 127.6, 126.2, 117.0, 60.8, 54.6, 50.0, 42.4, 33.1, 31.5, 19.7, 14.6. HRMS (ESI-TOF): *m/z* calculated for C₂₅H₃₁N₄O₃ [M+H]⁺, 435.2391. Found, 435.2395 (ΔM=1.0 ppm).

Ethyl 4-(4-(benzyloxy)-5-(naphthalen-2-ylmethyl)-1H-1,2,3-triazol-1-yl)piperidine-1-carboxylate (2.31b). A solution of ¹PrMgCl in THF (1.7M, 0.69 mL, 1.2 mmol) was added dropwise to a cooled solution (–10 °C) of **2.27** (0.50 g, 1.1 mmol) in anhydrous THF (7 mL). The mixture was stirred 1 h before a solution of 2-naphthaldehyde (0.19 g, 1.2 mmol) in anhydrous THF (3 mL) was added. The resulting mixture was allowed to reach rt. After 48 h, saturated aqueous NH₄Cl (5 mL) was added and the mixture stirred for 30 min before it was evaporated *in vacuo*. The residue was taken up in water (50 mL) and extracted with Et₂O (3 × 50 mL). The combined organic phase was washed with brine (50 mL), dried over anhydrous Na₂SO₄, and evaporated *in vacuo*. Purification by flash chromatography (petroleum ether 40–60 °C/EtOAc, gradient 0%–40% EtOAc) afforded the alcohol intermediate **2.29b** (0.42 g, 80%). HRMS (ESI-TOF): *m/z* calculated for C₂₈H₃₁N₄O₄ [M+H]⁺, 487.2340. Found, 487.2338 (ΔM=0.4 ppm). **2.29b** (0.40 g, 0.83 mmol) was dissolved in CH₂Cl₂ (30 mL) and Et₃SiH (0.21 mL, 1.3 mmol) was added. The solution was cooled at 0 °C, TFA (1.8 mL, 23 mmol) was added and the resulting mixture was allowed to reach rt and stirred for 20 h. CH₂Cl₂ was added up to 50 mL and the resulting mixture was washed with 2M NaOH (50 mL). The aqueous phase was extracted with CH₂Cl₂ (2 × 50 mL) and the combined organic phase was washed with brine (50 mL), dried over anhydrous Na₂SO₄, and evaporated *in vacuo*. Purification by flash chromatography (petroleum ether 40–60 °C/EtOAc, gradient 10%–35% EtOAc) afforded **2.31b** (0.30 g, 77%) as colourless oil. ¹H NMR (600 MHz, DMSO-*d*₆): δ 7.90–7.78 (m, 3H), 7.66 (s,

1H), 7.52–7.45 (m, 2H), 7.37–7.25 (m, 6H), 5.31 (s, 2H), 4.58 (tt, $J = 11.5, 4.0$ Hz, 1H), 4.20 (s, 2H), 4.02 (q, $J = 7.1$ Hz, 2H), 4.00–3.89 (m, 2H), 2.97–2.77 (m, 2H), 1.81 (qd, $J = 12.3, 4.5$ Hz, 2H), 1.73–1.62 (m, 2H), 1.15 (t, $J = 7.1$ Hz, 3H). ^{13}C NMR (150 MHz, DMSO- d_6) δ 156.8, 154.5, 137.0, 135.1, 133.0, 131.8, 128.3, 127.9, 127.85, 127.6, 127.4, 126.7, 126.4, 126.2, 125.8, 118.3, 71.3, 60.8, 55.0, 42.3, 31.5, 26.7, 14.5. HRMS (ESI-TOF): m/z calculated for $\text{C}_{28}\text{H}_{31}\text{N}_4\text{O}_3$ $[\text{M}+\text{H}]^+$, 471.2391. Found, 471.2387 ($\Delta\text{M}=0.8$ ppm).

Ethyl 4-(4-(benzyloxy)-5-(naphthalen-2-ylmethyl)-2H-1,2,3-triazol-2-yl)piperidine-1-carboxylate (2.32b). A solution of $i\text{PrMgCl}$ in THF (1.7M, 1.4 mL, 2.4 mmol) was added dropwise to a cooled solution (-10 °C) of **2.28** (1.0 g, 2.2 mmol) in anhydrous THF (15 mL). The mixture was stirred 1 h before a solution of 2-naphthaldehyde (0.38 g, 2.4 mmol) in anhydrous THF (5 mL) was added. The resulting mixture was allowed to reach rt. After 48 h, saturated aqueous NH_4Cl (10 mL) was added and the mixture stirred for 30 min before it was evaporated *in vacuo*. The residue was taken up in water (50 mL) and extracted with Et_2O (3×50 mL). The combined organic phase was washed with brine (50 mL), dried over anhydrous Na_2SO_4 , and evaporated *in vacuo*. Purification by flash chromatography (petroleum ether 40–60 °C/ EtOAc , gradient 0%–35% EtOAc) afforded the alcohol intermediate **2.30b** (0.64 g, 60%) as colourless oil. HRMS (ESI-TOF): m/z calculated for $\text{C}_{28}\text{H}_{30}\text{N}_4\text{O}_4\text{Na}$ $[\text{M}+\text{Na}]^+$, 509.2159. Found, 509.2167 ($\Delta\text{M}=1.5$ ppm). **2.30b** (0.62 g, 1.3 mmol) was dissolved in CH_2Cl_2 (45 mL) and Et_3SiH (0.33 mL, 2.0 mmol) was added. The solution was cooled at 0 °C, TFA (2.7 mL, 36 mmol) was added and the resulting mixture was allowed to reach rt and stirred for 20 h. CH_2Cl_2 was added up to 50 mL and the resulting mixture was washed with 2M NaOH (50 mL). The aqueous phase was extracted with CH_2Cl_2 (2×50 mL) and the combined organic phase was washed with brine (50 mL), dried over anhydrous Na_2SO_4 , and evaporated *in vacuo*. Purification by flash chromatography (petroleum ether 40–60 °C/ EtOAc , gradient 0%–20% EtOAc) afforded **2.32b** (0.30 g, 50%) as colourless oil. ^1H NMR (600 MHz, DMSO- d_6): δ 7.85 (d, $J = 7.7$ Hz, 1H), 7.83–7.78 (m, 2H), 7.69 (s, 1H), 7.51–7.43 (m, 2H), 7.37–7.26 (m, 6H), 5.19 (s, 2H), 4.49 (tt, $J = 10.9, 4.1$ Hz, 1H), 4.07–4.00 (m, 4H), 4.00–3.92 (m, 2H), 3.09–2.93 (m, 2H), 2.07–2.00 (m, 2H), 1.79 (qd, $J = 11.6, 4.4$ Hz, 2H), 1.18 (t, $J = 7.1$ Hz, 3H). ^{13}C NMR (150 MHz, DMSO- d_6) δ 157.0, 154.6, 136.5, 136.3, 133.0, 131.7, 130.5, 128.3, 128.0, 127.9, 127.8, 127.5, 127.4, 127.2, 126.4, 126.1, 125.5, 71.4, 60.8, 60.2, 41.9, 31.0, 29.5, 14.6. HRMS (ESI-TOF): m/z calculated for $\text{C}_{28}\text{H}_{31}\text{N}_4\text{O}_3$ $[\text{M}+\text{H}]^+$, 471.2391. Found, 471.2384 ($\Delta\text{M}=1.3$ ppm).

Ethyl 4-(4-(benzyloxy)-5-(3,3-diphenylpropyl)-2H-1,2,3-triazol-2-yl)piperidine-1-carboxylate (2.32c). A solution of $i\text{PrMgCl}$ in THF (1.7M, 1.4 mL, 2.5 mmol) was added dropwise to a cooled solution (-10 °C) of **2.28** (1.0 g, 2.2 mmol) in anhydrous THF (15 mL).

The mixture was stirred 1 h before a solution of 3,3-diphenylpropanal (**2.33**, 0.52 g, 2.5 mmol) in anhydrous THF (5 mL) was added. The resulting mixture was allowed to reach rt. After 48 h, saturated aqueous NH₄Cl (5 mL) was added and the mixture stirred for 30 min before it was evaporated *in vacuo*. The residue was taken up in water (50 mL) and extracted with Et₂O (3 × 50 mL). The combined organic phase was washed with brine (50 mL), dried over anhydrous Na₂SO₄, and evaporated *in vacuo*. Purification by flash chromatography (petroleum ether 40–60 °C/EtOAc, gradient 0%–35% EtOAc) afforded the alcohol intermediate **2.30c** (0.36 g, 30%) as colourless oil. ¹H NMR (600 MHz, DMSO-*d*₆): δ 7.41–7.30 (m, 5H), 7.30–7.20 (m, 8H), 7.18–7.11 (m, 2H), 5.24 (d, *J* = 5.2 Hz, 1H), 5.17 (s, 2H), 4.48 (tt, *J* = 10.7, 4.0 Hz, 1H), 4.32 (dt, *J* = 8.2, 5.6 Hz, 1H), 4.05 (q, *J* = 7.1 Hz, 2H), 4.03–4.00 (m, 1H), 3.99–3.92 (m, 2H), 3.11–2.95 (m, 2H), 2.56–2.43 (m, 2H), 2.06–2.00 (m, 2H), 1.83–1.74 (m, 2H), 1.19 (t, *J* = 7.1 Hz, 3H). ¹³C NMR (150 MHz, DMSO-*d*₆) δ 156.6, 154.6, 145.1, 144.3, 136.6, 134.2, 128.4, 128.36, 128.3, 128.2, 128.0, 127.9, 127.8, 127.6, 126.1, 126.0, 71.3, 61.7, 60.8, 60.2, 46.9, 41.9, 40.9, 30.9, 14.6. HRMS (ESI-TOF): *m/z* calculated for C₃₂H₃₆N₄O₄Na [M+Na]⁺, 563.2629. Found, 563.2618 (ΔM=1.8 ppm). **2.30c** (0.34 g, 0.62 mmol) was dissolved in CH₂Cl₂ (30 mL) and Et₃SiH (0.60 mL, 3.7 mmol) was added. The solution was cooled at 0 °C and TFA (1.3 mL, 17 mmol) was added and the resulting mixture was allowed to reach rt and stirred for 72 h. CH₂Cl₂ was added up to 50 mL and the resulting mixture was washed with 2M NaOH (50 mL). The aqueous phase was extracted with CH₂Cl₂ (2 × 50 mL) and the combined organic phase was washed with brine (50 mL), dried over anhydrous Na₂SO₄, and evaporated *in vacuo*. Purification by flash chromatography (petroleum ether 40–60 °C/EtOAc 85:15 *v/v*) afforded **2.32c** (0.25 g, 78%) as colourless oil. ¹H NMR (600 MHz, DMSO-*d*₆): δ 7.41–7.31 (m, 5H), 7.28–7.22 (m, 8H), 7.17–7.12 (m, 2H), 5.16 (s, 2H), 4.46 (tt, *J* = 10.8, 4.1 Hz, 1H), 4.05 (q, *J* = 7.1 Hz, 2H), 4.00–3.92 (m, 2H), 3.92 (t, *J* = 7.7 Hz, 1H), 3.10–2.94 (m, 2H), 2.41–2.37 (m, 2H), 2.32–2.27 (m, 2H), 2.04–1.99 (m, 2H), 1.77 (qd, *J* = 12.3, 4.3 Hz, 2H), 1.19 (t, *J* = 7.1 Hz, 3H). ¹³C NMR (150 MHz, DMSO-*d*₆) δ 156.9, 154.6, 144.7, 136.5, 131.1, 128.4, 128.37, 128.1, 128.0, 127.6, 126.1, 71.4, 60.8, 60.0, 49.9, 41.9, 33.4, 21.7, 14.6. HRMS (ESI-TOF): *m/z* calculated for C₃₂H₃₇N₄O₃ [M+H]⁺, 525.2860. Found, 525.2856 (ΔM=0.7 ppm).

5-(naphthalen-2-ylmethyl)-1-(piperidin-4-yl)-1*H*-1,2,3-triazol-4-ol hydrochloride (2.4b). A solution of **2.31b** (0.21 g, 0.46 mmol) in EtOH/35% HCl (1:2 *v/v*, 15 mL) was heated at reflux for 24 h. Upon cooling to rt, the solvents were evaporated *in vacuo*. Purification by preparative HPLC (gradient 20%–40% solvent B over 10 min) followed by conversion of the obtained product into the hydrochloric salt using 2M HCl afforded **2.4b** (73 mg, 46%) as pale yellow solid: mp 258–261 °C. ¹H NMR (600 MHz, DMSO-*d*₆): δ 9.34 (br s, 1H), 8.99 (br s, 1H), 7.90–7.81 (m, 3H), 7.71 (s, 1H), 7.51–7.44 (m, 2H), 7.37 (dd, *J* = 8.4, 1.7 Hz, 1H), 4.67 (tt, *J* = 10.9,

3.9 Hz, 1H), 4.19 (s, 2H), 3.31–3.25 (m, 2H), 3.03–2.94 (m, 2H), 2.21–2.11 (m, 2H), 1.85–1.77 (m, 2H). ¹³C NMR (150 MHz, DMSO-*d*₆) δ 155.8, 135.7, 133.0, 131.8, 128.3, 127.6, 127.4, 126.8, 126.3, 126.0, 125.7, 116.8, 52.3, 42.0, 28.4, 26.6. HRMS (ESI-TOF): *m/z* calculated for C₁₈H₂₁N₄O [M+H]⁺, 309.1710. Found, 309.1708 (ΔM=0.5 ppm).

5-(3,3-diphenylpropyl)-1-(piperidin-4-yl)-1*H*-1,2,3-triazol-4-ol hydrochloride (2.4c). A solution of **2.35c** (93 mg, 0.21 mmol) in EtOH/35% HCl (1:2 *v/v*, 15 mL) was heated at reflux for 24 h. Upon cooling to rt, the solvents were evaporated *in vacuo*. Recrystallization from MeOH/Et₂O afforded **2.4c** (43 mg, 51%) as white solid: mp 232–234 °C. ¹H NMR (600 MHz, DMSO-*d*₆): δ 9.82 (s, 1H), 9.16 (br s, 1H), 8.88 (br s, 1H), 7.37–7.24 (m, 8H), 7.23–7.13 (m, 2H), 4.28 (tt, *J* = 11.0, 4.0 Hz, 1H), 3.97 (t, *J* = 7.8 Hz, 1H), 3.40–3.37 (q, *J* = 7.0 Hz, 0.6H, (CH₃CH₂)₂O), 3.37–3.33 (m, 2H), 3.00–2.91 (m, 2H), 2.48–2.45 (m, 2H), 2.30–2.24 (m, 2H), 2.22–2.13 (m, 2H), 2.02–1.95 (m, 2H), 1.09 (t, *J* = 7.0 Hz, 0.9 H, (CH₃CH₂)₂O). ¹³C NMR (150 MHz, DMSO-*d*₆) δ 155.4, 144.5, 128.5, 127.6, 126.2, 117.2, 64.9, 51.9, 50.1, 42.1, 33.0, 28.4, 19.7, 15.1. HRMS (ESI-TOF): *m/z* calculated for C₂₂H₂₇N₄O [M+H]⁺, 363.2179. Found, 363.2179 (ΔM=0.2 ppm). Anal. calcd (C₂₂H₂₆N₄O·1.25HCl·0.1Et₂O): C, 64.76; H, 6.85; N, 13.49. Found: C, 65.14; H, 6.45; N 13.18.

5-(Naphthalen-2-ylmethyl)-2-(piperidin-4-yl)-2*H*-1,2,3-triazol-4-ol hydrochloride (2.5b). A solution of **2.32b** (0.23 g, 0.49 mmol) in EtOH/35% HCl (1:2 *v/v*, 15 mL) was heated at reflux for 24 h. Upon cooling to rt, the solvents were evaporated *in vacuo*. Purification by preparative HPLC (gradient 20%–50% solvent B over 15 min) followed by conversion of the obtained product into the hydrochloric salt using 2M HCl afforded **2.5b** (32 mg, 20%) as pale yellow solid: mp 200–203 °C. ¹H NMR (600 MHz, DMSO-*d*₆): δ 10.50 (s, 1H), 9.03 (br s, 2H), 7.87–7.79 (m, 3H), 7.68 (s, 1H), 7.50–7.42 (m, 2H), 7.39 (d, *J* = 8.4 Hz, 1H), 4.52 (tt, *J* = 9.8, 4.3 Hz, 1H), 4.01 (s, 2H), 3.33–3.24 (m, 2H), 3.09–2.99 (m, 2H), 2.21–2.06 (m, 4H). ¹³C NMR (150 MHz, DMSO-*d*₆) δ 156.1, 136.9, 133.0, 131.6, 130.5, 127.9, 127.5, 127.4, 127.2, 126.3, 126.1, 125.5, 57.3, 41.7, 29.3, 27.9. HRMS (ESI-TOF): *m/z* calculated for C₁₈H₂₁N₄O [M+H]⁺, 309.1710. Found, 309.1711 (ΔM=0.3 ppm).

5-(3,3-diphenylpropyl)-2-(piperidin-4-yl)-2*H*-1,2,3-triazol-4-ol hydrochloride (2.5c). A solution of **2.32c** (0.21 g, 0.38 mmol) in EtOH/35% HCl (1:2 *v/v*, 15 mL) was heated at reflux for 24 h. Upon cooling to rt, the solvents were evaporated *in vacuo*. Recrystallization from MeOH/Et₂O afforded **2.5c** (82 mg, 52%) as white solid: mp 246–249 °C. ¹H NMR (600 MHz, DMSO-*d*₆): δ 10.27 (s, 1H), 9.21 (s, 2H), 7.38–7.21 (m, 8H), 7.21–7.09 (m, 2H), 4.49 (tt, *J* = 10.0, 4.8 Hz, 1H), 3.96 (t, *J* = 7.5 Hz, 1H), 3.32–3.22 (m, 2H), 3.12–2.98 (m, 2H), 2.42–2.25 (m, 4H), 2.21–2.06 (m, 4H). ¹³C NMR (150 MHz, DMSO-*d*₆) δ 155.8, 144.8, 131.1, 128.4, 127.6,

126.0, 57.0, 50.1, 41.6, 33.5, 27.8, 21.8. HRMS (ESI-TOF): m/z calculated for $C_{22}H_{27}N_4O$ $[M+H]^+$, 363.2179. Found, 363.2182 ($\Delta M=0.8$ ppm).

4-(Benzyloxy)-1,2,5-thiadiazole-3-carbonitrile (2.37).⁸⁶ K_2CO_3 (5.2 g, 38 mmol) and benzyl bromide (3.8 mL, 32 mmol) were added to a solution of **2.36**⁹² (4.0 g, 32 mmol) in dry DMF (50 mL) and stirred at rt for 24 h. Water (500 mL) was added and the resulting mixture was extracted with EtOAc (4 \times 200 mL). The combined organic phase was washed with water (2 \times 100 mL) brine (2 \times 100 mL), dried over anhydrous Na_2SO_4 , and evaporated *in vacuo*. Purification by flash chromatography (petroleum ether 40–60 °C/EtOAc, 95:5 *v/v*) afforded **2.37** (4.4 g, 65%) as white solid: mp 43–44 °C. 1H NMR (300 MHz, $DMSO-d_6$): δ 7.63–7.38 (m, 5H), 5.52 (s, 2H). ^{13}C NMR (75 MHz, $DMSO-d_6$): δ 166.0, 134.8, 128.7, 128.6, 128.5, 121.6, 111.5, 73.0. MS (CI) 218 $[M+H]^+$.

4-(Benzyloxy)-1,2,5-thiadiazole-3-carboxylic acid (2.38).⁸⁶ 6M NaOH (3.7 mL, 22 mmol) was added to a solution of **2.37**⁸⁶ (1.6 g, 7.4 mmol) in EtOH (100 mL). The resulting mixture was stirred at 55 °C for 24 h. Upon cooling to rt, the reaction mixture was neutralized with 2M HCl and concentrated *in vacuo*. 2M HCl was added until pH 2 and the suspension was filtered affording **2.38** (1.6 g, 92%) as white solid: mp 154–155 °C. 1H NMR (300 MHz, $DMSO-d_6$): δ 13.73 (br. s, 1H), 7.58–7.28 (m, 5H), 5.48 (s, 2H). ^{13}C NMR (75 MHz, $DMSO-d_6$): δ 164.4, 159.9, 140.1, 135.7, 128.5, 128.3, 128.0, 72.1. MS (CI) 237 $[M+H]^+$.

Methyl 4-(benzyloxy)-1,2,5-thiadiazole-3-carboxylate (2.39). A 2M solution of oxalyl chloride in CH_2Cl_2 (3.6 mL, 0.72 mmol) and anhydrous DMF (60 μ L) were added to a cooled (0 °C) solution of **2.38** (0.5 g, 0.21 mmol) in anhydrous THF (30 mL) under a nitrogen atmosphere. After 2 h, MeOH (2 mL) was added at 0 °C, the reaction was allowed to reach rt and stirred 24 h. The volatiles were removed under reduced pressure. The product was taken up in water (100 mL) and extracted in EtOAc (3 \times 100 mL). The combined organic phase was washed with brine (100 mL), dried over anhydrous Na_2SO_4 , and evaporated *in vacuo*. Purification by flash chromatography (petroleum ether 40–60 °C/EtOAc, gradient 0%–5% EtOAc) afforded **2.39** (0.53 g, 100%) as amorphous yellow solid. 1H NMR (300 MHz, $DMSO-d_6$): δ 7.60–7.30 (m, 5H), 5.50 (s, 2H), 3.86 (s, 2H). ^{13}C NMR (75 MHz, $DMSO-d_6$): δ 164.5, 158.8, 138.4, 135.6, 128.5, 128.3, 127.9, 72.1, 52.6.

(4-(Benzyloxy)-1,2,5-thiadiazol-3-yl)methanol (2.40). $NaBH_4$ (0.38 g, 10 mmol) was added to a cooled (0 °C) solution of **2.39** (0.5 g, 2.0 mmol) in anhydrous THF (25 mL). After 48 h, water (200 mL) was added and the product extracted with CH_2Cl_2 (3 \times 75 mL). The combined organic phase was washed with brine (50 mL), dried over anhydrous Na_2SO_4 , and evaporated *in vacuo*.

Purification by flash chromatography (petroleum ether 40–60 °C/EtOAc, gradient 0%–40% EtOAc) afforded **2.40** (0.3 g, 67%) as pale yellow oil. ¹H NMR (300 MHz, DMSO-*d*₆): δ 7.56–7.32 (m, 5H), 5.48 (t, *J* = 5.9 Hz, 1H), 5.45 (s, 2H), 4.53 (d, *J* = 5.9 Hz, 2H). ¹³C NMR (75 MHz, DMSO-*d*₆): δ 162.3, 151.8, 135.9, 128.5, 128.3, 128.1, 71.6, 56.6.

3-(Benzyloxy)-4-(bromomethyl)-1,2,5-thiadiazole (2.41). PPh₃ (0.35 g, 1.3 mmol) was added to a stirred solution of **2.40** (0.25 g, 1.1 mmol) in anhydrous CH₂Cl₂ (10 mL) at –10 °C. To the resulting mixture, NBS (0.24 g, 1.3 mmol) was added in small portions over 30 min. The reaction mixture was stirred for 2 h at –10 °C before the solvent was evaporated *in vacuo*. Purification of the resulting residue by flash chromatography (petroleum ether 40–60 °C/EtOAc, 95:5 *v/v*) afforded compound **2.41** (0.24 g, 75%) as pale yellow oil. ¹H NMR (300 MHz, DMSO-*d*₆): δ 7.58–7.31 (m, 5H), 5.50 (s, 2H), 4.70 (s, 2H). ¹³C NMR (75 MHz, DMSO-*d*₆): δ 162.1, 146.7, 135.7, 128.5, 128.3, 127.9, 72.0, 23.0.

2-(4-(benzyloxy)-1,2,5-thiadiazol-3-yl)acetonitrile (2.42). A solution of **2.41** (0.19 g, 0.67 mmol) in EtOH (3 mL) was added dropwise to a solution of NaCN (0.39 g, 8.0 mmol) in EtOH/water (9:1 *v/v*, 8 mL). The reaction mixture was stirred for 48 h at rt before the volatiles were evaporated *in vacuo*. The resulting residue was taken up in water and extracted with EtOAc (3 × 100 mL). The combined organic phase was washed with water (1 × 50 mL), brine (1 × 50 mL), dried over anhydrous Na₂SO₄, and evaporated *in vacuo*. Purification by flash chromatography (petroleum ether 40–60 °C/EtOAc, gradient 0%–10% EtOAc) afforded **2.42** (65 mg, 42%) as pale brown amorphous solid. The product was difficult to purify with standard techniques and resulted unclear in all the attempts made. ¹H NMR (300 MHz, DMSO-*d*₆): δ 7.57–7.26 (m, 5H), 5.47 (s, 2H), 4.26 (s, 2H). ¹³C NMR (75 MHz, DMSO-*d*₆): δ 161.5, 141.9, 135.5, 128.4, 128.3, 128.0, 116.2, 72.0, 18.2.

4-(((Benzyloxy)carbonyl)amino)-2-((tert-butoxycarbonyl)amino)butanoic acid (2.45). A saturated solution of NaHCO₃ (50 mL) and di-*tert*-butyl dicarbonate (3.1 g, 14.3 mmol) were added to a stirred suspension of **2.44**⁹³ (2.0 g, 7.9 mmol) in 1,4-dioxane (50 mL). The reaction mixture was stirred for 24 h at rt. Water (100 mL) was added and the reaction mixture was washed with EtOAc (3 × 100 mL). The water phase was acidified to pH 1 with 2M HCl and extracted with EtOAc (3 × 100 mL). The combined organic phase was washed with brine (100 mL), dried over anhydrous Na₂SO₄, and evaporated *in vacuo* to afford **2.45** (2.7 g, 95%) as colourless sticky oil. ¹H NMR (300 MHz, DMSO-*d*₆): δ 12.48 (br. s., 1H), 7.38–7.24 (m, 6H), 7.11 (d, *J* = 8.2 Hz, 1H), 5.00 (s, 2H), 3.96–3.84 (m, 1H), 3.12–2.97 (m 2H), 1.91–1.60 (m, 2H), 1.38 (s, 9H). ¹³C NMR (75 MHz, DMSO-*d*₆): δ 174.1, 156.1, 155.6, 137.3, 128.4, 127.82,

127.78, 78.1, 66.2, 51.3, 37.5, 30.9, 28.3. HRMS (ESI-TOF): m/z calculated for $C_{17}H_{25}N_2O_6$ $[M+H]^+$, 353.1707. Found, 353.1699 ($\Delta M=2.4$ ppm).

Benzyl *tert*-butyl(4-amino-4-oxobutane-1,3-diyl)dicarbamate (2.46). Di-*tert*-butyl dicarbonate (1.6 g, 7.2 mmol), NH_4HCO_3 (2.8 g, 36 mmol), and pyridine (0.7 mmol) were added to a solution of **2.45** (2.5 g, 7.2 mmol) in acetonitrile (100 mL). The reaction mixture was stirred for 24 h at rt. The volatiles were removed under reduced pressure. The product was taken up in HCl 1M (100 mL) and extracted in EtOAc (3×100 mL). The combined organic phase was washed with brine (100 mL), dried over anhydrous Na_2SO_4 , and evaporated *in vacuo*. Purification by flash chromatography (petroleum ether 40–60 °C/EtOAc 20:80 *v/v*) afforded **2.46** (0.86 g, 34%) as white solid: mp 116–118 °C. 1H NMR (300 MHz, DMSO- d_6): δ 7.41–7.14 (m, 6H), 7.01 (s, 1H), 6.83 (d, $J = 8.2$ Hz, 1H), 5.01 (s, 2H), 3.93–3.80 (m, 1H), 3.10–2.95 (m, 2H), 1.86–1.51 (m, 2H), 1.38 (s, 9H). ^{13}C NMR (75 MHz, DMSO- d_6): δ 173.7, 155.9, 155.2, 137.1, 128.2, 127.7, 77.9, 65.1, 51.9, 37.4, 32.0, 28.1. HRMS (ESI-TOF): m/z calculated for $C_{17}H_{26}N_3O_5$ $[M+H]^+$, 352.1867. Found, 352.1859 ($\Delta M=2.3$ ppm).

Benzyl (3,4-diamino-4-oxobutyl)carbamate (2.47). **2.46** (0.66 g, 1.9 mmol) was dissolved in CH_2Cl_2 (30 mL) and trifluoroacetic acid (1.4 mL, 18.9 mmol) was added. The reaction mixture was stirred at rt for 12 h. The reaction mixture was diluted with dichloromethane (150 mL) and washed with 1M NaOH (2×20 mL). The organic phase was dried over anhydrous Na_2SO_4 , filtered, and evaporated *in vacuo* to afford **2.47** (0.47 g, 100%) as white solid: mp 123–127 °C (lit.⁹³ 112–114 °C). 1H NMR (300 MHz, DMSO- d_6): δ 7.40–7.27 (m, 5H), 7.23 (t, $J = 5.4$, 1H), 6.95 (s, 1H), 5.01 (s, 2H), 3.15–3.02 (m, 3H), 1.79–1.34 (m, 2H). ^{13}C NMR (DMSO- d_6): δ 177.1, 156.0, 137.1, 128.2, 127.7, 65.1, 52.5, 38.0, 35.1. HRMS (ESI-TOF): m/z calculated for $C_{12}H_{18}N_3O_3$ $[M+H]^+$, 252.1343. Found, 252.1339 ($\Delta M=1.5$ ppm).

Benzyl (2-(4-hydroxy-1,2,5-thiadiazol-3-yl)ethyl)carbamate (2.48). A solution of S_2Cl_2 (0.45 mL, 5.7 mmol) in anhydrous DMF (20 mL) was added dropwise to a solution of **2.47** (0.47 g, 1.9 mmol) in anhydrous DMF (10 mL). The reaction mixture was stirred for 12 hours at rt before poured into 200 mL of iced water. The mixture was filtered, the filtrate was acidified to pH 1 and extracted with Et_2O (4×100 mL). The combined organic phase was washed with brine (1×100 mL), dried over anhydrous Na_2SO_4 , and evaporated *in vacuo*. Purification by flash chromatography ($CH_2Cl_2/MeOH$ 95:5 *v/v*) afforded **2.48** (0.090 g, 17%) as white solid: mp 86–87 °C. 1H NMR (300 MHz, DMSO- d_6): δ 12.59 (br s, 1H), 7.42–7.26 (m, 5H), 4.99 (s, 2H), 3.37 (t, $J = 7.1$ Hz, 2H), 2.83 (t, $J = 7.1$ Hz, 2H). ^{13}C NMR (75 MHz, DMSO- d_6): δ 162.5, 155.9, 149.9, 137.1, 128.2, 127.6, 127.5, 65.0, 38.1, 29.0. HRMS (ESI-TOF): m/z calculated for $C_{12}H_{14}N_3O_3S$ $[M+H]^+$, 280.0750. Found, 280.0744 ($\Delta M=2.4$ ppm).

4-(2-Aminoethyl)-1,2,5-thiadiazol-3-ol hydrochloride (2.2). A solution of **2.48** (81 mg, 0.29 mmol) in MeOH/2M HCl (1:3, 16 mL) was refluxed for 72 h. The resulting solution was washed with EtOAc (3 × 10 mL) and evaporated *in vacuo*. Trituration of the resulting residue with $i\text{-Pr}_2\text{O}$ afforded **2.2** (34 mg, 64%) as white solid: mp 215–217 °C. ^1H NMR (600 MHz, D_2O): δ 3.49 (t, $J = 6.8$ Hz, 2H), 3.18 (t, $J = 6.8$ Hz, 2H). ^{13}C NMR (150 MHz, D_2O): δ 162.0, 148.1, 37.1, 26.1. HRMS (ESI-TOF): m/z calculated for $\text{C}_4\text{H}_8\text{N}_3\text{OS} [\text{M}+\text{H}]^+$, 146.0383. Found, 146.0385 ($\Delta M=1.8$ ppm).

Determination of ionization constants.

The ionization constants of compounds **2.2–2.5** were determined by potentiometric titration with the GLpKa apparatus (Sirius Analytical Instruments Ltd, Forest Row, East Sussex, UK). The pKa values were obtained as mean of four titrations: aqueous solutions (ionic strength adjusted to 0.15M with KCl) of the compound (20 mL, about 1 mM) were initially acidified to pH 1.8 with 0.5 N HCl and then titrated with standardized 0.5N KOH to pH 12.2 at constant temperature of $25(\pm 0.1)$ °C under argon atmosphere.

Pharmacology

Characterization in [^3H]muscimol binding affinity study: please refer to Petersen *et al.* for experimental details.⁵⁶ Alternatively please refer to manuscript in preparation in Supplementary Information.

3 Synthesis and pharmacological evaluation of novel amino bioisosteres for the GABA_ARs

3.1 Background and rationale

The bioisosteric replacement approach has been used extensively within the GABA_ARs area and most efforts have been directed to replace the acidic moiety of GABA.⁵⁶ On the other hand, besides many conformational restricted analogues (e.g. homo-β-proline **3.1**, isoguvacine etc.),^{76, 103} only few examples of bioisosteric replacement of the amino moiety of GABA are reported in literature, which include imidazole-4-acetic acid (IAA),^{59, 104} 2-(2-aminothiazol-4-yl)acetic acid (**3.2**),¹⁰⁵ 2-amino-1,4,5,6-tetrahydropyrimidine-5-carboxylic acid (**1.4**)⁶⁶ and 2-amino-3,4,5,6-tetrahydropyridine-5-carboxylic acid (**1.5**)⁶⁶ (Figure 3.1).

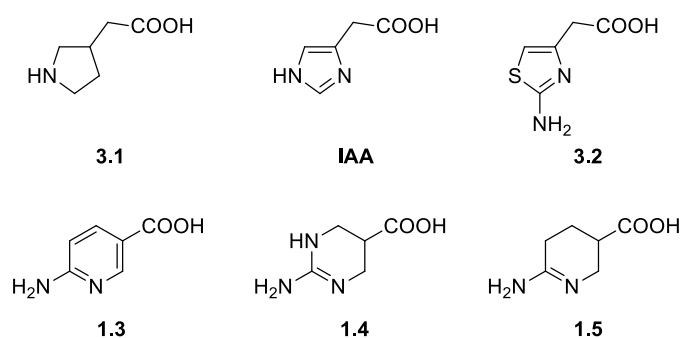


Figure 3.1 Structures of reference compounds homo-β-proline (**3.1**), IAA, 2-(2-aminothiazol-4-yl)acetic acid (**3.2**), 6-aminonicotinic acid (**1.3**), 2-amino-1,4,5,6-tetrahydropyrimidine-5-carboxylic acid (**1.4**) and 2-amino-3,4,5,6-tetrahydropyridine-5-carboxylic acid (**1.5**).

IAA is a natural metabolite of L-histidine and is reported as a partial GABA_AR agonist.⁵⁹ Compound **3.2** is structurally related to IAA and was shown to bind with low affinity to the GABA_ARs.¹⁰⁵ Compounds **1.4** and **1.5** are structurally related to 6-aminonicotinic acid (**1.3**) with markedly improved affinity for the GABA_ARs (Table 3.1).⁶⁶ Furthermore, compound **1.4** was shown to be a selective substrate for BGT1 among the other GABA transporters.¹⁵

Table 3.1 Pharmacological data of reference compounds GABA, IAA, **3.1–3.2** and **1.3–1.5**.^a

Compound	[³ H] Muscimol <i>K_i</i> (μM)
GABA	0.049 ^b
3.1	0.2 ^c
IAA	0.65 ^d
3.2	32
1.3	4.4 ^e
1.4	0.54 ^e
1.5	0.044 ^e

^aGABA_A receptor binding affinities at rat synaptic membranes. ^bData from Lolli *et al.*⁸³ ^cData from Nielsen *et al.*¹⁰³ ^dData from Madsen *et al.*⁵⁹ ^eData from Petersen *et al.*⁶⁶

IAA was pharmacologically characterized at GABA_ARs and GABA_CRs, displaying agonist effect with a non-selective profile at both receptors. Moreover, SAR study of IAA revealed that the introduction of small and big substituents in the 2- or 5- position was detrimental for the affinity to the native GABA_ARs.⁵⁹ The insertion of substituents in the α -position or changing the length and the position of the lateral side chain that bears the carboxylic acid moiety were also not tolerated, leading to ligands with impaired affinity (Figure 3.2 and Table 3.2).⁶⁷

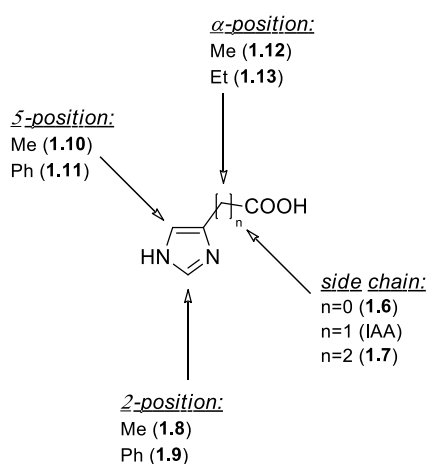
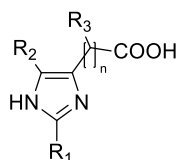


Figure 3.2 SAR of IAA: modulation of IAA (n=1) in the α -, 2- and 5- positions, and modulation of the length of the side chain.

However, 5-methyl IAA (**1.10**) was shown to be potent agonist at the homomeric ρ_1 GABA_ARs, whilst α -methyl IAA (**1.12**) was characterized as potent antagonist at the ρ_1 containing GABA_ARs in the FMP assay (Table 3.2). The two compounds were also shown devoid of activity at the $\alpha_1\beta_2\gamma_2\delta$ GABA_ARs meaning a selective profile for the ρ containing GABA_ARs.^{59, 67}

Table 3.2 Pharmacological data of reference compounds GABA, IAA and **1.6–1.13**.



Compound	R ₁	R ₂	R ₃	[CH ₂] _n	[³ H] Muscimol K _i (μM) ^a	$\alpha_1\beta_2\gamma_2\delta$ EC ₅₀ (μM) ^b	ρ_1 EC ₅₀ (μM) ^b	ρ_1 IC ₅₀ (μM) ^b
GABA					0.049 ^c	2.6 ^e	0.32 ^e	
IAA	H	H	H	1	0.65 ^d	24	4.6 ^e	
1.6	H	H	H	0	>100 ^e	ND	>300 ^e	
1.7	H	H	H	2	>100 ^e	ND	>300 ^e	
1.8	Me	H	H	1	>100 ^d	ND	>1000 ^d	
1.9	Ph	H	H	1	>100 ^d	ND	>1000 ^d	
1.10	H	Me	H	1	67 ^d	>1000 ^d	12 ^e	
1.11	H	Ph	H	1	>100 ^d	>1000 ^d	420 ^d	
1.12	H	H	Me	1	21 ^e	>1000 ^e		9.4 ^e
(+)-1.12	H	H	Me	1	13 ^e	>1000 ^e		4.7 ^e
1.13	H	H	Et	1	>100 ^e	ND		>300 ^e

^aGABA_A receptor binding affinities at rat synaptic membranes. ^bFunctional characterization at the human $\alpha_1\beta_2\gamma_2\delta$ and ρ_1 GABA_A receptors transiently expressed in tsA201 cells (or HEK293) using the FLIPR Membrane Potential Blue assay. ^cData from Lolli *et al.*⁸³ ^dData from Madsen *et al.*⁵⁹ ^eData from Krall *et al.*⁶⁷

The SAR study of IAA performed at the University of Copenhagen proves that successful bioisosteric replacement of the amino moiety of GABA not only leads to structural novel compounds, but can also lead to analogues with different pharmacological properties and, for the given example, to selective ligands.

In the present project, a bioisosteric replacement of the amino moiety of IAA was studied in order to expand the use of amino bioisosteres in the GABA_ARs area and to extend the SAR study of IAA analogues. The above mentioned SAR study was assumed as starting point for the design of novel structures. In particular, a variety of five membered partly saturated heterocycles was chosen to modulate chemical properties (e.g. ionization constants) and introduce chirality, aiming to explore more in detail the GABA_AR binding site. Among others, dihydroimidazole and 2-amino analogues of dihydrothiazole, dihydrooxazole, and dihydroimidazole were chosen as possible amino moieties for the synthesis of target compounds (Figure 3.3).

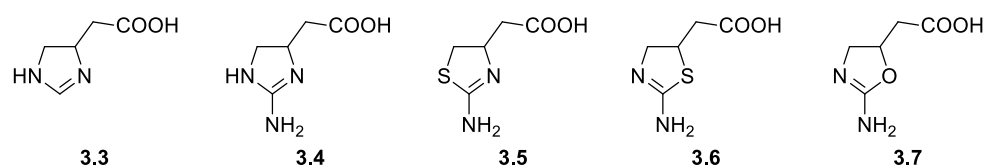


Figure 3.3 Target compounds 3.3–3.7.

A preliminary SAR study of **3.5** was performed by introducing a small substituent (i.e. methyl group) in the 4-, 5- and α -position (Figure 3.4). The methyl group was chosen as possible substituent among others because of previous experience. It is known that, especially for GABA_ARs agonists, the structural requirements imposed by the GABA_ARs to the ligands are strict and big substituents near the core scaffolds are usually not allowed.^{56, 59, 67} For these reasons, compounds **3.8**, **3.9** and **3.10** were included in the study as modulation of the compounds developed in the first series.

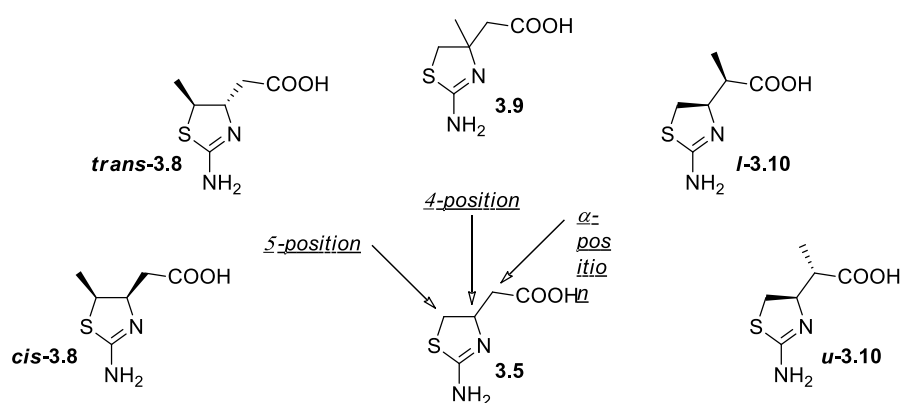


Figure 3.4 Preliminary SAR study of compound **3.5**. Relative configuration displayed for compounds **3.8** and **3.10**.

The synthesis and the pharmacological and physicochemical properties of these novel heterocycles are reported and discussed in this chapter. This study was designed to expand the use of novel amino bioisosteres in the GABA_ARs area, aiming to increase knowledge about

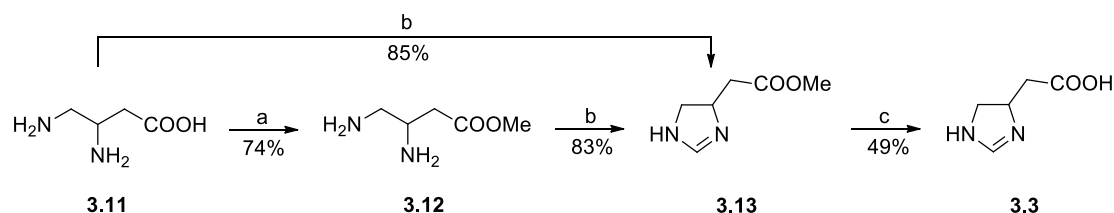
structural requirements of GABA_AR orthosteric binding site, modulate the pharmacodynamic properties of GABA analogues and develop novel GABA_ARs ligands towards functional subtype-selectivity.

3.2 Results and discussion

3.2.1 Chemistry

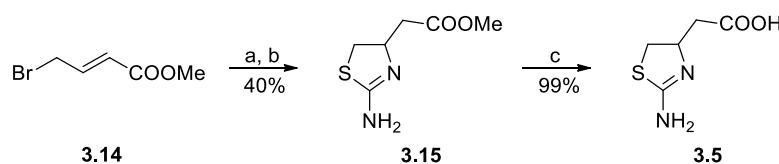
Compounds IAA, (*S*)-**3.1**, (*R*)-**3.1** and **3.2** were included in the study and obtained from commercial suppliers, while the remaining IAA analogues were synthesized as described in this section.

The synthesis of compound **3.3** was accomplished starting from commercially available 3,4-diaminobutanoic acid dihydrochloride (Scheme 3.1). The carboxylic acid of **3.11** was converted in the methyl ester **3.12** using thionyl chloride in methanol, followed by annulation reaction of the formed β,γ -diaminoester (**3.12**) into the imidazoline **3.13** using trimethyl orthoformate, according to previously reported procedures.^{106, 107} Alternatively, **3.13** was synthesized in one step from **3.11** using trimethyl orthoformate in methanol at reflux with higher overall yield. The consequent deprotection using diluted hydrochloric acid at 50 °C afforded the target compound **3.3**. In this respect, the formation of side products was observed with diluted hydrochloric acid at higher temperature or with basic conditions, probably due to decomposition of starting material.



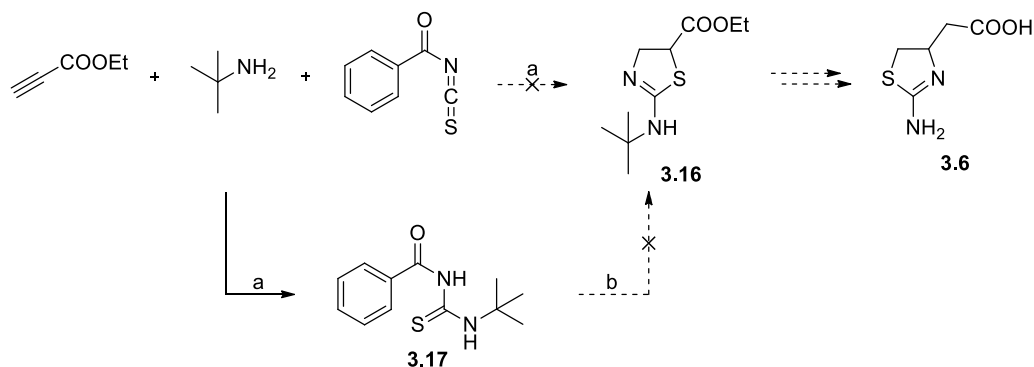
Scheme 3.1 Reagents and conditions: (a) SOCl₂, MeOH, rt, (b) HC(OMe)₃, MeOH, reflux, (c) 2M HCl, 50 °C.

Compound **3.5** was synthesized as outlined in Scheme 3.2. As previously reported by Campbell *et al.*, the 2-amino-4,5-dihydrothiazol-4-yl derivative **3.15** was obtained by a two-step synthesis: a first condensation between methyl 4-bromocrotonate (**3.14**) and thiourea in acetone followed by a cyclization reaction obtained by addition of sodium hydrogen carbonate.¹⁰⁸ In our experience, differently from the literature, the synthesis of **3.15** was not achieved in one-pot but only by adding sodium hydrogen carbonate after the formation of the isothiuronium intermediate. The subsequent deprotection of **3.15** under acidic conditions afforded **3.5**.



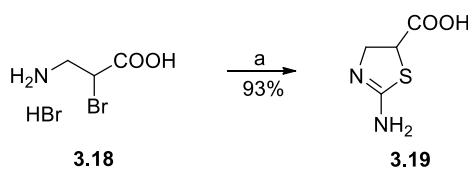
Scheme 3.2 Reagents and conditions: (a) thiourea, acetone, rt, (b) NaHCO₃, acetone, reflux, (c) 48% HBr, rt.

The synthesis of **3.6** was attempted using two different strategies as depicted in Scheme 3.3 and 3.5. Rostami-Charati *et al.* reported a convenient synthesis for compound **3.16**,¹⁰⁹ (Scheme 3.3) which could be used as starting material in our synthetic pathway consisting of a one carbon homologation of the lateral carboxylic moiety. However, in our experience the synthesis previously reported did not afford the expected product but only compound **3.17** which is an intermediate described by the authors.^{109, 110} The conversion was also tried at higher temperature or in two different steps, as well as in other solvents (i.e. dichloromethane), but not significant improvement was observed and the synthetic scheme was therefore abandoned.



Scheme 3.3 Reagents and conditions: (a) N-methylimidazole, H₂O, rt or 50 °C, (b) ethyl propiolate, N-methylimidazole, H₂O, rt.

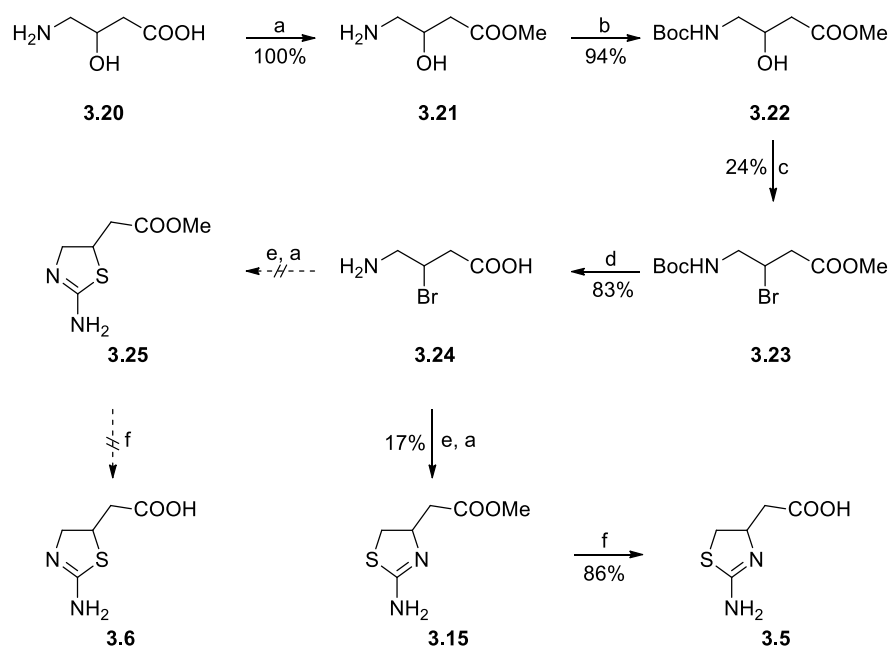
Golubev *et al.* reported the synthesis of **3.19** from 3-amino-2-bromopropanoic acid using potassium thiocyanate in water at pH 7 (Scheme 3.4).



Scheme 3.4 Reagents and conditions: (a) **3.18** as hydrobromic salt, KSCN, H₂O, NaH₂PO₄, pH 7, reflux.

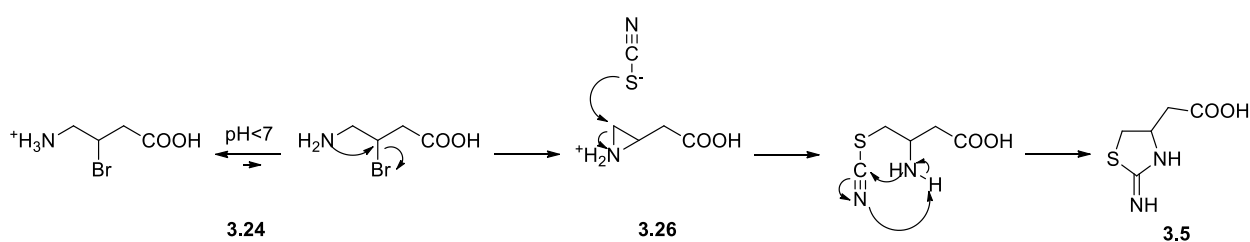
Analogously, the synthesis of the target compound **3.6** was tried from the key intermediate **3.24** (Scheme 3.5). Starting from 4-amino-3-hydroxybutanoic acid (**3.20**), the carboxylic and amino moieties were protected affording **3.22** in two steps.^{111, 112} The subsequent reaction of **3.22** with triphenylphosphine and *N*-bromosuccinimide in dichloromethane gave compound **3.23**, which was then deprotected using diluted hydrobromic acid yielding the key intermediate **3.24**. The following reaction between **3.24**, potassium thiocyanate and Na₂HPO₄ in water at pH 7 and subsequent protection of the carboxylic acid moiety to methyl ester afforded a product coherent with **3.25** in 8% yield (determined using NMR and MS analyses). The replacement of Na₂HPO₄ with NaH₂PO₄ (pH 4), one or two equivalents of NaHCO₃ (pH 5 and 7 respectively) and K₂CO₃ (pH 9) were attempted to improve the yield of this reaction. In particular, the use of one equivalent of NaHCO₃ (pH 5) seemed to be the best condition based on HPLC analysis and for this reason it was applied on large scale yielding **3.25** in 17% yield. Consequent deprotection in

acidic condition afforded compound **3.6**. However, the structure of the synthesized compound was proved to be equivalent to the isomer **3.5** (determined by x-ray analysis, see Figure 3.5) instead of **3.6** as previously stated (Scheme 3.5).



Scheme 3.5 Reagents and conditions: (a) SOCl_2 , dry MeOH, rt, (b) Boc_2O , NaHCO_3 , THF/ H_2O , rt, (c) PPh_3 , NBS, dry CH_2Cl_2 , 0 °C, (d) 2M HBr, 50 °C, (e) KSCN, NaHCO_3 , H_2O , 70 °C, (f) 2M HCl, 50 °C.

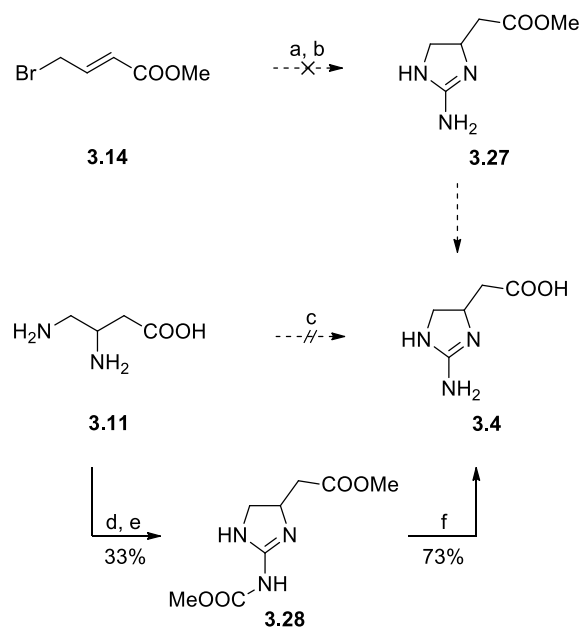
The formation of the side product **3.5** instead of the target compound **3.6** could be explained by the mechanism of reaction showed in Scheme 3.6. The aziridine **3.26** was postulated as possible intermediate which could lead to the formation of the side product. However, the mechanism of reaction has not been confirmed and, in interest of time, the synthesis of compound **3.6** was postponed and could be part of upcoming research projects.



Scheme 3.6 Proposed mechanism of reaction for the synthesis of **3.5** via aziridine.

Compound **3.4** was synthesized as described in Scheme 3.7. Methyl 4-bromocrotonate **3.14** was made reacted with guanidine in acetone using NaHCO_3 or K_2CO_3 as base, but the reaction did not allow the synthesis of **3.27** (conditions a and b, Scheme 3.7). The reaction between 3,4-diaminobutanoic acid (**3.11**) and cyanogen bromide (condition c, Scheme 3.7) should yield the desired product as previously reported for other analogues.^{113, 114} However, considering the toxicity of the reagent, the 2-aminoimidazoline moiety was obtained using the method previously reported by Weinhardt *et al.*¹¹⁵ that consist of annulation between vicinal diamino moiety of **3.11**

and thiopseudourea. Therefore, annulation of **3.11** and 1,3-bis(methoxycarbonyl)-2-methyl-2-thiopseudourea at 70 °C followed by protection of the carboxylic acid moiety as methyl ester gave **3.28** (conditions d and e, Scheme 3.7). The carboxylic acid moiety was protected to facilitate the purification of the intermediate by flash chromatography. Consequent deprotection of **3.28** by treatment with diluted hydrochloric acid at reflux afforded the target compound **3.4**.

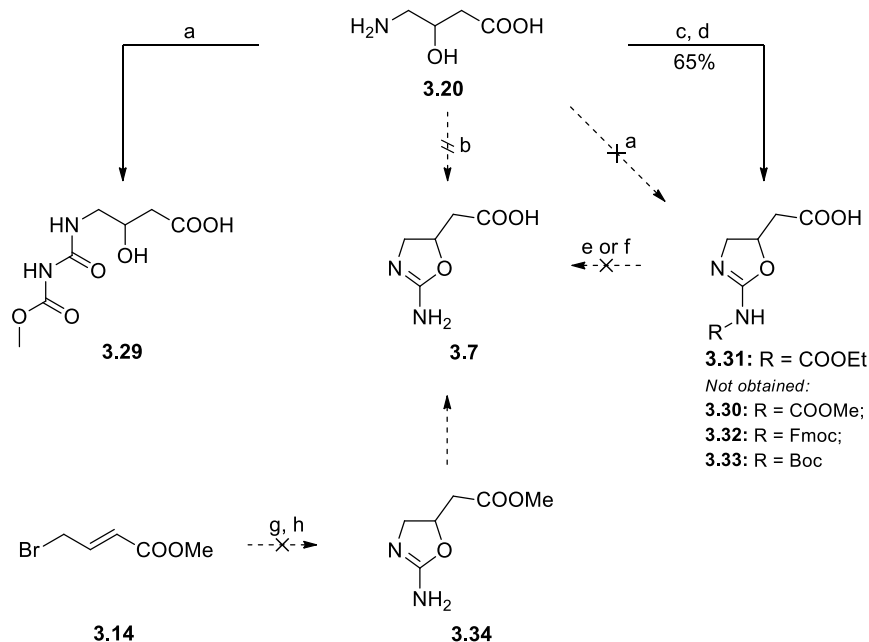


Scheme 3.7 Reagents and conditions: (a) guanidine hydrochloride, NaHCO₃, acetone, rt, (b) NaHCO₃ or K₂CO₃, acetone, reflux, (c) BrCN, MeOH, reflux, (d) CH₃O₂CN=C(SCH₃)NHCOC₂H₅, NaHCO₃, MeOH/H₂O, 70 °C, (e) SOCl₂, dry MeOH, rt. (f) 2M HCl, reflux.

The synthesis of the last target compound of the first series (**3.7**) was not accomplished even if several attempts were done (Scheme 3.8). The method employed for the synthesis of the 2-aminoimidazoline moiety of **3.4** (please refer to condition d, Scheme 3.7) was initially applied for the synthesis of the 2-aminooxazoline moiety. 4-Amino-3-hydroxybutanoic acid (**3.20**) was made reacted with 1,3-bis(methoxycarbonyl)-2-methyl-2-thiopseudourea at 70 °C in methanol/water (condition a, Scheme 3.8), but compound **3.29** was obtained instead of **3.30**.

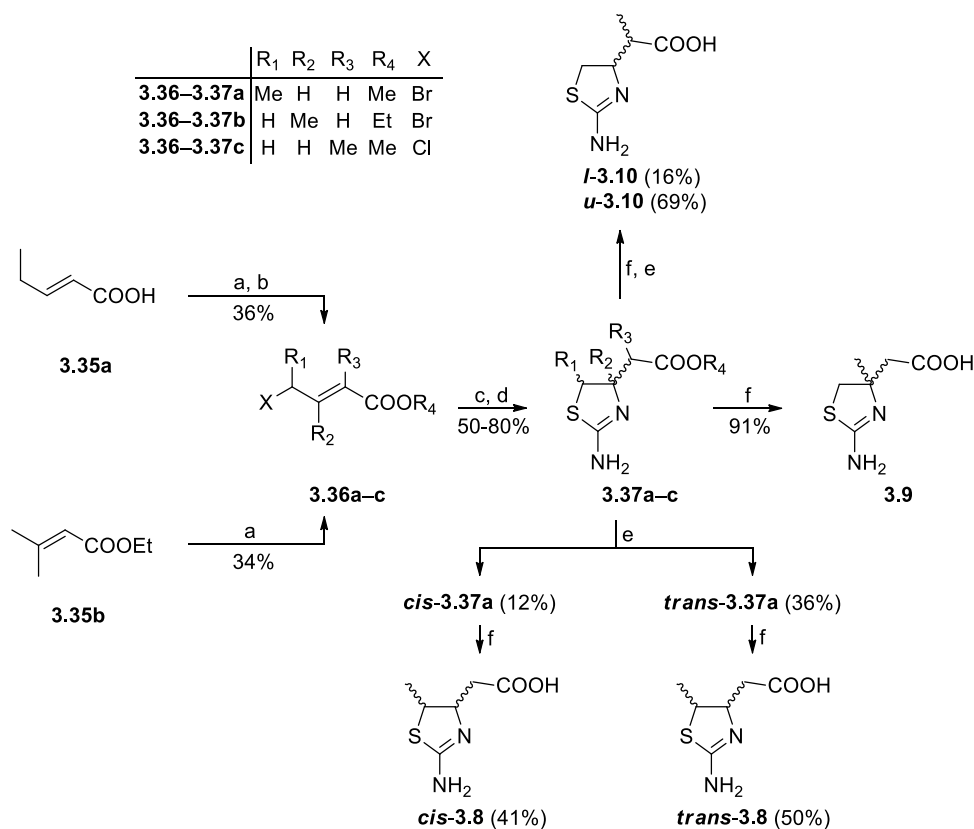
The preparation of 2-aminooxazoline ring is reported in literature using cyanogen bromide or alkyl- or alkoxy-carbonyl isothiocyanates.^{116, 117} At first, the reaction between **3.20** and cyanogen bromide (condition b, Scheme 3.8) was tried affording a mixture of polar products difficult to be purified. In contrast, **3.20** was then made reacted with ethoxycarbonyl isothiocyanate, followed by the addition of mercury (II) acetate to promote the cyclization affording **3.31** (conditions c and d, Scheme 3.8). The deprotection of **3.31** was attempted in both acidic and basic conditions, but these attempts resulted in decomposition of the starting material without yielding the target compound **3.7**. The use of other isothiocyanates may be suggested to synthesize analogues of **3.31** (e.g. **3.32** or **3.33**). These analogues could be subsequently deprotected using mild condition and avoiding aqueous reagents which might lead to ring opening.

Following a modified procedure previously reported for the synthesis of 2-aminothiazolidine moiety (please refer to Scheme 3.2),¹⁰⁸ methyl 4-bromocrotonate **3.14** was made reacted with urea in acetone using NaHCO₃ as base, but the reaction did not allow the synthesis of **3.34** (conditions g and h, Scheme 3.8). Moreover, the addition of sodium iodide to enhance the reactivity of **3.14** did not allow the formation of the product. In interest of time, the synthesis of compound **3.7** was postponed and could be part of upcoming research project.



Scheme 3.8 Reagents and conditions: (a) CH₃O₂CN=C(SCH₃)NHCO₂CH₃, NaHCO₃, MeOH/H₂O, 70 °C, (b) BrCN, dry MeOH, rt, (c) EtOCOCNS, dry THF, 40 °C, (d) Hg(OAc)₂, 40 °C, (e) 6M HCl, reflux, (f) NaOH, EtOH, reflux, (g) urea, acetone, rt, (h) NaHCO₃, acetone, reflux.

Compound **3.5** was chosen among the other compounds included in the first series for a preliminary SAR study because of the easy synthesis that allowed simple structural changes and because of high affinity of the ligand to the native GABA_ARs. Methyl or ethyl γ -halo- α,β -enoate (**3.36a–c**) were used as key starting materials for the synthesis of the compounds included in the second series (**3.8–3.10**, Scheme 3.9). **3.36c** was obtained from commercial suppliers, while **3.36a** and **3.36b** were synthesized as depicted in Scheme 3.9 and in accordance with previously reported procedures.^{118, 119} Using the method previously described for the synthesis of **3.5**, the reaction of alkyl γ -halo- α,β -enoate (**3.36a–c**) with thiourea in acetone and subsequent cyclization using sodium hydrogen carbonate in two steps gave **3.37a–c**. The diastereomeric mixture of **3.37a** was then resolved into the two pairs of enantiomers *cis*-**3.37a** and *trans*-**3.37a** by preparative HPLC. The configuration of the two isomers was determined by 2D NMR analysis (please refer to section 3.2.3). Deprotection under acidic conditions afforded compounds *cis*-**3.8**, *trans*-**3.8** and **3.9–3.10**. The diastereomeric mixture of compound **3.37c** was separated after deprotection using preparative HPLC obtaining *l*-**3.10** and *u*-**3.10**, and the configuration of the two isomers was determined by X-ray crystallography (section 3.2.2).

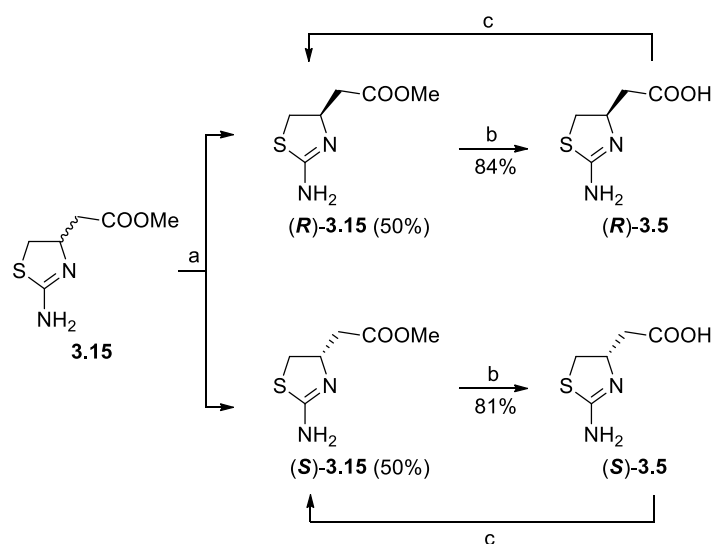


Scheme 3.9 Reagents and conditions: (a) NBS, AIBN, ClCH₂CH₂Cl, reflux, (b) H₂SO₄ cat, MeOH, rt, (c) thiourea, acetone, (d) NaHCO₃, acetone, reflux, (e) preparative HPLC: column RP Phenomenex Gemini NX-C18 column, (f) 2M HCl, 50 °C.

3.2.2 Stereochemistry

The importance of stereochemistry for the affinity of GABA_AR ligands is known and described in literature. For instance, (*R*)-**3.1** has higher binding affinity for GABA_ARs than the (*S*)-enantiomer.¹⁰³

Taking this information, it would be relevant to verify the importance of the stereochemistry for the new class of GABA_AR ligands reported in the chapter. For this reason, the compounds included in the first series (**3.3–3.5**, **3.13**, **3.15** and **3.28**) were screened using chiral HPLC columns in either normal or reversed phase (please refer to Table SI.1 in Supplementary Information). Although a large number of conditions and columns was screened, only one column was identified to resolve compound **3.15** in normal phase. Therefore, the enantiomers of compound **3.5** were obtained by separation of the methyl ester analogue (**3.15**) using preparative HPLC and a Chiralpak IF column, followed by acid catalysed hydrolysis (Scheme 3.10). Since it was not possible to directly determine the enantiomeric excess (ee) of compounds (*R*)-**3.5** and (*S*)-**3.5** using the available columns, the ee was indirectly determined by converting the compounds in the methyl esters (*R*)-**3.15** and (*S*)-**3.15** and then analysing them using Chiralpak IF column. Finally, X-ray crystallography was used to determine the absolute configuration of (*S*)-**3.5** (Figure 3.5) and the other enantiomer was consequently determined (please refer to Supplementary Information for the experimental details).



Scheme 3.10 Reagents and conditions: (a) preparative HPLC: column CHIRALPAK IF, mobile phase: heptane/EtOH (8:2 v/v) + 0.5% TFA, (b) 2M HCl, 50 °C, (c) SOCl₂, dry MeOH, rt.

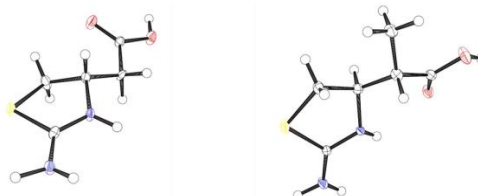
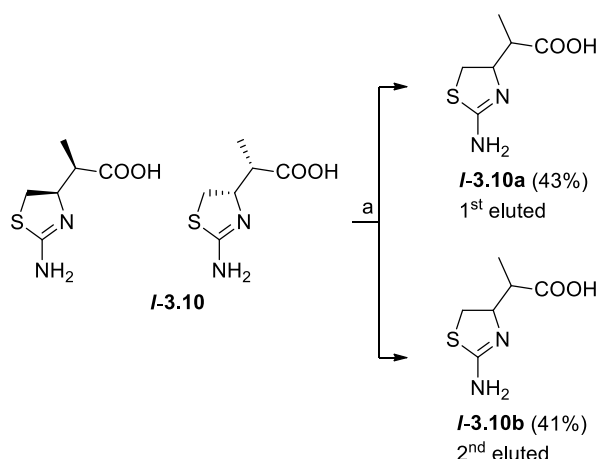


Figure 3.5 Crystal structures of compounds (*S*)-**3.5** (left) and *u*-**3.10** (right). Nitrogen atoms are depicted in blue, sulphur atoms in yellow and oxygen atoms in red. Please refer to Figures SI.1 and 2 in Supplementary Information for high resolution images.

The two diastereomers *u*-**3.10** and *l*-**3.10** have different pharmacological properties as described in section 3.2.4. For this reason, the structure of *u*-**3.10** was determined by X-ray crystallography (Figure 3.5) and the other pair of enantiomers (*l*-**3.10**) was consequently determined (please refer to Supplementary Information for the experimental details). Based on pharmacological results, the most interesting pair of enantiomers (*l*-**3.10**) was resolved using preparative HPLC and a Chirobiotic T column and the ee was determined for *l*-**3.10a** and *l*-**3.10b** by analytical HPLC (Scheme 3.11). The absolute configuration is still unknown and will be determined by X-ray crystallography.



Scheme 3.11 Reagents and conditions: (a) preparative HPLC: column CHIROBIOTIC T, mobile phase: H₂O/MeOH (9:1 v/v).

3.2.3 Characterization

As outlined in the chemistry section 3.2.1, a diastereoisomeric mixture of *cis*- and *trans*-**3.37a** was obtained and resolved using reversed phase preparative HPLC. The obtained two pairs of enantiomers were then deprotected affording *cis*-**3.8** and *trans*-**3.8**. The structural determination of the compounds is based on the analysis of these latter.

ROESY experiments were performed and key ROE correlations were identified as diagnostic signals and used to distinguish between *cis*- and *trans*- isomers of compound **3.8**. Even though the correlation between δCH_3 and γCH is present in either *cis*-**3.8** (red/pink, Figure 3.6) or *trans*-**3.8** (blue/green, Figure 3.6), the correlations between δCH_3 and αCH_2 and between βCH and γCH are characteristic of *cis*-**3.8**, as outlined Figure 3.7 (C and D). On the other hand, the analysis of *trans*-**3.8** showed characteristic correlations between δCH_3 and βCH , as well as between αCH_2 and γCH (Figure 3.6 and Figure 3.7 A, B).

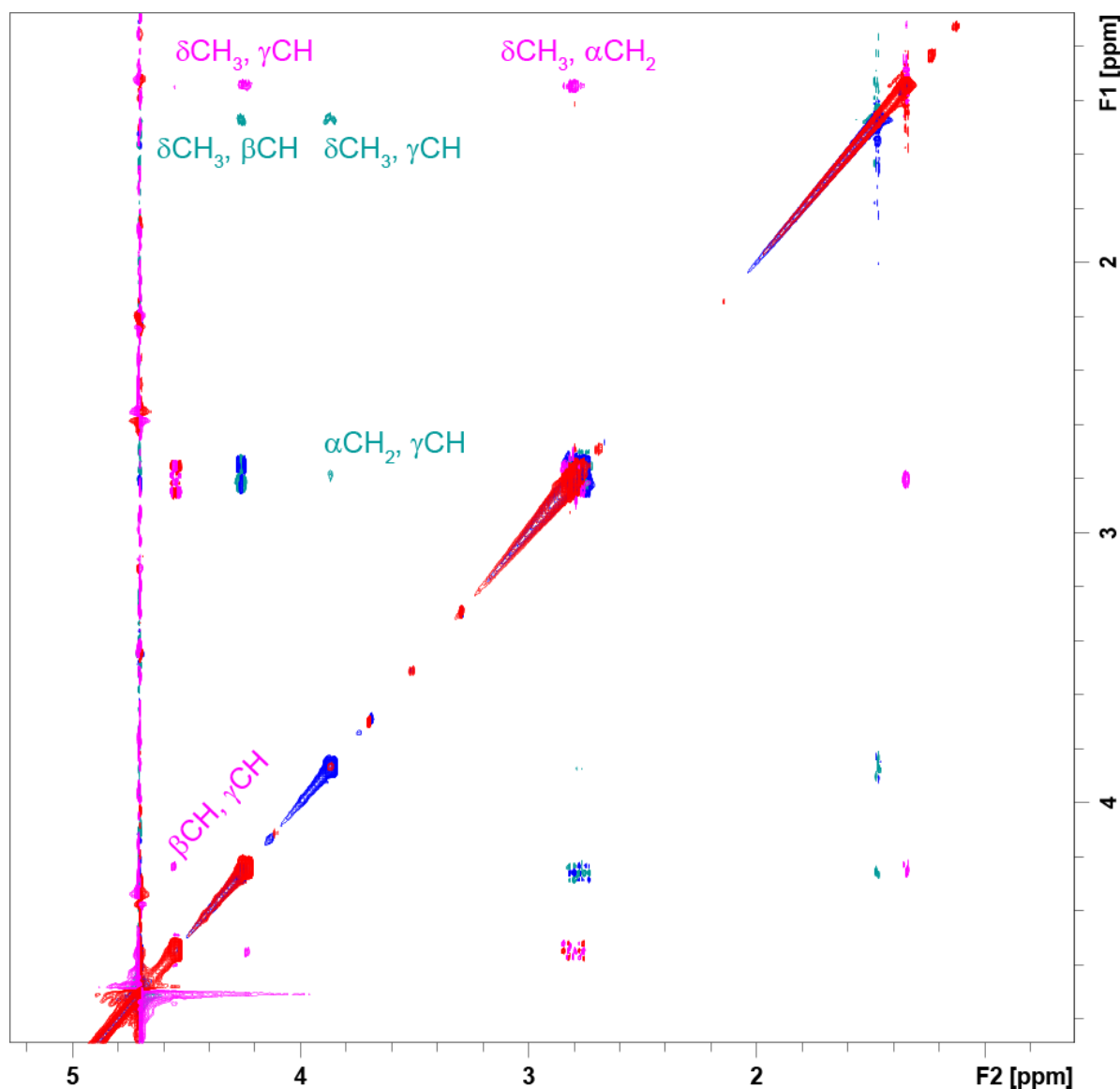


Figure 3.6 Overlay of ROESY spectra (600 MHz acquired in D_2O) of *trans*-**3.8** (blue/green) and *cis*-**3.8** (red/pink) with key ROE correlations used for identification of the *cis*/*trans* diastereomers highlighted.

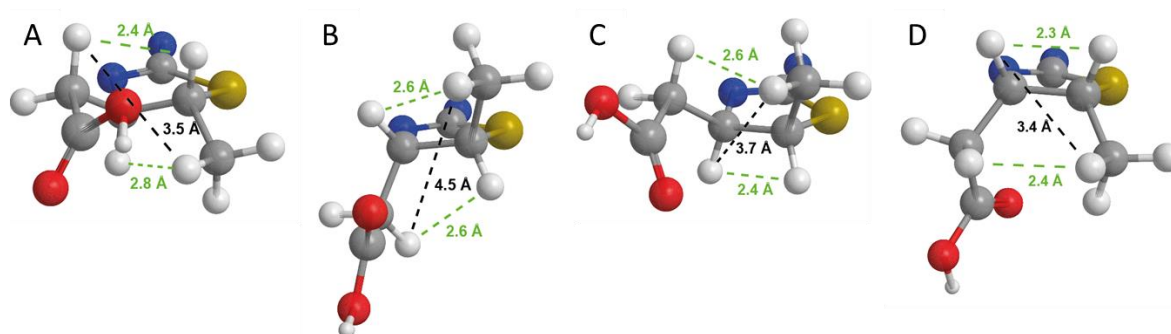


Figure 3.7 MM2 energy minimized 3D representations of the two *trans*-**3.8** (A and B) and *cis*-**3.8** enantiomers (C and D). Key intramolecular distances are shown, with observed ROE correlations used for identification of the diastereomers marked in green. Nitrogen atoms are blue, sulphur atoms yellow and oxygen atoms red.

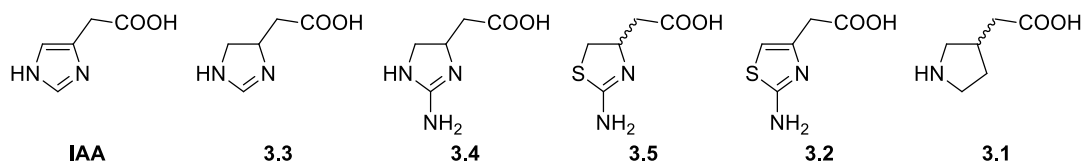
3.2.4 Pharmacology

The binding affinities of the synthesized and purchased compounds (IAA, **3.1–3.5** and **3.8–3.10**) at native GABA_ARs were measured by displacement of [³H]muscimol in rat brain membrane preparations. Functional characterization of the compounds was carried out at human $\alpha_1\beta_2\gamma_{2S}$, $\alpha_3\beta_2\gamma_{2S}$, $\alpha_4\beta_2\gamma_{2S}$, $\alpha_5\beta_2\gamma_{2S}$, and ρ_1 GABA_ARs transiently expressed in tsA201 cells using the FLIPRTM Membrane Potential (FMP) Blue Assay.¹²⁰

Within the first series of compounds, **3.3**, **3.4**, and **3.5** showed binding affinities to the native GABA_ARs in the mid to high nanomolar range and functional properties at GABA_ARs subtypes comparable to those of GABA (Table 3.3). With respect to functional properties, these compounds were characterized as full agonist at $\alpha_1\beta_2\gamma_{2S}$, $\alpha_3\beta_2\gamma_{2S}$, $\alpha_4\beta_2\gamma_{2S}$, and $\alpha_5\beta_2\gamma_{2S}$ GABA_ARs, displaying maximal responses in the range 71–100% of maximal response elicited by GABA with low micromolar potencies. In contrast, they were characterized as partial agonist at ρ_1 GABA_ARs, with maximal responses in the range 45–64% of maximal response of GABA and with potencies in the low micromolar range. Usually, if compared to synaptic subtypes, a tendency of higher potency at the extrasynaptic $\alpha_5\beta_2\gamma_{2S}$ is observed for GABA_AR agonists and was also evident in this study. Based on the obtained experimental results, the use of dihydroimidazole and 2-amino analogues of dihydroimidazole and dihydrothiazole as bioisosteres of the amino moiety in the GABA_ARs area is validated.

The aromatic heterocyclic compounds IAA and **3.2** showed a significant decrease in binding affinities with respect to the partly saturated analogues **3.3** and **3.5** respectively. The p*K*_a value of the amino moiety of these compounds was determined and, from the obtained results, compounds **3.3** and **3.5** (p*K*_{a2} 9.63 and 8.62 respectively) probably have larger extent of protonation and may form stronger interactions in the binding pocket when compared with the aromatic analogues IAA and **3.2** (p*K*_{a2} 7.13 and 6.08 respectively). For this reason, the p*K*_a value of the amino moiety seems to play an essential role in determining the pharmacological properties of these GABA_AR ligands (Table 3.3).

Table 3.3 Pharmacological data and ionization constants for reference compounds GABA and IAA, and compounds **3.1**–**3.5**.^a



	[³ H]muscimol binding K_i (μM) ^b [$pK_i \pm \text{SEM}$]	$\alpha_1\beta_2\gamma_2\text{S}$ EC_{50} (μM) ^c [$p\text{EC}_{50} \pm \text{SEM}$] $R_{\text{max}} \pm \text{SEM}$	$\alpha_3\beta_2\gamma_2\text{S}$ EC_{50} (μM) ^c [$p\text{EC}_{50} \pm \text{SEM}$] $R_{\text{max}} \pm \text{SEM}$	$\alpha_4\beta_2\gamma_2\text{S}$ EC_{50} (μM) ^c [$p\text{EC}_{50} \pm \text{SEM}$] $R_{\text{max}} \pm \text{SEM}$	$\alpha_5\beta_2\gamma_2\text{S}$ EC_{50} (μM) ^c [$p\text{EC}_{50} \pm \text{SEM}$] $R_{\text{max}} \pm \text{SEM}$	ρ_1 EC_{50} (μM) ^c [$p\text{EC}_{50} \pm \text{SEM}$] $R_{\text{max}} \pm \text{SEM}$	pK_{a2} ^d
GABA	0.049 ^e	3.7 [5.42 ± 0.03] 100	1.6 [5.90 ± 0.04] 100	3.7 [5.43 ± 0.03] 100	0.23 [6.63 ± 0.03] 100	0.34 [6.47 ± 0.03] 100	10.7 ^f
IAA	0.65 ^g	24 [4.61 ± 0.07] 46 ± 4	8.1 [5.09 ± 0.03] 89 ± 4	19 [4.73 ± 0.08] 81 ± 4	1.8 [5.76 ± 0.07] 92 ± 2	4.6 ^h [5.34 ± 0.06] 46 ± 7	7.13 ±0.04
3.3	0.090 [7.05 ± 0.03]	7.6 [5.12 ± 0.07] 71 ± 3	5.4 [5.27 ± 0.05] 91 ± 4	7.9 [5.10 ± 0.09] 74 ± 2	0.79 [6.10 ± 0.06] 88 ± 5	2.8 [5.56 ± 0.07] 45 ± 2	9.63 ±0.02
3.4	0.45 [6.37 ± 0.07]	11 [4.95 ± 0.08] 81 ± 5	12 [4.94 ± 0.03] 105 ± 7	14 [4.85 ± 0.09] 81 ± 1	1.6 [5.81 ± 0.08] 90 ± 7	3.8 [5.41 ± 0.06] 64 ± 4	10.05 ±0.05
3.5	0.11 [6.97 ± 0.04]	1.8 [5.73 ± 0.05] 86 ± 3	1.1 [5.96 ± 0.07] 95 ± 7	1.3 [5.88 ± 0.07] 93 ± 2	0.22 [6.66 ± 0.08] 98 ± 9	6.5 [5.19 ± 0.05] 43 ± 3	8.62 ±0.04
(S)-3.5	0.36 [6.44 ± 0.02]	12 [4.91 ± 0.05] 65 ± 5	2.4 [5.63 ± 0.08] 102 ± 3	8.6 [5.07 ± 0.05] 53 ± 5	0.56 [6.25 ± 0.09] 103 ± 3	3.7 [5.43 ± 0.07] 34 ± 4	-
(R)-3.5	0.059 [7.23 ± 0.03]	1.5 [5.81 ± 0.07] 97 ± 5	0.37 [6.43 ± 0.09] 98 ± 4	0.59 [5.23 ± 0.02] 105 ± 5	0.12 [6.92 ± 0.07] 104 ± 4	5.4 [5.27 ± 0.06] 75 ± 7	-
3.2	32 [4.50 ± 0.06]	Weak agonist ⁱ	Weak agonist ⁱ	Weak agonist ⁱ	24 [4.61 ± 0.03] 85 ± 7	Weak agonist ⁱ	6.08 ±0.04
(R)-3.1	0.21 [6.69 ± 0.07]	12 [4.92 ± 0.05] 93 ± 6	5.6 [5.25 ± 0.03] 102 ± 2	8.1 [5.09 ± 0.05] 94 ± 6	0.94 [6.02 ± 0.09] 99 ± 8	8.4 [5.08 ± 0.05] 101 ± 3	-
(S)-3.1	5.6 [5.26 ± 0.04]	Weak agonist ^l	Weak agonist ⁱ	Weak agonist ^l	24 [4.62 ± 0.06] 86 ± 2	Weak agonist ⁱ	-

^aGABA_A receptor binding affinities at rat synaptic membranes and functional characterization at the human $\alpha_1\beta_2\gamma_2\text{S}$, $\alpha_3\beta_2\gamma_2\text{S}$, $\alpha_4\beta_2\gamma_2\text{S}$, $\alpha_5\beta_2\gamma_2\text{S}$ and ρ_1 GABA_A receptors transiently expressed in tsA201 cells using the FLIPR membrane potential blue assay. ^b IC_{50} values were calculated from inhibition curves and converted to K_i values. Data are given as the mean [mean $pK_i \pm \text{SEM}$] of three to five independent experiments. ^cThe agonist data are given as EC_{50} values (μM) with $p\text{EC}_{50} \pm \text{SEM}$ values in bracket. $R_{\text{max}} \pm \text{SEM}$ values are given in % of the maximal response induced by GABA. ^dThe ionization constants of compounds **3.2**–**3.5** and IAA were determined by potentiometric titration using a GLpK_a apparatus (Sirius Analytical Instruments Ltd., Forest Row, East Sussex, UK). ^eData from Lolli *et al.*⁸³ ^fData from Albert *et al.*⁹⁶ ^gData from Madsen *et al.*⁵⁹ ^hData from Krall *et al.*⁶⁷ ⁱSignificant agonist response at 100 μM and higher concentrations. ^lSignificant agonist response at 300 μM and higher concentrations.

As outlined before, the enantiopharmacology is also an important factor to be considered in the GABA_ARs. The rationale design of the ligands involved in this study permitted a further evaluation of the concept. When compared with (*S*)-**3.1**, (*R*)-Homo- β -proline ((*R*)-**3.1**) has higher binding affinity for GABA_ARs¹⁰³ and the compound showed also higher potency at the

evaluated GABA_AR subtypes (Table 3.3). Analogously, (**R**)-**3.5** showed a 6-fold preference for binding at the GABA_ARs and showed the highest affinity among the compounds included in this study. Functional properties at the $\alpha\beta\gamma$ -GABA_ARs are in accordance with obtained binding affinities but the characterization of the compounds at the ρ_1 containing GABA_ARs displayed a comparable potency of the two enantiomers.

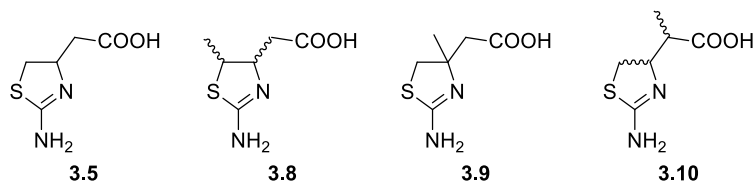
A second series of compounds (**3.8–3.10**) was obtained as part of a preliminary SAR study of compound **3.5**, which was chosen as lead compound among the other analogues included in the first series because of the accessible chemistry and the high binding affinity at the GABA_ARs. Introduction of a methyl group in the 4- or 5-position of the 2-aminodihydrothiazole ring (**3.9** and *trans*-**3.8**, *cis*-**3.8** respectively) led to 20- to 110-fold reduced affinity for the GABA_ARs when compared with the lead compound **3.5** (Table 3.4). Introduction of a methyl group in the α -position with respect to the carboxylic acid moiety led to two pairs of enantiomers that, after separation and characterization, showed the following profile: *u*-**3.10** was shown to have impaired binding affinity at the GABA_ARs if compared with the lead **3.5**, while *l*-**3.10** regained affinity for the native GABA_ARs.

With respect to the functional properties, *trans*-**3.8** showed weak agonist profile at the tested GABA_AR subtypes. **3.9**, *cis*-**3.8**, and *u*-**3.10** showed weak to moderate potent agonist activity at the $\alpha\beta\gamma$ -GABA_ARs, while they were characterized as weak antagonist at the ρ_1 GABA_AR, without reflecting significant subtype selectivity. However, *l*-**3.10** displayed partial agonist activity at the $\alpha_1\beta_2\gamma_{2S}$ and $\alpha_3\beta_2\gamma_{2S}$ subtypes with maximal response around 20% of maximal response induced by GABA, weak agonist activity at $\alpha_4\beta_2\gamma_{2S}$ subtype, and full agonist activity (81% of R_{max} of GABA) at the $\alpha_5\beta_2\gamma_{2S}$ GABA_ARs. The compound also showed high potency and low efficacy for the ρ_1 GABA_ARs with maximal response of 35% of maximal response elicited by GABA.

The high binding affinity and the interesting pharmacological profile displayed by *l*-**3.10** encouraged the resolution and pharmacological characterization of the pure enantiomers. The binding affinity of the first eluted pure enantiomer *l*-**3.10a** was shown to be 4-fold greater than *l*-**3.10b**. With respect to the functional properties, *l*-**3.10a** was shown to be full agonist at all the $\alpha\beta\gamma$ -GABA_ARs with potencies reflecting the obtained binding affinities and, in general, 4-fold greater than *l*-**3.10b**. Moreover, the latter compound displayed a 6-fold preference for the ρ -containing GABA_ARs than *l*-**3.10a**.

A molecular modelling study is currently being performed to explain the different activity at the ρ -containing GABA_ARs possessed by the ligands of the second series. In particular, compounds *trans*-**3.8**, *cis*-**3.8**, **3.9**, *u*-**3.10** and *l*-**3.10** will be analysed in the homology model of GABA_CRs based on multiple template at the University of Copenhagen.

Table 3.4 Pharmacological data for reference compound GABA and compounds **3.5**, **3.8–3.10**.^a



	[³ H]muscimol binding K_i (μM) ^b [p $K_i \pm$ SEM]	$\alpha_1\beta_2\gamma_{2S}$ EC ₅₀ (μM) ^c [pEC ₅₀ \pm SEM] $R_{max} \pm SEM$	$\alpha_3\beta_2\gamma_{2S}$ EC ₅₀ (μM) ^c [pEC ₅₀ \pm SEM] $R_{max} \pm SEM$	$\alpha_4\beta_2\gamma_{2S}$ EC ₅₀ (μM) ^c [pEC ₅₀ \pm SEM] $R_{max} \pm SEM$	$\alpha_5\beta_2\gamma_{2S}$ EC ₅₀ (μM) ^c [pEC ₅₀ \pm SEM] $R_{max} \pm SEM$	ρ_1 EC ₅₀ (μM) ^c [pEC ₅₀ \pm SEM] $R_{max} \pm SEM$
GABA	0.049 ^d	3.7 [5.42 \pm 0.03] 100	1.6 [5.90 \pm 0.04] 100	3.7 [5.43 \pm 0.03] 100	0.23 [6.63 \pm 0.03] 100	0.34 [6.47 \pm 0.03] 100
3.5	0.11 [6.97 \pm 0.04]	1.8 [5.73 \pm 0.05] 86 \pm 3	1.1 [5.96 \pm 0.07] 95 \pm 7	1.3 [5.88 \pm 0.07] 93 \pm 2	0.22 [6.66 \pm 0.08] 98 \pm 9	6.5 [5.19 \pm 0.05] 43 \pm 3
<i>trans</i> - 3.8	12 [4.96 \pm 0.09]	Weak agonist ^g	Weak agonist ^g	Weak agonist ^g	17 [4.77 \pm 0.06] 90 \pm 4	Weak agonist ^f
<i>cis</i> - 3.8	5.5 [5.26 \pm 0.04]	Weak agonist ^h	54 [4.26 \pm 0.07] 76 \pm 5	Weak agonist ^g	8.2 [5.08 \pm 0.02] 92 \pm 3	^e IC ₅₀ : ~100
3.9	2.2 [5.66 \pm 0.02]	Weak agonist ^f	26 [4.59 \pm 0.08] 80 \pm 4	Weak agonist ^g	4.5 [5.35 \pm 0.08] 92 \pm 6	^e IC ₅₀ : ~300
<i>u</i> - 3.10	1.6 [5.79 \pm 0.03]	48 [4.32 \pm 0.04] 59 \pm 5	17 [4.78 \pm 0.08] 96 \pm 6	Weak agonist ^f	2.6 [5.58 \pm 0.04] 94 \pm 4	^e IC ₅₀ : ~300
<i>l</i> - 3.10	0.36 [6.45 \pm 0.03]	9.7 [5.01 \pm 0.08] 22 \pm 2	36 [4.45 \pm 0.04] 19 \pm 1	Weak agonist ^h	3.0 [5.52 \pm 0.03] 81 \pm 6	1.6 [5.80 \pm 0.07] 35 \pm 1
<i>l</i> - 3.10a	0.33 [6.49 \pm 0.05]	25 [4.60 \pm 0.10] 69 \pm 6	30 [4.52 \pm 0.13] 83 \pm 5	26 [4.58 \pm 0.11] 32 \pm 2	2.7 [5.57 \pm 0.11] 97 \pm 6	7.4 [5.13 \pm 0.04] 63 \pm 6
<i>l</i> - 3.10b	1.3 [5.91 \pm 0.02]	Weak agonist ⁱ	Weak agonist ^l	Weak agonist ^f	11 [4.96 \pm 0.12] 34 \pm 4	1.2 [5.92 \pm 0.06] 31 \pm 2

^aGABA_A receptor binding affinities at rat synaptic membranes and functional characterization at the human $\alpha_1\beta_2\gamma_{2S}$, $\alpha_3\beta_2\gamma_{2S}$, $\alpha_4\beta_2\gamma_{2S}$, $\alpha_5\beta_2\gamma_{2S}$, and ρ_1 GABA_A receptors transiently expressed in tsA201 cells using the FLIPR Membrane Potential Blue assay.

^bIC₅₀ values were calculated from inhibition curves and converted to K_i values. Data is given as the mean [mean p $K_i \pm$ SEM] of three to five independent experiments. ^cThe agonist data are given as EC₅₀ values (μM) with pEC₅₀ \pm SEM values in bracket. $R_{max} \pm SEM$ values are given in % of the maximal response induced by GABA. ^dData from Lolli *et al.*⁸³ ^eIC₅₀ values (determined using GABA EC₈₀ as agonist concentration) are given in μM . ^fSignificant agonist response at 100 μM and higher concentrations. ^gSignificant agonist response at 300 μM and higher concentrations. ^hSignificant agonist response at 1000 μM and higher concentrations. ⁱSignificant agonist response at 10 μM and higher concentrations. ^lSignificant agonist response at 30 μM and higher concentrations.

The compounds included in the first and second series of the study were also evaluated as possible amino bioisosteres at the human GATs. Using a cell-based [³H]GABA uptake assay the compounds were investigated for their ability to inhibit the human GATs expressed in mammalian cell lines. The obtained inhibitory activities at a concentration of 100 μM are displayed in Figure 3.8 and data for compounds showing >30% inhibition at a concentration of 100 μM are given as IC₅₀ values in Table 3.5.

The first series of compounds (**3.1**, **3.3–3.5**) showed inhibitory activities in the mid- to low micromolar range (IC_{50} 2.1–155 μ M) where (*R*)-**3.1**, (*S*)-**3.1** and **3.3** displayed higher inhibitory activities compared with the compounds containing the exo-cyclic amino group (i.e. **3.4** and **3.5**). As previously shown, the stereochemistry of compound **3.1** was proved to be not relevant for the inhibitory activity at the GABA uptake and displayed no selectivity. For this reason, compounds (*S*)-**3.5** and (*R*)-**3.5** were not assayed. Interestingly, compound **3.4** showed greater potency for BGT1 over the other subtypes. The 4-, 5- and α - substituted analogues of **3.5** (**3.8–3.10**) showed low inhibitory activity at all four *h*GATs (< 30% inhibitory activity at 100 μ M, Figure 3.8), meaning that GABA binding site of the GATs is sensible to steric bulk near the core scaffold.

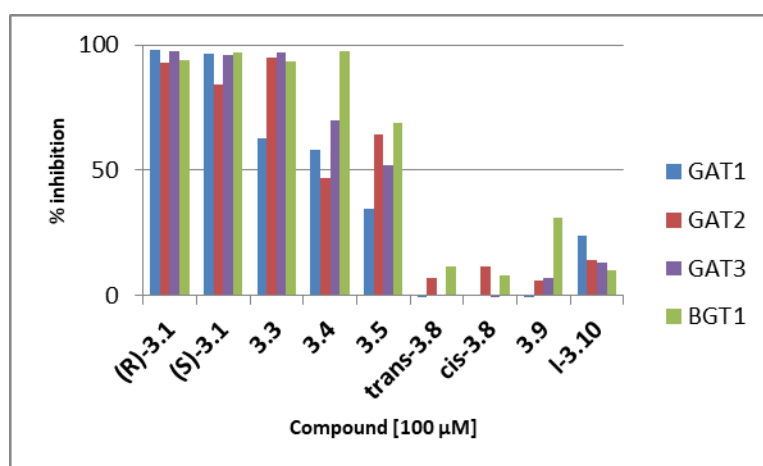
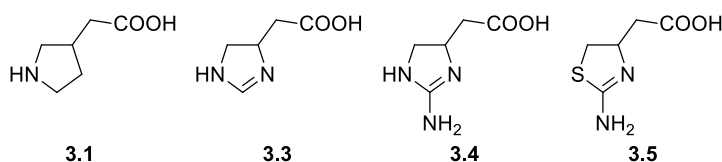


Figure 3.8 Inhibition (%) of compounds **3.1**, **3.3–3.5** and **3.8–3.10** (100 μ M) at human GATs.

Table 3.5 Inhibitory activities of selected compounds (**3.1**, **3.3–3.5**) at human GATs.^a



	<i>h</i> GAT1 ^b IC_{50} (μ M)	<i>h</i> GAT2 ^b IC_{50} (μ M)	<i>h</i> GAT3 ^b IC_{50} (μ M)	<i>h</i> BGT1 ^b IC_{50} (μ M)
GABA	10	26	11	10
(R)-3.1	2.5	6.0	2.3	5.2
(S)-3.1	3.5	19	2.1	2.4
3.3	68	2.7	2.1	7.8
3.4	76	155	31	2.6
3.5	134	79	110	41

^aThe compounds were tested for their ability to inhibit the uptake of 30 nM [³H]GABA. ^b[³H]GABA uptake assay conducted at CHO cells stably expressing the *h*GATs. IC_{50} are given as mean of 3 independent experiments. $pIC_{50} \pm SEM$ are not given.

3.3 Conclusions

In the present chapter, a bioisosteric replacement of the amino moiety of IAA was evaluated using a variety of five-membered aromatic and partly saturated heterocycles. The synthesis of two small series of compounds have been developed and successfully performed.

The pharmacological evaluation of the compounds in the first series (**3.3–3.5**) proved that the bioisosteric replacement of the imidazole moiety of IAA using dihydroimidazole and 2-amino analogues of dihydroimidazole and dihydrothiazole was successful. The enantiopharmacology was proved to be important for the new analogues at the GABA_ARs, as evident for compound **3.5**. The ionization constants of the novel GABA analogues have been determined and resulted an important chemical properties influencing the activity at the GABA_ARs. The compounds included in the first series were also evaluated as possible amino bioisosteres in the *h*GATs system, proving to be suitable bioisosteres. In this perspective, the most interesting compound was **3.4**, which possesses a partial preference for BGT1 over the three other subtypes.

In addition, one analogue included in the first series (i.e. **3.5**) was chosen for a preliminary SAR study where a methyl group was introduced in three different position (i.e. 4-, 5- and α -positions). Compounds **3.8–3.10** were synthesized and the binding affinities were evaluated at the native GABA_ARs. Except compound *l*-**3.10**, all the analogues showed lower binding affinities than the lead compound **3.5**. The results proved that GABA_AR is sensible to minor modification near the core scaffold of the orthosteric agonists.

However, one enantiomeric pair of the α -substituted **3.5** (i.e. *l*-**3.10**) retained affinity for the GABA_ARs, and also displayed an interesting pharmacological profile when characterized at $\alpha\beta\gamma$ - and ρ - GABA_ARs. The compound showed partial agonist activity for all the considered subtypes except for the extrasynaptic $\alpha_5\beta_2\gamma_{2S}$ GABA_ARs, where it exploited full agonist activity and high potency. The compound was subsequently resolved into the pure enantiomers which displayed only a 4-fold preference for one enantiomer for the $\alpha\beta\gamma$ GABA_ARs and 6-fold preference for the other enantiomer for the ρ_1 containing GABA_ARs. However, the racemic mixture displayed interesting pharmacological properties which will be examined in depth in the future.

Interestingly, the pharmacological evaluation of the second series of compounds at *h*GATs also proved that the substitution of the available position of the core scaffold of **3.5** was detrimental for the inhibitory activity.

In conclusion, the results reported in this chapter shed more light on the architecture and structural requirements of the GABA_ARs and *h*GATs. The use of the bioisosteric replacement toward the amino moiety of GABA was expanded by the use of partly saturated nitrogen containing heterocycles and, in accordance to experimental results, they can be considered as useful tool leading to possible functional selective ligands.

3.4 Experimental section

Chemistry

(*R*)-**3.1**, (*S*)-**3.1** and **3.2** were obtained from commercial suppliers: (*R*)-**3.1**, AstaTech, Inc. (USA); (*S*)-**3.1**, AstaTech, Inc. (USA); **3.2**, Sigma Aldrich. All reagents and solvents (reagent or chromatography grade) were obtained from commercial suppliers and used without further purification, if not stated differently. Air- and/or moisture-sensitive reactions were performed under a nitrogen atmosphere using syringe-septum cap techniques and with the use of flame-dried glassware. Anhydrous solvents were obtained by using a solvent purification system (THF, DMF and CH₂Cl₂) or by storage over 3 Å molecular sieves. Thin-layer chromatography (TLC) was carried out using Merck silica gel 60 F₂₅₄ plates, and compounds were visualized by UV (254 nm), KMnO₄ or ninhydrin spray reagent. Flash chromatography (FC) was carried out according to standard procedures using Merck silica gel 60 (0.040–0.063 mm). Preparative reversed phase HPLC was carried out on an Ultimate 3000 HPLC system (Dionex) with a multi-wavelength UV detector (200, 210, 225 and 254 nm) and 10 mL loop using a preparative RP Phenomenex Gemini NX-C₁₈ column (5 μm, 21.2×250 mm) using eluent A (Milli-Q H₂O/TFA, 100/0.1) and eluent B (CH₃CN/Milli-Q H₂O/TFA, 90/10/0.1) at a flow rate of 20 mLmin⁻¹. For HPLC control, data collection, and data handling, Chromeleon Software ver. 6.80 was used. Compounds *l*-**3.10a** and *l*-**3.10b** were obtained by preparative chiral HPLC on an Ultimate 3000 HPLC system (Dionex) with a multi-wavelength UV detector (200, 210, 225 and 254 nm) and 10 mL loop using a preparative Chirobiotic T column (5 μm, 21.2×250 mm), a mobile phase consisting of Milli-Q H₂O/MeOH (90/10), and a flow rate of 20 mLmin⁻¹. For HPLC control, data collection, and data handling Chromeleon Software ver. 6.80 was used. Determination of enantiomeric excess (ee) for compounds *l*-**3.10a** and *l*-**3.10b** were performed using an analytical HPLC system consisting of an Ultimate 3000 pump (Dionex, Thermo Scientific), an Ultimate WPS-3000SL autosampler (Dionex, Thermo Scientific), and an Ultimate Photodiode Array Detector (Dionex, Thermo Scientific). The column used was a Astec® Chirobiotic® T column (5 μm, 4.6×250 mm) using a mobile phase consisting of Milli-Q H₂O/MeOH (70/30) at a flow rate of 1 mLmin⁻¹. For HPLC control, data collection, and data handling, Chromeleon Software ver. 6.80 was used. Compounds (*R*)-**3.15** and (*S*)-**3.15** were obtained by preparative chiral HPLC on an Ultimate 3000 HPLC system (Dionex) with a multi-wavelength UV detector (200, 210, 225 and 254 nm) and 10 mL loop using a semi-preparative CHIRALPAK IF column (5 μm, 10×250 mm), a mobile phase consisting of Heptane/EtOH/TFA (80/20/0.5), and a flow rate of 5 mLmin⁻¹. For HPLC control, data collection, and data handling Chromeleon Software ver. 6.80 was used. Determination of enantiomeric excess (ee) of compounds (*R*)-**3.15** and (*S*)-**3.15** was

determined using chiral HPLC on an Ultimate 3000 HPLC system (Dionex) with a multi-wavelength UV detector (200, 210, 225 and 254 nm) and 10 mL loop equipped with a CHIRALPAK IF column (5 μ m, 4.6 \times 250 mm) using a mobile phase consisting of Heptane/EtOH/TFA (80/20/0.5), and a flow rate of 1 mLmin⁻¹. For HPLC control, data collection, and data handling, Chromeleon Software ver. 6.80 was used. Determination of enantiomeric excess (ee) of compounds (**R**)-**3.5** and (**S**)-**3.5** was determined by converting the compounds in the methyl esters (**R**)-**3.15** and (**S**)-**3.15** and then analyzed using the method described above. Melting points were recorded on an SRS OptiMelt apparatus in open capillary tubes and are uncorrected. ¹H and ¹³C NMR data were recorded on a Bruker Avance 400 MHz spectrometer equipped with a 5 mm PABBO BB[¹H, ¹⁹F] Z-GRD probe, or a Bruker Avance 600 MHz spectrometer equipped with a cryogenically cooled 5 mm CPDCH ¹³C[¹H] Z-GRD probe, at 300 K. Data are tabulated in the following order: chemical shift (δ) [multiplicity (br, broad; s, singlet; d, doublet; t, triplet; q, quartet; m, multiplet), coupling constant(s) *J* (Hz), number of protons]. The solvent residual peak was used as internal reference.¹⁰² Compound synthesized as pair of enantiomers containing two chiral centres were named in accordance with IUPAC recommendations.¹²¹ The purity of all tested compounds was analysed using combustion analysis and calculated elementary analyses are within 0.4% of found values. Elementary analyses were performed by Mr. J. Theiner, Department of Physical Chemistry, University of Vienna, Austria.

Methyl 3,4-diaminobutanoate dihydrochloride (3.12). 3,4-diaminobutanoic acid dihydrochloride (**3.11**, 12, 0.5 g, 2.6 mmol) was suspended in anhydrous MeOH (20 mL) at 0 °C. After 45 min, thionyl chloride (0.29 ml, 3.9 mmol) was added and the reaction mixture was allowed to reach rt. Upon completion of the reaction (monitored by TLC, nBuOH/H₂O/AcOH/EtOAc 1:1:1:1 v/v), the solvent was removed under reduced pressure. The product was taken up in MeOH and the solvent was evaporated three times. The crude product was dissolved in MeOH (100 mL) and filtrated to remove the insoluble. The solvent was removed under reduced pressure, re-dissolved in the smallest amount of MeOH and precipitated with Et₂O to give compound **3.12** as white solid (0.40 g, 74%): mp 182 °C dec. ¹H NMR (600 MHz, DMSO-*d*₆): δ 8.68 (br s, 6H, NH), 3.79 (m, 1H, β CHN), 3.66 (s, 3H, OCH₃), 3.20 (dd, *J* = 13.7, 6.8 Hz, 1H, γ CH₂N), 3.17–3.12 (m, 1H, γ CH₂N), 2.97 (dd, *J* = 17.5, 5.8 Hz, 1H, α CH₂), 2.86 (dd, *J* = 17.5, 7.1 Hz, 1H, α CH₂). ¹³C NMR (150 MHz, DMSO-*d*₆): δ 169.8 (COO), 52.0 (OCH₃), 45.7 (β CHN), 40.2 (γ CH₂N), 34.4 (α CH₂). LC-MS (ESI) 133 [M+H]⁺.

Methyl 2-(4,5-dihydro-1H-imidazol-4-yl)acetate hydrochloride (3.13). Compound **3.12** (0.27 g, 1.3 mmol) was dissolved in MeOH (35 mL). Trimethyl orthoformate (1.28 mL, 11.7 mmol) was added and the reaction mixture was refluxed for 48 h (TLC silica plate

nBuOH/H₂O/AcOH/EtOAc 1:1:1:1 *v/v* showed completion of the reaction). The solvent was then evaporated under reduced pressure. The crude product was re-dissolved in the smallest amount of MeOH and Et₂O was added. The suspension was filtered and the solid was discarded. The filtrate was evaporated and dried to give compound **3.13** (0.19 g, 83%) as yellow viscous oil. ¹H NMR (600 MHz, DMSO-*d*₆): δ 10.45 (br s, 2H, NH), 8.53 (s, 1H, NCHN), 4.49 (td, *J* = 14.1, 6.7 Hz, 1H, βCHN), 3.97 (t, *J* = 11.7 Hz, 1H, γCH₂N), 3.64 (s, 3H, OCH₃), 3.57 (dd, *J* = 11.8, 7.8 Hz, 1H, γCH₂N), 2.83–2.73 (m, 2H, αCH₂). ¹³C NMR (150 MHz, DMSO-*d*₆): δ 170.3 (COO), 157.1 (NCHN), 53.0 (βCHN), 51.7 (OCH₃), 48.9 (γCH₂N), 38.2 (αCH₂). LC-MS (ESI) 143 [M+H]⁺.

2-(4,5-dihydro-1H-imidazol-4-yl)acetic acid hydrochloride (3.3). Compound **3.13** (0.20 g, 1.1 mmol) was dissolved in 2M HCl (20 mL). The reaction mixture was stirred at 50 °C for three hours. Then the solvent was evaporated under reduced pressure. The product was taken in water and the solvent was evaporated two times. The crude product (0.17 g, 93% yield) was crystallized twice with MeOH/Et₂O affording compound **3.3** (90 mg, 49%) as white solid: mp 161–164 °C. ¹H NMR (600 MHz, D₂O): δ 8.21 (s, 1H, NCHN), 4.72–4.66 (m, 1H, βCHN), 4.16 (t, *J* = 12.1 Hz, 1H, γCH₂N), 3.75 (dd, *J* = 11.9, 7.7 Hz, 1H, γCH₂N), 2.95–2.81 (m, 2H, αCH₂). ¹³C NMR (150 MHz, D₂O): δ 174.1 (COO), 156.7 (NCHN), 53.2 (βCHN), 49.0 (γCH₂N), 38.7 (αCH₂). LC-MS (ESI) 129 [M+H]⁺. Anal. calcd (C₅H₈N₂O₂·1.15HCl): C, 35.31; H, 5.42; N, 16.47. Found: C, 35.53; H, 5.64; N, 16.32.

Methyl 2-(2-amino-4,5-dihydrothiazol-4-yl)acetate (3.15).¹⁰⁸ To a solution of methyl 4-bromocrotonate (**3.14**, 0.66 mL, 5.6 mmol, 85% technical grade) in acetone (22 mL) was added thiourea (425 mg, 5.6 mmol) and the resulting mixture was stirred for 5 h at rt. Then solid NaHCO₃ (0.94 g, 11.2 mmol) was added and the temperature was raised to 70 °C. After 2 h the reaction mixture was cooled to room temperature, filtered, and evaporated *in vacuo*. Purification by flash chromatography (CH₂Cl₂/(MeOH/aq NH₃, 9:1 *v/v*), 95:5 *v/v*) brought **3.15** (390 mg, 40%) as white solid. mp 96–97 °C. ¹H NMR (400 MHz; CDCl₃): δ 4.76 (br s, 2H, NH₂), 4.63–4.56 (m, 1H, βCHN), 3.70 (s, 3H, OCH₃), 3.56 (dd, *J* = 10.8, 7.4 Hz, 1H, γCH₂S), 3.13 (dd, *J* = 10.8, 6.9 Hz, 1H, γCH₂S), 2.70 (dd, *J* = 15.6, 6.4 Hz, 1H, αCH₂), 2.54 (dd, *J* = 15.6, 7.7 Hz, 1H, αCH₂). ¹³C NMR (100 MHz, CDCl₃): δ 172.0 (COO), 160.9 (N₂CS), 69.1 (βCHN), 51.9 (OCH₃), 40.7 (αCH₂), 39.8 (γCH₂S).

Alternatively the compound was synthesized as follow:

NaHCO₃ (0.546 g, 6.50 mmol) and KSCN (0.631 g, 6.50 mmol) were added to a solution of **3.24** (1.75 g, 6.50 mmol) in water (50 mL) and refluxed for 24 h. The solvent was evaporated. The crude product was then dissolved in MeOH (50 mL) and stirred at 0 °C for 30 min. Thionyl

chloride (2.37 mL, 32.5 mmol) was added. The reaction mixture was allowed to reach rt and stirred for 24 h. The solvent was evaporated under reduced pressure, dissolved again in MeOH and dried to give the crude product. Flash chromatography (EtOAc/tetrahydrofuran 7:3 v/v + 0.05% aq NH₃) was performed to afford compound **3.15** as white solid (0.19 g, 17%): mp 96–97 °C. R_f 0.3 (EtOAc/THF 8:2 v/v + 0.5% aq NH₃). ¹H NMR (600 MHz, D₂O): δ 4.60–4.50 (m, 1H, βCHN), 3.75 (s, 3H, OCH₃), 3.60 (dd, *J* = 11.1, 7.5 Hz, 1H, γCH₂S), 3.20 (dd, *J* = 11.1, 6.7 Hz, 1H, γCH₂S), 2.77–2.62 (m, 2H, αCH₂). ¹³C NMR (150 MHz, D₂O): δ 174.5 (COO), 165.8 (N₂CS), 67.0 (βCHN), 52.3 (OCH₃), 39.2 (αCH₂), 38.8 (γCH₂S). LC-MS (ESI) 175 [M+H]⁺.

(R)-Methyl 2-(2-amino-4,5-dihydrothiazol-4-yl)acetate 2,2,2-trifluoroacetate ((R)-3.15) and **(S)-methyl 2-(2-amino-4,5-dihydrothiazol-4-yl)acetate 2,2,2-trifluoroacetate ((S)-3.15)**. Compound **3.15** (104 mg, 0.60 mmol) was dissolved in heptane/EtOH (50:50 v/v) to a concentration of 11 mg mL⁻¹, filtered (45 μm, Millipore) and separated using a CHIRALPAK IF column, heptane/EtOH (80:20 v/v) + 0.5% TFA as mobile phase and injections volumes of 400 μL. The fractions containing the first eluting enantiomer were evaporated *in vacuo* affording **(S)-3.15** as pale brown oil (86 mg, 100%): > 99% ee. *t*_R 9.9 min. ¹H-NMR and ¹³C-NMR were identical to those of the racemic mixture. The fractions containing the second eluting enantiomer were evaporated *in vacuo* affording **(R)-3.15** as pale brown oil (86 mg, 100%): > 99% ee. *t*_R 13.6 min. ¹H-NMR and ¹³C-NMR were identical to those of the racemic mixture.

2-(2-amino-4,5-dihydrothiazol-4-yl)acetic acid, hydrobromide (3.5).¹⁰⁸ **3.15** (300 mg, 1.7 mmol) was dissolved in 48% aqueous HBr (5 mL) and the mixture was stirred at rt for 16 h. Evaporation of the mixture *in vacuo* brought **3.5** (414 mg, 99%) as light brown crystals: mp 192–195 °C. ¹H NMR (400 MHz, D₂O): δ 4.64 (dddd, *J* = 7.8, 7.3, 6.1, 5.6 Hz, 1H, βCHN), 3.78 (dd, *J* = 11.5, 7.8 Hz, 1H, γCH₂S), 3.37 (dd, *J* = 11.5, 5.6 Hz, 1H, γCH₂S), 2.87 (dd, *J* = 17.1, 7.3 Hz, 1H, αCH₂), 2.81 (dd, *J* = 17.1, 6.1 Hz, 1H, αCH₂). ¹³C NMR (100 MHz, D₂O): δ 174.1 (COO), 173.5 (N₂CS), 57.5 (βCHN), 37.2 (αCH₂), 35.3 (γCH₂S). Anal. calcd (C₅H₈N₂O₂S·1HBr): C, 24.91; H, 3.76; N, 11.62; S, 13.30. Found: C, 25.21; H, 3.52; N, 11.52; S, 13.13.

2-(2-amino-4,5-dihydrothiazol-4-yl)acetic acid hydrochloride (3.5). Compound **3.15** (90 mg, 0.52 mmol) was dissolved in 2M HCl (20 mL) and stirred at 55 °C for 6 h. The reaction mixture was washed with EtOAc (2 × 20 mL) and then the aqueous phase was evaporated *in vacuo*. Crystallization from MeOH/Et₂O afforded compound **3.5** as white crystals (88 mg, 86%): mp 206–210 °C. ¹H NMR (600 MHz, D₂O): δ 4.75–4.66 (m, 1H, βCHN), 3.85 (dd, *J* = 11.5, 7.8 Hz, 1H, γCH₂S), 3.44 (dd, *J* = 11.5, 5.6 Hz, 1H, γCH₂S), 2.98–2.82 (m, 2H, αCH₂). ¹³C NMR (150 MHz, D₂O): δ 174.3 (COO), 173.5 (N₂CS), 57.7 (βCHN), 37.4 (αCH₂), 35.3 (γCH₂S). LC-MS

(ESI) 161 [M+H]⁺. Anal. calcd (C₅H₈N₂O₂S·1.15HCl): C, 29.71; H, 4.56; N, 13.86; S, 15.86. Found: C, 30.00; H, 4.53; N, 13.51; S, 15.99.

(S)-2-(2-amino-4,5-dihydrothiazol-4-yl)acetic acid hydrochloride ((S)-3.5). Compound **(S)-3.15** (86 mg, 0.30 mmol) was dissolved in 2M HCl (10 mL) and stirred at 50 °C for 6 h. The reaction mixture was washed with EtOAc (2 × 4 mL) and then the aqueous phase was evaporated *in vacuo* to give compound **(S)-3.5** as pale yellow crystals (50 mg, 84%): > 99% ee. mp 198–202 °C. ¹H-NMR and ¹³C-NMR were identical to those of the racemic mixture. Anal. calcd (C₅H₈N₂O₂S·0.8HCl·0.15CF₃COOH): C, 30.83; H, 4.37; N, 13.57; S, 15.53. Found: C, 30.89; H, 4.55; N, 13.64; S, 15.48. The enantiomeric excess was determined on the corresponding methyl ester **(S)-3.15**: **(S)-3.5** (5 mg, 0.025 mmol) was dissolved in MeOH (3 mL) and stirred at 0 °C for 20 min. Thionyl chloride (11 μL, 0.15 mmol) was added. The reaction mixture was allowed to reach rt and stirred for 24 h. The solvent was evaporated under reduced pressure, dissolved again in MeOH and dried to give **(S)-3.15**. *t*_R 9.9 min. > 99% ee.

(R)-2-(2-amino-4,5-dihydrothiazol-4-yl)acetic acid hydrochloride ((R)-3.5). Compound **(R)-3.15** (86 mg, 0.30 mmol) was dissolved in 2M HCl (10 mL) and stirred at 50 °C for 6 h. The reaction mixture was washed with EtOAc (2 × 4 mL) and then the aqueous phase was evaporated *in vacuo* to give compound **(R)-3.5** as pale yellow crystals (49 mg, 84%): > 99% ee. mp 198–202 °C. ¹H-NMR and ¹³C-NMR were identical to those of the racemic mixture. Anal. calcd (C₅H₈N₂O₂S·0.85HCl·0.2CF₃COOH): C, 30.31; H, 4.26; N, 13.09; S, 14.98. Found: C, 30.35; H, 4.57; N, 13.57; S, 14.51. The enantiomeric excess was determined on the corresponding methyl ester **(R)-3.15**: **(R)-3.5** (5 mg, 0.025 mmol) was dissolved in MeOH (3 mL) and stirred at 0 °C for 20 min. Thionyl chloride (11 μL, 0.15 mmol) was added. The reaction mixture was allowed to reach rt and stirred for 24 h. The solvent was evaporated under reduced pressure, dissolved again in MeOH and dried to give **(R)-3.15**. *t*_R 13.6 min. > 99% ee.

N-(tert-butylcarbamoithiyl)benzamide (3.17). A stirred suspension of benzyl isothiocyanate (0.32 mL, 2.4 mmol) and *tert*-butylamine (0.25 mL, 2.4 mmol) in water (5 mL) was added to a stirred mixture of ethyl propiolate (0.24 mL, 2.4 mmol) and *N*-methylimidazole (9 μL, 0.12 mmol) in water (5 mL). The resulting reaction mixture was stirred at rt for 24 h. The solid was filtered and washed with cooled Et₂O affording **3.17** (50 mg, 9%). ¹H NMR (400 MHz, DMSO-*d*₆): δ 11.12 (br. s, 1H), 10.97 (br. s, 1H), 7.92–7.86 (m, 2H), 7.66–7.60 (m, 1H), 7.54–7.47 (m, 2H), 1.54 (s, 9H).

Alternatively the compound was synthesized as follow:

A stirred suspension of benzoyl isothiocyanate (0.32 mL, 2.4 mmol) and *tert*-butylamine (0.25 mL, 2.4 mmol) in CH₂Cl₂ (7 mL) was added to a stirred mixture of ethyl propiolate (0.24 mL,

2.4 mmol) and *N*-methylimidazole (9 μ L, 0.12 mmol) in CH_2Cl_2 (7 mL). The resulting reaction mixture was stirred at rt for 48 h and the solvent was evaporated *in vacuo*. Purification by flash chromatography (heptane/EtOAc 90:10) afforded **3.17** (150 mg, 27%). $^1\text{H-NMR}$ was identical to previously reported spectrum.

Methyl 4-amino-3-hydroxybutanoate hydrochloride (3.21).¹¹¹ 4-amino-3-hydroxybutanoic acid (**3.20**, 5.0 g, 42 mmol) was suspended in anhydrous methanol (100 mL) at 0 °C and stirred for 30 min. Thionyl chloride (6.1 mL, 84 mmol) was added and the reaction mixture allowed to reach rt upon stirring for 48 h. The solvent was evaporated under reduced pressure. The product was taken in methanol and the solvent was evaporated three times to give the compound **3.21** (7.1 g, 100%) as yellow viscous oil. $^1\text{H NMR}$ (600 MHz, $\text{DMSO-}d_6$): δ 7.95 (br s, 3H, NH), 5.56 (br s, 1H, OH), 4.10 (tt, $J = 8.3, 4.0$ Hz, 1H, βCHO), 3.61 (s, 3H, OCH_3), 2.96–2.84 (m, 1H, $\gamma\text{CH}_2\text{N}$), 2.79–2.68 (m, 1H, $\gamma\text{CH}_2\text{N}$), 2.58 (dd, $J = 15.6, 4.8$ Hz, 1H, αCH_2), 2.44 (dd, $J = 15.6, 8.0$ Hz, 1H, αCH_2). LC-MS (ESI) 134 $[\text{M}+\text{H}]^+$.

Methyl 4-((*tert*-butoxycarbonyl)amino)-3-hydroxybutanoate (3.22).¹¹² Compound **3.21** (7.1 g, 42 mmol) was dissolved in water/tetrahydrofuran (1:1 *v/v*, 250 mL). Di-*tert*-butyl dicarbonate (9.2 g, 42 mmol) and NaHCO_3 (10.6 g, 126 mmol) were added and the reaction stirred for 24 h. The organic solvent was removed under reduced pressure and water was added (up to 250 mL). Extraction with EtOAc (4 \times 100 mL) was performed. The combined organic phase was washed with brine (100 mL), dried over anhydrous MgSO_4 , and evaporated to give compound **3.22** as a colourless oil (9.2 g, 94%). $^1\text{H NMR}$ (400 MHz, $\text{DMSO-}d_6$): δ 6.74 (t, $J = 6.0$, 1H, NH), 4.91 (d, $J = 5.6$, 1H, OH), 3.91–3.80 (m, 1H, βCHO), 3.58 (s, 3H, OCH_3), 3.01–2.85 (m, 2H, $\gamma\text{CH}_2\text{N}$), 2.44 (dd, $J = 15.1, 3.9$ Hz, 1H, αCH_2), 2.20 (dd, $J = 15.1, 8.9$ Hz, 1H, αCH_2), 1.37 (s, 9H, Boc). $^{13}\text{C NMR}$ (100 MHz, $\text{DMSO-}d_6$): δ 171.6 (COO), 155.7 (BocCO), 77.6 (BocC_q), 66.8 (βCHO), 51.2 (OCH_3), 45.9 ($\gamma\text{CH}_2\text{N}$), 39.8 (αCH_2), 28.2 (BocCH₃). LC-MS (ESI) 134 $[\text{M}+\text{H-Boc}]^+$.

Methyl 3-bromo-4-((*tert*-butoxycarbonyl)amino)butanoate (3.23). PPh_3 (20.64 g, 78.7 mmol) was added to a cooled (0 °C) solution of **3.22** (9.18 g, 39.3 mmol) in CH_2Cl_2 (150 mL). *N*-bromosuccinimide (14.0 g, 78.7 mmol) was then added portion wise over 1 h and the reaction monitored by TLC until completion of the reaction. The solvent was removed under reduced pressure. The crude product was purified by flash chromatography (heptane/EtOAc 80:20 *v/v*) affording compound **3.23** as white solid (2.78 g, 24%): mp 46–50 °C. $^1\text{H NMR}$ (600 MHz, $\text{DMSO-}d_6$): δ 7.21 (t, $J = 6.0$ Hz, 1H, NH), 4.36–4.29 (m, 1H, βCHBr), 3.64 (s, 3H, OCH_3), 3.39–3.32 (m, 1H, $\gamma\text{CH}_2\text{N}$), 3.32–3.26 (m, 1H, $\gamma\text{CH}_2\text{N}$), 3.11 (dd, $J = 16.7, 3.7$ Hz, 1H, αCH_2), 2.74 (dd, $J = 16.7, 9.9$ Hz, 1H, αCH_2), 1.39 (s, 1H, Boc). $^{13}\text{C NMR}$ (150 MHz, $\text{DMSO-}d_6$): δ

170.2 (COO), 155.6 (BocCO), 78.1 (BocC_q), 51.7 (OCH₃), 49.3 (βCHBr), 46.3 (γCH₂N), 40.6 (αCH₂), 28.1 (BocCH₃). LC-MS (ESI) 196, 198 [M+H-Boc]⁺.

4-amino-3-bromobutanoic acid hydrobromide (3.24). Compound **3.23** (2.78 g, 9.4 mmol) was dissolved in MeOH (5 mL) and added 2M HBr (100 mL). The reaction mixture was stirred at 55 °C for 36 h. The reaction mixture was washed with EtOAc (2 × 50 mL) and then the aqueous phase was evaporated. The crude product was dissolved in EtOH and precipitated using Et₂O. The white solid was collected by filtration affording compound **3.24** (2.10 g, 83%): mp 124–125 °C. ¹H NMR (600 MHz, D₂O): δ 4.62–4.55 (m, 1H, βCHBr), 3.61 (dd, *J* = 14.0, 3.4 Hz, 1H, γCH₂N), 3.45 (dd, *J* = 14.0, 9.8 Hz, 1H, γCH₂N), 3.19 (dd, *J* = 17.0, 5.0 Hz, 1H, αCH₂), 3.07 (dd, *J* = 16.9, 8.7 Hz, 1H, αCH₂). ¹³C NMR (150 MHz, D₂O): δ 173.7 (COO), 45.1 (γCH₂N), 43.7 (βCHBr), 41.0 (αCH₂). LC-MS (ESI) 182, 184 [M+H]⁺.

Methyl 2-(2-((methoxycarbonyl)amino)-4,5-dihydro-1H-imidazol-4-yl)acetate (3.28). 3,4-diaminobutanoic acid dihydrochloride (12, 0.25 g, 1.3 mmol) was dissolved in MeOH/water (5:1 v/v, 48 mL). NaHCO₃ (0.22 g, 2.6 mmol) and 1,3-bis(methoxycarbonyl)-2-methyl-2-thiopseudourea (0.30 g, 1.4 mmol) were added. The reaction mixture was stirred at 70 °C for 20 h. The solvent was then evaporated and the residue taken in water (15 mL). The pH was adjusted to pH 1 using aqueous HCl (1M) and the resulting precipitate was filtered off. The filtrate was washed with EtOAc (3 × 25 mL) and the aqueous phase was evaporated *in vacuo* to give 2-(2-((methoxycarbonyl)amino)-4,5-dihydro-1H-imidazol-4-yl)acetic acid. The raw product was dissolved in anhydrous MeOH (20 mL), cooled to 0 °C, and added thionyl chloride (0.35 mL, 4.8 mmol) drop wise. The reaction mixture was allowed to reach rt and stirred for 24 h before the volatiles were evaporated *in vacuo*. The resulting residue was taken up in MeOH and evaporated two times. The crude product was purified by flash chromatography (EtOAc/Acetone 1:1 v/v) to give compound **3.28** (0.10 g, 33%) as white solid: mp 176–177 °C. R_f 0.25 (CH₂Cl₂/MeOH 95:5 v/v). ¹H NMR (600 MHz, DMSO-*d*₆): δ 7.83 (br s, 1H, NH), 7.63 (br s, 1H, NH), 4.09 (dq, *J* = 9.3, 6.7 Hz, 1H, βCHN), 3.61 (t, *J* = 9.8, 1H, γCH₂N), 3.61 (s, 3H, OCH₃), 3.46 (s, 3H, OCH₃), 3.16 (dd, *J* = 9.9, 6.6 Hz, 1H, γCH₂N), 2.66 (dd, *J* = 16.4, 6.5 Hz, 1H, αCH₂), 2.61 (dd, *J* = 16.4, 6.9 Hz, 1H, αCH₂). ¹³C NMR (150 MHz, DMSO-*d*₆): δ 171.0 (COO), 164.5 (CN₃), 163.8 (NHCOO), 51.5 (OCH₃), 51.3 (OCH₃), 50.1 (βCHN), 46.3 (γCH₂N), 38.9 (αCH₂). LC-MS (ESI) 216 [M+H]⁺.

2-(2-amino-4,5-dihydro-1H-imidazol-4-yl)acetic acid hydrochloride (3.4). Compound **3.28** (90 mg, 0.42 mmol) was dissolved in 2M HCl (20 mL). The reaction mixture was stirred at reflux for five days. The reaction mixture was washed with EtOAc (2 × 10 mL) and the water phase was evaporated under reduced pressure. The product was taken in water and the solvent

was evaporated two times. The crude product (69 mg, 92%) was triturated with Et₂O to give compound **3.4** (55 mg, 73% yield) as pale yellow solid: mp 136–142 °C. ¹H NMR (600 MHz, D₂O): δ 4.42 (dq, *J* = 9.5, 6.5 Hz, 1H, βCHN), 3.92 (t, *J* = 9.8 Hz, 1H, γCH₂N), 3.48 (dd, *J* = 10.0, 6.3 Hz, 1H, γCH₂N), 2.80 (d, *J* = 6.6 Hz, 2H, αCH₂). ¹³C NMR (150 MHz, D₂O): δ 174.8 (COO), 159.4 (CN₃), 51.6 (βCHN), 47.7 (γCH₂N), 38.7 (αCH₂). Anal. calcd (C₅H₉N₃O₂·1.35HCl): C, 31.22; H, 5.42; N, 21.84. Found: C, 31.39; H, 5.71; N 21.53. LC-MS (ESI) 144 [M+H]⁺.

3-hydroxy-4-(3-(methoxycarbonyl)ureido)butanoic acid (3.29). 1,3-Bis(methoxycarbonyl)-2-methyl-2-thiopseudourea (0.48 g, 2.3 mmol) was added to a solution of 4-Amino-3-hydroxybutanoic acid (**3.20**, 0.25 g, 2.1 mmol) in MeOH/water (4:1 *v/v*, 50 mL). The reaction mixture was stirred at 75 °C for 48 h and then the solvent was evaporated *in vacuo*. Purification by flash chromatography (CH₂Cl₂/MeOH, gradient from 10% to 50% MeOH) afforded **3.29** (0.16, 34%) as amorphous solid. ¹H NMR (600 MHz, D₂O): δ 10.01 (br. s, 1H), 7.91 (t, *J* = 5.4 Hz, 1H), 3.79–3.72 (m, 1H), 3.64 (s, 3H), 3.22 (ddd, *J* = 13.0, 5.9, 4.4 Hz, 1H), 3.03–2.97 (m, 1H), 2.09 (dd, *J* = 15.1, 4.0 Hz, 1H), 1.99 (dd, *J* = 15.0, 8.4 Hz, 1H). ¹³C NMR (150 MHz, D₂O): δ 175.5, 154.9, 152.8, 66.6, 52.3, 45.0, 40.7.

2-(2-((ethoxycarbonyl)amino)-4,5-dihydrooxazol-5-yl)acetic acid (3.31). Ethoxycarbonyl isothiocyanate (1.1 mL, 9.2 mmol) was added to a stirred suspension of 4-amino-3-hydroxybutanoic acid (**3.20**, 1.0 g, 8.4 mmol) in anhydrous tetrahydrofuran (60 mL) and stirred at 40 °C for 12 h. Mercury (II) acetate (2.9 g, 9.2 mmol) was added to the resulting yellow solution and stirred at 40 °C for 24 h. The black suspension was filtered through a short layer of celite, and the solvent was evaporated *in vacuo*. Trituration with Et₂O afforded **3.31** (1.17 g, 65%) as white solid. ¹H NMR (600 MHz, DMSO-*d*₆): δ 12.54 (br. s, 1H), 8.81 (br. s, 1H), 4.94 (dtd, *J* = 8.9, 7.3, 5.8 Hz, 1H), 3.97 (qd, *J* = 7.1, 1.7 Hz, 2H), 3.82 (dd, *J* = 9.8, 8.9 Hz, 1H), 3.41 (dd, *J* = 9.9, 7.4 Hz, 1H), 2.79 (dd, *J* = 16.7, 5.8 Hz, 1H), 2.72 (dd, *J* = 16.7, 7.2 Hz, 1H), 1.15 (t, *J* = 7.1 Hz, 3H). ¹³C NMR (150 MHz, DMSO-*d*₆): δ 170.9, 165.6, 162.8, 73.7, 60.0, 47.3, 38.4, 14.4.

(E)-methyl 4-bromopent-2-enoate (3.36a). A solution of ethyl (*E*)-pent-2-enoic acid (**3.35a**, 3.0 g, 29.9 mmol) in dichloroethane (30 mL) was made reacted with *N*-bromosuccinimide (5.32 g, 29.9 mmol) and AIBN (30 mg, 0.18 mmol). (Attention: it is reported that the reaction may become uncontrollable if not cooled properly). The reaction mixture was then stirred at reflux for 6 h. After cooling to rt, the solid was removed by filtration and washed with heptane (30 mL). The organic layers were concentrated under vacuum to give (*E*)-4-bromopent-2-enoic acid as a pale brown sticky oil (6.61 g). The crude product was used in the next reaction without any

further purification. ^1H NMR (400 MHz, DMSO- d_6): δ 12.55 (br s, 1H, COOH), 6.89 (dd, J = 15.4, 8.2 Hz, 1H, βCH), 5.97 (d, J = 15.4 Hz, 1H, αCH), 4.94–5.12 (m, 1H, γCHBr), 1.76 (d, J = 6.6 Hz, 3H, δCH_3). A catalytic amount of sulphuric acid was added to a solution of crude (*E*)-4-bromopent-2-enoic acid (6.61 g) in methanol (100 mL). The mixture was stirred at rt for 24 h. Saturated aqueous solution of NaHCO_3 was added till pH 7, and the organic solvent was then removed by evaporation *in vacuo*. The resulting residue was extracted with Et_2O (2×20 mL). The organic layers were then combined, washed with brine, dried over anhydrous MgSO_4 , filtered and evaporated to yield the crude product. The product was purified by flash chromatography (heptane/ EtOAc 95:5 *v/v*) to obtain compound **3.36a** (2.09 g, 36%) as colourless oil. ^1H NMR (400 MHz, DMSO- d_6): δ 6.97 (dd, J = 15.5, 8.2 Hz, 1H, βCH), 6.09 (dd, J = 15.5, 1.0 Hz, 1H, αCH), 5.10–5.01 (m, 1H, γCHBr), 3.69 (s, 3H, OCH_3), 1.76 (d, J = 6.7 Hz, 3H, δCH_3). LC-MS (ESI) 193, 195 $[\text{M}+\text{H}]^+$.

Methyl 2-((4*R,5*R**)-2-amino-5-methyl-4,5-dihydrothiazol-4-yl)acetate 2,2,2-trifluoroacetate (*trans*-3.37a) and methyl 2-((4*R**,5*S**)-2-amino-5-methyl-4,5-dihydrothiazol-4-yl)acetate 2,2,2-trifluoroacetate (*cis*-3.37a).** A solution of compound **3.36a** (0.70 g, 3.6 mmol) and thiourea (0.27 g, 3.6 mmol) in acetone (20 mL) was stirred for 72 h. Then, NaHCO_3 (0.608 g, 7.24 mmol) was added and the solution was heated at reflux for two hours. The resulting mixture was filtered and the filtrate concentrated under vacuum. The crude product was purified by flash chromatography (EtOAc + 0.5% aq NH_3) to obtain the expected product (0.56 g, 82%) as sticky oil. The diastereomeric mixture was resolved using preparative HPLC (15 min gradient from 0% B to 5% B) to obtain two pairs of enantiomer: *trans*-**3.37a** (first eluted) and *cis*-**3.37a** (second eluted) as colourless sticky oils. *trans*-**3.37a** (0.24 g, 36%). t_R 9.57 min. ^1H NMR (400 MHz, D_2O): δ 4.40–4.34 (m, 1H, βCHN), 3.95 (dq, J = 6.9, 3.4 Hz, 1H, γCHS), 3.78 (s, 3H, OCH_3), 2.96–2.82 (m, 2H, αCH_2), 1.56 (d, J = 6.9 Hz, 3H, δCH_3). ^{13}C NMR (150 MHz, D_2O): δ 172.8 (COO), 172.5 (CN_2S), 63.7 (βCHN), 52.5 (OCH_3), 48.3 (γCHS), 36.8 (αCH_2), 20.3 (δCH_3). *cis*-**3.37a** (80 mg, 12%). t_R 10.71 min. ^1H NMR (400 MHz, D_2O): δ 4.75 (dt, J = 8.2, 6.2, 1H, βCHN), 4.38–4.29 (m, 1H, γCHS), 3.78 (s, 2H, OCH_3), 2.99–2.84 (m, 2H, αCH_2), 1.42 (d, J = 7.0 Hz, 3H, δCH_3). ^{13}C NMR (150 MHz, D_2O): δ 173.1 (COO), 172.9 (CN_2S), 60.1 (βCHN), 52.6 (OCH_3), 46.5 (γCHS), 32.9 (αCH_2), 14.3 (δCH_3).

2-((4*R,5*R**)-2-amino-5-methyl-4,5-dihydrothiazol-4-yl)acetic acid hydrochloride (*trans*-3.8).** Compound *trans*-**3.37a** (0.24 g, 1.3 mmol) was dissolved in 2M HCl (15 mL) and stirred for 12 h at 55 °C. The reaction mixture was washed twice with EtOAc (2×5 mL) and the water phase was evaporated *in vacuo*. The solid thus obtained was dissolved in water (10 mL) and evaporated again. This procedure was repeated three times. The product obtained was dissolved

in a little amount of MeOH and precipitated adding Et₂O. The solid was isolated by filtration to afford **trans-3.8** as white crystals (0.13 g, 50%). mp 182–185 °C. ¹H NMR (600 MHz, D₂O): δ 4.34 (ddd, *J* = 7.8, 5.6, 3.3 Hz, 1H, βCHN), 3.95 (dq, *J* = 6.9, 3.4 Hz, 1H, γCHS), 2.89 (dd, *J* = 17.0, 5.6 Hz, 1H, αCH₂), 2.84 (dd, *J* = 17.0, 7.9 Hz, 1H, αCH₂), 1.55 (d, *J* = 6.9 Hz, 3H, δCH₃). ¹³C NMR (150 MHz, D₂O): δ 174.4 (COO), 172.5 (CN₂S), 63.8 (βCHN), 48.4 (γCHS), 36.9 (αCH₂), 20.3 (δCH₃). Anal. calcd (C₆H₁₀N₂O₂S·1HCl): C, 34.21; H, 5.26; N, 13.3; S, 15.22. Found: C, 33.89; H, 5.27; N, 13.14; S, 14.99.

2-((4*R,5*S**)-2-amino-5-methyl-4,5-dihydrothiazol-4-yl)acetic acid hydrochloride (*cis*-3.8).**

Compound **cis-3.37a** (82 mg, 0.44 mmol) was dissolved in 2M HCl (10 mL) and stirred for 12 h at 55 °C. The procedure for the synthesis of **trans-3.8** was then followed to afford compound **cis-3.8** (34 mg, 41%) as white crystals. mp 214–216 °C. ¹H NMR (600 MHz, D₂O): δ 4.63 (dt, *J* = 8.6, 6.1 Hz, 1H, βCHN), 4.35–4.30 (m, 1H, γCHS), 2.91 (d, *J* = 17.1, 8.7 Hz, 1H, αCH₂), 2.86 (dd, *J* = 17.1, 5.6 Hz, 1H, αCH₂), 1.43 (d, *J* = 7.0 Hz, 3H, δCH₃). ¹³C NMR (150 MHz, D₂O): δ 174.6 (COO), 173.1 (CN₂S), 60.4 (βCHN), 46.5 (γCHS), 33.1 (αCH₂), 14.4 (δCH₃). Anal. calcd (C₆H₁₀N₂O₂S·1.4HCl): C, 31.99; H, 5.10; N, 12.44; S, 14.23. Found: C, 32.14; H, 4.98; N, 12.29; S, 14.37.

Ethyl 4-bromo-3-methylbut-2-enoate (3.36b).¹¹⁸ To an ice-cooled (0 °C) solution of ethyl 3-methylbut-2-enoate (**3.35b**, 3.0 g, 23.4 mmol) in dichloroethane (30 mL), N-bromosuccinimide (4.17 g, 23.4 mmol) and AIBN (30 mg, 0.183 mmol) were added in small portions under a nitrogen atmosphere (Attention: it is reported that the reaction may become uncontrollable if not cooled properly). Upon completion of the addition, the reaction mixture was heated at reflux for 6 h. After cooling to rt, the solid was removed by filtration and washed with heptane (30 mL). The organic layers were evaporated *in vacuo* to give an oil, which was purified by flash chromatography (heptane/EtOAc 99:1 v/v). A 85:15 mixture of (*E*)- and (*Z*)- **3.36b** (1.63 g, 34%) was obtained as yellowish oil. ¹H NMR (400 MHz, DMSO-*d*₆): δ 6.09 (q, *J* = 1.0 Hz, 1H, αCH), 5.86 (q, *J* = 1.4 Hz, 1H, αCH), 4.62 (s, 2H, γCH₂), 4.23 (s, 2H, γCH₂), 4.12 (q, *J* = 7.1, 2H, OCH₂CH₃), 4.10 (q, *J* = 7.1, 2H, OCH₂CH₃), 2.17 (d, *J* = 1.3, 3H, CH₃), 2.00 (d, *J* = 1.4, 3H, CH₃), 1.21 (t, *J* = 7.1, 3H, OCH₂CH₃), 1.20 (t, *J* = 7.1, 3H, OCH₂CH₃). LC-MS (ESI) 207-209 [M+H]⁺.

Ethyl 2-(2-amino-4-methyl-4,5-dihydrothiazol-4-yl)acetate (3.37b). A solution of compound **3.36b** (0.70 g, 3.4 mmol), and thiourea (0.26 g, 3.4 mmol) in acetone (20 mL) was stirred for 12 h. Then NaHCO₃ (0.57 g, 6.7 mmol) was added and the solution was heated at reflux for two hours. The resulting mixture was filtered and the filtrate concentrated *in vacuo*. The crude product was purified by flash chromatography (EtOAc + 0.5% aq NH₃) to afford compound

3.37b as sticky oil (0.345 g, 50%). ^1H NMR (400 MHz, D_2O): δ 4.20 (qd, $J = 7.1, 2.6$ Hz, 2H, OCH_2CH_3), 3.59 (d, $J = 11.2$ Hz, 1H, $\gamma\text{CH}_2\text{S}$), 3.31 (d, $J = 11.2$ Hz, 1H, $\gamma\text{CH}_2\text{S}$), 2.67 (d, $J = 3.5$ Hz, 2H, αCH_2), 1.42 (s, 3H, CH_3), 1.30 (t, $J = 7.1$ Hz, 3H, OCH_2CH_3). ^{13}C NMR (100 MHz, $\text{DMSO}-d_6$): δ 170.5, 157.7, 74.2, 59.7, 44.6, 43.8, 26.2, 14.1. LC-MS (ESI) 203 $[\text{M}+\text{H}]^+$.

2-(2-amino-4-methyl-4,5-dihydrothiazol-4-yl)acetic acid hydrochloride (3.9). A solution of **3.37b** (0.30 g, 1.5 mmol) in 2M HCl (15 mL) was stirred at 55 °C for 12 h. The reaction mixture was washed twice with EtOAc (2×5 mL) and the water phase was evaporated *in vacuo*. The yellow solid thus obtained was dissolved in water (10 mL) and evaporated again. This procedure was repeated three times. The product obtained was dissolved in a little amount of MeOH and precipitated adding Et_2O . The white crystals were isolated by filtration to afford compound **3.9** (0.29 g, 91%). mp 222–224 °C. ^1H NMR (600 MHz, D_2O): δ 3.71 (d, $J = 11.6$ Hz, 1H, $\gamma\text{CH}_2\text{S}$), 3.57 (d, $J = 11.9$ Hz, 1H, $\gamma\text{CH}_2\text{S}$), 2.97 (d, $J = 15.8$ Hz, 1H, αCH_2), 2.87 (d, $J = 15.8$ Hz, 1H, αCH_2), 1.61 (s, 3H, CH_3). ^{13}C NMR (150 MHz, D_2O): δ 173.8 (COO), 172.0 (CN_2S), 65.7 (βCNC_3), 42.4 (αCH_2), 41.1 ($\gamma\text{CH}_2\text{S}$), 23.8 (CH_3). LC-MS (ESI) 175 $[\text{M}+\text{H}]^+$. Anal. calcd ($\text{C}_6\text{H}_{10}\text{N}_2\text{O}_2\text{S}\cdot\text{HCl}$): C, 34.21; H, 5.26; N, 13.30; S, 15.22. Found: C, 34.30; H, 5.24; N, 12.90; S, 15.25.

(*R)-2-((*R**)-2-amino-4,5-dihydrothiazol-4-yl)propanoic acid hydrochloride (*l*-3.10)** and **(*R**)-2-((*S**)-2-amino-4,5-dihydrothiazol-4-yl)propanoic acid hydrochloride (*u*-3.10)**. Methyl 4-chloro-2-methylbut-2-enoate (**3.36c**, 0.417 g, 2.81 mmol) was dissolved in acetone (20 mL), thiourea (0.213 g, 2.81 mmol) was added and the reaction mixture was stirred at 55 °C for 24 h. NaHCO_3 (0.471 g, 5.61 mmol) was added and the reaction mixture refluxed for 16 h. The suspension was filtered, the solid washed with acetone and the filtrate evaporated to afford a yellowish oil. Flash chromatography ($\text{CH}_2\text{Cl}_2/\text{MeOH}$ 95:5 *v/v* + 0.5% aq NH_3) was performed affording a 8:2 mixture of *l*- and *u*- pairs of enantiomer of methyl 2-(2-amino-4,5-dihydrothiazol-4-yl)propanoate (**3.37c**, 0.44 g, 83%) as pale yellow solid. Compound **3.37c** (0.44 g, 2.3 mmol) was dissolved in 2M HCl (25 mL) and stirred at 60 °C for 8 h. The reaction mixture was allowed to reach rt and then evaporated affording the desired compound (0.50 g, 100%) as white solid. The diastereomeric mixture was resolved using preparative HPLC (8 min 0% B) and then converted in the hydrochloric salt using 2M HCl. Two pairs of enantiomers were obtained: ***l*-3.10** (first eluted) and ***u*-3.10** (second eluted) as white solids. ***l*-3.10** (80 mg, 16%): mp 168–172 °C. t_{R} 6.42 min. ^1H NMR (600 MHz, D_2O): δ 4.65 (dt, $J = 8.4, 5.5$ Hz, 1H, βCHN), 3.85 (dd, $J = 11.7, 8.5$ Hz, 1H, $\gamma\text{CH}_2\text{S}$), 3.51 (dd, $J = 11.6, 5.3$ Hz, 1H, $\gamma\text{CH}_2\text{S}$), 2.97 (m, 1H, αCH), 1.29 (d, $J = 7.1$ Hz, 3H, $\text{CH}_3\alpha\text{CH}$). ^{13}C NMR (150 MHz, D_2O): δ 177.5 (COO), 173.9 (CN_2S), 62.2 (βCHN), 42.3 (αCH), 33.4 ($\gamma\text{CH}_2\text{S}$), 11.8 ($\text{CH}_3\alpha\text{CH}$). Anal. calcd. ($\text{C}_6\text{H}_{10}\text{N}_2\text{O}_2\text{S}\cdot 1.65\text{HCl}$): C,

30.75; H, 5.01; N, 11.95; S, 13.68. Found: C, 30.99; H, 4.94; N, 11.78; S, 13.42. **u-3.10** (0.34 g, 69%): mp 215–217 °C. t_R 7.56 min. ^1H NMR (600 MHz, D_2O): δ 4.57 (td, $J = 7.8, 6.1$ Hz, 1H, βCHN), 3.81 (dd, $J = 11.6, 8.1$ Hz, 1H, $\gamma\text{CH}_2\text{S}$), 3.53 (dd, $J = 11.6, 6.1$ Hz, 1H, $\gamma\text{CH}_2\text{S}$), 2.96 (m, 1H, αCH), 1.29 (d, $J = 7.2$ Hz, 3H $\text{CH}_3\alpha\text{CH}$). ^{13}C NMR (150 MHz, D_2O): δ 177.4 (COO), 173.7 (CN₂S), 62.6 (βCHN), 42.5 (αCH_2), 33.1 ($\gamma\text{CH}_2\text{S}$), 12.5 ($\text{CH}_3\alpha\text{CH}$). Anal. calcd ($\text{C}_6\text{H}_{10}\text{N}_2\text{O}_2\text{S}\cdot 1.4\text{HCl}$): C, 34.21; H, 5.26; N, 13.3; S, 15.22. Found: C, 34.13; H, 5.27; N, 12.97; S, 15.18.

2-(2-amino-4,5-dihydrothiazol-4-yl)propanoic acid (l-3.10a) and **2-(2-amino-4,5-dihydrothiazol-4-yl)propanoic acid (l-3.10b)**. Compound **l-3.10** (40 mg, 0.19 mmol) was dissolved in Milli-Q H_2O to a concentration of 3.7 mg mL^{-1} , filtered (45 μm , Millipore) and separated using a CHIROBIOTIC T column, Milli-Q $\text{H}_2\text{O}/\text{MeOH}$ (9:1) as mobile phase and injections volumes of 150 μL . The fractions containing the pure enantiomers were evaporated *in vacuo* affording **l-3.10a** (first eluted) and **l-3.10b** (second eluted) as pale yellow solids. **l-3.10a** (14 mg, 86%): > 99% ee. t_R 54.4 min. ^1H NMR (600 MHz, $\text{D}_2\text{O}+\text{NaOD}$, int. ref. 1,4-dioxane): δ 3.10–3.02 (m, 1H), 2.70–2.61 (m, 1H), 2.47 (dd, $J = 12.4, 6.1$ Hz, 1H), 2.41 (dd, $J = 12.5, 8.4$ Hz, 1H), 0.92 (d, $J = 7.4$ Hz, 3H). ^{13}C NMR (150 MHz, $\text{D}_2\text{O}+\text{NaOD}$, int. ref. 1,4-dioxane): δ 186.3, 169.4, 64.7, 45.9, 30.7, 11.7. ^1H -NMR and ^{13}C -NMR were identical to those of the racemic mixture in the same solvent. **l-3.10b** (13.5 mg, 83%): > 95% ee. t_R 58.3 min. ^1H -NMR and ^{13}C -NMR were identical to those of the racemic mixture in the same solvent.

Determination of ionization constants.

The ionization constants of compounds IAA and **3.2–3.5** were determined by potentiometric titration with the GLpKa apparatus (Sirius Analytical Instruments Ltd, Forest Row, East Sussex, UK). The pKa values were obtained as mean of four titrations: aqueous solutions (ionic strength adjusted to 0.15M with KCl) of the compound (20 mL, about 1 mM) were initially acidified to pH 1.8 with 0.5 N HCl and then titrated with standardized 0.5N KOH to pH 12.2 at constant temperature of 25 (± 0.1) °C under argon atmosphere.

Pharmacology

Characterization in [^3H]muscimol binding affinity study: please refer to Petersen *et al.* for experimental details.⁵⁶

Functional characterization in the FMP assay: please refer to Petersen *et al.* for experimental details.⁵⁶

Cell-based [^3H]GABA uptake assay: please refer to Al-Khawaja *et al.*¹⁵ and to Kragholm *et al.* for experimental details.¹²²

Structure elucidation of compounds (*S*)-3.5 and *u*-3.10.

Please refer to Supplementary Information.

References

1. Roberts, E.; Frankel, S. γ -Aminobutyric acid in brain: its formation from glutamic acid. *J. Biol. Chem.* **1950**, *187*, 55-63.
2. Wingo, W. J.; Awapara, J. Decarboxylation of L-glutamic acid by brain. *J. Biol. Chem.* **1950**, *187*, 267-71.
3. Roberts, E.; Frankel, S. Glutamic acid decarboxylase in brain. *J. Biol. Chem.* **1951**, *188*, 789-95.
4. Battaglioli, G.; Martin, D. L. GABA synthesis in brain slices is dependent on glutamine produced in astrocytes. *Neurochem. Res.* **1991**, *16*, 151-6.
5. Bak, L. K.; Schousboe, A.; Waagepetersen, H. S. The glutamate/GABA-glutamine cycle: aspects of transport, neurotransmitter homeostasis and ammonia transfer. *J. Neurochem.* **2006**, *98*, 641-653.
6. Nicholls, D. G. Release of glutamate, aspartate, and γ -aminobutyric acid from isolated nerve terminals. *J. Neurochem.* **1989**, *52*, 331-41.
7. Koch, U.; Magnusson, A. K. Unconventional GABA release: mechanisms and function. *Curr. Opin. Neurobiol.* **2009**, *19*, 305-310.
8. Bormann, J. B. The 'ABC' of GABA receptors. *Trends Pharmacol. Sci.* **2000**, *21*, 16-19.
9. Bettler, B.; Kaupmann, K.; Mosbacher, J.; Gassmann, M. Molecular structure and physiological functions of GABAB receptors. *Physiol. Rev.* **2004**, *84*, 835-867.
10. Rowley, N. M.; Madsen, K. K.; Schousboe, A.; White, H. S. Glutamate and GABA synthesis, release, transport and metabolism as targets for seizure control. *Neurochem. Int.* **2012**, *61*, 546-558.
11. Owens, D. F.; Kriegstein, A. R. Is there more to GABA than synaptic inhibition? *Nat. Rev. Neurosci.* **2002**, *3*, 715-727.
12. Scimemi, A. Structure, function, and plasticity of GABA transporters. *Front. Cell. Neurosci.* **2014**, *8*, 161/1-161/14.
13. Damgaard, M.; Al-Khawaja, A.; Vogensen, S. B.; Jurik, A.; Sijm, M.; Lie, M. E. K.; Baek, M. I.; Rosenthal, E.; Jensen, A. A.; Ecker, G. F.; Froelund, B.; Wellendorph, P.; Clausen, R. P. Identification of the First Highly Subtype-Selective Inhibitor of Human GABA Transporter GAT3. *ACS Chem. Neurosci.* **2015**, *6*, 1591-1599.
14. Meldrum, B. S.; Chapman, A. G. Basic mechanisms of gabitril (tiagabine) and future potential developments. *Epilepsia* **1999**, *40*, S2-S6.
15. Al-Khawaja, A.; Petersen, J. G.; Damgaard, M.; Jensen, M. H.; Vogensen, S. B.; Lie, M. E. K.; Kragholm, B.; Brauner-Osborne, H.; Clausen, R. P.; Froelund, B.; Wellendorph, P. Pharmacological Identification of a Guanidine-Containing β -Alanine Analogue with Low Micromolar Potency and Selectivity for the Betaine/GABA Transporter 1 (BGT1). *Neurochem. Res.* **2014**, *39*, 1988-1996.
16. Sigel, E.; Steinmann, M. E. Structure, Function, and Modulation of GABAA Receptors. *J. Biol. Chem.* **2012**, *287*, 40224-40231.
17. Moss, S. J.; Smart, T. G. Constructing inhibitory synapses. *Nat. Rev. Neurosci.* **2001**, *2*, 240-250.
18. Simon, J.; Wakimoto, H.; Fujita, N.; Lalande, M.; Barnard, E. A. Analysis of the Set of GABAA Receptor Genes in the Human Genome. *J. Biol. Chem.* **2004**, *279*, 41422-41435.
19. Sieghart, W. Structure, pharmacology, and function of GABAA receptor subtypes. *Adv. Pharmacol. (San Diego, CA, U. S.)* **2006**, *54*, 231-263.
20. Olsen, R. W.; Sieghart, W. International union of pharmacology. LXX. Subtypes of γ -aminobutyric acidA receptors: classification on the basis of subunit composition, pharmacology, and function. Update. *Pharmacol. Rev.* **2008**, *60*, 243-260.
21. Whiting, P. J. GABA-A receptor subtypes in the brain: a paradigm for CNS drug discovery? *Drug Discov Today* **2003**, *8*, 445-450.

22. Sieghart, W.; Sperk, G. Subunit composition, distribution and function of GABAA receptor subtypes. *Curr. Top. Med. Chem. (Hilversum, Neth.)* **2002**, *2*, 795-816.
23. Olsen, R. W.; Sieghart, W. GABA A receptors: subtypes provide diversity of function and pharmacology. *Neuropharmacology* **2009**, *56*, 141-8.
24. Knoflach, F.; Hernandez, M.-C.; Bertrand, D. GABAA receptor-mediated neurotransmission: Not so simple after all. *Biochem. Pharmacol. (Amsterdam, Neth.)* **2016**, *115*, 10-17.
25. Mody, I. Distinguishing between GABAA receptors responsible for tonic and phasic conductances. *Neurochem. Res.* **2001**, *26*, 907-913.
26. Belelli, D.; Harrison, N. L.; Maguire, J.; Macdonald, R. L.; Walker, M. C.; Cope, D. W. Extrasynaptic GABAA receptors: form, pharmacology, and function. *J. Neurosci.* **2009**, *29*, 12757-12763.
27. Olsen, R. W. Analysis of γ -Aminobutyric Acid (GABA) Type A Receptor Subtypes Using Isosteric and Allosteric Ligands. *Neurochem. Res.* **2014**, *39*, 1924-1941.
28. Johnston, G. A. R. Advantages of an antagonist: bicuculline and other GABA antagonists. *Br. J. Pharmacol.* **2013**, *169*, 328-336.
29. Bergmann, R.; Kongsbak, K.; Soerensen, P. L.; Sander, T.; Balle, T. A unified model of the GABAA receptor comprising agonist and benzodiazepine binding sites. *PLoS One* **2013**, *8*, e52323.
30. Woods, J. H.; Katz, J. L.; Winger, G. Benzodiazepines: use, abuse, and consequences. *Pharmacol. Rev.* **1992**, *44*, 151-347.
31. Sigel, E. Mapping of the benzodiazepine recognition site on GABAA receptors. *Curr. Top. Med. Chem. (Hilversum, Neth.)* **2002**, *2*, 833-839.
32. Rudolph, U.; Moehler, H. Analysis of GABAA receptor function and dissection of the pharmacology of benzodiazepines and general anesthetics through mouse genetics. *Annu. Rev. Pharmacol. Toxicol.* **2004**, *44*, 475-498.
33. Rudolph, U.; Crestani, F.; Benke, D.; Brunig, I.; Benson, J. A.; Fritschy, J.-M.; Martin, J. R.; Bluethmann, H.; Mohler, H. Benzodiazepine actions mediated by specific γ -aminobutyric acidA receptor subtypes. *Nature (London)* **1999**, *401*, 796-800.
34. Low, K.; Crestani, F.; Keist, R.; Benke, D.; Brunig, I.; Benson, J. A.; Fritschy, J.-M.; Ruiticke, T.; Bluethmann, H.; Mohler, H.; Rudolph, U. Molecular and neuronal substrate for the selective attenuation of anxiety. *Science (Washington, D. C.)* **2000**, *290*, 131-134.
35. Crestani, F.; Keist, R.; Fritschy, J. M.; Benke, D.; Vogt, K.; Prut, L.; Bluethmann, H.; Mohler, H.; Rudolph, U. Trace fear conditioning involves hippocampal $\alpha 5$ GABAA receptors. *Proc. Natl. Acad. Sci. U. S. A.* **2002**, *99*, 8980-8985.
36. Reynolds, D. S.; Rosahl, T. W.; Cirone, J.; O'Meara, G. F.; Haythornthwaite, A.; Newman, R. J.; Myers, J.; Sur, C.; Howell, O.; Rutter, A. R.; Atack, J.; Macaulay, A. J.; Hadingham, K. L.; Hutson, P. H.; Belelli, D.; Lambert, J. J.; Dawson, G. R.; McKernan, R.; Whiting, P. J.; Wafford, K. A. Sedation and anesthesia mediated by distinct GABAA receptor isoforms. *J. Neurosci.* **2003**, *23*, 8608-8617.
37. Jurd, R.; Arras, M.; Lambert, S.; Drexler, B.; Siegwart, R.; Crestani, F.; Zaugg, M.; Vogt, K. E.; Ledermann, B.; Antkowiak, B.; Rudolph, U. General anesthetic actions in vivo strongly attenuated by a point mutation in the GABAA receptor $\beta 3$ subunit. *FASEB J.* **2003**, *17*, 250-252, 10.1096/fj.02-0611fje.
38. Rudolph, U.; Mohler, H. GABAA receptor subtypes: therapeutic potential in down syndrome, affective disorders, schizophrenia, and autism. *Annu. Rev. Pharmacol. Toxicol.* **2014**, *54*, 483-507.
39. Foster, A. C.; Kemp, J. A. Glutamate- and GABA-based CNS therapeutics. *Curr. Opin. Pharmacol.* **2006**, *6*, 7-17.
40. <https://clinicaltrials.gov/>
41. Braat, S.; Kooy, R. F. the GABAA receptor as a therapeutic target for neurodevelopmental disorders. *Neuron* **2015**, *86*, 1119-1130.

42. Dougherty, D. A. Cys-Loop Neuroreceptors: Structure to the Rescue? *Chem. Rev. (Washington, DC, U. S.)* **2008**, 108, 1642-1653.
43. Miller, P. S.; Smart, T. G. Binding, activation and modulation of Cys-loop receptors. *Trends Pharmacol. Sci.* **2010**, 31, 161-174.
44. Miller, P. S.; Aricescu, A. R. Crystal structure of a human GABAA receptor. *Nature (London, U. K.)* **2014**, 512, 270-275.
45. Laverty, D.; Thomas, P.; Field, M.; Andersen, O. J.; Gold, M. G.; Biggin, P. C.; Gielen, M.; Smart, T. G. Crystal structures of a GABAA-receptor chimera reveal new endogenous neurosteroid-binding sites. *Nat. Struct. Mol. Biol.* **2017**, 24, 977-985.
46. Miller, P. S.; Scott, S.; Masiulis, S.; De Colibus, L.; Pardon, E.; Steyaert, J.; Aricescu, A. R. Structural basis for GABAA receptor potentiation by neurosteroids. *Nat. Struct. Mol. Biol.* **2017**, 24, 986-992.
47. Corringer, P.-J.; Poitevin, F.; Prevost, M. S.; Sauguet, L.; Delarue, M.; Changeux, J.-P. Structure and pharmacology of pentameric receptor channels: From bacteria to brain. *Structure (Oxford, U. K.)* **2012**, 20, 941-956.
48. Unwin, N. Refined Structure of the Nicotinic Acetylcholine Receptor at 4Å Resolution. *J. Mol. Biol.* **2005**, 346, 967-989.
49. Brejc, K.; van Dijk, W. J.; Klaassen, R. V.; Schuurmans, M.; van der Oost, J.; Smit, A. B.; Sixma, L. K. Crystal structure of an ACh-binding protein reveals the ligand-binding domain of nicotinic receptors. *Nature (London, U. K.)* **2001**, 411, 269-276.
50. Hilf, R. J. C.; Dutzler, R. X-ray structure of a prokaryotic pentameric ligand-gated ion channel. *Nature (London, U. K.)* **2008**, 452, 375-379.
51. Bocquet, N.; Nury, H.; Baaden, M.; Le Poupon, C.; Changeux, J.-P.; Delarue, M.; Corringer, P.-J. X-ray structure of a pentameric ligand-gated ion channel in an apparently open conformation. *Nature (London, U. K.)* **2009**, 457, 111-114.
52. Hibbs, R. E.; Gouaux, E. Principles of activation and permeation in an anion-selective Cys-loop receptor. *Nature (London, U. K.)* **2011**, 474, 54-60.
53. Sander, T.; Frolund, B.; Bruun, A. T.; Ivanov, I.; McCammon, J. A.; Balle, T. New insights into the GABA(A) receptor structure and orthosteric ligand binding: receptor modeling guided by experimental data. *Proteins* **2011**, 79, 1458-77.
54. Law, R. J.; Lightstone, F. C. Modeling neuronal nicotinic and GABA receptors: important interface salt-links and protein dynamics. *Biophys. J.* **2009**, 97, 1586-1594.
55. Naffaa, M. M.; Chebib, M.; Hibbs, D. E.; Hanrahan, J. R. Comparison of templates for homology model of $\rho 1$ GABAC receptors: More insights to the orthosteric binding site's structure and functionality. *J. Mol. Graphics Modell.* **2015**, 62, 43-55.
56. Petersen, J. G.; Bergmann, R.; Krosggaard-Larsen, P.; Balle, T.; Frolund, B. Probing the Orthosteric Binding Site of GABAA Receptors with Heterocyclic GABA Carboxylic Acid Bioisosteres. *Neurochem. Res.* **2014**, 39, 1005-1015.
57. Krosggaard-Larsen, P.; Frolund, B.; Kristiansen, U.; Frydenvang, K.; Ebert, B. GABAA and GABAB receptor agonists, partial agonists, antagonists and modulators: design and therapeutic prospects. *Eur. J. Pharm. Sci.* **1997**, 5, 355-384.
58. Krall, J.; Krosggaard-Larsen, P.; Kristiansen, U.; Balle, T.; Krosggaard-Larsen, N.; Sorensen, T. E.; Frolund, B. GABAA receptor partial agonists and antagonists: structure, binding mode, and pharmacology. *Adv Pharmacol* **2015**, 72, 201-27.
59. Madsen, C.; Jensen, A. A.; Liljefors, T.; Kristiansen, U.; Nielsen, B.; Hansen, C. P.; Larsen, M.; Ebert, B.; Bang-Andersen, B.; Krosggaard-Larsen, P.; Frolund, B. 5-Substituted Imidazole-4-acetic Acid Analogues: Synthesis, Modeling, and Pharmacological Characterization of a Series of Novel γ -Aminobutyric AcidC Receptor Agonists. *J. Med. Chem.* **2007**, 50, 4147-4161.
60. Krosggaard-Larsen, P.; Frolund, B.; Frydenvang, K. GABA uptake inhibitors: design, molecular pharmacology and therapeutic aspects. *Curr. Pharm. Des.* **2000**, 6, 1193-1209.

61. Frolund, B.; Tagmose, L.; Liljefors, T.; Stensbol, T. B.; Engblom, C.; Kristiansen, U.; Krogsgaard-Larsen, P. A Novel Class of Potent 3-Isoxazolol GABAA Antagonists: Design, Synthesis, and Pharmacology. *J. Med. Chem.* **2000**, *43*, 4930-4933.
62. Krogsgaard-Larsen, P.; Frolund, B.; Liljefors, T. Specific GABAA agonists and partial agonists. *Chem. Rec.* **2002**, *2*, 419-430.
63. Krogsgaard-Larsen, P.; Frolund, B.; Liljefors, T.; Ebert, B. GABAA agonists and partial agonists: THIP (Gaboxadol) as a non-opioid analgesic and a novel type of hypnotic. *Biochem. Pharmacol.* **2004**, *68*, 1573-1580.
64. Hoeg, S.; Greenwood, J. R.; Madsen, K. B.; Larsson, O. M.; Froelund, B.; Schousboe, A.; Krogsgaard-Larsen, P.; Clausen, R. P. Structure-activity relationships of selective GABA uptake inhibitors. *Curr. Top. Med. Chem. (Sharjah, United Arab Emirates)* **2006**, *6*, 1861-1882.
65. Moller, H. A.; Sander, T.; Kristensen, J. L.; Nielsen, B.; Krall, J.; Bergmann, M. L.; Christiansen, B.; Balle, T.; Jensen, A. A.; Frolund, B. Novel 4-(piperidin-4-yl)-1-hydroxypyrazoles as γ -aminobutyric acidA receptor ligands: synthesis, pharmacology, and structure-activity relationships. *J. Med. Chem.* **2010**, *53*, 3417-3421.
66. Petersen, J. G.; Sorensen, T.; Damgaard, M.; Nielsen, B.; Jensen, A. A.; Balle, T.; Bergmann, R.; Frolund, B. Synthesis and pharmacological evaluation of 6-aminonicotinic acid analogues as novel GABA(A) receptor agonists. *Eur J Med Chem* **2014**, *84*, 404-16.
67. Krall, J.; Brygger, B. M.; Sigurethardottir, S. B.; Ng, C. K. L.; Bundgaard, C.; Kehler, J.; Nielsen, B.; Bek, T.; Jensen, A. A.; Frolund, B. Discovery of α -Substituted Imidazole-4-acetic Acid Analogues as a Novel Class of $\rho 1$ γ -Aminobutyric Acid Type A Receptor Antagonists with Effect on Retinal Vascular Tone. *ChemMedChem* **2016**, *11*, 2299-2310.
68. Hoestgaard-Jensen, K.; Dalby, N. O.; Krall, J.; Hammer, H.; Krogsgaard-Larsen, P.; Froelund, B.; Jensen, A. A. Probing $\alpha 4\beta\delta$ GABAA receptor heterogeneity: differential regional effects of a functionally selective $\alpha 4\beta 1\delta / \alpha 4\beta 3\delta$ receptor agonist on tonic and phasic inhibition in rat brain. *J. Neurosci.* **2014**, *34*, 16256-16272/1-16256-16272/17, 17 pp.
69. Hoestgaard-Jensen, K.; O'Connor, R. M.; Dalby, N. O.; Simonsen, C.; Finger, B. C.; Golubeva, A.; Hammer, H.; Bergmann, M. L.; Kristiansen, U.; Krogsgaard-Larsen, P.; Braeuner-Osborne, H.; Ebert, B.; Frolund, B.; Cryan, J. F.; Jensen, A. A. The orthosteric GABAA receptor ligand Thio-4-PIOL displays distinctly different functional properties at synaptic and extrasynaptic receptors. *Br. J. Pharmacol.* **2013**, *170*, 919-932.
70. Boddum, K.; Froelund, B.; Kristiansen, U. The GABAA Antagonist DPP-4-PIOL Selectively Antagonises Tonic over Phasic GABAergic Currents in Dentate Gyrus Granule Cells. *Neurochem. Res.* **2014**, *39*, 2078-2084.
71. Meanwell, N. A. Synopsis of Some Recent Tactical Application of Bioisosteres in Drug Design. *J. Med. Chem.* **2011**, *54*, 2529-2591.
72. Lolli, M.; Narramore, S.; Fishwick, C. W. G.; Pors, K. Refining the chemical toolbox to be fit for educational and practical purpose for drug discovery in the 21st Century. *Drug Discovery Today* **2015**, *20*, 1018-1026.
73. Ballatore, C.; Huryn, D. M.; Smith, A. B. Carboxylic Acid (Bio)Isosteres in Drug Design. *ChemMedChem* **2013**, *8*, 385-395.
74. Johnston, G. A. R.; Curtis, D. R.; De Groat, W. C.; Duggan, A. W. Central actions of ibotenic acid and muscimol. *Biochem. Pharmacol.* **1968**, *17*, 2488-9.
75. Bowden, K.; Drysdale, A. C.; Mogyey, G. A. Constituents of Amanita muscaria. *Nature (London, U. K.)* **1965**, *206*, 1359-60.
76. Krogsgaard-Larsen, P.; Johnston, G. A. R.; Lodge, D.; Curtis, D. R. A new class of GABA agonist. *Nature (London)* **1977**, *268*, 53-5.
77. Krogsgaard-Larsen, P.; Hjeds, H.; Curtis, D. R.; Lodge, D.; Johnston, G. A. R. Dihydromuscimol, thiomuscimol and related heterocyclic compounds as GABA analogs. *J. Neurochem.* **1979**, *32*, 1717-24.
78. Byberg, J. R.; Labouta, I. M.; Falch, E.; Hjeds, H.; Krogsgaard-Larsen, P.; Curtis, D. R.; Gynther, B. D. Synthesis and biological activity of a GABAA agonist which has no effect on

- benzodiazepine binding and of structurally related glycine antagonists. *Drug Des Deliv* **1987**, 1, 261-74.
79. Kristiansen, U.; Lambert, J. D. C.; Falch, E.; Krogsgaard-Larsen, P. Electrophysiological studies of the GABAA receptor ligand, 4-PIOL, on cultured hippocampal neurons. *Br. J. Pharmacol.* **1991**, 104, 85-90.
80. Petersen, J. G.; Bergmann, R.; Moller, H. A.; Jorgensen, C. G.; Nielsen, B.; Kehler, J.; Frydenvang, K.; Kristensen, J.; Balle, T.; Jensen, A. A.; Kristiansen, U.; Frolund, B. Synthesis and biological evaluation of 4-(aminomethyl)-1-hydroxypyrazole analogues of muscimol as gamma-aminobutyric acid(a) receptor agonists. *J Med Chem* **2013**, 56, 993-1006.
81. Hjeds, H.; Krogsgaard-Larsen, P. Synthesis of some 4-aminoalkyl-5-methyl-3-isoxazolols structurally related to muscimol and γ -aminobutyric acid (GABA). *Acta Chem. Scand., Ser. B* **1976**, B30, 567-73.
82. Krehan, D.; Frolund, B.; Ebert, B.; Nielsen, B.; Krogsgaard-Larsen, P.; Johnston, G. A. R.; Chebib, M. Aza-THIP and related analogues of THIP as GABAC antagonists. *Bioorg. Med. Chem.* **2003**, 11, 4891-4896.
83. Lolli, M. L.; Hansen, S. L.; Rolando, B.; Nielsen, B.; Wellendorph, P.; Madsen, K.; Larsen, O. M.; Kristiansen, U.; Fruttero, R.; Gasco, A.; Johansen, T. N. Hydroxy-1,2,5-oxadiazolyl moiety as bioisoster of the carboxy function. Synthesis, ionization constants, and pharmacological characterization of gamma-aminobutyric acid (GABA) related compounds. *J Med Chem* **2006**, 49, 4442-6.
84. Tosco, P.; Lolli, M. L. Hydroxy-1,2,5-oxadiazolyl moiety as bioisoster of the carboxy function. A computational study on gamma-aminobutyric acid (GABA) related compounds. *J Mol Model* **2008**, 14, 279-91.
85. Pippione, A. C.; Dosio, F.; Ducime, A.; Federico, A.; Martina, K.; Sainas, S.; Froelund, B.; Gooyit, M.; Janda, K. D.; Boschi, D.; Lolli, M. L. Substituted 4-hydroxy-1,2,3-triazoles: synthesis, characterization and first drug design applications through bioisosteric modulation and scaffold hopping approaches. *MedChemComm* **2015**, 6, 1285-1292.
86. Sainas, S.; Pippione, A. C.; Giorgis, M.; Lupino, E.; Goyal, P.; Ramondetti, C.; Buccinna, B.; Piccinini, M.; Braga, R. C.; Andrade, C. H.; Andersson, M.; Moritzer, A.-C.; Friemann, R.; Mensa, S.; Al-Kadaraghi, S.; Boschi, D.; Lolli, M. L. Design, synthesis, biological evaluation and X-ray structural studies of potent human dihydroorotate dehydrogenase inhibitors based on hydroxylated azole scaffolds. *Eur. J. Med. Chem.* **2017**, 129, 287-302.
87. Frolund, B.; Jorgensen, A. T.; Tagmose, L.; Stensbol, T. B.; Vestergaard, H. T.; Engblom, C.; Kristiansen, U.; Sanchez, C.; Krogsgaard-Larsen, P.; Liljefors, T. Novel class of potent 4-arylalkyl substituted 3-isoxazolol GABAA antagonists: synthesis, pharmacology, and molecular modeling. *J. Med. Chem.* **2002**, 45, 2454-2468.
88. Krall, J.; Kongstad, K. T.; Nielsen, B.; Sorensen, T. E.; Balle, T.; Jensen, A. A.; Frolund, B. 5-(Piperidin-4-yl)-3-hydroxypyrazole: A novel scaffold for probing the orthosteric gamma-aminobutyric acid type A receptor binding site. *ChemMedChem* **2014**, 9, 2475-85.
89. Pippione, A. C.; Giraud, A.; Bonanni, D.; Carnovale, I. M.; Marini, E.; Cena, C.; Costale, A.; Zonari, D.; Pors, K.; Sadiq, M.; Boschi, D.; Oliaro-Bosso, S.; Lolli, M. L. Hydroxytriazole derivatives as potent and selective aldo-keto reductase 1C3 (AKR1C3) inhibitors discovered by bioisosteric scaffold hopping approach. *Eur. J. Med. Chem.* **2017**, 139, 936-946.
90. Caddick, S.; Judd, D. B.; Lewis, A. K. d. K.; Reich, M. T.; Williams, M. R. V. A generic approach for the catalytic reduction of nitriles. *Tetrahedron* **2003**, 59, 5417-5423.
91. Kursanov, D. N.; Parnes, Z. N.; Loim, N. M. Applications of ionic hydrogenation to organic synthesis. *Synthesis* **1974**, 633-51.
92. Weinstock, L. M.; Davis, P.; Handelsman, B.; Tull, R. J. General synthetic system for 1,2,5-thiadiazoles. *J. Org. Chem.* **1967**, 32, 2823-8.
93. Treder, A. A New Approach to the Synthesis of Selectively Protected (2S)-1,2,4-Triaminobutane Derivatives. *Synthesis* **2005**, 14, 2281-2283.

94. Pozdnev, V. F. Activation of Carboxylic-Acids by Pyrocarbonates - Application of Di-Tert-Butyl Pyrocarbonate as Condensing Reagent in the Synthesis of Amides of Protected Amino-Acids and Peptides. *Tetrahedron Letters* **1995**, 36, 7115-7118.
95. Sainas, S.; Pippione, A.; Giraud, A.; Martina, K.; Bosca, F.; Rolando, B.; Barge, A.; Ducime, A.; Federico, A.; Grosset, S.; White, R.; Boschi, D.; Lolli, M. Regioselective N alkylation of ethyl 4-benzyloxy-1,2,3-triazolecarboxylate: a useful tool for the synthesis of carboxylic acids bioisosteres. In Submitted, 2018.
96. Albert, A.; Serjeant, E. P. *The Determination of Ionization Constants: A Laboratory Manual*. 3rd Ed. Methuen, Inc.: 1984; p 150 pp.
97. Jaguar Version 7.9. Schrödinger LLC, N. Y., NY (USA), 2012.
98. Frolund, B.; Kristiansen, U.; Brehm, L.; Hansen, A. B.; Krogsgaard-Larsen, P.; Falch, E. Partial GABAA Receptor Agonists. Synthesis and in Vitro Pharmacology of a Series of Nonannulated Analogs of 4,5,6,7-Tetrahydroisoxazolo[4,5-c]pyridin-3-ol. *J. Med. Chem.* **1995**, 38, 3287-96.
99. Krehan, D.; Storustovu, S.; Liljefors, T.; Ebert, B.; Nielsen, B.; Krogsgaard-Larsen, P.; Frolund, B. Potent 4-Arylalkyl-Substituted 3-Isothiazolol GABAA Competitive/Noncompetitive Antagonists: Synthesis and Pharmacology. *J. Med. Chem.* **2006**, 49, 1388-1396.
100. Krall, J.; Jensen, C. H.; Soerensen, T. E.; Nielsen, B.; Jensen, A. A.; Sander, T.; Balle, T.; Frolund, B. Exploring the Orthosteric Binding Site of the γ -Aminobutyric Acid Type A Receptor Using 4-(Piperidin-4-yl)-1-hydroxypyrazoles 3- or 5-Imidazolyl Substituted: Design, Synthesis, and Pharmacological Evaluation. *J. Med. Chem.* **2013**, 56, 6536-6540.
101. Watson, S. C.; Eastham, J. F. Colored indicators for simple direct titration of magnesium and lithium reagents. *J. Organomet. Chem.* **1967**, 9, 165-8.
102. Gottlieb, H. E.; Kotlyar, V.; Nudelman, A. NMR chemical shifts of common laboratory solvents as trace impurities. *J. Org. Chem.* **1997**, 62, 7512-7515.
103. Nielsen, L.; Brehm, L.; Krogsgaard-Larsen, P. GABA agonists and uptake inhibitors. Synthesis, absolute stereochemistry, and enantioselectivity of (R)-(-)- and (S)-(+)-homo- β -proline. *J. Med. Chem.* **1990**, 33, 71-7.
104. Constanti, A.; Quilliam, J. P. Comparison of the effects of GABA [γ -aminobutyric acid] and imidazoleacetic acid on the membrane conductance of lobster muscle fibers. *Brain Res.* **1974**, 79, 306-10.
105. Breckenridge, R. J.; Nicholson, S. H.; Nicol, A. J.; Suckling, C. J.; Leigh, B.; Iversen, L. Inhibition of [3H]GABA binding to postsynaptic receptors in human cerebellar synaptic membranes by carboxyl and amino derivatives of GABA. *J. Neurochem.* **1981**, 37, 837-44.
106. Defacqz, N.; Van, T.-T.; Cordi, A.; Marchand-Brynaert, J. Synthesis of C5-substituted imidazolines. *Tetrahedron Lett.* **2003**, 44, 9111-9114.
107. Martin, P. K.; Matthews, H. R.; Rapoport, H.; Thyagarajan, G. Synthesis of 1,4-substituted imidazoles. *J. Org. Chem.* **1968**, 33, 3758-61.
108. Campbell, M. M.; Mickel, S. J.; Singh, G. (\pm)-2-Amino-2-thiazoline-4-ethanoic acid; a novel, specific GABAA receptor agonist. *Bioorg. Med. Chem. Lett.* **1991**, 1, 247-8.
109. Rostami-Charati, F. Synthesis of pyrroles and thiazolanes promoted by N-methylimidazole in water. *Synlett* **2014**, 25, 2030-2032.
110. Hossaini, Z.; Rostami-Charati, F.; Moghadam, M. E.; Moghaddasi-Kochaksaraee, F. Expedient solvent-free synthesis of 1,3-thiazolanes via multicomponent reactions. *Chin. Chem. Lett.* **2014**, 25, 794-796.
111. Mulder, M. P. C.; El Oualid, F.; ter Beek, J.; Ovaa, H. A Native Chemical Ligation Handle that Enables the Synthesis of Advanced Activity-Based Probes: Diubiquitin as a Case Study. *ChemBioChem* **2014**, 15, 946-949.
112. Forrester, S. G.; Foster, J.; Robert, S.; Salim, L.; Desaulniers, J.-P. Efficient synthesis of the GABAA receptor agonist trans-4-aminocrotonic acid (TACA). *Bioorg. Med. Chem. Lett.* **2017**, 27, 4512-4513.

113. Schreiber, J.; Witkop, B. The reaction of cyanogen bromide with mono- and diamino acids. *J. Am. Chem. Soc.* **1964**, *86*, 2441-5.
114. Weinhardt, K.; Wallach, M. B.; Marx, M. Synthesis and antidepressant profiles of phenyl-substituted 2-amino- and 2-[(alkoxycarbonyl)amino]-1,4,5,6-tetrahydropyrimidines. *J. Med. Chem.* **1985**, *28*, 694-8.
115. Weinhardt, K.; Beard, C. C.; Dvorak, C.; Marx, M.; Patterson, J.; Roszkowski, A.; Schuler, M.; Unger, S. H.; Wagner, P. J.; Wallach, M. B. Synthesis and central nervous system properties of 2-[(alkoxycarbonyl)amino]-4(5)-phenyl-2-imidazolines. *J. Med. Chem.* **1984**, *27*, 616-27.
116. McCormick, K. D.; Dong, L.; Boyce, C. W.; De Lera Ruiz, M.; Zheng, J.; Won, W. S. Spiroaminoxazoline analogs as alpha2C adrenergic receptor modulators and their preparation and use in the treatment of diseases. WO2010042475A1, 2010.
117. Ueda, S.; Terauchi, H.; Yano, A.; Ido, M.; Matsumoto, M.; Kawasaki, M. 4,5-Disubstituted-1,3-oxazolidin-2-imine derivatives: a new class of orally bioavailable nitric oxide synthase inhibitor. *Bioorg. Med. Chem. Lett.* **2004**, *14*, 313-316.
118. Atigadda, V. R.; Xia, G.; Deshpande, A.; Wu, L.; Kedishvili, N.; Smith, C. D.; Krontiras, H.; Bland, K. I.; Grubbs, C. J.; Brouillette, W. J.; Muccio, D. D. Conformationally Defined Rexinoids and Their Efficacy in the Prevention of Mammary Cancers. *J. Med. Chem.* **2015**, *58*, 7763-7774.
119. Blenderman, W. G.; Joullie, M. M.; Preti, G. Lithium ammonia reductions of 2-thiophenecarboxylic acids. *J. Org. Chem.* **1983**, *48*, 3206-13.
120. Jensen, A. A.; Bergmann, M. L.; Sander, T.; Balle, T. Ginkgolide X is a potent antagonist of anionic Cys-loop receptors with a unique selectivity profile at glycine receptors. *J Biol Chem* **2010**, *285*, 10141-53.
121. Moss, G. P. Basic terminology of stereochemistry. *Pure Appl. Chem.* **1996**, *68*, 2193-2222.
122. Kragholm, B.; Kvist, T.; Madsen, K. K.; Joergensen, L.; Vogensen, S. B.; Schousboe, A.; Clausen, R. P.; Jensen, A. A.; Brauner-Osborne, H. Discovery of a subtype selective inhibitor of the human betaine/GABA transporter 1 (BGT-1) with a non-competitive pharmacological profile. *Biochem. Pharmacol. (Amsterdam, Neth.)* **2013**, *86*, 521-528.
123. Bruker 2011. Apex2 Suite. Bruker AXS, M., Wisconsin, USA.
124. Bruker 2013. SAINT Version 8.34A. Data reduction and correction program. Bruker AXS Inc., M., Wisconsin, USA.
125. Bruker 2012. SADABS-2012/1. Bruker/Siemens Area Detector Absorption Correction program. Bruker AXS Inc., M., Wisconsin, USA.
126. Sheldrick, G. M. A short history of SHELX. *Acta Crystallogr., Sect. A: Found. Crystallogr.* **2008**, *64*, 112-122.
127. Flack, H. D. On enantiomorph-polarity estimation. *Acta Crystallogr., Sect. A: Found. Crystallogr.* **1983**, *A39*, 876-81.
128. International Tables for Crystallography; Wilson, A. J. C., Ed.; Kluwer Academic Publishers: Dordrecht, The Netherlands, 1995; Vol. C, Tables 4.2.6.8 and 6.1.1.4.
129. Farrugia, L. J. ORTEP-3 for windows - a version of ORTEP-III with a graphical user interface (GUI). *J. Appl. Crystallogr.* **1997**, *30*, 565.

Supplementary Information

HPLC chiral screening: Table SI.1	Page 86
X-ray Crystallographic Analysis of Compound (<i>S</i>)- 3.5 .	Page 87–88
X-ray Crystallographic Analysis of Compound <i>u</i> - 3.10 .	Page 89–90
Manuscript in preparation: “5-(Piperidin-4-yl)-4-hydroxy-1,2,3-triazole: A novel scaffold to probe the orthosteric γ -aminobutyric acid receptor binding site”	Page 91–104
NMR analyses of compounds included in chapter 2 (only available in the pdf version).	Page 105–140
NMR analyses of compounds included in chapter 3 (only available in the pdf version).	Page 141–162

Table SI.1 Chiral HPLC screening of compounds **3.3–3.5**, **3.13**, **3.15** and **3.28**. Ultimate 3000 HPLC system (Dionex) with a multi-wavelength UV detector (200, 210, 225, and 254 nm) and 10 mL loop. For HPLC control, data collection, and data handling, Chromeleon Software ver. 6.80 was used.

	Condition	Compounds	t_R	R_s	Comments
CHIROBIOTIC T	MeOH/H ₂ O 70/30 1.0 mLmin ⁻¹	3.3	16.1	0	The following changes did not improve the resolution: different solvent ratio, EtOH/ H ₂ O in different ratio, addition of AcOH
		3.4	17.7	0	
		3.5	16.1-17	0 small shoulder	
CROWNPAK CR(-)	HClO ₄ , pH 2, 0 °C 0.4 mLmin ⁻¹	3.4	6.0	0	Room temperature did not change the resolution
		3.5	6.6	0	
CHIRALCEL OD-H	Heptane/ EtOH/ TFA 80/20/0.5 0.8 mLmin ⁻¹	3.13	7.2	0	Flow rate of 0.4 mLmin ⁻¹ did not improve the resolution
		3.3	6.8-7.3	0 small shoulder	
		3.28	20.5	0	
		3.4	6.8-6.9	0 small shoulder	
		3.15	8.5	0	
		3.5	7.2	0	
CHIRALPAK AD-H	Heptane/ EtOH/ TFA 80/20/0.5 1.0 mLmin ⁻¹	3.13	6.0	0	
		3.3	5.7	0	
		3.28	8.6	0	
		3.4	6.2	0	
		3.15	6.4	0 small shoulder	
		3.5	6.2	0	
CELLULOSE 2	Heptane/ EtOH/ TFA 80/20/0.5 1.0 mLmin ⁻¹	3.3	11.3-12.5	0.75	Higher temperature slightly improved the resolution ($R_s \ll 1.5$)
		3.5	9.7-10.1	0 small shoulder	
CHIRALPAK AS-H	Heptane/ EtOH/ TFA 80/20/0.5 1.0 mLmin ⁻¹	3.13	12.8	0	
		3.3	10.4	0	
		3.28	12.3	0 broad tailing peaks	
		3.4	12.5-13.9	0 shoulder-tailing	
		3.15	10.7-16.8	0 broad tailing peaks	
		3.5	16.2	0 broad tailing peaks	
CHIRALPAK IF	Heptane/ EtOH/ TFA 80/20/0.5 1.0 mLmin ⁻¹	3.13	13.5	0	3.15 was resolved using CHIRALPAK IF in the condition tested and was suitable for preparative HPLC
		3.3	10.9	0	
		3.28	16.7	0	
		3.4	8.4-9.1	0 small shoulder	
		3.15	10.1-14.1	3.6	
		3.5	8.2	0	

X-ray Crystallographic Analysis of Compound (S)-3.5. (D8V3133).

Single crystals suitable for X-ray diffraction studies were grown from a solution in methanol and diethyl ether. A single crystal was mounted and immersed in a stream of nitrogen gas [$T = 123(1)$ K]. Data were collected, using graphite-monochromated $\text{CuK}\alpha$ radiation ($\lambda = 1.54178$ Å) on a Bruker D8 Venture diffractometer. Data collection and cell refinement were performed using the Bruker Apex2 Suite software.¹²³ Data reduction using SAINT¹²⁴ and multi-scan correction for absorption using SADABS-2012/1¹²⁵ were performed within the Apex2 Suite. The crystal data, data collection and the refinement data are given in Table SI.2.

Structure Solution and Preliminary Refinement.

Positions of all non-hydrogen atoms were found by direct methods (SHELXS97).¹²⁶ Full-matrix least-squares refinements (SHELXL97)¹²⁶ were performed on F^2 , minimizing $\sum w(F_o^2 - kF_c^2)^2$, with anisotropic displacement parameters of the non-hydrogen atoms. The positions of hydrogen atoms were located in subsequent difference electron density maps and were included in calculated position with fixed isotropic displacement parameters ($U_{\text{iso}} = 1.2U_{\text{eq}}$ for CH_2), except for hydrogen atoms connected to chiral C, O or N atoms. These hydrogen atoms were refined with fixed isotropic displacement parameters ($U_{\text{iso}} = 1.2U_{\text{eq}}$ for CH and NH; $U_{\text{iso}} = 1.5U_{\text{eq}}$ for OH and NH_2). Refinement (space group $P1$: 230 parameters, 2311 unique reflections) converged at $R_F = 0.0282$, $wR_F^2 = 0.0712$ [2109 reflections with $F_o > 4\sigma(F_o)$; $w^{-1} = (\sigma^2(F_o^2) + (0.0288P)^2)$, where $P = (F_o^2 + 2F_c^2)/3$; $S = 1.035$]. The residual electron density varied between -0.24 and 0.30 e \AA^{-3} . Non-centrosymmetric space group is assigned, and the absolute configuration can be determined (Flack = $0.00(2)$).¹²⁷

Two molecules are found in the asymmetric unit in the triclinic space group $P1$. The unit cell is monoclinic and the structure will be analysed for missing symmetry elements.

Complex scattering factors for neutral atoms were taken from International Tables for Crystallography as incorporated in SHELXL97.^{126, 128} Fractional atomic coordinates, a list of anisotropic displacement parameters, and a complete list of geometrical data will be deposited in the Cambridge Crystallographic Data Centre.

Table SI.2 Crystal data, data collection and preliminary refinement data for compound (*S*)-3.5.

Formula	C ₅ H ₈ N ₂ O ₂ S; HCl
Mw (g/mol)	196.65
Temperature, K	123(1)
Crystal class	triclinic (unit cell monoclinic)
Space group	<i>P1</i> *
Cell parameters	a = 7.2533(16) Å b = 6.8367(16) Å c = 8.5584(18) Å β = 101.243(11)°
V (Å ³), Z	416.25(16) / 2
F(000)	204
d _{calc} (g/cm ³)	1.569
λ (CuKα radiation)	1.54178 Å
θ _{max} (°)	5.27 < θ < 66.58
Reflections total/unique	3913/2311
R _{merge}	0.0396
Number of parameters	230
Reflections (<i>I</i> > 2 σ(<i>I</i>))	2109
<i>RI/wR2</i> (<i>I</i> > 2 σ(<i>I</i>))	0.0282/0.0712
<i>RI/wR2</i> (all reflections)	0.0332/0.0752
Goodness-of-fit on <i>F</i> ²	1.035
ρ _{max} / ρ _{min} (eÅ ⁻³)	0.30 / -0.24

* (space group will be analysed in the upcoming refinements)

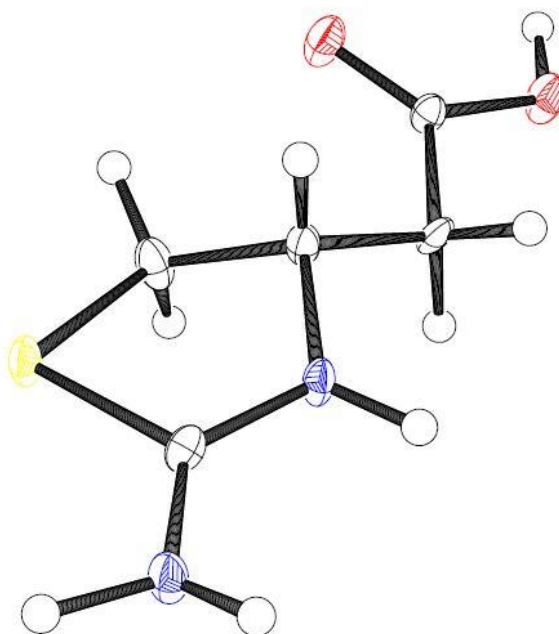


Figure SI.1 Perspective drawing (ORTEP-3¹²⁹) of compounds (*S*)-3.5. Displacement ellipsoids of the non-hydrogen atoms are shown at the 50% probability level. Hydrogen atoms have been shown as spheres of arbitrary size. Nitrogen atoms are blue, sulphur atom yellow and oxygen atoms red.

X-ray Crystallographic Analysis of Compound *u*-3.10 (D8V3132).

Single crystals suitable for X-ray diffraction studies were grown from a solution in methanol and diethyl ether. A single crystal was mounted and immersed in a stream of nitrogen gas [$T = 123(1)$ K]. Data were collected, using graphite-monochromated MoK α radiation ($\lambda = 0.71073$ Å) on a Bruker D8 Venture diffractometer. Data collection and cell refinement were performed using the Bruker Apex2 Suite software.¹²³ Data reduction using SAINT¹²⁴ and multi-scan correction for absorption using SADABS-2012/1¹²⁵ were performed within the Apex2 Suite. The crystal data, data collection and the refinement data are given in Table SI.3.

Structure Solution and Preliminary Refinement.

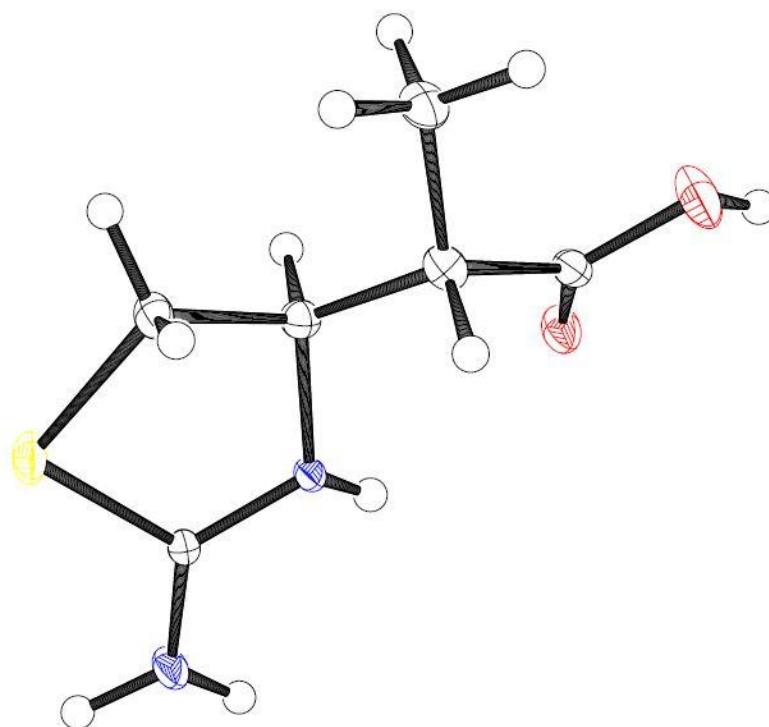
Positions of all non-hydrogen atoms were found by direct methods (SHELXS97).¹²⁶ Full-matrix least-squares refinements (SHELXL97)¹²⁶ were performed on F^2 , minimizing $\sum w(F_o^2 - kF_c^2)^2$, with anisotropic displacement parameters of the non-hydrogen atoms. The positions of hydrogen atoms were located in subsequent difference electron density maps and were included in calculated position with fixed isotropic displacement parameters ($U_{iso} = 1.2U_{eq}$ for CH₂ and $U_{iso} = 1.5U_{eq}$ for CH₃), except for hydrogen atoms connected to chiral C, O or N atoms. These hydrogen atoms were refined with fixed isotropic displacement parameters ($U_{iso} = 1.2U_{eq}$ for CH and NH; $U_{iso} = 1.5U_{eq}$ for OH, NH₂ and CH₃). Refinement (128 parameters, 5243 unique reflections) converged at $R_F = 0.0739$, $wR_F^2 = 0.1767$ [4631 reflections with $F_o > 4\sigma(F_o)$; $w^{-1} = (\sigma^2(F_o^2) + (0.0673P)^2 + 3.2063P)$, where $P = (F_o^2 + 2F_c^2)/3$; $S = 1.051$]. The residual electron density varied between -2.21 and 5.75 e Å⁻³. These residual densities will be analysed further in upcoming refinements.

Complex scattering factors for neutral atoms were taken from International Tables for Crystallography as incorporated in SHELXL97.^{126, 128} Fractional atomic coordinates, a list of anisotropic displacement parameters, and a complete list of geometrical data will be deposited in the Cambridge Crystallographic Data Centre.

Table SI.3 Crystal data, data collection and preliminary refinement data for compound ***u-3.10***.

Formula	C ₆ H ₁₀ N ₂ O ₂ S; HCl
Mw (g/mol)	210.68
Temperature, K	123(1)
Crystal class	monoclinic
Space group	<i>P</i> 2 ₁ / <i>n</i>
Cell parameters	<i>a</i> = 8.0830(11) Å <i>b</i> = 11.2667(16) Å <i>c</i> = 10.6861(16) Å β = 108.821(5)°
<i>V</i> (Å ³), <i>Z</i>	921.1(2) / 4
<i>F</i> (000)	440
<i>d</i> _{calc} (g/cm ³)	1.519
λ (CuK α radiation)	0.71073 Å
θ_{\max} (°)	2.71 < θ < 38.67
Reflections total/unique	47745/5243
<i>R</i> _{merge}	0.0351
Number of parameters	128
Reflections (<i>I</i> > 2 σ (<i>I</i>))	4631
<i>R</i> 1/ <i>wR</i> 2 (<i>I</i> > 2 σ (<i>I</i>))	0.0739/0.1767
<i>R</i> 1/ <i>wR</i> 2 (all reflections)	0.0828/0.1833
Goodness-of-fit on <i>F</i> ²	1.051
ρ_{\max} / ρ_{\min} (eÅ ⁻³)	5.75 / -2.21*

* (residual density will be analysed in the upcoming refinements)

**Figure SI.2** Perspective drawing (ORTEP-3¹²⁹) of compounds ***u-3.10***. Displacement ellipsoids of the non-hydrogen atoms are shown at the 50% probability level. Hydrogen atoms have been shown as spheres of arbitrary size. Nitrogen atoms are blue, sulphur atoms yellow and oxygen atoms red.

5-(Piperidin-4-yl)-4-hydroxy-1,2,3-triazole: A novel scaffold to probe the orthosteric γ -aminobutyric acid receptor binding site

Alessandro Giraud, Jacob Krall, Birgitte Nielsen, Troels E. Sørensen, Kenneth T. Kongstad, Barbara Rolando, Donatella Boschi, Bente Frølund* and Marco L. Lolli*

Manuscript in preparation: to be soon submitted to *Organic and Biomolecular Chemistry*

Synthesis of 5-(piperidin-4-yl)-4-hydroxy-1,2,3-triazoles: a novel scaffold to probe the orthosteric γ -aminobutyric acid receptor binding site

Received 00th January 20xx,
Accepted 00th January 20xx

DOI: 10.1039/x0xx00000x

www.rsc.org/

Alessandro Giraudo,^{a,b} Jacob Krall,^b Birgitte Nielsen,^b Troels E. Sørensen,^{b,c} Kenneth T. Kongstad,^b Barbara Rolando,^a Donatella Boschi,^a Bente Frølund,^{b,*} and Marco L. Lollo^{a,*}

Abstract. To test the potential of the hydroxytriazole moiety as bioisosteric replacement of the carboxylic acid group in GABA and related ligands, a series of N_1 - and N_2 -substituted 4-hydroxy-1,2,3-triazole analogues of the previous reported GABA_AR ligands, including muscimol, 4-PIOL, and 4-PHP, has been synthesized and characterized pharmacologically. We here report on straightforward chemical strategies, which include a directed alkylation scheme opening for further elaborative studies on the core hydroxytriazole scaffold. The unsubstituted N_1 - and N_2 -piperidin-4-yl substituted 4-hydroxy-1,2,3-triazoles analogues (**3a**, **4a**) of 4-PIOL and 4-PHP showed very low affinity (high to medium micromolar range), whereas substituting the 5-position with a 2-naphthyl or 3,3-diphenylpropyl, in general, led to binding affinities in the low micromolar range. Based on electrostatic analysis and docking studies using a $\alpha_1\beta_2\gamma_2$ GABA_AR homology model we were able to rationalize the observed divergence in SAR for the series of N_1 - and N_2 -substituted analogues offering more detailed insight into the orthosteric GABA_AR binding site.

Introduction

γ -Aminobutyric acid (GABA), the major inhibitory neurotransmitter in the central nervous system, activates the GABA_A receptors (GABA_ARs), which belongs to the family of ligand-gated ion channels. A high degree of structural heterogeneity of the GABA_ARs has been revealed and is reflected in multiple receptor subtypes built up as pentameric assemblies comprised of 19 different GABA_AR subunits; α_{1-6} , β_{1-3} , γ_{1-3} , δ , ϵ , θ , π , and ρ_{1-3} .¹ A rich and complex pharmacology has been observed based on multiple subtypes, allosteric binding sites, and diverse subcellular and regional localization.² More detailed structural insight is emerging for the GABA_ARs in terms of full-length crystal structures of related receptors and the more recent publication of the β_3 homopentameric GABA_AR.³⁻⁶ Furthermore, extensive structure-activity relationship (SAR) studies have been performed over the years.^{7,8} Consequently, a large number of potent and selective ligands for the orthosteric GABA_AR binding site have been reported. Especially, the conformational restriction of the structure of GABA by bioisosteric replacement of the carboxylic acid moiety with acidic heterocycles has been successful. Besides being carboxylic acid bioisosteres, these

heterocyclic rings allow for introduction of substituents of different shape, size, and electronic properties in well-defined positions useful for mapping the binding site.⁹

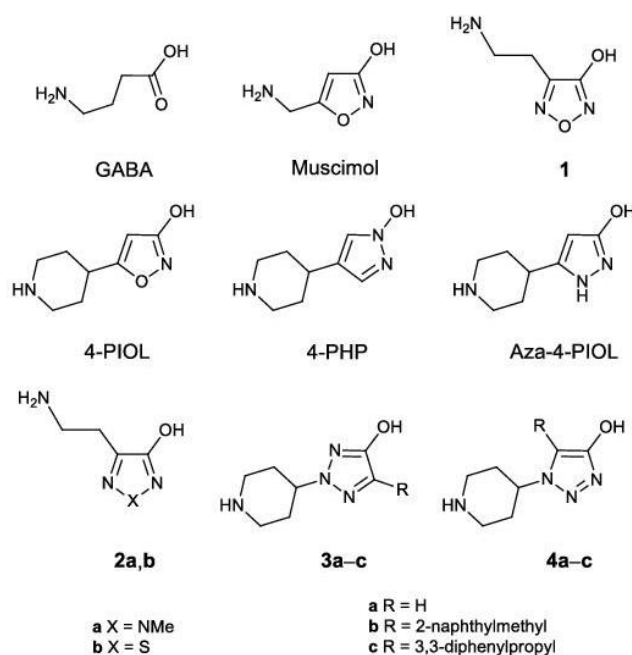


Figure 1 Reference compounds GABA, Muscimol, 4-PIOL, 4-PHP, Aza-4-PIOL and compounds **1**, **2a–b**, **3a–c** and **4a–c**.

The broad range of ligands include muscimol, 5-(piperidin-4-yl)-3-isoxazolol (4-PIOL), 4-(piperidin-4-yl)-1-hydroxypyrazole (4-PHP), and 5-(piperidin-4-yl)-3-hydroxypyrazol (aza-4-PIOL)

^a Department of Science and Drug Technology, University of Torino, Via Pietro Giuria 9, 10125 Torino, Italy. E-mail: marco.lollo@unito.it

^b Department of Drug Design and Pharmacology, University of Copenhagen, 2100 Copenhagen, Denmark. E-mail: bfr@sund.ku.dk

^c Faculty of Pharmacy, The University of Sydney, Camperdown Campus, Sydney NSW 2006 (Australia)

*Electronic Supplementary Information (ESI) available: Copies of NMR spectra, HSQC and HMBC experiment for compounds 15–18. Detailed experimental procedures for compounds 10, 19, 20 and 27. See DOI: 10.1039/x0xx00000x

analogues (Figure 1), which all have supported the development of solid GABA_AR homology models optimized for agonists or antagonist binding and identified specific cavities in the vicinity of the core part of the binding site for GABA.^{10,11}

In recent years, we have applied the *scaffold hopping* approach on various hydroxylated azole systems including thiadiazoles,¹² 1,2,5-oxadiazoles,¹³ pyrazoles,^{14, 15} isoxazoles,¹⁶ and 1,2,3-triazoles,¹⁷ whereof the hydroxy-1,2,3-triazole represents one of the most versatile but less investigated heterocycle. Due to its acidic properties (pK_a ranged from 5 to 7, depending on the nature the substituents), the hydroxy-1,2,3-triazole scaffold is deprotonated to a large extent at physiological pH and a potential isostere of the carboxylic acid function. Unlike the hydroxy-1,2,5-oxadiazole system represented in compound **1** (Figure 1), the hydroxytriazole allows effective scaffold hopping¹⁸ through regio substitution of the nitrogens in the triazole ring. Supporting the bioisosteric hypothesis for such system, we have previously reported on successful bioisosteric application of the 4-hydroxy-1,2,3-triazole mimicking the distal (*S*)-glutamic acid carboxyl group¹⁷ and the benzoic acid in brequinar,¹⁹ a dihydroorotate dehydrogenase (DHODH) inhibitor.

In the present study, we investigated the orthosteric GABA_AR binding site by introducing the 4-hydroxy-1,2,3-triazole as a new bioisostere to the carboxyl group of GABA as described for the 3-hydroxyisoxazole, hydroxy-1,2,5-oxadiazole, and 1- and 3-hydroxypyrazole moieties of reported GABA_AR ligands. To challenge the above mentioned homology model and verify the structural similarity, binding modes, and bioisosteric potential of the 4-hydroxy-1,2,3-triazole, two regioisomeric series *N*₁- and *N*₂-substituted 4-hydroxy-1,2,3-triazole analogues were synthesized (compounds **3a-c** and **4a-c**, respectively, Figure 1) corresponding to a selected subgroup of previously reported 4-PIOL, 4-PHP, and aza-4-PIOL analogues.^{14, 15, 20} The syntheses and pharmacological properties at native GABA_ARs in rat brain homogenate are reported and SARs are discussed using the above mentioned homology model.

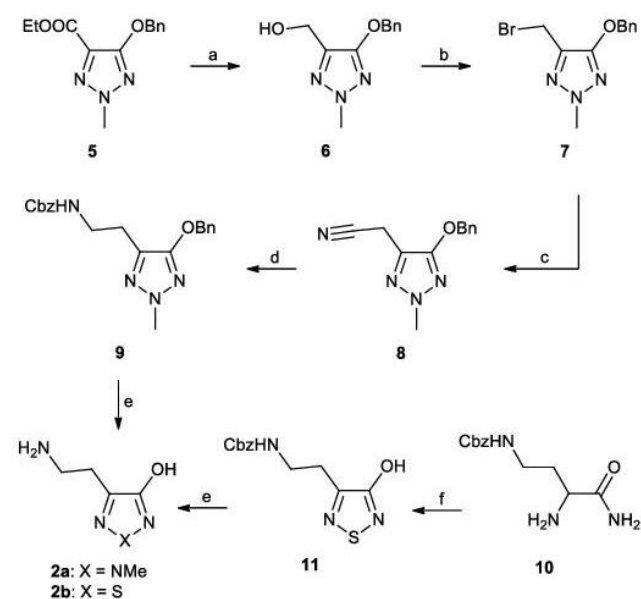
Results and discussion

Chemistry

The target compounds **2a** and **2b** were synthesized as described in Scheme 1. The alcohol **6** was obtained from compound **5**¹⁷ by reduction of the ethyl ester using LiAlH₄. Treatment of **6** with *N*-bromosuccinimide and triphenylphosphine afforded **7**, which was converted into **8** using sodium cyanide immediately upon purification due to instability of compound **7**. Following a one-pot procedure, previously described by Petersen *et al.*,^{21, 22} compound **8** was converted into **9** by reduction of the nitrile group followed by benzyloxycarbonyl (Cbz) protection of the formed amine. This latter protection of the amino group was performed to optimize the purification procedure of **9**. Deprotection of **9** under acidic conditions afforded target compound **2a**. In order to complete the scenario that involves compound **1**^{13, 23} (Figure

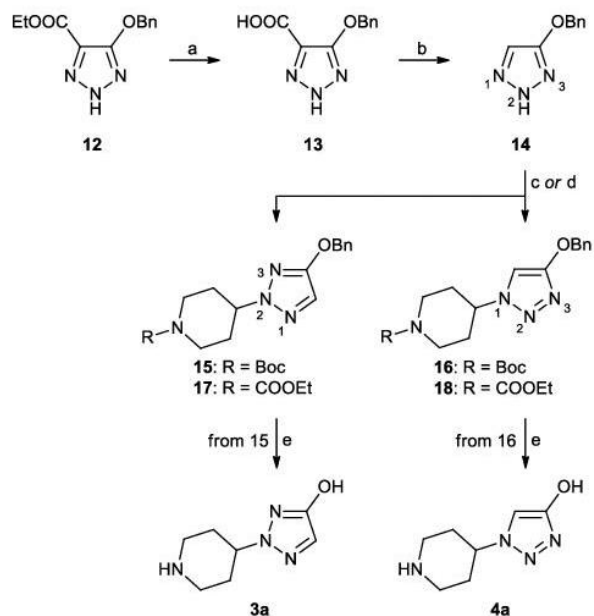
1), we synthesized the hydroxythiadiazole GABA (**2b**, Figure 1). Compound **2b** was synthesized starting from **10** (Scheme 1), a compound previously described by Treder *et al.* in high yields.²⁴ Because, in our hands, the published synthetic scheme was not reproduced in satisfactory yields, we developed an alternative method starting from glutamic acid for the synthesis of **10** (please refer to Supplementary Information for synthetic details), which was obtained in an overall yield of 8% (four steps).

Annulation of **10** and sulphur monochloride, a method previously described by Weinstock *et al.*,²⁵ and subsequent deprotection under acidic condition afforded target compound **2b**.

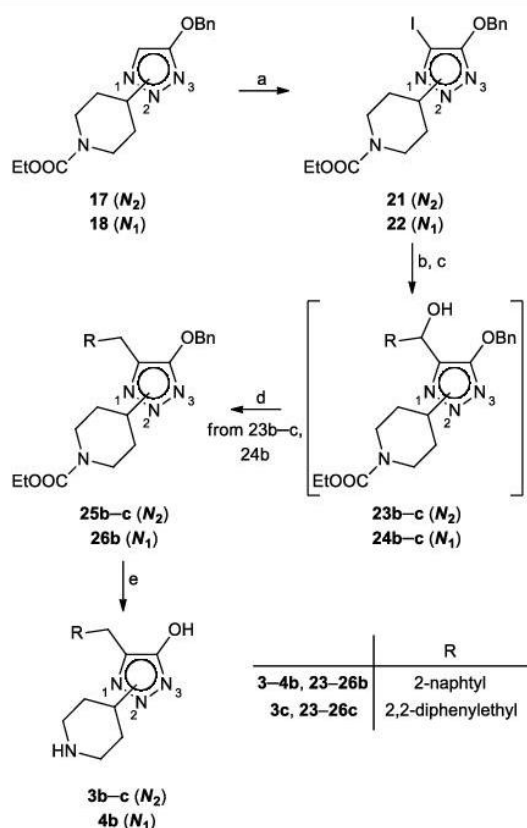


Scheme 1 Reagents and conditions: (a) LiAlH₄, THF, 0 °C to rt, (b) PPh₃, NBS, CH₂Cl₂, -10 °C, (c) NaCN, EtOH/H₂O, rt, (d) BnOCOCI, NaBH₄, NiCl₂, MeOH, 0 °C to rt, (e) 2M HCl, reflux, (f) S₂Cl₂, DMF, rt.

Target compounds **3a-c** and **4a-c** were synthesized (Scheme 2 to 4) starting from **12**, which was prepared as previously described.¹⁷ Compound **14** was obtained in two steps starting by first, hydrolysis of the ethoxycarbonyl moiety followed by decarboxylation at elevated temperatures of the formed acid (**13**). As for **12**, also compound **14** represent a valuable intermediate for the synthesis of regio substituted hydroxytriazoles. In analogy to **12**¹⁷ also **14** follow an alkylation scheme directed toward the *N*₂- and *N*₁-position of the triazole ring. Alkylation of **14** using *tert*-butyl 4-bromopiperidine-1-carboxylate (**19**) afforded a mixture of the *N*₂- (**15**) and *N*₁- (**16**) substituted regioisomers, which were isolated using standard column chromatography in 60% and 10% yields, respectively. The substitution pattern between the *N*₂ and *N*₁ position was determined by 2D NMR analyses (please refer to Supplementary Information). Subsequent deprotection of compounds **15** and **16** under acidic conditions afforded compounds **3a** and **4a**, respectively.



Scheme 2 Reagents and conditions: (a) 6M NaOH, EtOH, 50 °C, (b) DMF, 130 °C, 6h, (c) *tert*-butyl 4-bromopiperidine-1-carboxylate (**19**), K₂CO₃, CH₃CN, reflux, (d) ethyl 4-bromopiperidine-1-carboxylate (**20**), Cs₂CO₃, 1,4-dioxane, reflux, (e) 6M HCl, reflux.

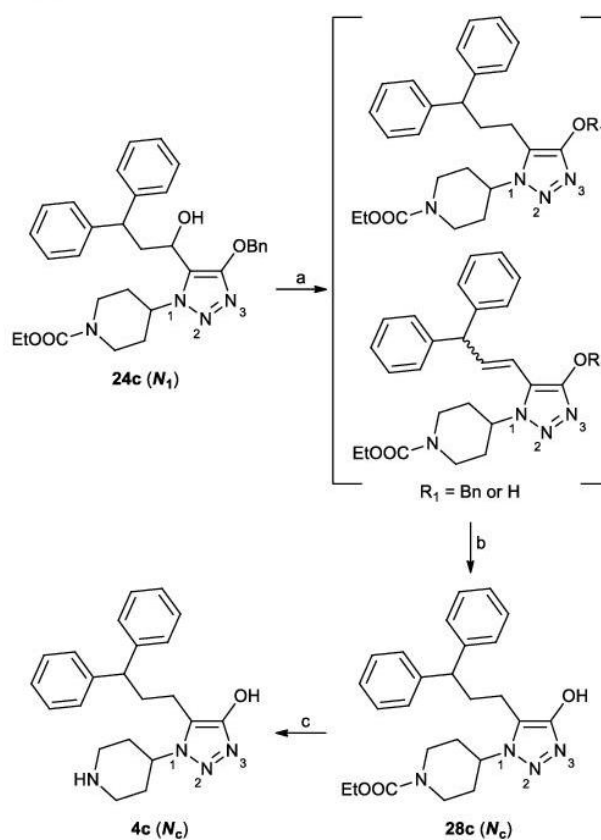


Scheme 3 Reagents and conditions: (a) ICl, AcOH, H₂O, 80 °C, (b) *i*PrMgCl, THF, -10 °C, (c) 2-naphthaldehyde or 3,3-diphenylpropanal (**27**), THF, 0 °C to rt, (d) Et₃SiH, TFA, CH₂Cl₂, 0 °C to rt, (e) 35% HCl, EtOH, reflux.

Target compounds **3b-c** and **4b-c** (Scheme 3 and 4) were obtained from intermediates **17** and **18**, which were

synthesized as described for **15** and **16** (Scheme 2), using ethyl 4-bromopiperidine-1-carboxylate (**20**). Analogously to **15** and **16**, the *N*₂ (**17**) and *N*₁ (**18**) regioisomers were obtained in 63% and 17% yield, respectively. In order to obtain a higher yield of the *N*₁ isomer, different alkylation conditions were attempted. Interestingly, caesium carbonate in anhydrous 1,4-dioxane at reflux improved the ratio between the *N*₁ and *N*₂ regioisomers and a 1:1 mixture of **18** and **17** was obtained (isolated yields of 41% and 39%, respectively).

Iodination of **17** and **18** (Scheme 3) using iodine monochloride afforded compounds **21** and **22**, which were converted into the corresponding Grignard reagents using *iso*-propylmagnesium chloride. Quenching of the Grignard reagents in situ with either 2-naphthaldehyde or 3,3-diphenylpropanal afforded the corresponding alcohol derivatives **23b-c** and **24b-c**. Ionic hydrogenation of the formed alcohol using triethylsilane and trifluoroacetic acid²⁶ followed by deprotection under acidic conditions afforded target compounds **3b-c** and **4b**.



Scheme 4 Reagents and conditions: (a) Et₃SiH, TFA, CH₂Cl₂, 50 °C, sealed tube, (b) H₂, Pd/C, MeOH, rt, (c) 35% HCl, EtOH, reflux.

In contrast to compounds **23b-c** and **24b**, the ionic hydrogenation of **24c** (Scheme 4) afforded a mixture of saturated and unsaturated products (determined using LC-MS analysis), which could not be separated using conventional purification methods. However, the crude mixture was hydrogenated using palladium on carbon, which afforded

compound **28c**. Subsequent deprotection under acidic conditions afforded target compound **4c**.

Structure-activity relationship and electrostatic properties

The synthesized compounds **2a–b**, **3a–c**, and **4a–c** were characterized in receptor binding studies using rat brain membrane preparations, where the binding affinities of the compounds at native GABA_ARs were measured by displacement of [³H]muscimol (Table 1).

As previously reported for the corresponding 3-hydroxyisoxazole²⁷ and 3-hydroxy-1,2,5-oxadiazole analogues,^{13, 23} the monocyclic analogues **2a** and **2b** showed no or low affinity for native GABA_ARs. Since these carboxylic acid isosteres show pK_a values in a range (pK_a 3.12–5.92) comparable to muscimol, a potent GABA_AR agonist, the lack of affinity might reflect a suboptimal conformation of the pharmacophoric elements of the compounds.

Also, the N₂- and N₁-substituted 4-hydroxy-1,2,3-triazole analogues of 4-PIOL (**3a** and **4a**, respectively) displayed low GABA_AR affinities in the high to medium micromolar range comparable to aza-4-PIOL and more than 5-fold lower than 4-PIOL and 4-PHP. Introduction of 2-naphthylmethyl in the 5-position of the N₁-substituted 4-hydroxy-1,2,3-triazole analogue (**4b**) led to a 20-fold increase in affinity compared to the non-substituted analogue. Similar receptor affinity was observed by introduction of the 2-naphthylmethyl substituent in the 5-position of the N₂-substituted 4-hydroxy-1,2,3-triazole analogue (**3b**). Replacing the naphthylmethyl to a more flexible 3-biphenylpropyl moiety did not change the receptor affinity for the 5-substituted N₁-substituted 4-hydroxy-1,2,3-triazole analogue (**4c**). In contrast, the corresponding structural change for the N₂-substituted 4-hydroxy-1,2,3-triazole analogue (**3c**) was detrimental for affinity and led to a compound with complete loss of GABA_AR affinity.

Considering the overall structural similarity of the core scaffolds of 4-PIOL, 4-PHP, **3a** and **4a**, and because the substituted analogues of **3a** and **4a** to an extent showed affinity, a high desolvation energy of the non-substituted analogues **3a** and **4a** could be the reason for the lack of receptor affinity observed in the binding study. A similar case was previously reported for the corresponding 3-hydroxypyrazol analogue of 4-PIOL (aza-4-PIOL).¹⁵ Using the program Jaguar,²⁸ the free energies of solvation for the zwitterionic forms of 4-PHP (−77.9 kcal/mol), aza-4-PIOL (−101.2 kcal/mol), **3a** (−88.5 kcal/mol), and **4a** (−97.2 kcal/mol) were calculated, indicating a significantly higher desolvation energy penalty for compounds **3a** and **4a** than for 4-PHP.

The heterocyclic carboxylic acid bioisosteres interacting with the GABA_AR in general resembles the electrostatic properties of the carboxylic acid in GABA.⁸ As shown for 4-PHP and aza-4-PIOL in Figure 2A,B, the electronegative charge is centred in the area around the hydroxy group and the neighbouring nitrogen allowing the ligands to interact in a bidentate manner with the conserved α₁-Arg66 in the GABA binding site. In contrast, the electrostatic profile shows a slightly different charge distribution for compounds **3a** and **4a** (Figure 2C,D)

which could indicate that this bidentate interaction could be compromised leading to reduced binding affinity.

Table 1 Pharmacological data and ionization constants for reference compounds GABA, 4-PIOL, 4-PHP, Aza-4-PIOL, 3- and 5-(2-naphMe)-4-PHP, and compounds **1**, **2a–b**, **3a–c** and **4a–c**.

	[³ H]muscimol binding K _i (μM) ^a [pK _i ±SEM]	pK _{a1} ^b
GABA	0.049 ^c	4.04 ±0.02 ^c
1	13 ^c	3.12 ±0.02 ^c
2a	>100	5.92 ±0.02
2b	75 [4.13±0.04]	4.54 ±0.03
4-PIOL	9 ^d	5.3 ^d
4-PHP	10 ^d	5.4 ^d
Aza-4-PIOL	>100 ^d	6.7 ^d
3a	>100	6.36 ±0.01
4a	55 [4.26±0.05]	6.51 ±0.03
3b	3.3 [5.49±0.04]	-
4b	2.4 [5.62±0.04]	-
3c	>100	-
4c	1.6 [5.80±0.03]	-

^a GABA_A receptor binding affinities at rat synaptic membranes: IC₅₀ values were calculated from inhibition curves and converted to K_i values. Data is given as the mean [mean pK_i ± SEM] of three to five independent experiments. ^b The ionization constants of compounds **2a–b**, **3a**, and **4a** were determined by potentiometric titration using a GLPK_s apparatus (Sirius Analytical Instruments Ltd., Forest Row, East Sussex, UK). ^c Data from Lolli *et al.*¹³ ^d Data from Krall *et al.*⁷

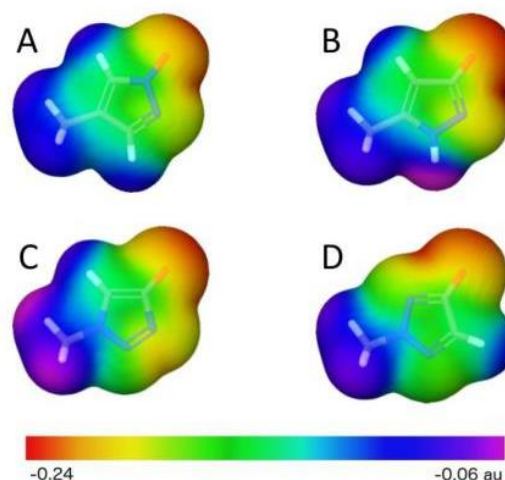


Figure 2 Electrostatic potential mapped on the surface of the molecular density for the anionic form of (A) 4-methyl-1-hydroxypyrazole, (B) 5-methyl-3-hydroxypyrazole, (C) 1-methyl-4-hydroxy-1,2,3-triazole, and (D) 2-methyl-4-hydroxy-1,2,3-triazole ring systems. Increasing negative potential coloured from purple/blue over green to red. Calculations were carried out with Jaguar²⁸ using the cc-PVDZS basis set and the B3LYP hybrid potential. Au, atomic units.

The higher pK_a values observed for the hydroxytriazoles (pK_a 6.36–6.51) compared to that of 4-PHP (pK_a 5.4), and 4-PIOL (pK_a 5.3) (Table 1) might also add to lower binding. The N₁- and N₂-substituted hydroxytriazoles, as the 3-hydroxypyrazole aza-4-PIOL, are thus less acidic than 4-PHP and protonated to a greater extent under physiological pH, which in turn might

lead to a weaker interaction in the orthosteric GABA_AR binding site.

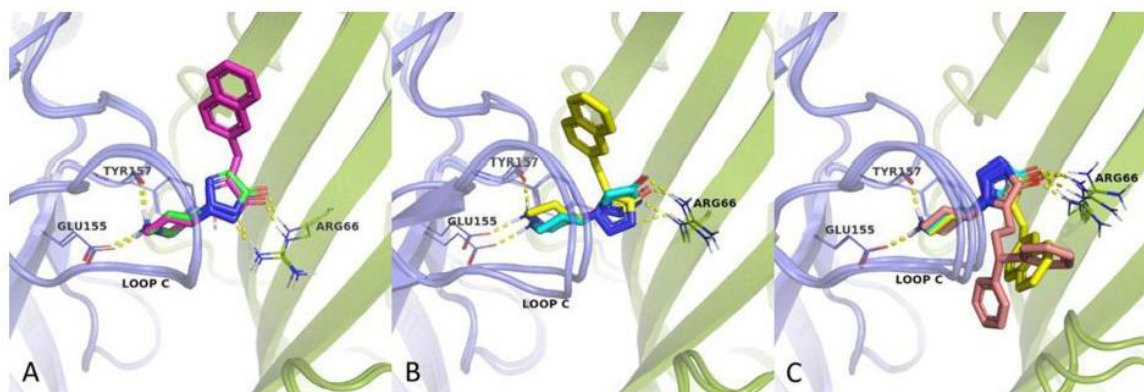


Figure 3 Compounds **3a** (A, green), **3b** (A, pink), **4a** (B and C, cyan), **4b** (B and C, yellow) and **4c** (C, salmon) docked into the $\alpha_1\beta_2\gamma_2$ GABA_AR homology model. Residues surrounding the ligand binding site from the principal side (light-teal carbons) and complementary side (olive-green carbons) are shown. Hydrogen bonds are depicted with yellow dashes.

Molecular modelling

To further assess the obtained pharmacological data the binding modes of the synthesized compounds were evaluated using the reported homology model of the $\alpha_1\beta_2\gamma_2$ GABA_AR in the antagonist bound state.¹¹ The obtained docking poses for the ligands match the binding mode previously reported,¹¹ with the amine moiety forming hydrogen bonds with β_2 -Glu155 and the backbone carbonyl of β_2 -Tyr157 and the hydroxytriazole moiety forming a bidentate interaction to α_1 -Arg66 mimicking the binding interactions of GABA.

As reported for 4-PIOL and 4-PHP, two different orientations of the triazole-piperidine core scaffold of **4a** are possible while still maintaining the bidentate interactions described above (Figure 3B,C). The naphthylmethyl substituted analogue, **4b**, is able to bind in either of the two orientations (Figure 3B,C), whereas the diphenylpropyl substituted analogue, **4c**, adopts a binding pose where the triazole moiety is found in the aforementioned alternative orientation (180° flip), thus the substituent is accommodated in the more spacious cavity below the core scaffold (Figure 3C).

The binding site optimized for **3a** shows a marked difference in the conformation of α_1 -Arg66, with the side chain moving to a position further towards the membrane, thus allowing it to form a bidentate interaction with **3a** and **3b**, and with the hydrophobic substituent reaching out into the previously reported cavity above the core scaffold (Figure 3A). The more bulky diphenylpropyl substituted analogue, **3c**, is not able to interact with α_1 -Arg66 in this conformation, likely due to limited space in the aforementioned cavity (Figure 3A). Unlike **4c**, the suggested 180° flip as described for **4a** and analogues is not optimal for this series of compounds (**5a–c**).

Conclusions

In this study we show that the 4-hydroxy-1,2,3-triazole ring system is able to replace previous identified five membered heterocyclic carboxylic acid bioisosteres as ligands for the GABA_AR. A series of 4-hydroxy-1,2,3-triazole analogues were synthesized and characterized pharmacologically at native rat

GABA_AR. In general, the synthesized N_1 - and N_2 -substituted analogues displayed affinities in the medium to low micromolar range (K_i values of 1.6–55 μ M). Despite previous identified cavities above and below the orthosteric binding site the two structural closely related series of analogues displayed slightly different SAR indicating different binding modes. These results were rationalized by using a homology model for the orthosteric binding site of the $\alpha_1\beta_2\gamma_2$ GABA_AR implying a 180° flip of the core scaffold of the N_1 -substituted analogues **4b** and **4c** enabling accommodation of the larger substituent of **4c** in the more spacious cavity below the core scaffold. This binding mode is not optimal for the corresponding N_2 -substituted analogue **3c**. All in all, the synthesis strategy applied in this study included directed alkylation of the triazole ring system useful for future application of this heterocyclic moiety, which, in the present study, has offered a more detailed insight into the architecture and flexibility of the orthosteric binding site in the GABA_AR.

Experimental section

Chemistry

Compounds **10**, **19**, **20** and **27** were synthesized as reported in Supplementary Information, while compounds **5** and **12** were prepared as described in the literature.¹⁷ All chemical reagents and solvents (analytical grade) were obtained from commercial sources (Sigma Aldrich, Alfa Aesar, or TCI) and used without further purification. Air- and/or moisture sensitive reactions were performed under a nitrogen atmosphere using syringe-septum techniques and dried glass-ware. Anhydrous solvents were dried over 4 Å molecular sieves or by distillation (THF) prior to use from Na and benzophenone under nitrogen atmosphere. ⁱPrMgCl (in THF) was titrated prior to use as described elsewhere.²⁹ Thin layer chromatography (TLC) on silica gel was carried out using 5 × 20 cm plates with a silica layer of 0.25 mm in thickness. Purification of synthesized compounds were performed using flash column chromatography on silica gel (Merck Kieselgel 60, 230-400 mesh ASTM) or by the use of a CombiFlash Rf 200

apparatus (Teledyne Isco) with 5–200 mL/min, 200 psi (with automatic injection valve) using RediSep Rf Silica columns (Teledyne Isco). Melting points (mp) were measured on a Büchi 540 apparatus in open capillary tubes and are uncorrected. Analytical high performance liquid chromatography (HPLC) analysis were performed on a Perkin Elmer Flexar UHPLC system equipped with an UHPLC Acquity BEH C18 column (1.7 μm , 2.1 \times 50 mm, Waters) and a 20 μL loop. Elution of analysed samples were performed using mixtures of eluent A ($\text{H}_2\text{O}/\text{TFA}$, 100/0.1) and eluent B ($\text{CH}_3\text{CN}/\text{TFA}$, 100/0.1) at a flow rate of 0.5 mL/min. For HPLC control, data collection, and data handling Chromera Software ver. 4.1.0 was used. Alternatively, analytical HPLC analyses were performed on an Ultimate 3000 HPLC system (Thermo Scientific) with an LPG-3400A pump, a WPS-3000SL autosampler, and a DAD-3000D detector using a Gemini[®] NX-C₁₈ column (3 μm , 110 \AA , 4.6 \times 250 mm) and eluents A ($\text{H}_2\text{O}/\text{TFA}$, 100/0.1) and B ($\text{CH}_3\text{CN}/\text{H}_2\text{O}/\text{TFA}$, 90/10/0.1) at a flow rate of 1 mL/min. For HPLC control, data collection, and data handling, Chromeleon Software ver. 6.80 was used. The purity of the analyzed compounds is $\geq 95\%$, unless otherwise stated. Preparative reversed phase HPLC was carried out on an Ultimate 3000 HPLC system (Thermo Scientific) with a LPG-3200BX pump, a Rheodyne 7125i injector, a 10 mL loop, and a MWD-3000SD detector (200, 210, 225, and 254 nm) using a preparative Phenomenex Gemini NX-C₁₈ column (5 μm , 21.2 \times 250 mm) and eluents A ($\text{H}_2\text{O}/\text{TFA}$, 100/0.1) and B ($\text{CH}_3\text{CN}/\text{H}_2\text{O}/\text{TFA}$, 90/10/0.1) at a flow rate of 20 mL/min. For HPLC control, data collection, and data handling, Chromeleon Software ver. 6.80 was used. ¹H and ¹³C NMR were recorded either on a Bruker Avance 300 MHz, a Jeol JNM-ECZR 600 MHz, or a Bruker Avance 600 MHz spectrometer equipped with a cryogenically cooled 5 mm CPDCH ¹³C[¹H] Z-GRD probe, at 300 K. Data are tabulated in the following order: chemical shift (δ) [multiplicity (b, broad; s, singlet; d, doublet; t, triplet; q, quartet; m, multiplet), coupling constant(s) *J* (Hz), number of protons]. The solvent residual peak or TMS were used as internal reference.³⁰ HPLC-HRMS analyses were performed on a system comprised of an Agilent 1200 HPLC system comprising of a quaternary pump with a built-in degasser, a thermostated column compartment, an autosampler, and a photodiode array detector, coupled with a Bruker microOTOF-QII mass spectrometer equipped with an electrospray ionization (ESI) source and operated via a 1:99 flow splitter. Mass spectra were acquired in positive ionization mode, using drying temperature of 200 $^\circ\text{C}$, a capillary voltage of -4100V , nebulizer pressure of 2.0 bar, and drying gas flow of 7 L/min. A solution of sodium formate clusters was injected in the beginning of each run to enable internal mass calibration. Chromatographic separation was acquired on a Phenomenex Luna C₁₈(2) column (150 mm \times 4.6 mm, 3 μm , 100 \AA) maintained at 40 $^\circ\text{C}$, using a flow rate of 0.8 mL/min and a linear gradient of the binary solvent system water-acetonitrile-formic acid (eluent A: 95/5/0.1, and eluent B: 5/95/0.1) rising from 0% to 100% of eluent B over 20 minutes. Data was acquired using Compass HyStar Ver. 3.2 (Bruker Daltonic

GmbH, Germany) and processed using Compass DataAnalysis Ver. 4.0 (Bruker Daltonic GmbH, Germany).

(5-(Benzyloxy)-2-methyl-2H-1,2,3-triazol-4-yl)methanol (6). LiAlH₄ (0.36 g, 9.6 mmol) was added to a cooled (0 $^\circ\text{C}$) solution of compound **5**¹⁷ (2.50 g, 9.6 mmol) in anhydrous THF (125 mL). The reaction mixture was stirred for 2 h at 0 $^\circ\text{C}$ before it was quenched with adding in sequence water (0.37 mL), 15% w/w NaOH (0.37 mL) and then water (0.37 mL). The volatiles were evaporated *in vacuo* and the residue was taken up in water. The resulting mixture was extracted with Et₂O (3 \times 100 mL) and the combined organic phase was washed with brine (150 mL), dried over anhydrous Na₂SO₄, and evaporated *in vacuo* to afford compound **6** as colourless oil (1.82 g, 87%). ¹H NMR (300 MHz, DMSO-*d*₆): δ 7.50–7.28 (m, 5H), 5.22 (s, 2H), 5.05 (t, *J* = 5.5 Hz, 1H), 4.36 (d, *J* = 5.5 Hz, 2H), 3.95 (s, 3H). ¹³C NMR (75 MHz, DMSO-*d*₆): δ 157.4, 136.5, 131.8, 128.3, 128.0, 127.8, 71.4, 52.2, 41.3. HRMS (ESI-TOF): *m/z* calculated for C₁₁H₁₂N₃O [M+H]⁺, 202.0975. Found, 202.0974 (ΔM =0.3 ppm).

4-(Benzyloxy)-5-(bromomethyl)-2-methyl-2H-1,2,3-triazole (7). PPh₃ (1.58 g, 6.0 mmol) was added to a stirred solution of **6** (1.10 g, 5.0 mmol) in anhydrous CH₂Cl₂ (30 mL) at -10 $^\circ\text{C}$. To the resulting mixture, NBS (1.07 g, 6.03 mmol) was added in small portions over 30 min. The reaction mixture was stirred for 1 h at -10 $^\circ\text{C}$ before the solvent was evaporated *in vacuo*. Purification of the resulting residue by flash chromatography (CH₂Cl₂) afforded compound **7** as colourless oil (1.13 g, 81%), which was used immediately upon purification in the synthesis of compound **8** due to stability issues of **7**. ¹H NMR (300 MHz, CDCl₃): δ 7.43–7.22 (m, 5H), 5.18 (s, 2H), 4.38 (s, 2H), 3.93 (s, 3H). ¹³C NMR (75 MHz, CDCl₃): δ 158.0, 136.2, 128.7, 128.6, 128.4, 128.0, 72.2, 42.0, 20.4.

2-(5-(Benzyloxy)-2-methyl-2H-1,2,3-triazol-4-yl)acetonitrile (8). A solution of **7** (1.13 g, 4.0 mmol) in EtOH (20 mL) was added dropwise to a solution of NaCN (0.39 g, 8.0 mmol) in EtOH/water (9:1 v/v, 25 mL). The reaction mixture was stirred for 48 h at rt before the volatiles were evaporated *in vacuo*. The resulting residue was taken up in water and extracted with EtOAc (3 \times 100 mL). The combined organic phase was washed with water (1 \times 100 mL), brine (1 \times 100 mL), dried over anhydrous Na₂SO₄, and evaporated *in vacuo*. Purification by flash chromatography (petroleum ether 40–60 $^\circ\text{C}$ /EtOAc, gradient 0%–20% EtOAc) afforded **8** as colourless oil (0.63 g, 69%). ¹H NMR (300 MHz, DMSO-*d*₆): δ 7.50–7.30 (m, 5H), 5.24 (s, 2H), 4.05–3.90 (m, 5H). ¹³C NMR (75 MHz, DMSO-*d*₆): δ 156.8, 136.1, 128.3, 128.1, 127.8, 121.8, 117.0, 71.7, 41.7, 12.3. HRMS (ESI-TOF): *m/z* calculated for C₁₂H₁₃N₄O [M+H]⁺, 229.1084. Found, 229.1085 (ΔM =0.5 ppm).

Benzyl (2-(5-(benzyloxy)-2-methyl-2H-1,2,3-triazol-4-yl)ethyl)carbamate (9). Benzyl chloroformate (0.65 mL, 4.6 mmol) and NiCl₂·6H₂O (54 mg, 0.23 mmol) were added to a stirred solution of **8** (0.52 g, 2.3 mmol) in MeOH (20 mL) at 0 $^\circ\text{C}$. NaBH₄ (0.69 g, 18 mmol) was then added in small portions

over 1 h while keeping the temperature at 0 °C, whereupon the reaction mixture was allowed to reach rt and stirred for 24 h before water was added (300 mL). The resulting mixture was extracted with CH₂Cl₂ (6 × 100 mL) and the combined organic phase was washed with brine (200 mL), dried over anhydrous Na₂SO₄, and evaporated *in vacuo*. Purification by column chromatography (petroleum ether 40–60 °C/EtOAc, gradient 0%–70% EtOAc) afforded **9** (0.28 g, 35%) as white solid: mp 44–46 °C. ¹H NMR (300 MHz, DMSO-*d*₆): δ 7.51–7.23 (m, 10H), 5.19 (s, 2H), 4.99 (s, 2H), 3.92 (s, 3H), 3.21 (q, *J* = 6.9 Hz, 2H), 2.64 (t, *J* = 7.5 Hz, 2H). ¹³C NMR (75 MHz, DMSO-*d*₆): δ 157.4, 155.9, 137.1, 136.5, 128.9, 128.3, 128.2, 127.9, 127.7, 127.65, 127.6, 71.4, 65.1, 41.2, 39.2, 23.8. HRMS (ESI-TOF): *m/z* calculated for C₂₀H₂₃N₄O₃ [M+H]⁺, 367.1765. Found, 367.1760 (ΔM=1.3 ppm).

5-(2-Aminoethyl)-2-methyl-2H-1,2,3-triazol-4-ol

hydrochloride (2a). A solution of **9** (0.18 g, 0.50 mmol) in MeOH/2M HCl (1:4 v/v, 25 mL) was refluxed for 72 hours. The resulting solution was washed with EtOAc (3 × 15 mL) and evaporated *in vacuo*. Recrystallization from ¹PrOH/Et₂O afforded **2a** (40 mg, 45%) as white solid: mp 191–192 °C. ¹H NMR (300 MHz, D₂O): δ 3.94 (s, 3H), 3.29 (t, *J* = 7.0 Hz, 2H), 2.96 (t, *J* = 7.0 Hz, 2H). ¹³C NMR (75 MHz, D₂O, int. std. MeOH): δ 156.1, 128.2, 41.5, 38.8, 21.7. HRMS (ESI-TOF): *m/z* calculated for C₅H₁₁N₄O [M+H]⁺, 143.0927. Found, 143.0927 (ΔM=0.5 ppm).

Benzyl (2-(4-hydroxy-1,2,5-thiadiazol-3-yl)ethyl)carbamate (11). A solution of S₂Cl₂ (0.45 mL, 5.7 mmol) in anhydrous DMF (20 mL) was added dropwise to a solution of **10** (0.47 g, 1.9 mmol) in anhydrous DMF (10 mL). The reaction mixture was stirred for 12 hours at rt before poured into 200 mL of iced water. The mixture was filtered, the filtrate was acidified to pH 1 and extracted with Et₂O (4 × 100 mL). The combined organic phase was washed with brine (1 × 100 mL), dried over anhydrous Na₂SO₄, and evaporated *in vacuo*. Purification by flash chromatography (CH₂Cl₂/MeOH 95:5 v/v) afforded **11** (0.090 g, 17%) as white solid: mp 86–87 °C. ¹H NMR (300 MHz, DMSO-*d*₆): δ 12.59 (br s, 1H), 7.42–7.26 (m, 5H), 4.99 (s, 2H), 3.37 (t, *J* = 7.1 Hz, 2H), 2.83 (t, *J* = 7.1 Hz, 2H). ¹³C NMR (75 MHz, DMSO-*d*₆): δ 162.5, 155.9, 149.9, 137.1, 128.2, 127.6, 127.5, 65.0, 38.1, 29.0. HRMS (ESI-TOF): *m/z* calculated for C₁₂H₁₄N₃O₃S [M+H]⁺, 280.0750. Found, 280.0744 (ΔM=2.4 ppm).

4-(2-Aminoethyl)-1,2,5-thiadiazol-3-ol hydrochloride (2b). A solution of **11** (81 mg, 0.29 mmol) in MeOH/2M HCl (1:3 v/v, 16 mL) was refluxed for 72 h. The resulting solution was washed with EtOAc (3 × 10 mL) and evaporated *in vacuo*. Trituration of the resulting residue with ¹Pr₂O afforded **2b** (34 mg, 64%) as white solid: mp 215–217 °C. ¹H NMR (600 MHz, D₂O): δ 3.49 (t, *J* = 6.8 Hz, 2H), 3.18 (t, *J* = 6.8 Hz, 2H). ¹³C NMR (150 MHz, D₂O): δ 162.0, 148.1, 37.1, 26.1. HRMS (ESI-TOF): *m/z* calculated for C₄H₈N₃OS [M+H]⁺, 146.0383. Found, 146.0385 (ΔM=1.8 ppm).

5-(Benzyloxy)-2H-1,2,3-triazole-4-carboxylic acid (13). 6M NaOH (14.2 mL, 85.0 mmol) was added to a solution of **12**¹⁷ (3.5 g, 14.2 mmol) in EtOH (100 mL). The reaction mixture was heated at 50 °C for 24 h. Upon cooling to rt, the reaction mixture was neutralized with 6M HCl and the solvents were evaporated. The residue was taken up in water and 1M HCl was added until pH 1. The resulting suspension was filtered and the solid was washed with hexane to give **13** (3.1 g, quant.) as white solid: mp 172 °C (dec.). ¹H NMR (600 MHz, DMSO-*d*₆): δ 14.05 (br s, 1H), 7.54–7.27 (m, 5H), 5.32 (s, 2H). ¹³C NMR (75 MHz, DMSO-*d*₆): δ 161.2, 159.8, 136.5, 128.4, 128.1, 128.0, 121.6, 71.5. HRMS (ESI-TOF): *m/z* calculated for C₁₀H₁₀N₃O₃ [M+H]⁺, 220.0717. Found, 220.0712 (ΔM=2.3 ppm).

4-(Benzyloxy)-2H-1,2,3-triazole (14). **13** (3.5 g, 16.0 mmol) was dissolved in anhydrous DMF (50 mL) and the resulting solution heated at 130 °C for 6 h. Upon cooling to rt, water (500 mL) was added and the mixture was extracted with Et₂O (5 × 100 mL). The combined organic phase was washed with water (2 × 100 mL), brine (2 × 100 mL), dried over anhydrous Na₂SO₄, and evaporated *in vacuo*. Purification by flash chromatography (CH₂Cl₂/EtOAc, 95:5 v/v) afforded **14** (2.25 g, 70%) as white solid: mp 100–102 °C. ¹H NMR (600 MHz, DMSO-*d*₆): δ 14.1 (br s, 1H), 7.29–7.49 (m, 6H), 5.19 (s, 2H). ¹³C NMR (75 MHz, DMSO-*d*₆): δ 160.5, 136.6, 128.4, 128.1, 128.0, 118.7, 71.4. HRMS (ESI-TOF): *m/z* calculated for C₉H₁₀N₃O [M+H]⁺, 176.0818. Found, 176.0812 (ΔM=3.6 ppm).

tert-Butyl 4-(4-(benzyloxy)-2H-1,2,3-triazol-2-yl)piperidine-1-carboxylate (15) and **tert-butyl 4-(4-(benzyloxy)-1H-1,2,3-triazol-1-yl)piperidine-1-carboxylate (16).** K₂CO₃ (1.7 g, 12.6 mmol) was added to a solution of **14** (1.1 g, 6.3 mmol) in CH₃CN (35 mL). The reaction mixture was heated at reflux and *tert*-butyl 4-bromopiperidine-1-carboxylate (**19**, 2.2 g, 8.2 mmol) was added in portions over 48 h. The reaction mixture was cooled at rt and the solvent was evaporated *in vacuo*. The resulting residue was taken up in water (200 mL) and extracted with EtOAc (3 × 100 mL). The combined organic phase was washed with brine (50 mL), dried over anhydrous Na₂SO₄, and evaporated *in vacuo*. Purification by flash chromatography (petroleum ether 40–60 °C/EtOAc, gradient 10%–40% EtOAc) afforded **15** (first eluting, *N*₂ isomer) and **16** (second eluting, *N*₁ isomer) as white solids. **15** (1.36 g, 60%): mp 87–88 °C. ¹H NMR (300 MHz, DMSO-*d*₆): δ 7.48–7.30 (m, 6H), 5.17 (s, 2H), 4.52 (tt, *J* = 10.8, 4.0 Hz, 1H), 3.94 (d, *J* = 13.3 Hz, 2H), 3.08–2.86 (m, 2H), 2.09–1.96 (m, 2H), 1.78 (qd, *J* = 4.3, 11.6 Hz, 2H), 1.41 (s, 9H). ¹³C NMR (75 MHz, DMSO-*d*₆): δ 160.1, 153.9, 136.3, 128.4, 128.2, 128.1, 118.6, 78.9, 71.5, 60.6, 41.8, 31.0, 28.0. HRMS (ESI-TOF): *m/z* calculated for C₁₉H₂₆N₄O₃Na [M+Na]⁺, 381.1897. Found, 381.1895 (ΔM=0.6 ppm). **16** (0.21 g, 10%): mp 106–107 °C. ¹H NMR (300 MHz, DMSO-*d*₆): δ 7.85 (s, 1H), 7.49–7.29 (m, 5H), 5.15 (s, 2H), 4.59 (tt, *J* = 11.3, 3.8 Hz, 1H), 4.03 (d, *J* = 12.9 Hz, 2H), 3.05–2.80 (m, 2H), 2.08–1.96 (m, 2H), 1.79 (qd, *J* = 12.2, 4.3 Hz, 2H), 1.41 (s, 9H). ¹³C NMR (75 MHz, DMSO-*d*₆): δ 160.1, 153.7, 136.5, 128.4, 128.1, 128.0, 105.6, 78.9, 71.5, 57.7, 42.1, 31.7, 28.1. HRMS (ESI-TOF): *m/z*

calculated for $C_{19}H_{27}N_4O_3$ $[M+H]^+$, 359.2078. Found, 359.2068 ($\Delta M=2.7$ ppm).

2-(Piperidine-4-yl)-2H-1,2,3-triazol-4-ol hydrochloride (3a). 15 (0.25 g, 0.70 mmol) was suspended in 6M HCl (10 mL) and the suspension was heated at reflux for 48 h. Upon cooling to rt, the reaction mixture was washed with EtOAc (2 × 10 mL) and the aqueous phase evaporated *in vacuo*. Recrystallization from EtOH/Et₂O afforded **3a** (90 mg, 63%) as white crystals: mp 259–263 °C. ¹H NMR (300 MHz, D₂O): δ 7.17 (s, 1H), 4.65 (tt, J = 10.3, 4.3 Hz, 1H), 3.52 (dt, J = 13.3, 3.9 Hz, 2H), 3.28–3.13 (m, 2H), 2.42–2.14 (m, 4H). ¹³C NMR (75 MHz, D₂O): δ 158.4, 120.1, 58.1, 42.7, 27.9. HRMS (ESI-TOF): m/z calculated for $C_7H_{13}N_4O$ $[M+H]^+$, 169.1084. Found, 169.1083 ($\Delta M=0.6$ ppm).

1-(Piperidine-4-yl)-1H-1,2,3-triazol-4-ol hydrochloride (4a). 16 (0.17 g, 0.47 mmol) was suspended in 6M HCl (10 mL) and the suspension heated at reflux for 48 h. Upon cooling to rt, the reaction mixture was washed with EtOAc (2 × 10 mL) and the aqueous phase evaporated *in vacuo*. Recrystallization from EtOH/Et₂O afforded **4a** (20 mg, 21%) as white crystals: mp 243 °C (dec.). ¹H NMR (300 MHz, D₂O): δ 7.36 (s, 1H), 4.73 (m, 1H), 3.57 (dt, J = 6.9, 3.2 Hz, 2H), 3.22 (td, J = 13.2, 3.2 Hz, 2H), 2.49–2.36 (m, 2H), 2.34–2.16 (m, 2H). ¹³C NMR (75 MHz, D₂O): δ 157.5, 107.8, 56.3, 42.9, 28.3. HRMS (ESI-TOF): m/z calculated for $C_7H_{13}N_4O$ $[M+H]^+$, 169.1084. Found, 169.1085 ($\Delta M=0.9$ ppm).

Ethyl 4-(4-(benzyloxy)-2H-1,2,3-triazol-2-yl)piperidine-1-carboxylate (17) and **ethyl 4-(4-(benzyloxy)-1H-1,2,3-triazol-1-yl)piperidine-1-carboxylate (18)**. Cs₂CO₃ (17.3 g, 53 mmol) was added to a solution of **14** (4.6 g, 26.5 mmol) in anhydrous 1,4-dioxane (100 mL). The reaction mixture was heated at reflux and ethyl 4-bromopiperidine-1-carboxylate (**20**, 18.8 g, 80 mmol) was added in small portions over 72 h. The reaction mixture was cooled to rt, neutralized by adding 1M HCl, and the volatiles were removed *in vacuo*. The resulting residue was taken up in water (100 mL) and extracted with EtOAc (3 × 100 mL). The combined organic phase was washed with brine (50 mL), dried over anhydrous Na₂SO₄, and evaporated *in vacuo*. Purification by flash chromatography (petroleum ether 40–60 °C/EtOAc, gradient 15%–40% EtOAc) afforded **17** (first eluting, N₂ isomer) and **18** (second eluting, N₁ isomer) as colourless oil and white solid, respectively. **17** (3.45 g, 39%). ¹H NMR (300 MHz, DMSO-*d*₆): δ 7.50–7.30 (m, 6H), 5.17 (s, 2H), 4.54 (tt, J = 10.7, 4.0 Hz, 1H), 4.05 (q, J = 7.1 Hz, 2H), 4.03–3.89 (m, 2H), 3.18–2.90 (m, 2H), 2.05 (dd, J = 12.8, 3.0 Hz, 2H), 1.79 (ddd, J = 15.9, 12.1, 4.3 Hz, 2H), 1.19 (t, J = 7.1 Hz, 3H). ¹³C NMR (75 MHz, DMSO-*d*₆): δ 160.1, 154.6, 136.3, 128.4, 128.2, 128.1, 118.6, 71.5, 60.8, 60.4, 41.9, 31.0, 14.6. HRMS (ESI-TOF): m/z calculated for $C_{17}H_{23}N_4O_3$ $[M+H]^+$, 331.1765. Found, 331.1760 ($\Delta M=1.5$ ppm). **18** (3.6 g, 41%): mp 98–100 °C. ¹H NMR (600 MHz, DMSO-*d*₆): δ 7.85 (s, 1H), 7.48–7.31 (m, 5H), 5.15 (s, 2H), 4.62 (tt, J = 11.3, 4.0 Hz, 1H), 4.14–4.01 (m, 4H), 3.09–2.89 (m, 2H), 2.06–1.99 (m, 2H), 1.82 (qd, J = 12.3, 4.4 Hz, 2H), 1.19 (t, J = 7.1 Hz, 3H). ¹³C NMR (150 MHz, DMSO-*d*₆): δ 160.1, 154.5, 136.5, 128.4, 128.1, 128.0, 105.6, 71.5, 60.9, 57.6, 42.2, 31.6,

14.6. HRMS (ESI-TOF): m/z calculated for $C_{17}H_{23}N_4O_3$ $[M+H]^+$, 331.1765. Found, 331.1761 ($\Delta M=1.0$ ppm).

Ethyl 4-(4-(benzyloxy)-5-iodo-2H-1,2,3-triazol-2-yl)piperidine-1-carboxylate (21). A solution of ICl (0.12 g, 0.73 mmol) in AcOH (2 mL) were added to a solution of **17** (0.20 g, 0.61 mmol) in AcOH (3 mL). Water (7 mL) was added and the resulting mixture was heated at 80 °C for 24 h. A solution of sodium thiosulfate 15–20% w/w was added and the reaction mixture was concentrated *in vacuo*. Water (50 mL) was added and the mixture was extracted with Et₂O (3 × 50 mL). The combined organic phase was washed with brine (50 mL), dried over anhydrous Na₂SO₄, and evaporated *in vacuo*. Purification by flash chromatography (petroleum ether 40–60 °C/EtOAc, gradient 0%–25% EtOAc) afforded **21** as colourless oil (0.21 g, 76%). ¹H NMR (300 MHz, DMSO-*d*₆): δ 7.54–7.28 (m, 5H), 5.23 (s, 2H), 4.67–4.50 (m, 1H), 4.05 (q, J = 7.1 Hz, 2H), 4.02–3.88 (m, 2H), 3.14–2.90 (m, 2H), 2.12–1.97 (m, 2H), 1.78 (qd, J = 12.2, 4.1 Hz, 2H), 1.19 (t, J = 7.1 Hz, 3H). ¹³C NMR (75 MHz, DMSO-*d*₆): δ 161.3, 154.6, 136.0, 128.5, 128.3, 128.2, 77.2, 72.0, 61.3, 60.8, 41.8, 30.9, 14.6. HRMS (ESI-TOF): m/z calculated for $C_{17}H_{22}N_4O_3I$ $[M+H]^+$, 457.0731. Found, 457.0732 ($\Delta M=0.3$ ppm).

Ethyl 4-(4-(benzyloxy)-5-iodo-1H-1,2,3-triazol-1-yl)piperidine-1-carboxylate (22). A solution of ICl (0.14 g, 0.88 mmol) in AcOH (4 mL) were added to a solution of **18** (0.22 g, 0.68 mmol) in AcOH (6 mL). Water (14 mL) was added and the resulting mixture was heated at 80 °C for 24 h. A solution of sodium thiosulfate 15–20% w/w was added and the reaction mixture was concentrated *in vacuo*. Water (50 mL) was added and the mixture was extracted with Et₂O (3 × 50 mL). The combined organic phase was washed with brine (50 mL), dried over anhydrous Na₂SO₄, and evaporated *in vacuo*. Purification by flash chromatography (petroleum ether 40–60 °C/EtOAc, gradient 0%–30% EtOAc) afforded **22** as white solid (0.19 g, 60%): mp 103–107 °C. ¹H NMR (600 MHz, DMSO-*d*₆): δ 7.48–7.31 (m, 5H), 5.31 (s, 2H), 4.54 (tt, J = 11.4, 4.1 Hz, 1H), 4.14–4.07 (m, 2H), 4.06 (q, J = 7.1 Hz, 2H), 3.15–2.94 (m, 2H), 2.04–1.96 (m, 2H), 1.89 (qd, J = 12.1, 4.4 Hz, 2H), 1.19 (t, J = 7.1 Hz, 3H). ¹³C NMR (150 MHz, DMSO-*d*₆): δ 161.9, 154.6, 136.6, 128.5, 128.2, 128.1, 71.4, 65.0, 60.9, 57.9, 42.2, 31.1, 14.6. HRMS (ESI-TOF): m/z calculated for $C_{17}H_{21}N_4O_3I$ Na $[M+Na]^+$, 479.0551. Found, 479.0556 ($\Delta M=1.2$ ppm).

Ethyl 4-(4-(benzyloxy)-5-(1-hydroxy-3,3-diphenylpropyl)-1H-1,2,3-triazol-1-yl)piperidine-1-carboxylate (24c). A 1.7M solution of ¹PrMgCl in THF (0.67 mL, 1.1 mmol) was added dropwise to a cooled (–10 °C) solution of **22** (0.48 g, 1.0 mmol) in anhydrous THF (7 mL). The resulting mixture was stirred at the same temperature for 2 h. A solution of 3,3-diphenylpropanal (**27**, 0.24 g, 1.1 mmol) in anhydrous THF (3 mL) was added and the mixture was allowed to reach rt. After 48 h, saturated aqueous NH₄Cl (7 mL) was added and the mixture stirred for 30 min

before it was evaporated *in vacuo*. The residue was taken up in water (50 mL) and extracted with Et₂O (3 × 50 mL). The combined organic phase was washed with brine (50 mL), dried over anhydrous Na₂SO₄, and evaporated *in vacuo*. Purification by flash chromatography (CH₂Cl₂/EtOAc, 85:15 v/v) afforded **24c** (0.26 g, 46%) as white solid: mp 62–66 °C. ¹H NMR (600 MHz, DMSO-*d*₆): δ 7.38–7.31 (m, 5H), 7.29–7.21 (m, 8H), 7.20–7.14 (m, 2H), 5.62 (d, *J* = 5.3 Hz, 1H), 5.27 (s, 2H), 4.47 (dt, *J* = 8.2, 5.9 Hz, 1H), 4.38 (tt, *J* = 10.6, 4.6 Hz, 1H), 4.05 (q, *J* = 7.1 Hz, 2H), 4.01 (t, *J* = 8.0 Hz, 1H), 4.01–3.95 (m, 2H), 2.96–2.71 (m, 2H), 2.64–2.53 (m, 2H), 1.96–1.87 (m, 2H), 1.80–1.67 (m, 2H), 1.19 (t, *J* = 7.1 Hz, 3H). ¹³C NMR (150 MHz, DMSO-*d*₆) δ 155.8, 154.5, 144.5, 144.1, 136.9, 128.5, 128.4, 128.2, 127.8, 127.7, 127.65, 127.6, 126.2, 126.1, 120.8, 71.1, 60.8, 60.3, 55.7, 47.0, 42.4, 42.3, 31.9, 31.3, 14.6. HRMS (ESI-TOF): *m/z* calculated for C₃₂H₃₇N₄O₄ [M+H]⁺, 541.2809. Found, 541.2804 (ΔM=1.0 ppm).

Ethyl 4-(5-(3,3-diphenylpropyl)-4-hydroxy-1H-1,2,3-triazol-1-yl)piperidine-1-carboxylate (28c). Et₃SiH (0.3 mL, 1.8 mmol) and TFA (0.67 mL, 8.7 mmol) were added to a solution of **24c** (0.17 g, 0.31 mmol) in CH₂Cl₂ (6 mL). The reaction mixture was heated at 50 °C in a sealed tube for 48 h. After cooling, CH₂Cl₂ was added up to 50 mL and the resulting mixture washed with 2M NaOH (50 mL). The aqueous phase was extracted with CH₂Cl₂ (2 × 50 mL). The combined organic phases were washed with brine (50 mL), dried over anhydrous MgSO₄, and evaporated. The crude product was dissolved in MeOH (20 mL) and added Pd/C (15 mg). The reaction mixture was put under a hydrogen atmosphere and stirred for 16 h. The reaction mixture was filtered through a PVDF filter (0.45 μm) and the volatiles were evaporated *in vacuo*. Purification by preparative HPLC (gradient 50%–70% solvent B over 10 min) afforded **28c** (0.11 g, 81%) as colourless oil. ¹H NMR (600 MHz, DMSO-*d*₆): δ 7.37–7.25 (m, 8H), 7.21–7.15 (m, 2H), 4.05 (q, *J* = 7.0 Hz, 2H), 4.05–3.98 (m, 2H), 3.95 (t, *J* = 7.8 Hz, 1H), 2.90–2.72 (m, 2H), 2.49–2.44 (m, 2H), 2.30–2.23 (m, 2H), 1.84–1.74 (m, 4H), 1.19 (t, *J* = 7.1 Hz, 3H). ¹³C NMR (150 MHz, DMSO-*d*₆) δ 155.4, 154.5, 144.5, 128.5, 127.6, 126.2, 117.0, 60.8, 54.6, 50.0, 42.4, 33.1, 31.5, 19.7, 14.6. HRMS (ESI-TOF): *m/z* calculated for C₂₅H₃₁N₄O₃ [M+H]⁺, 435.2391. Found, 435.2395 (ΔM=1.0 ppm).

Ethyl 4-(4-(benzyloxy)-5-(naphthalen-2-ylmethyl)-1H-1,2,3-triazol-1-yl)piperidine-1-carboxylate (26b). A solution of ⁱPrMgCl in THF (1.7M, 0.69 mL, 1.2 mmol) was added dropwise to a cooled solution (–10 °C) of **22** (0.50 g, 1.1 mmol) in anhydrous THF (7 mL). The mixture was stirred 1 h before a solution of 2-naphthaldehyde (0.19 g, 1.2 mmol) in anhydrous THF (3 mL) was added. The resulting mixture was allowed to reach rt. After 48 h, saturated aqueous NH₄Cl (5 mL) was added and the mixture stirred for 30 min before it was evaporated *in vacuo*. The residue was taken up in water (50 mL) and extracted with Et₂O (3 × 50 mL). The combined organic phase was washed with brine (50 mL), dried over anhydrous Na₂SO₄, and

evaporated *in vacuo*. Purification by flash chromatography (petroleum ether 40–60 °C/EtOAc, gradient 0%–40% EtOAc) afforded the alcohol intermediate **24b** (0.42 g, 80%). HRMS (ESI-TOF): *m/z* calculated for C₂₈H₃₁N₄O₄ [M+H]⁺, 487.2340. Found, 487.2338 (ΔM=0.4 ppm). **24b** (0.40 g, 0.83 mmol) was dissolved in CH₂Cl₂ (30 mL) and Et₃SiH (0.21 mL, 1.3 mmol) was added. The solution was cooled at 0 °C, TFA (1.8 mL, 23 mmol) was added and the resulting mixture was allowed to reach rt and stirred for 20 h. CH₂Cl₂ was added up to 50 mL and the resulting mixture was washed with 2M NaOH (50 mL). The aqueous phase was extracted with CH₂Cl₂ (2 × 50 mL) and the combined organic phase was washed with brine (50 mL), dried over anhydrous Na₂SO₄, and evaporated *in vacuo*. Purification by flash chromatography (petroleum ether 40–60 °C/EtOAc, gradient 10%–35% EtOAc) afforded **26b** (0.30 g, 77%) as colourless oil. ¹H NMR (600 MHz, DMSO-*d*₆): δ 7.90–7.78 (m, 3H), 7.66 (s, 1H), 7.52–7.45 (m, 2H), 7.37–7.25 (m, 6H), 5.31 (s, 2H), 4.58 (tt, *J* = 11.5, 4.0 Hz, 1H), 4.20 (s, 2H), 4.02 (q, *J* = 7.1 Hz, 2H), 4.00–3.89 (m, 2H), 2.97–2.77 (m, 2H), 1.81 (qd, *J* = 12.3, 4.5 Hz, 2H), 1.73–1.62 (m, 2H), 1.15 (t, *J* = 7.1 Hz, 3H). ¹³C NMR (150 MHz, DMSO-*d*₆) δ 156.8, 154.5, 137.0, 135.1, 133.0, 131.8, 128.3, 127.9, 127.85, 127.6, 127.4, 126.7, 126.4, 126.2, 125.8, 118.3, 71.3, 60.8, 55.0, 42.3, 31.5, 26.7, 14.5. HRMS (ESI-TOF): *m/z* calculated for C₂₈H₃₁N₄O₃ [M+H]⁺, 471.2391. Found, 471.2387 (ΔM=0.8 ppm).

Ethyl 4-(4-(benzyloxy)-5-(naphthalen-2-ylmethyl)-2H-1,2,3-triazol-2-yl)piperidine-1-carboxylate (25b). A solution of ⁱPrMgCl in THF (1.7M, 1.4 mL, 2.4 mmol) was added dropwise to a cooled solution (–10 °C) of **21** (1.0 g, 2.2 mmol) in anhydrous THF (15 mL). The mixture was stirred 1 h before a solution of 2-naphthaldehyde (0.38 g, 2.4 mmol) in anhydrous THF (5 mL) was added. The resulting mixture was allowed to reach rt. After 48 h, saturated aqueous NH₄Cl (10 mL) was added and the mixture stirred for 30 min before it was evaporated *in vacuo*. The residue was taken up in water (50 mL) and extracted with Et₂O (3 × 50 mL). The combined organic phase was washed with brine (50 mL), dried over anhydrous Na₂SO₄, and evaporated *in vacuo*. Purification by flash chromatography (petroleum ether 40–60 °C/EtOAc, gradient 0%–35% EtOAc) afforded the alcohol intermediate **23b** (0.64 g, 60%) as colourless oil. HRMS (ESI-TOF): *m/z* calculated for C₂₈H₃₀N₄O₄Na [M+Na]⁺, 509.2159. Found, 509.2167 (ΔM=1.5 ppm). **23b** (0.62 g, 1.3 mmol) was dissolved in CH₂Cl₂ (45 mL) and Et₃SiH (0.33 mL, 2.0 mmol) was added. The solution was cooled at 0 °C, TFA (2.7 mL, 36 mmol) was added and the resulting mixture was allowed to reach rt and stirred for 20 h. CH₂Cl₂ was added up to 50 mL and the resulting mixture was washed with 2M NaOH (50 mL). The aqueous phase was extracted with CH₂Cl₂ (2 × 50 mL) and the combined organic phase was washed with brine (50 mL), dried over anhydrous Na₂SO₄, and evaporated *in vacuo*. Purification by flash chromatography (petroleum ether 40–60 °C/EtOAc, gradient 0%–20% EtOAc) afforded **25b** (0.30 g, 50%) as colourless oil. ¹H

NMR (600 MHz, DMSO-*d*₆): δ 7.85 (d, *J* = 7.7 Hz, 1H), 7.83–7.78 (m, 2H), 7.69 (s, 1H), 7.51–7.43 (m, 2H), 7.37–7.26 (m, 6H), 5.19 (s, 2H), 4.49 (tt, *J* = 10.9, 4.1 Hz, 1H), 4.07–4.00 (m, 4H), 4.00–3.92 (m, 2H), 3.09–2.93 (m, 2H), 2.07–2.00 (m, 2H), 1.79 (qd, *J* = 11.6, 4.4 Hz, 2H), 1.18 (t, *J* = 7.1 Hz, 3H). ¹³C NMR (150 MHz, DMSO-*d*₆) δ 157.0, 154.6, 136.5, 136.3, 133.0, 131.7, 130.5, 128.3, 128.0, 127.9, 127.8, 127.5, 127.4, 127.2, 126.4, 126.1, 125.5, 71.4, 60.8, 60.2, 41.9, 31.0, 29.5, 14.6. HRMS (ESI-TOF): *m/z* calculated for C₂₈H₃₁N₄O₃ [M+H]⁺, 471.2391. Found, 471.2384 (ΔM=1.3 ppm).

Ethyl 4-(4-(benzyloxy)-5-(3,3-diphenylpropyl)-2H-1,2,3-triazol-2-yl)piperidine-1-carboxylate (25c). A solution of ¹PrMgCl in THF (1.7M, 1.4 mL, 2.5 mmol) was added dropwise to a cooled solution (−10 °C) of **21** (1.0 g, 2.2 mmol) in anhydrous THF (15 mL). The mixture was stirred 1 h before a solution of 3,3-diphenylpropanal (**27**, 0.52 g, 2.5 mmol) in anhydrous THF (5 mL) was added. The resulting mixture was allowed to reach rt. After 48 h, saturated aqueous NH₄Cl (5 mL) was added and the mixture stirred for 30 min before it was evaporated *in vacuo*. The residue was taken up in water (50 mL) and extracted with Et₂O (3 × 50 mL). The combined organic phase was washed with brine (50 mL), dried over anhydrous Na₂SO₄, and evaporated *in vacuo*. Purification by flash chromatography (petroleum ether 40–60 °C/EtOAc, gradient 0%–35% EtOAc) afforded the alcohol intermediate **23c** (0.36 g, 30%) as colourless oil. ¹H NMR (600 MHz, DMSO-*d*₆): δ 7.41–7.30 (m, 5H), 7.30–7.20 (m, 8H), 7.18–7.11 (m, 2H), 5.24 (d, *J* = 5.2 Hz, 1H), 5.17 (s, 2H), 4.48 (tt, *J* = 10.7, 4.0 Hz, 1H), 4.32 (dt, *J* = 8.2, 5.6 Hz, 1H), 4.05 (q, *J* = 7.1 Hz, 2H), 4.03–4.00 (m, 1H), 3.99–3.92 (m, 2H), 3.11–2.95 (m, 2H), 2.56–2.43 (m, 2H), 2.06–2.00 (m, 2H), 1.83–1.74 (m, 2H), 1.19 (t, *J* = 7.1 Hz, 3H). ¹³C NMR (150 MHz, DMSO-*d*₆) δ 156.6, 154.6, 145.1, 144.3, 136.6, 134.2, 128.4, 128.36, 128.3, 128.2, 128.0, 127.9, 127.8, 127.6, 126.1, 126.0, 71.3, 61.7, 60.8, 60.2, 46.9, 41.9, 40.9, 30.9, 14.6. HRMS (ESI-TOF): *m/z* calculated for C₃₂H₃₆N₄O₄Na [M+Na]⁺, 563.2629. Found, 563.2618 (ΔM=1.8 ppm). **23c** (0.34 g, 0.62 mmol) was dissolved in CH₂Cl₂ (30 mL) and Et₃SiH (0.60 mL, 3.7 mmol) was added. The solution was cooled at 0 °C and TFA (1.3 mL, 17 mmol) was added and the resulting mixture was allowed to reach rt and stirred for 72 h. CH₂Cl₂ was added up to 50 mL and the resulting mixture was washed with 2M NaOH (50 mL). The aqueous phase was extracted with CH₂Cl₂ (2 × 50 mL) and the combined organic phase was washed with brine (50 mL), dried over anhydrous Na₂SO₄, and evaporated *in vacuo*. Purification by flash chromatography (petroleum ether 40–60 °C/EtOAc, 85:15 v/v) afforded **25c** (0.25 g, 78%) as colourless oil. ¹H NMR (600 MHz, DMSO-*d*₆): δ 7.41–7.31 (m, 5H), 7.28–7.22 (m, 8H), 7.17–7.12 (m, 2H), 5.16 (s, 2H), 4.46 (tt, *J* = 10.8, 4.1 Hz, 1H), 4.05 (q, *J* = 7.1 Hz, 2H), 4.00–3.92 (m, 2H), 3.92 (t, *J* = 7.7 Hz, 1H), 3.10–2.94 (m, 2H), 2.41–2.37 (m, 2H), 2.32–2.27 (m, 2H), 2.04–1.99 (m, 2H), 1.77 (qd, *J* = 12.3, 4.3 Hz, 2H), 1.19 (t, *J* = 7.1 Hz, 3H). ¹³C NMR (150 MHz, DMSO-*d*₆) δ 156.9, 154.6, 144.7, 136.5, 131.1, 128.4, 128.37, 128.1,

128.0, 127.6, 126.1, 71.4, 60.8, 60.0, 49.9, 41.9, 33.4, 30.9, 21.7, 14.6. HRMS (ESI-TOF): *m/z* calculated for C₃₂H₃₇N₄O₃ [M+H]⁺, 525.2860. Found, 525.2856 (ΔM=0.7 ppm).

5-(Naphthalen-2-ylmethyl)-2-(piperidin-4-yl)-2H-1,2,3-triazol-4-ol hydrochloride (3b). A solution of **25b** (0.23 g, 0.49 mmol) in EtOH/35% HCl (1:2 v/v, 15 mL) was heated at reflux for 24 h. Upon cooling to rt, the solvents were evaporated *in vacuo*. Purification by preparative HPLC (gradient 20%–50% solvent B over 15 min) followed by conversion of the obtained product into the hydrochloric salt using 2M HCl afforded **3b** (32 mg, 20%) as pale yellow solid: mp 200–203 °C. ¹H NMR (600 MHz, DMSO-*d*₆): δ 10.50 (s, 1H), 9.03 (br s, 2H), 7.87–7.79 (m, 3H), 7.68 (s, 1H), 7.50–7.42 (m, 2H), 7.39 (d, *J* = 8.4 Hz, 1H), 4.52 (tt, *J* = 9.8, 4.3 Hz, 1H), 4.01 (s, 2H), 3.33–3.24 (m, 2H), 3.09–2.99 (m, 2H), 2.21–2.06 (m, 4H). ¹³C NMR (150 MHz, DMSO-*d*₆) δ 156.1, 136.9, 133.0, 131.6, 130.5, 127.9, 127.5, 127.4, 127.2, 126.3, 126.1, 125.5, 57.3, 41.7, 29.3, 27.9. HRMS (ESI-TOF): *m/z* calculated for C₁₈H₂₁N₄O [M+H]⁺, 309.1710. Found, 309.1711 (ΔM=0.3 ppm).

5-(3,3-Diphenylpropyl)-2-(piperidin-4-yl)-2H-1,2,3-triazol-4-ol hydrochloride (3c). A solution of **25c** (0.21 g, 0.38 mmol) in EtOH/35% HCl (1:2 v/v, 15 mL) was heated at reflux for 24 h. Upon cooling to rt, the solvents were evaporated *in vacuo*. Recrystallization from MeOH/Et₂O afforded **3c** (82 mg, 52%) as white solid: mp 246–249 °C. ¹H NMR (600 MHz, DMSO-*d*₆): δ 10.27 (s, 1H), 9.21 (s, 2H), 7.38–7.21 (m, 8H), 7.21–7.09 (m, 2H), 4.49 (tt, *J* = 10.0, 4.8 Hz, 1H), 3.96 (t, *J* = 7.5 Hz, 1H), 3.32–3.22 (m, 2H), 3.12–2.98 (m, 2H), 2.42–2.25 (m, 4H), 2.21–2.06 (m, 4H). ¹³C NMR (150 MHz, DMSO-*d*₆) δ 155.8, 144.8, 131.1, 128.4, 127.6, 126.0, 57.0, 50.1, 41.6, 33.5, 27.8, 21.8. HRMS (ESI-TOF): *m/z* calculated for C₂₂H₂₇N₄O [M+H]⁺, 363.2179. Found, 363.2182 (ΔM=0.8 ppm).

5-(Naphthalen-2-ylmethyl)-1-(piperidin-4-yl)-1H-1,2,3-triazol-4-ol hydrochloride (4b). A solution of **26b** (0.21 g, 0.46 mmol) in EtOH/35% w/w HCl (1:2 v/v, 15 mL) was heated at reflux for 24 h. Upon cooling to rt, the solvents were evaporated *in vacuo*. Purification by preparative HPLC (gradient 20%–40% solvent B over 10 min) followed by conversion of the obtained product into the hydrochloric salt using 2M HCl afforded **4b** (73 mg, 46%) as pale yellow solid: mp 258–261 °C. ¹H NMR (600 MHz, DMSO-*d*₆): δ 9.34 (br s, 1H), 8.99 (br s, 1H), 7.90–7.81 (m, 3H), 7.71 (s, 1H), 7.51–7.44 (m, 2H), 7.37 (dd, *J* = 8.4, 1.7 Hz, 1H), 4.67 (tt, *J* = 10.9, 3.9 Hz, 1H), 4.19 (s, 2H), 3.31–3.25 (m, 2H), 3.03–2.94 (m, 2H), 2.21–2.11 (m, 2H), 1.85–1.77 (m, 2H). ¹³C NMR (150 MHz, DMSO-*d*₆) δ 155.8, 135.7, 133.0, 131.8, 128.3, 127.6, 127.4, 126.8, 126.3, 126.0, 125.7, 116.8, 52.3, 42.0, 28.4, 26.6. HRMS (ESI-TOF): *m/z* calculated for C₁₈H₂₁N₄O [M+H]⁺, 309.1710. Found, 309.1708 (ΔM=0.5 ppm).

5-(3,3-Diphenylpropyl)-1-(piperidin-4-yl)-1H-1,2,3-triazol-4-ol hydrochloride (4c). A solution of **28c** (93 mg, 0.21 mmol) in

EtOH/35% HCl (1:2 v/v, 15 mL) was heated at reflux for 24 h. Upon cooling to rt, the solvents were evaporated in vacuo. Recrystallization from MeOH/Et₂O afforded **4c** (43 mg, 51%) as white solid: mp 232–234 °C. Anal. calcd (C₂₂H₂₆N₄O·1.25HCl·0.1Et₂O): C, 64.76; H, 6.85; N, 13.49. Found: C, 65.14; H, 6.45; N 13.18. ¹H NMR (600 MHz, DMSO-*d*₆): δ 9.82 (s, 1H), 9.16 (br s, 1H), 8.88 (br s, 1H), 7.37–7.24 (m, 8H), 7.23–7.13 (m, 2H), 4.28 (tt, *J* = 11.0, 4.0 Hz, 1H), 3.97 (t, *J* = 7.8 Hz, 1H), 3.40–3.37 (q, *J* = 7.0 Hz, 0.6H, (CH₃CH₂)₂O), 3.37–3.33 (m, 2H), 3.00–2.91 (m, 2H), 2.48–2.45 (m, 2H), 2.30–2.24 (m, 2H), 2.22–2.13 (m, 2H), 2.02–1.95 (m, 2H), 1.09 (t, *J* = 7.0 Hz, 0.9 H, (CH₃CH₂)₂O). ¹³C NMR (150 MHz, DMSO-*d*₆) δ 155.4, 144.5, 128.5, 127.6, 126.2, 117.2, 64.9, 51.9, 50.1, 42.1, 33.0, 28.4, 19.7, 15.1. HRMS (ESI-TOF): *m/z* calculated for C₂₂H₂₇N₄O [M+H]⁺, 363.2179. Found, 363.2179 (ΔM=0.2 ppm).

Determination of ionization constants. The ionization constants of compounds **2a–b**, **3a–c** and **4a–c** were determined by potentiometric titration with the GLpK_a apparatus (Sirius Analytical Instruments Ltd, Forest Row, East Sussex, UK). The pK_a values were obtained as mean of four titrations: aqueous solutions (ionic strength adjusted to 0.15M with KCl) of the compound (20 mL, about 1 mM) were initially acidified to pH 1.8 with 0.5 N HCl and then titrated with standardized 0.5N KOH to pH 12.2 at constant temperature of 25(±0.1) °C under argon atmosphere.

Molecular modelling

Docking of selected compounds. A model of the extracellular domain of GABA_AR constructed using an iterative approach with the orthosteric binding site optimized using an induced fit docking protocol,^{31–34} has previously been reported,¹¹ and is used here with the compounds **3a** and **4a**. Subsequently ligands **3b–c**, and **4b–c**, were docked into the binding site as described previously,¹¹ except 200 poses per ligand were included in the post-docking minimization step. The attained docking poses were subsequently refined using the “None (refine only)” ligand sampling option in the Glide 7.7 docking program.^{35–38} Finally the obtained models were minimized using the MacroModel 11.8 program.³⁹

Calculation of solvation energies of 4-PHP and 2a. Solvation energies were calculated in Jaguar^{28, 40} version 9.8 on B3LYP/6-31+G** optimized geometries using the Poisson Boltzmann Finite (PDF)^{41–43} element method as implemented in Jaguar. Gas phase optimized geometries (B3LYP/6-31+G**) were used as reference. Default settings were used except for the SCF convergence threshold, which was set to “ultrafine”. Calculations were performed on the anionic forms the triazole moiety of the compounds.

Pharmacology

Characterization of compounds **2a–b**, **3a–c**, and **4a–c** in muscimol binding: the binding assay was performed using rat

brain synaptic membranes of cortex and the central hemispheres from male SPRD rats with tissue preparation as described in the literature.⁴⁴ On the day of the experiment, the membrane preparation was quickly thawed, homogenized in 50 volumes of ice-cold buffer (50 mM Tris–HCl buffer, pH 7.4), and centrifuged at 48,000g for 10 min at 4 °C. This washing step was repeated four times and the final pellet was re-suspended in buffer. The assay was carried out in 96-wells plates, by incubation of membranes (70–80 μg protein) in 200 μL buffer, 25 μL [³H]muscimol (5 nM final concentration), and 25 μL test substance in various concentrations, for 60 min at 0 °C. The reaction was terminated by rapid filtration through GF/C filters (Perkin Elmer Life Sciences), using a 96 well Packard FilterMate cellharvester, followed by washing with 3 × 250 μL of ice-cold buffer. The dried filters were added Microscint scintillation fluid (PerkinElmer Life Sciences), and the amount of filterbound radioactivity was quantified in a Packard TopCount microplate scintillator counter. The experiments were performed in triplicate at least three times for each compound. Non-specific binding was determined using 1.0 mM GABA. The binding data was analysed by a non-linear regression curve-fitting procedure using GraphPad Prism v. 6.00 (GraphPad Software, CA, USA). IC₅₀ values were calculated from inhibition curves and converted to K_i values using the modified Cheng–Prusoff equation.⁴⁵

Conflicts of interest

The authors declare no financial conflicts of interest.

Acknowledgements

This research was supported by funding from the University of Turin, Ricerca Locale 2015 and 2016 (Grant numbers LOLM_RILO_17_01 and BOSD_RILO_17_01). The authors also wish to thank several people who have contributed to this work. In particular, we would like to mention Livio Stevanato for maintaining the NMR instrumentation.

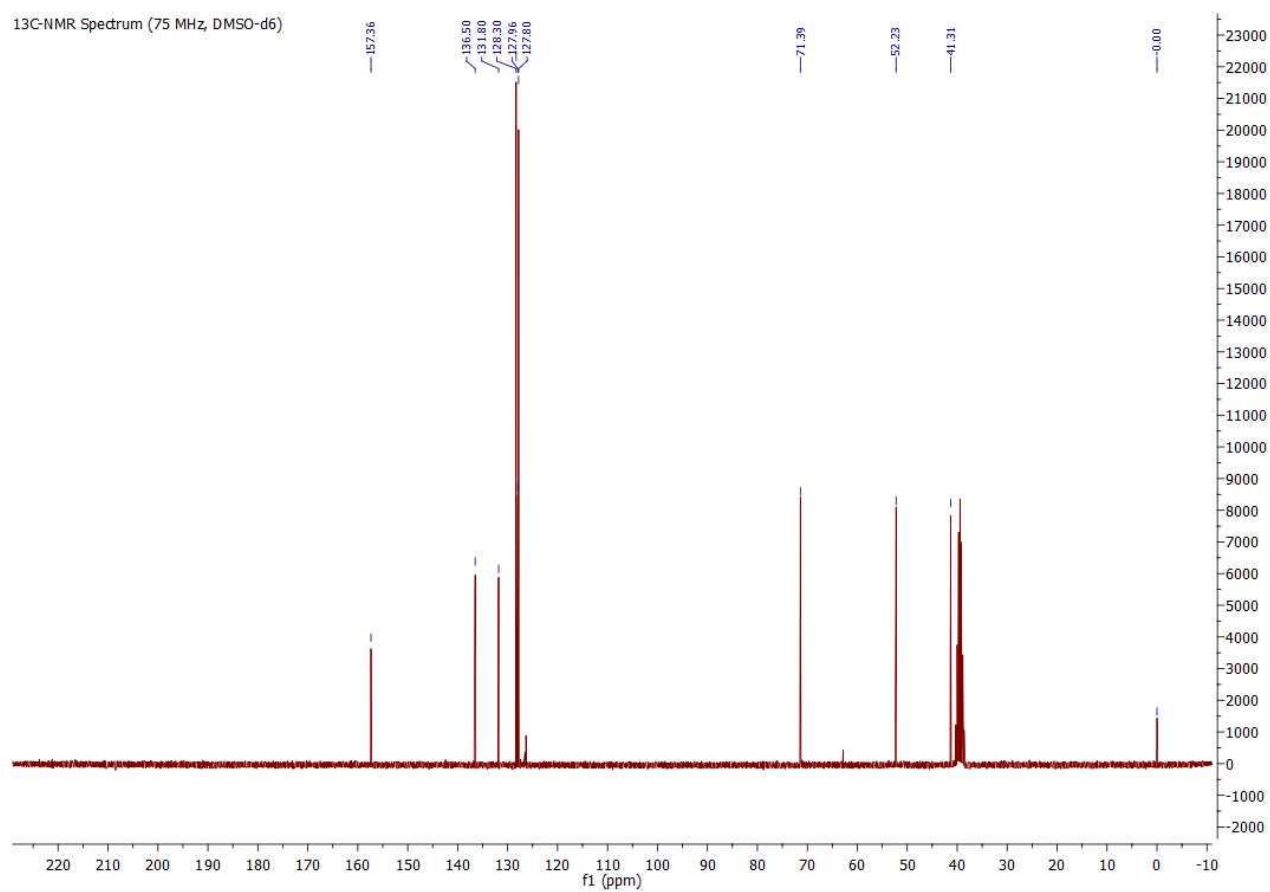
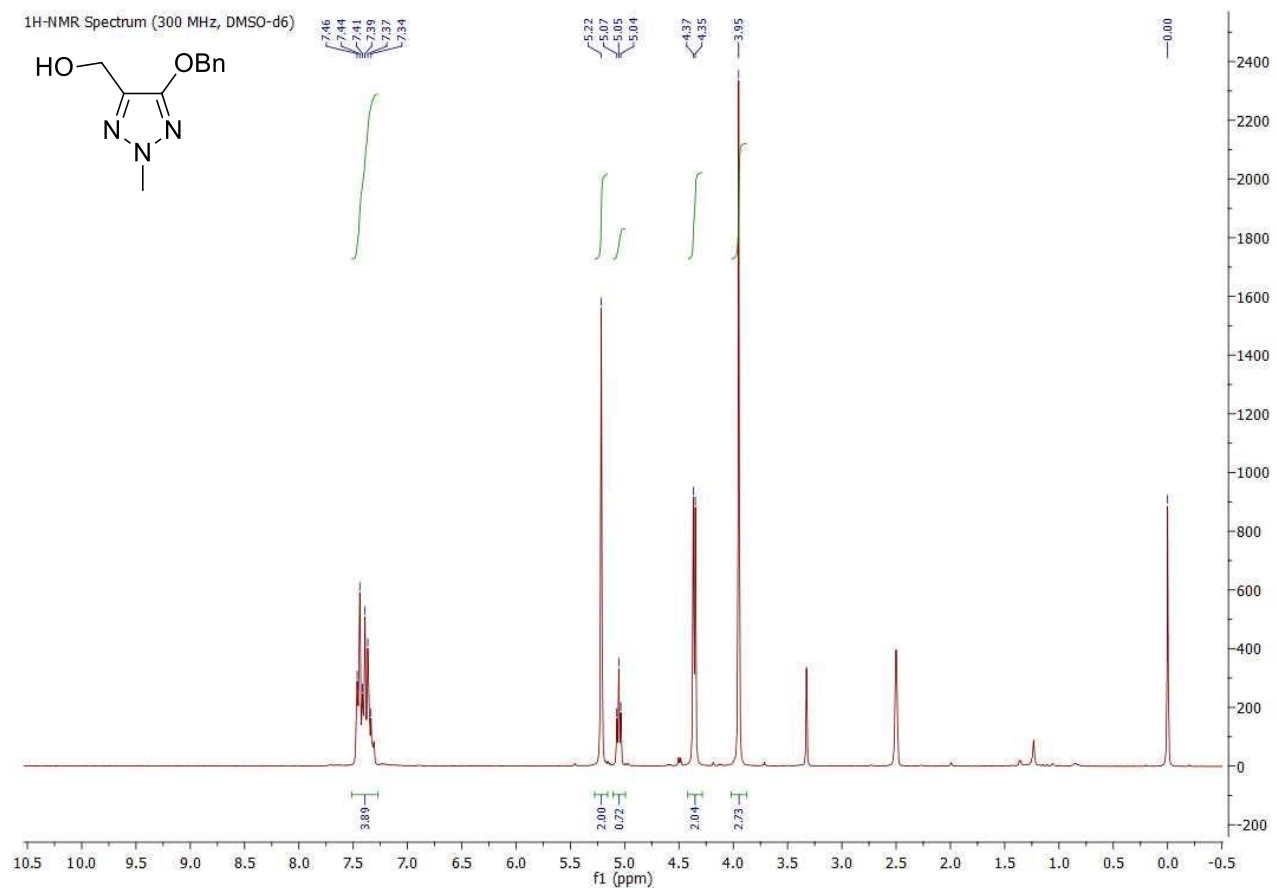
Notes and references

1. P. J. Whiting, *Drug Discov Today*, 2003, **8**, 445–450.
2. R. W. Olsen and W. Sieghart, *Neuropharmacology*, 2009, **56**, 141–148.
3. R. E. Hibbs and E. Gouaux, *Nature*, 2011, **474**, 54–60.
4. R. J. Hilf and R. Dutzler, *Nature*, 2008, **452**, 375–379.
5. R. J. Hilf and R. Dutzler, *Nature*, 2009, **457**, 115–118.
6. P. S. Miller and A. R. Aricescu, *Nature*, 2014, **512**, 270–275.
7. J. Krall, T. Balle, N. Krosggaard-Larsen, T. E. Sorensen, P. Krosggaard-Larsen, U. Kristiansen and B. Frolund, *Adv Pharmacol*, 2015, **72**, 201–227.
8. J. G. Petersen, R. Bergmann, P. Krosggaard-Larsen, T. Balle and B. Frolund, *Neurochem Res*, 2014, **39**, 1005–1015.
9. M. Lolli, S. Narramore, C. W. Fishwick and K. Pors, *Drug Discov Today*, 2015, **20**, 1018–1026.
10. R. Bergmann, K. Kongsbak, P. L. Sorensen, T. Sander and T. Balle, *PLoS One*, 2013, **8**, e52323.

11. T. Sander, B. Frolund, A. T. Bruun, I. Ivanov, J. A. McCammon and T. Balle, *Proteins*, 2011, **79**, 1458-1477.
12. A. C. Pippione, A. Federico, A. Ducime, S. Sainas, D. Boschi, A. Barge, E. Lupino, M. Piccinini, M. Kubbutat, J.-M. Contreras, C. Morice, S. Al-Karadaghi and M. L. Lolli, *MedChemComm*, 2017, **8**, 1850-1855.
13. M. L. Lolli, S. L. Hansen, B. Rolando, B. Nielsen, P. Wellendorph, K. Madsen, O. M. Larsen, U. Kristiansen, R. Fruttero, A. Gasco and T. N. Johansen, *J. Med. Chem.*, 2006, **49**, 4442-4446.
14. H. A. Moller, T. Sander, J. L. Kristensen, B. Nielsen, J. Krall, M. L. Bergmann, B. Christiansen, T. Balle, A. A. Jensen and B. Frolund, *J Med Chem*, 2010, **53**, 3417-3421.
15. J. Krall, K. T. Kongstad, B. Nielsen, T. E. Sorensen, T. Balle, A. A. Jensen and B. Frolund, *ChemMedChem*, 2014, **9**, 2475-2485.
16. B. Frolund, L. Tagmose, T. Liljefors, T. B. Stensbol, C. Engblom, U. Kristiansen and P. Krogsgaard-Larsen, *J. Med. Chem.*, 2000, **43**, 4930-4933.
17. A. C. Pippione, F. Dosio, A. Ducime, A. Federico, K. Martina, S. Sainas, B. Froelund, M. Gooyit, K. D. Janda, D. Boschi and M. L. Lolli, *MedChemComm*, 2015, **6**, 1285-1292.
18. H. Sun, G. Tawa and A. Wallqvist, *Drug Discovery Today*, 2012, **17**, 310-324.
19. S. Sainas, A. C. Pippione, M. Giorgis, E. Lupino, P. Goyal, C. Ramondetti, B. Buccinna, M. Piccinini, R. C. Braga, C. H. Andrade, M. Andersson, A.-C. Moritzer, R. Friemann, S. Mensa, S. Al-Kadaraghi, D. Boschi and M. L. Lolli, *Eur. J. Med. Chem.*, 2017, **129**, 287-302.
20. B. Frolund, A. T. Jorgensen, L. Tagmose, T. B. Stensbol, H. T. Vestergaard, C. Engblom, U. Kristiansen, C. Sanchez, P. Krogsgaard-Larsen and T. Liljefors, *J Med Chem*, 2002, **45**, 2454-2468.
21. S. Caddick, D. B. Judd, A. K. d. K. Lewis, M. T. Reich and M. R. V. Williams, *Tetrahedron*, 2003, **59**, 5417-5423.
22. J. G. Petersen, R. Bergmann, H. A. Moeller, C. G. Joergensen, B. Nielsen, J. Kehler, K. Frydenvang, J. Kristensen, T. Balle, A. A. Jensen, U. Kristiansen and B. Froelund, *J. Med. Chem.*, 2013, **56**, 993-1006.
23. P. Tosco and M. L. Lolli, *J. Mol. Model.*, 2008, **14**, 279-291.
24. A. P. Treder, A. Walkowiak, W. Zgoda and R. Andruszkiewicz, *Synthesis*, 2005, DOI: 10.1055/s-2005-869989, 2281-2283.
25. L. M. Weinstock, P. Davis, B. Handelsman and R. J. Tull, *J. Org. Chem.*, 1967, **32**, 2823-2828.
26. D. N. Kursanov, Z. N. Parnes and N. M. Loim, *Synthesis*, 1974, DOI: 10.1055/s-1974-23387, 633-651.
27. D. Krehan, B. Frolund, B. Ebert, B. Nielsen, P. Krogsgaard-Larsen, G. A. R. Johnston and M. Chebib, *Bioorg. Med. Chem.*, 2003, **11**, 4891-4896.
28. *Schrödinger Release 2017-4: Jaguar*, Schrödinger, LLC, New York, NY, 2017.
29. S. C. Watson and J. F. Eastham, *J. Organomet. Chem.*, 1967, **9**, 165-168.
30. H. E. Gottlieb, V. Kotlyar and A. Nudelman, *J. Org. Chem.*, 1997, **62**, 7512-7515.
31. *Schrödinger Release 2017-4: Schrödinger Suite 2017-4 Induced Fit Docking protocol; Glide*, Schrödinger, LLC, New York, NY, 2016; *Prime*, Schrödinger, LLC, New York, NY, 2017.
32. R. Farid, T. Day, R. A. Friesner and R. A. Pearlstein, *Bioorg. Med. Chem.*, 2006, **14**, 3160-3173.
33. W. Sherman, H. S. Beard and R. Farid, *Chem. Biol. Drug Des.*, 2006, **67**, 83-84.
34. W. Sherman, T. Day, M. P. Jacobson, R. A. Friesner and R. Farid, *J. Med. Chem.*, 2006, **49**, 534-553.
35. *Schrödinger Release 2017-4. Glide*, Schrödinger, LLC, New York, NY, 2017.
36. T. A. Halgren, R. B. Murphy, R. A. Friesner, H. S. Beard, L. L. Frye, W. T. Pollard and J. L. Banks, *J. Med. Chem.*, 2004, **47**, 1750-1759.
37. R. A. Friesner, J. L. Banks, R. B. Murphy, T. A. Halgren, J. J. Klicic, D. T. Mainz, M. P. Repasky, E. H. Knoll, M. Shelley, J. K. Perry, D. E. Shaw, P. Francis and P. S. Shenkin, *J. Med. Chem.*, 2004, **47**, 1739-1749.
38. R. A. Friesner, R. B. Murphy, M. P. Repasky, L. L. Frye, J. R. Greenwood, T. A. Halgren, P. C. Sanschagrin and D. T. Mainz, *J. Med. Chem.*, 2006, **49**, 6177-6196.
39. *Schrödinger Release 2017-4: MacroModel*, Schrödinger, LLC, New York, NY, 2017.
40. A. D. Bochevarov, E. Harder, T. F. Hughes, J. R. Greenwood, D. A. Braden, D. M. Philipp, D. Rinaldo, M. D. Halls, J. Zhang and R. A. Friesner, *Int. J. Quantum Chem.*, 2013, **113**, 2110-2142.
41. C. M. Cortis, J.-M. Langlois, M. D. Beachy and R. A. Friesner, *J. Chem. Phys.*, 1996, **105**, 5472-5484.
42. C. M. Cortis and R. A. Friesner, *J. Comput. Chem.*, 1997, **18**, 1570-1590.
43. C. M. Cortis and R. A. Friesner, *J. Comput. Chem.*, 1997, **18**, 1591-1608.
44. R. W. Ransom and N. L. Stec, *J. Neurochem.*, 1988, **51**, 830-836.
45. P. Leff and I. G. Dougall, *Trends Pharmacol. Sci.*, 1993, **14**, 110-112.

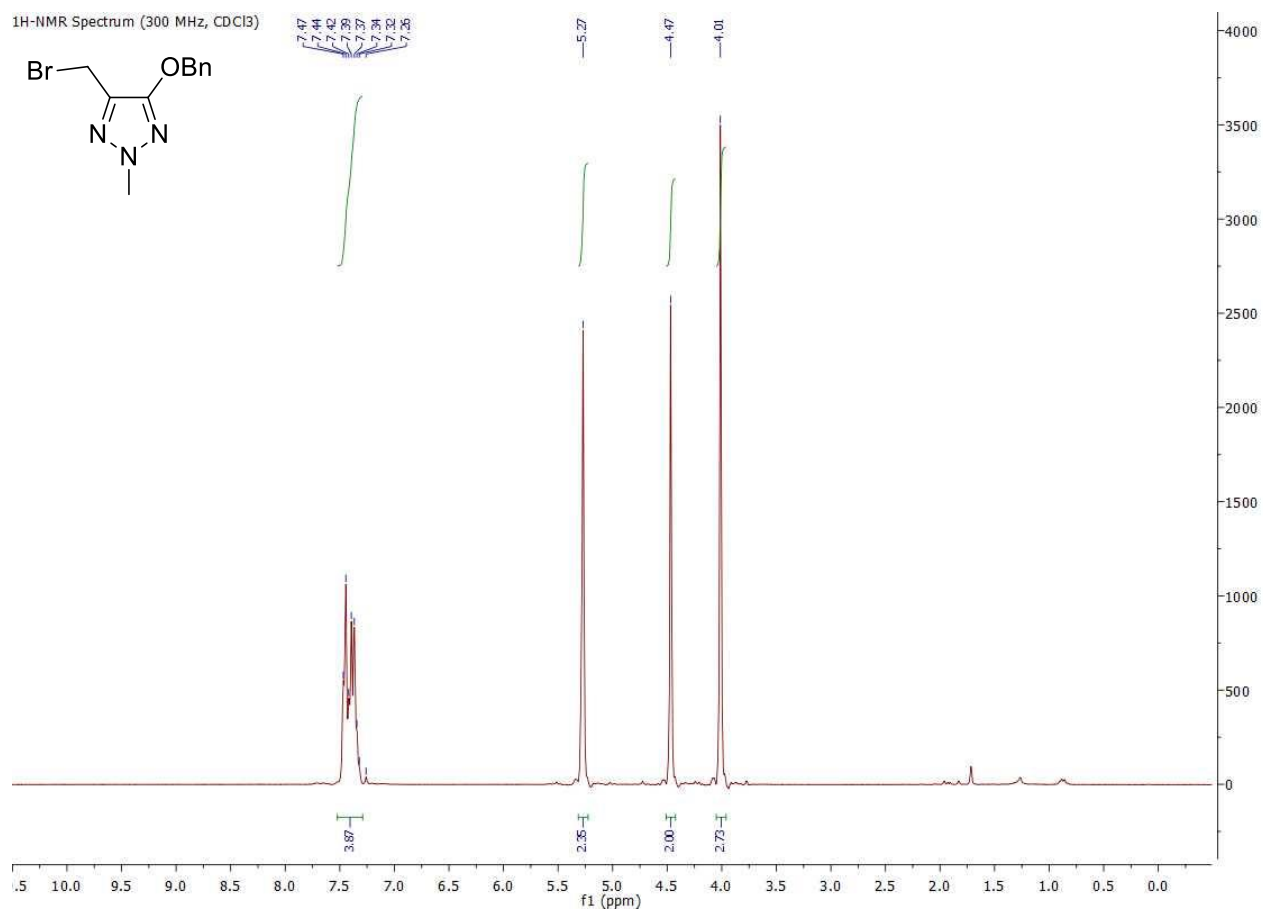
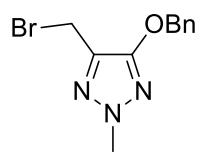
NMR analyses chapter 2

(5-(Benzyloxy)-2-methyl-2H-1,2,3-triazol-4-yl)methanol (2.11).

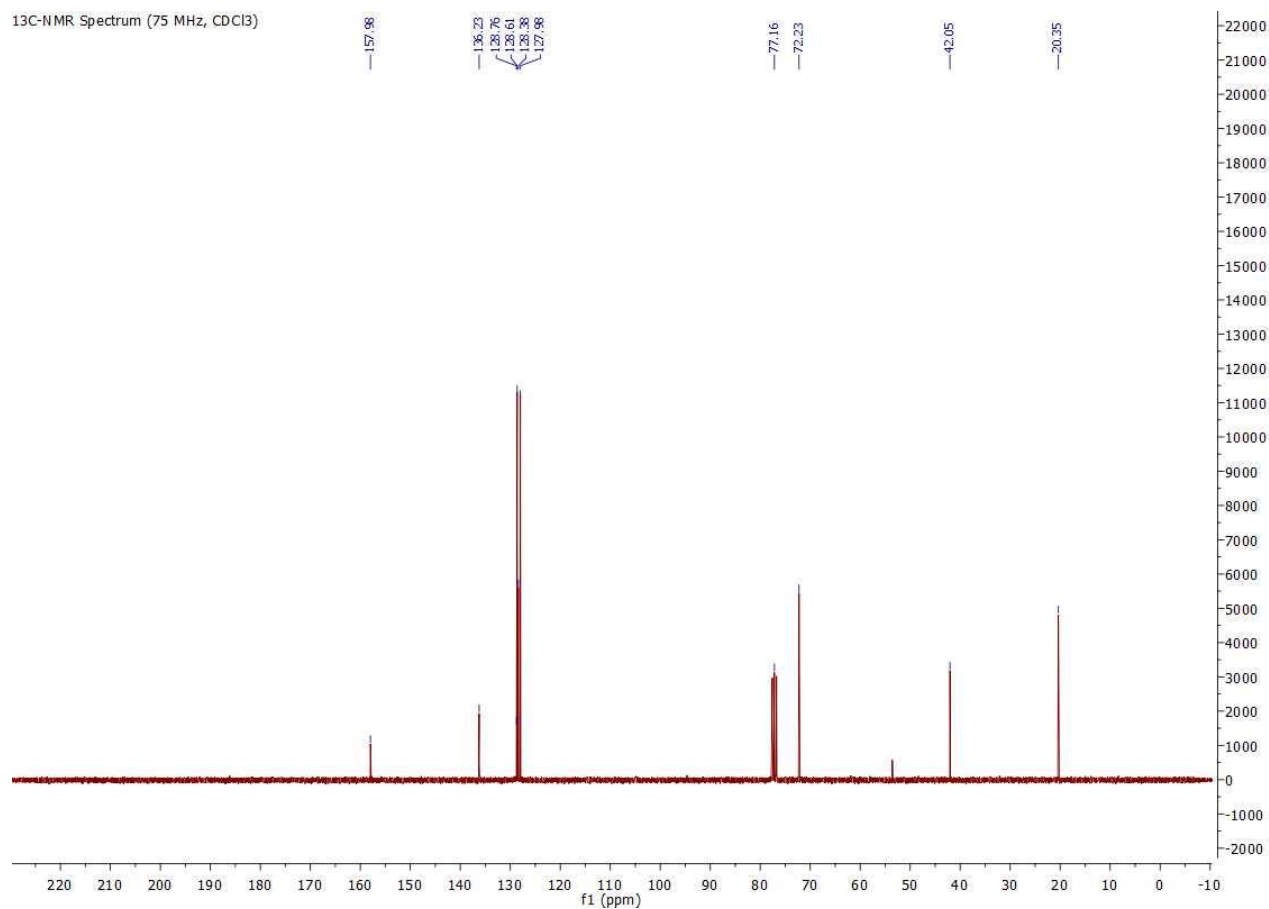


4-(Benzyloxy)-5-(bromomethyl)-2-methyl-2H-1,2,3-triazole (2.12).

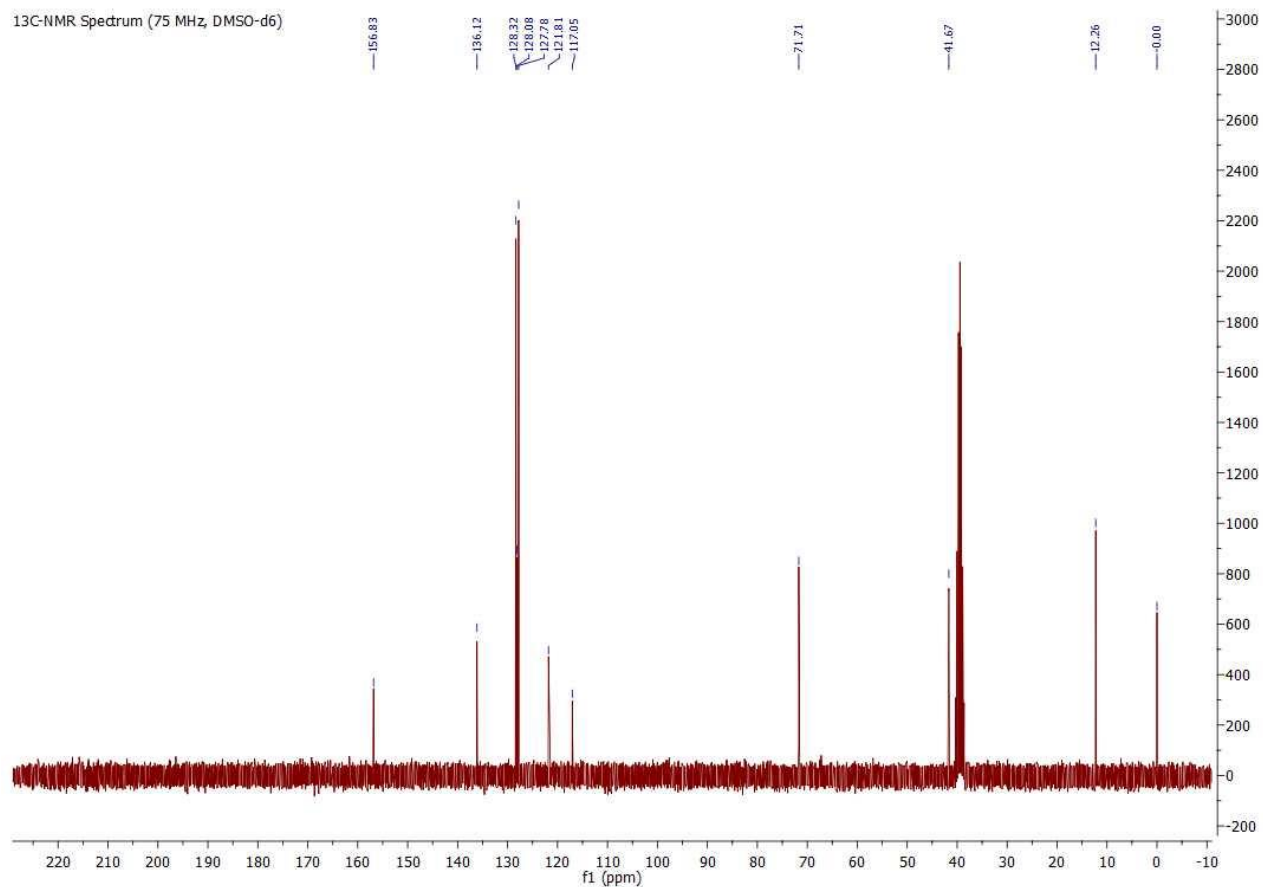
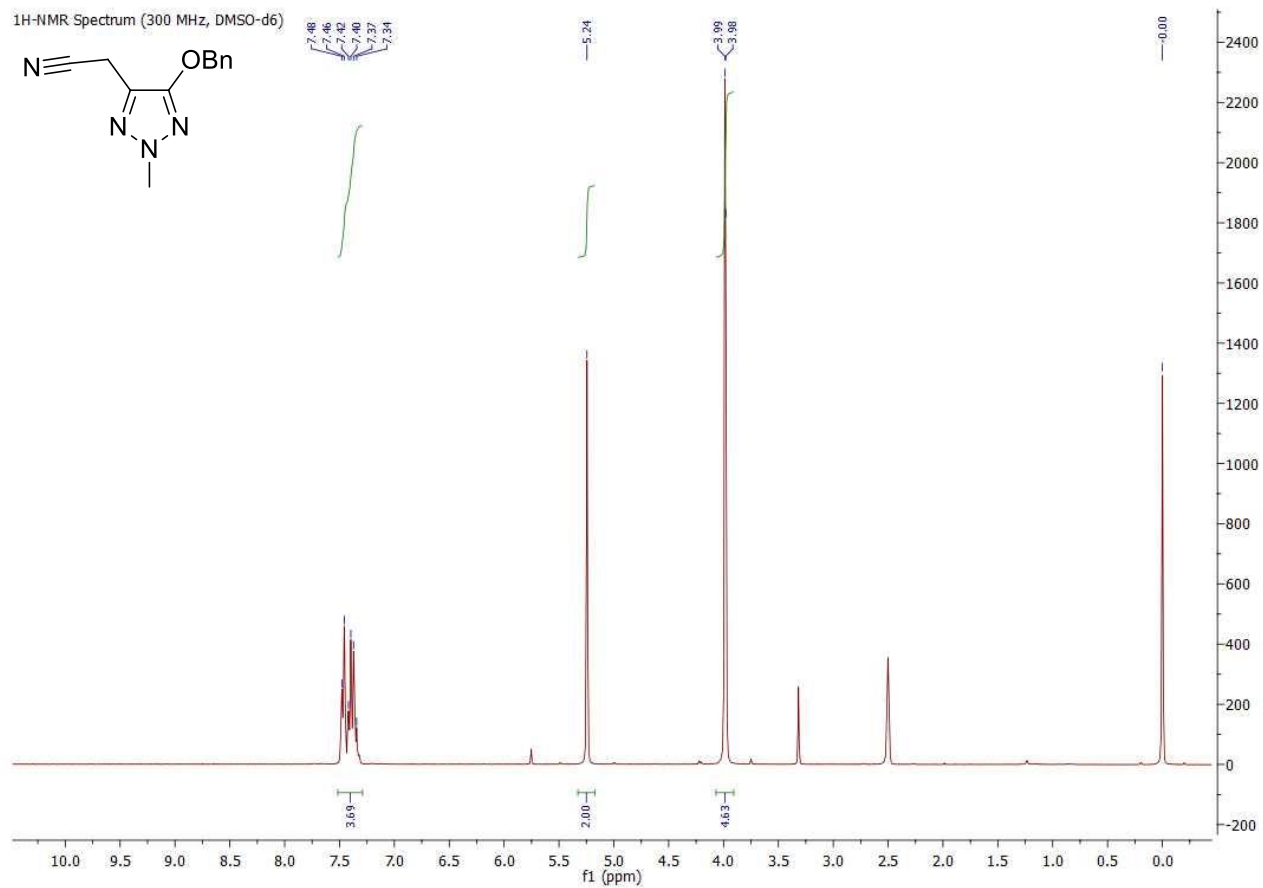
¹H-NMR Spectrum (300 MHz, CDCl₃)



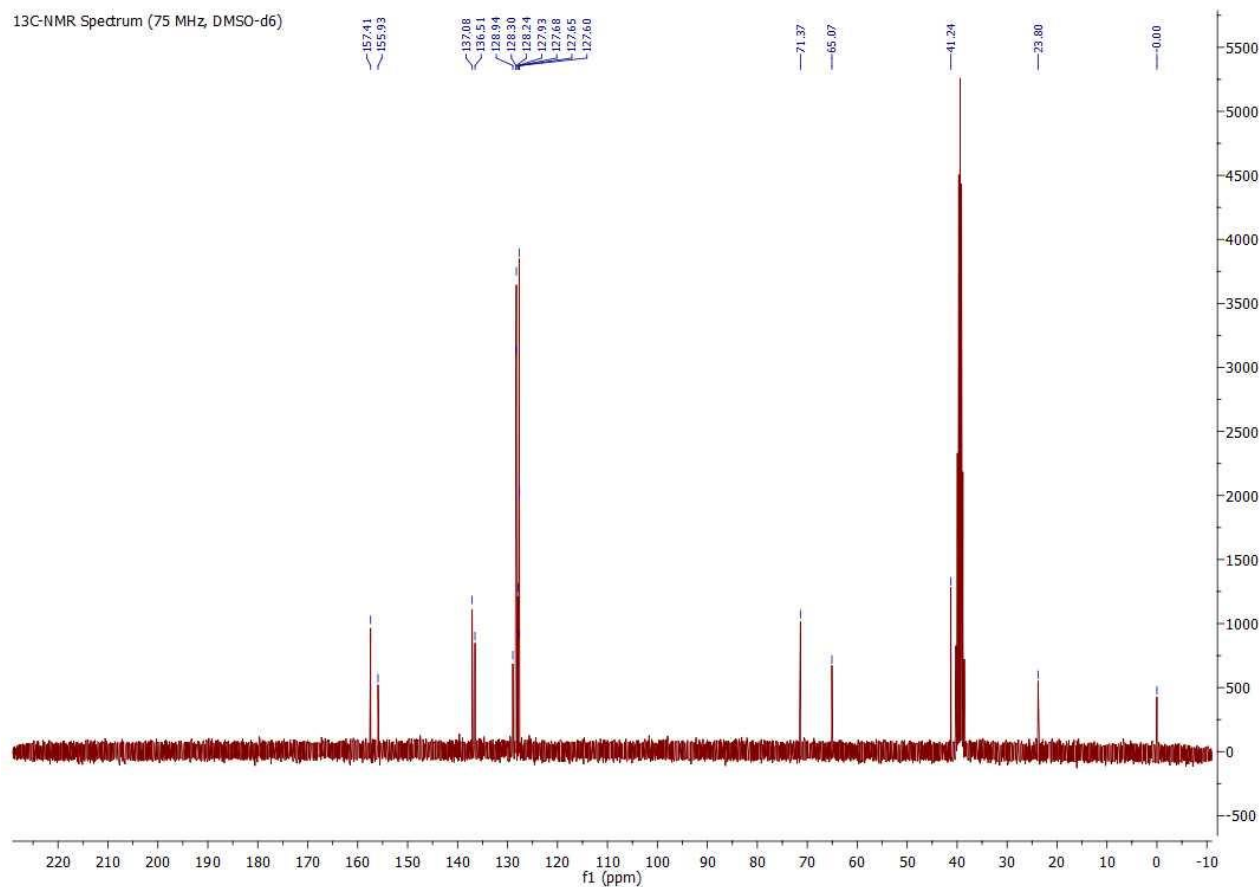
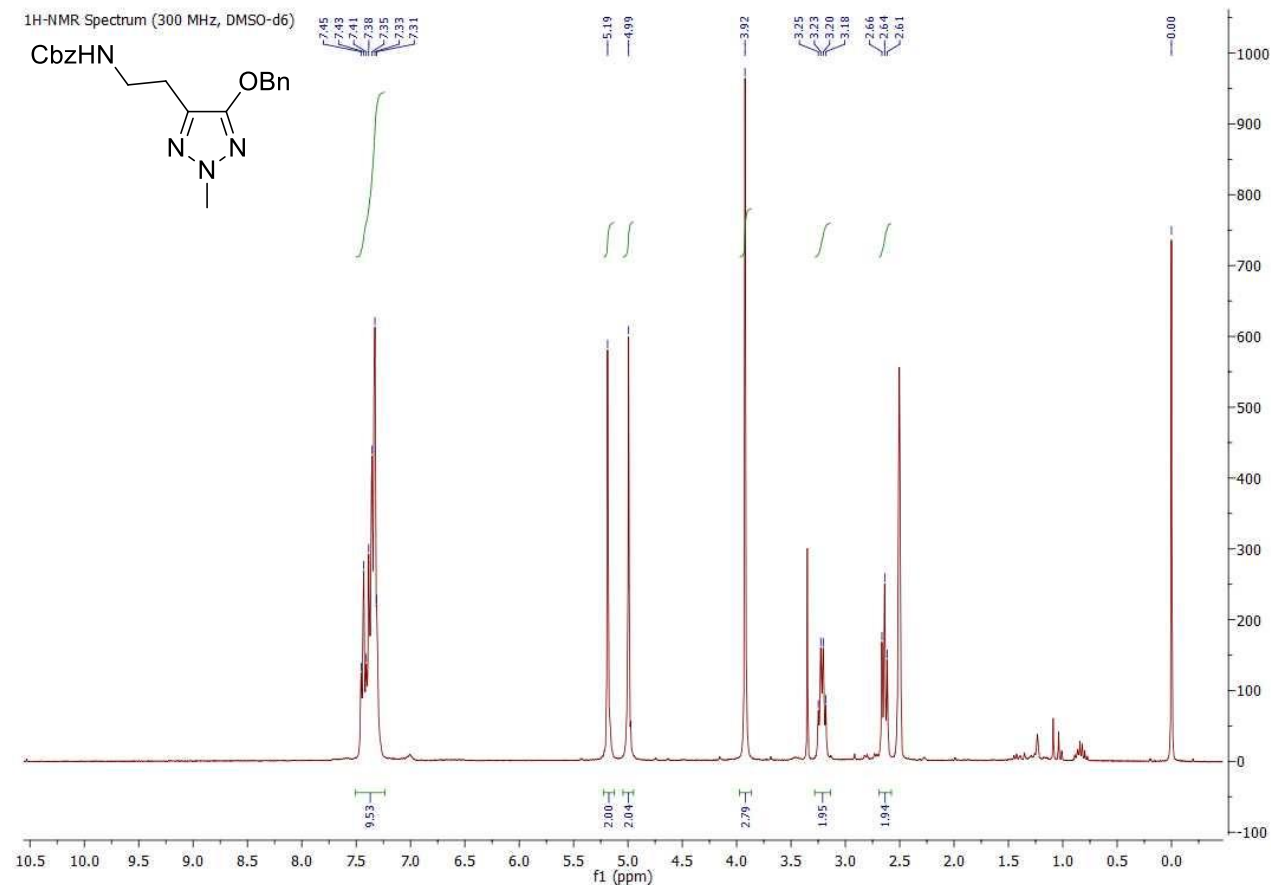
¹³C-NMR Spectrum (75 MHz, CDCl₃)



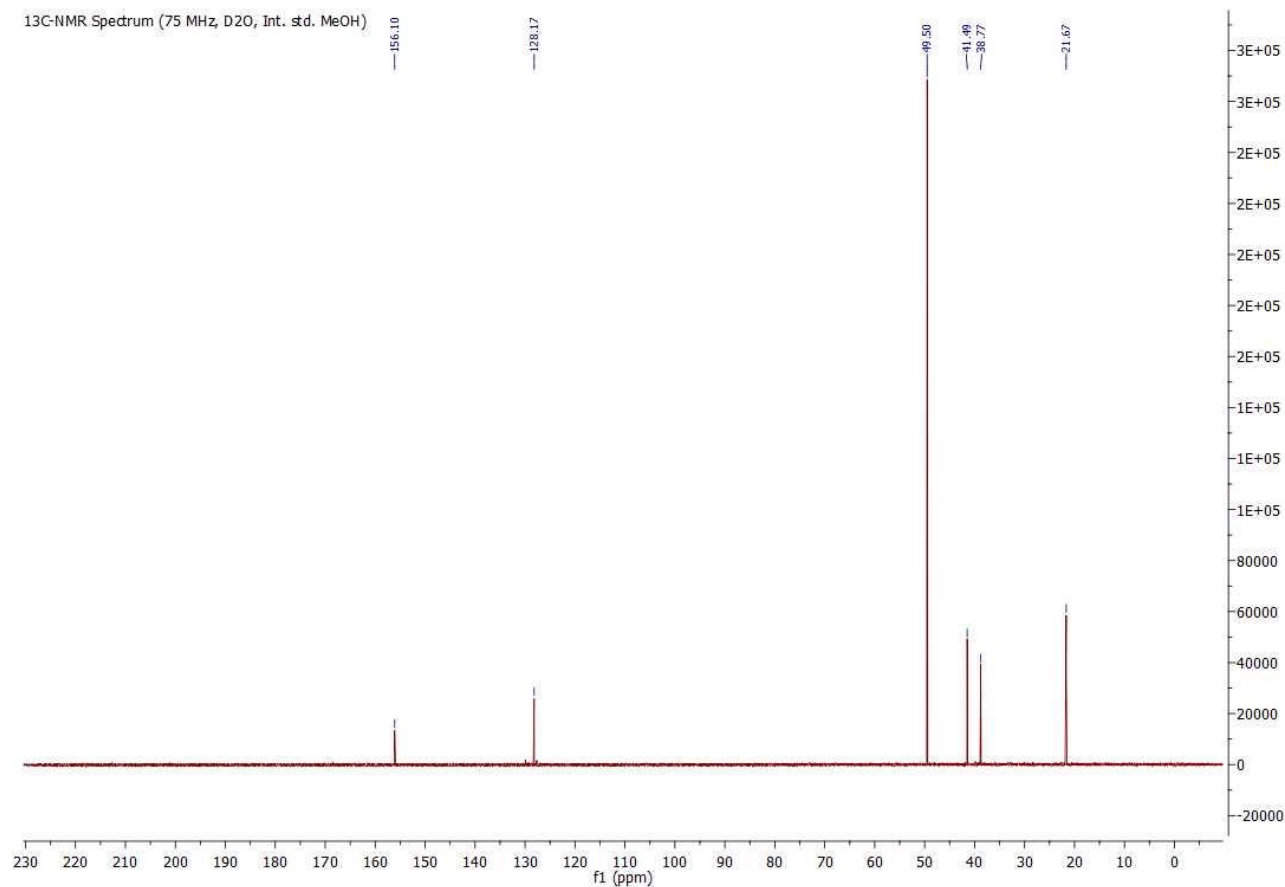
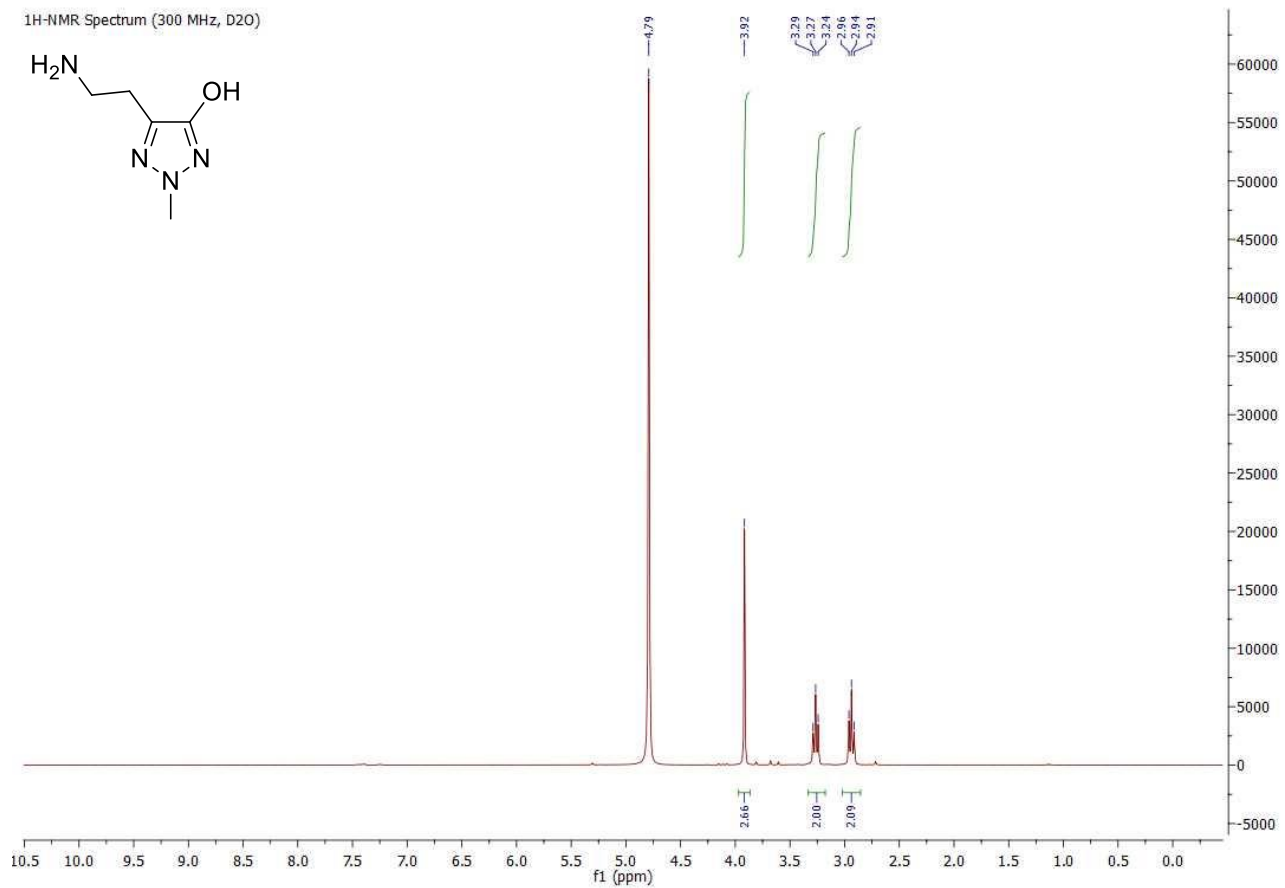
2-(5-(Benzyloxy)-2-methyl-2H-1,2,3-triazol-4-yl)acetonitrile (2.13).



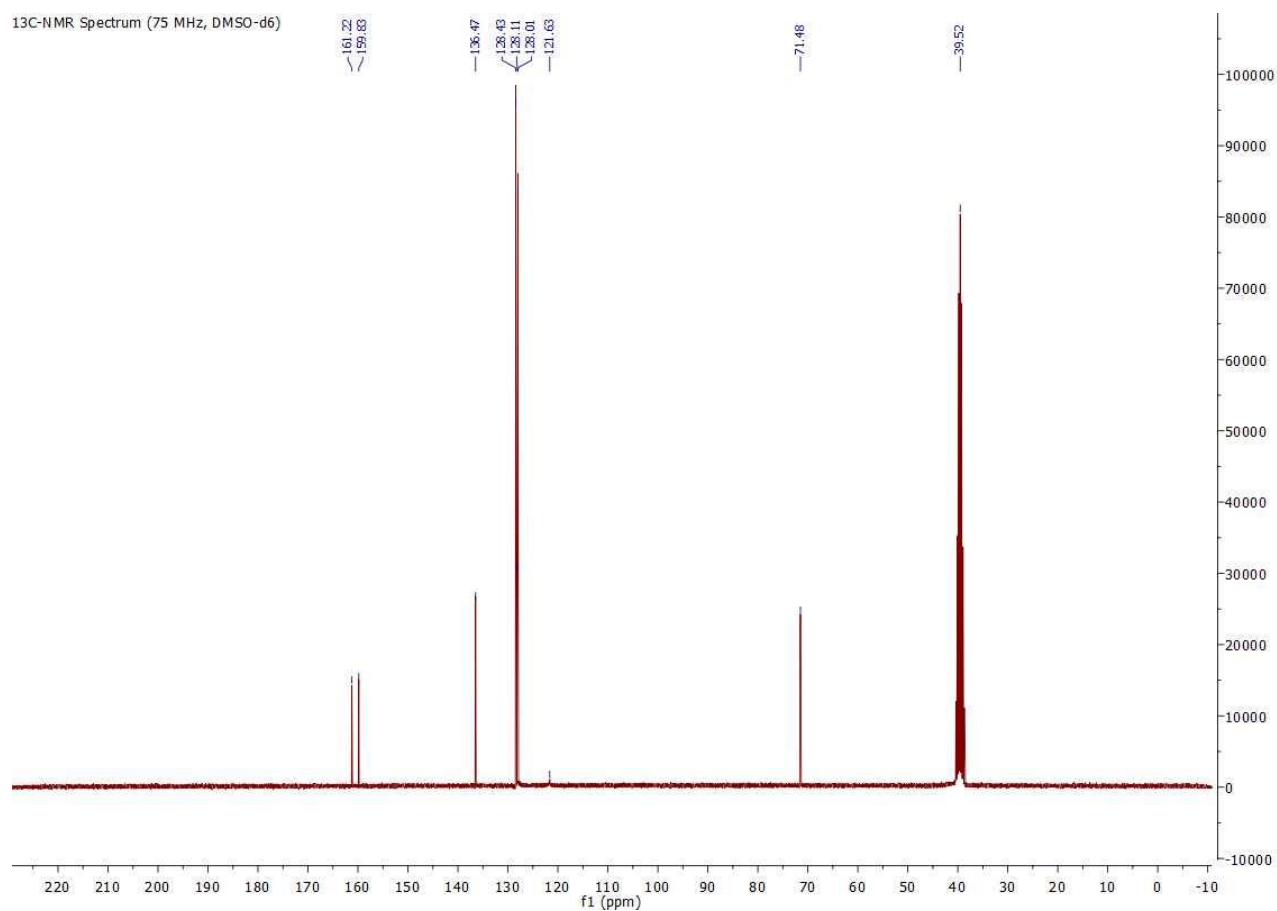
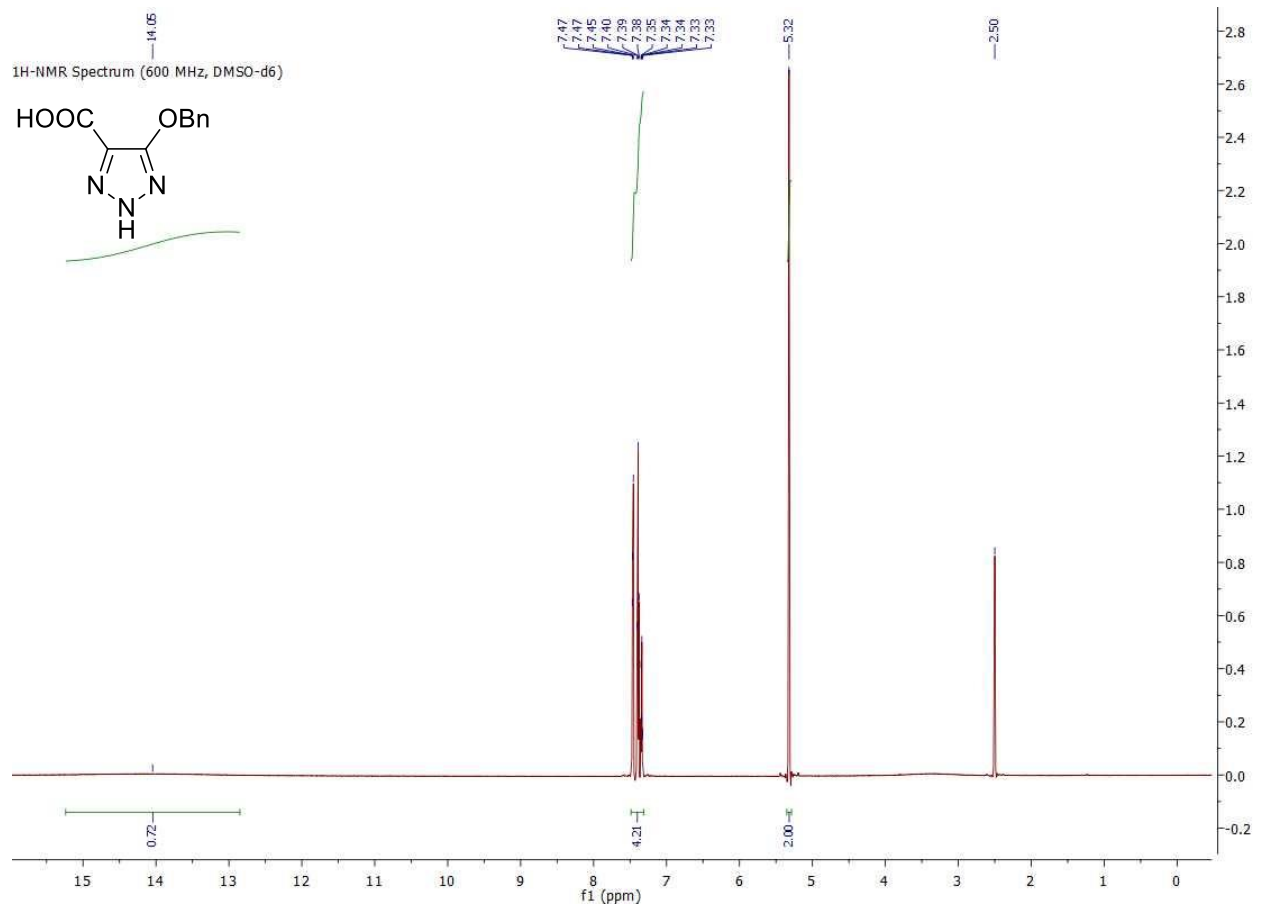
Benzyl (2-(5-(benzyloxy)-2-methyl-2H-1,2,3-triazol-4-yl)ethyl)carbamate (2.14).



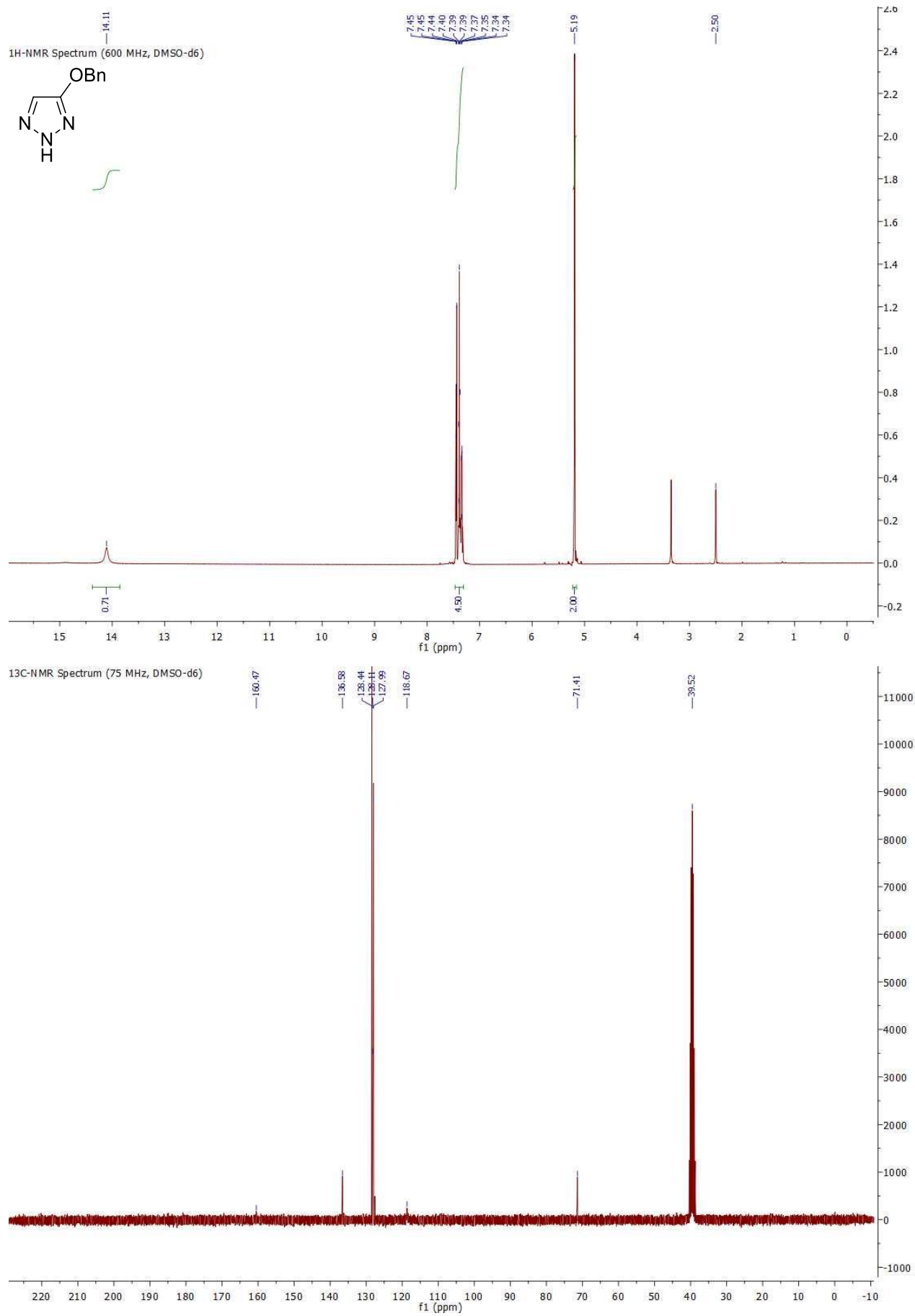
5-(2-aminoethyl)-2-methyl-2H-1,2,3-triazol-4-ol hydrochloride (2.3).



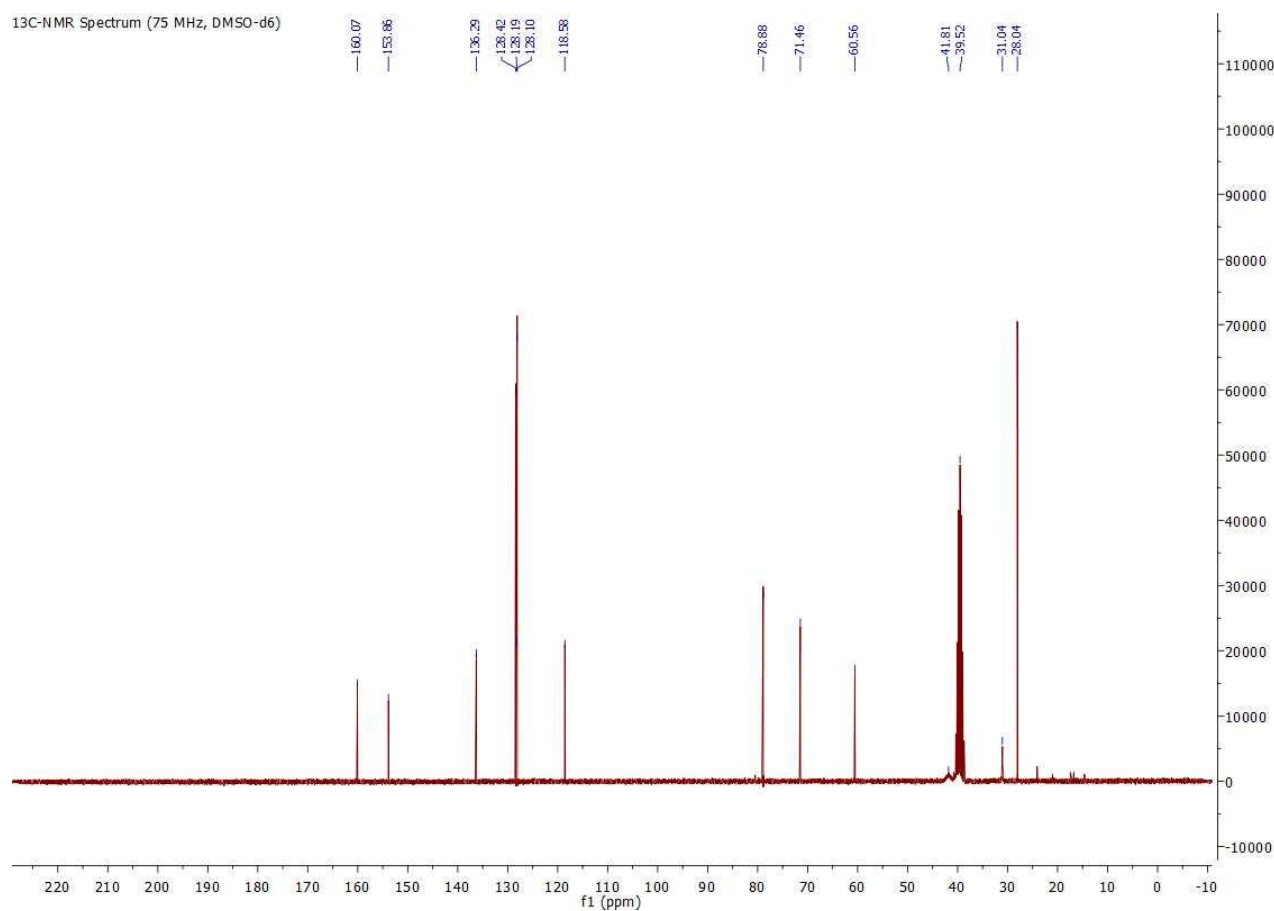
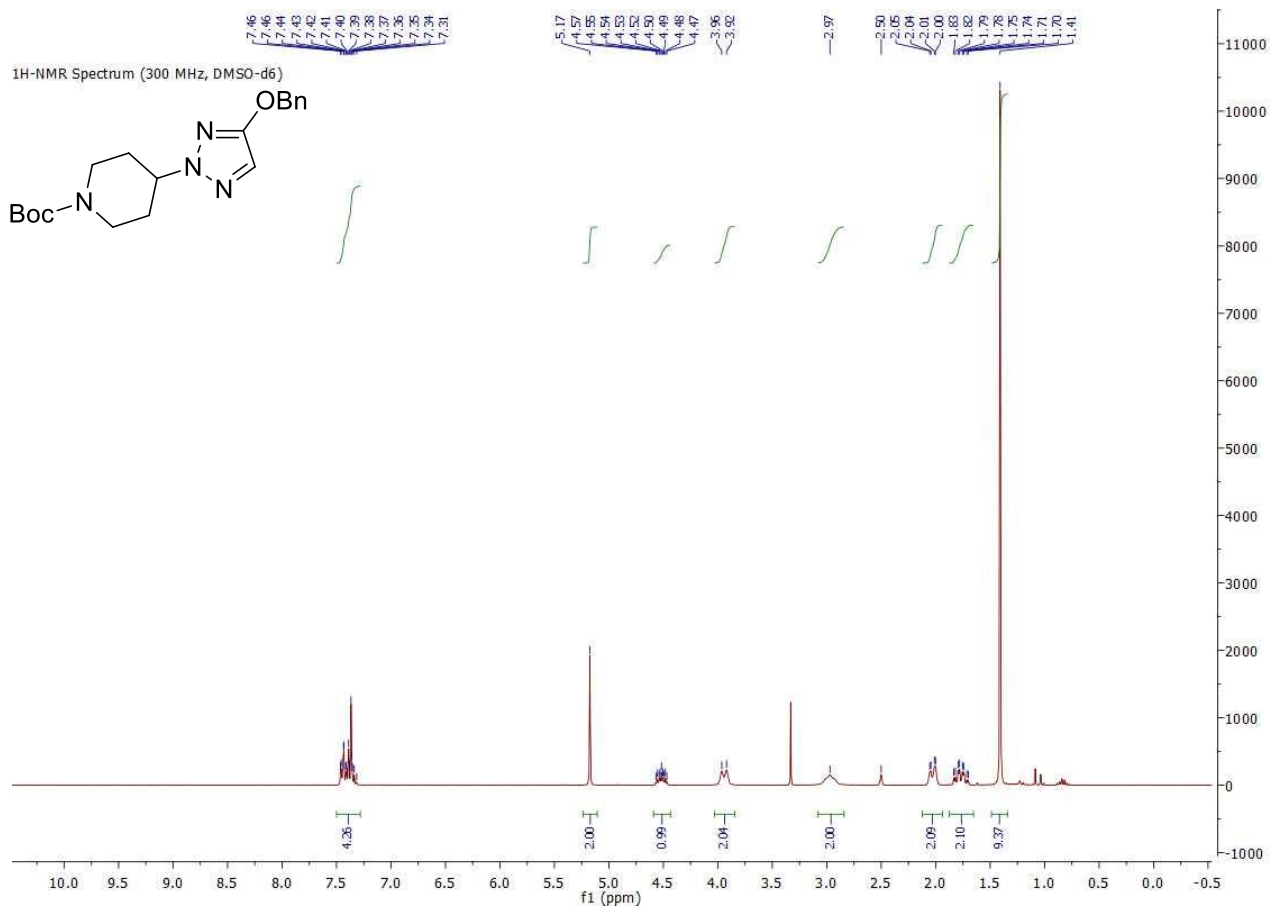
5-(benzyloxy)-2H-1,2,3-triazole-4-carboxylic acid (2.20).

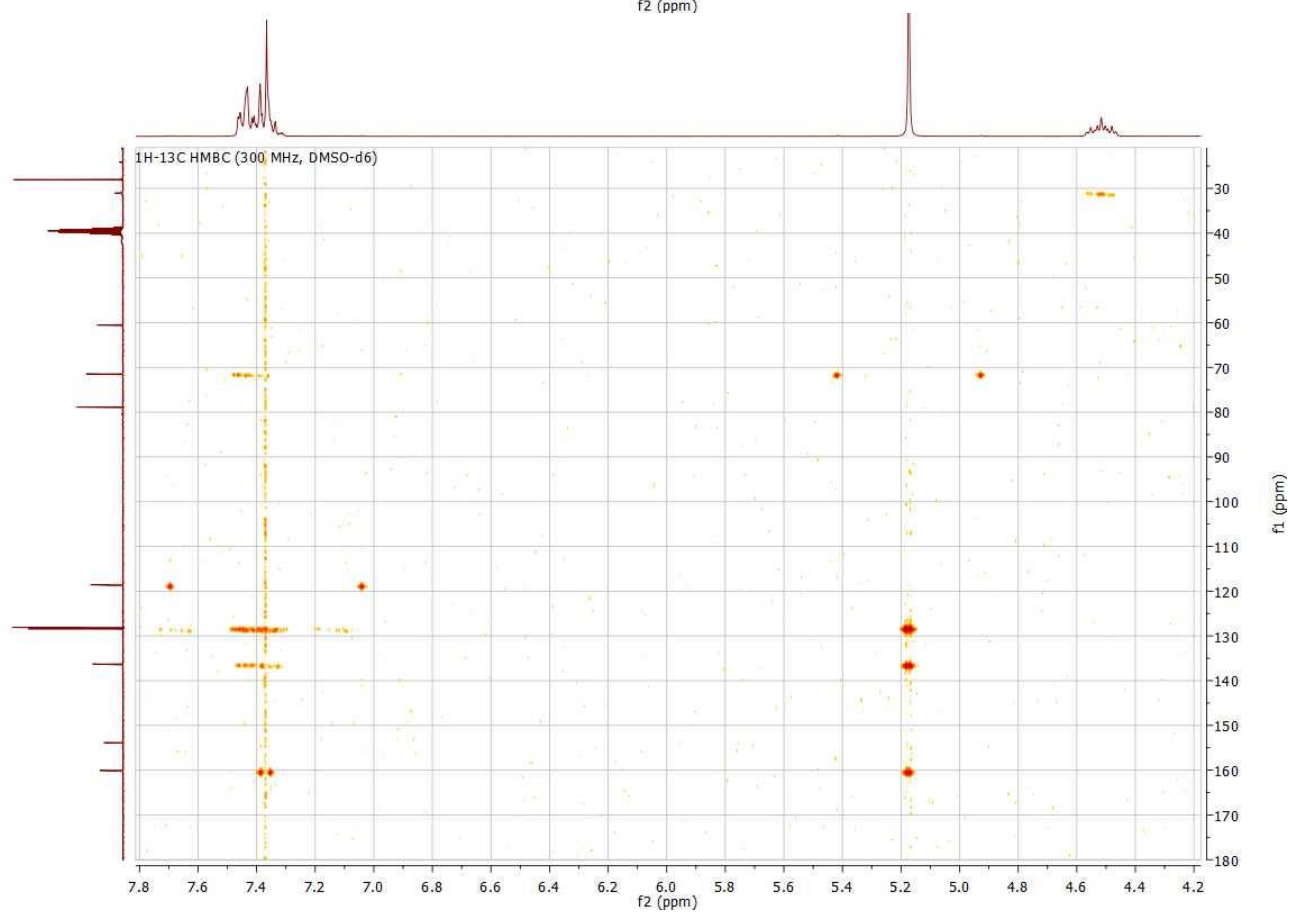
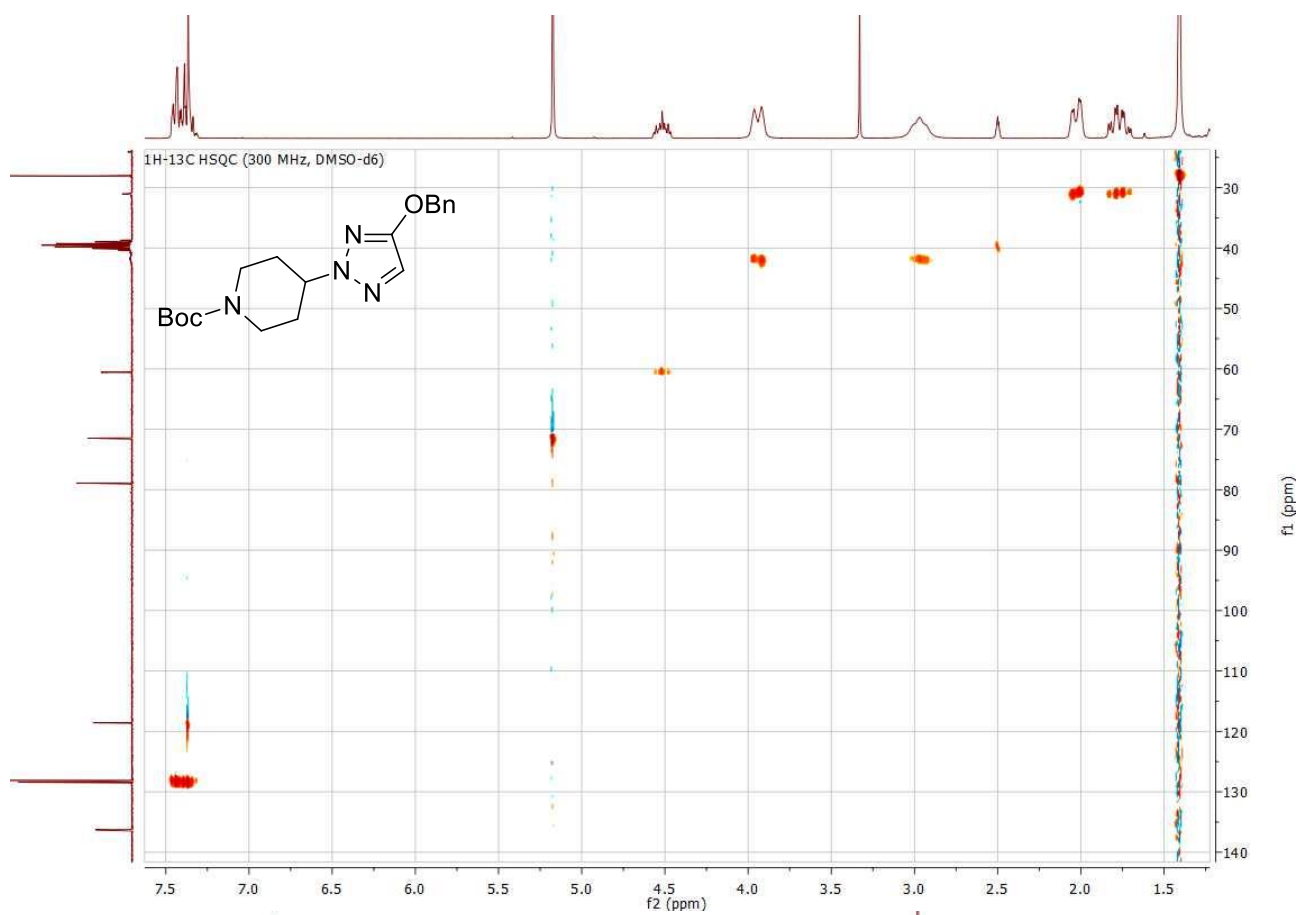


4-(benzyloxy)-2H-1,2,3-triazole (2.21).

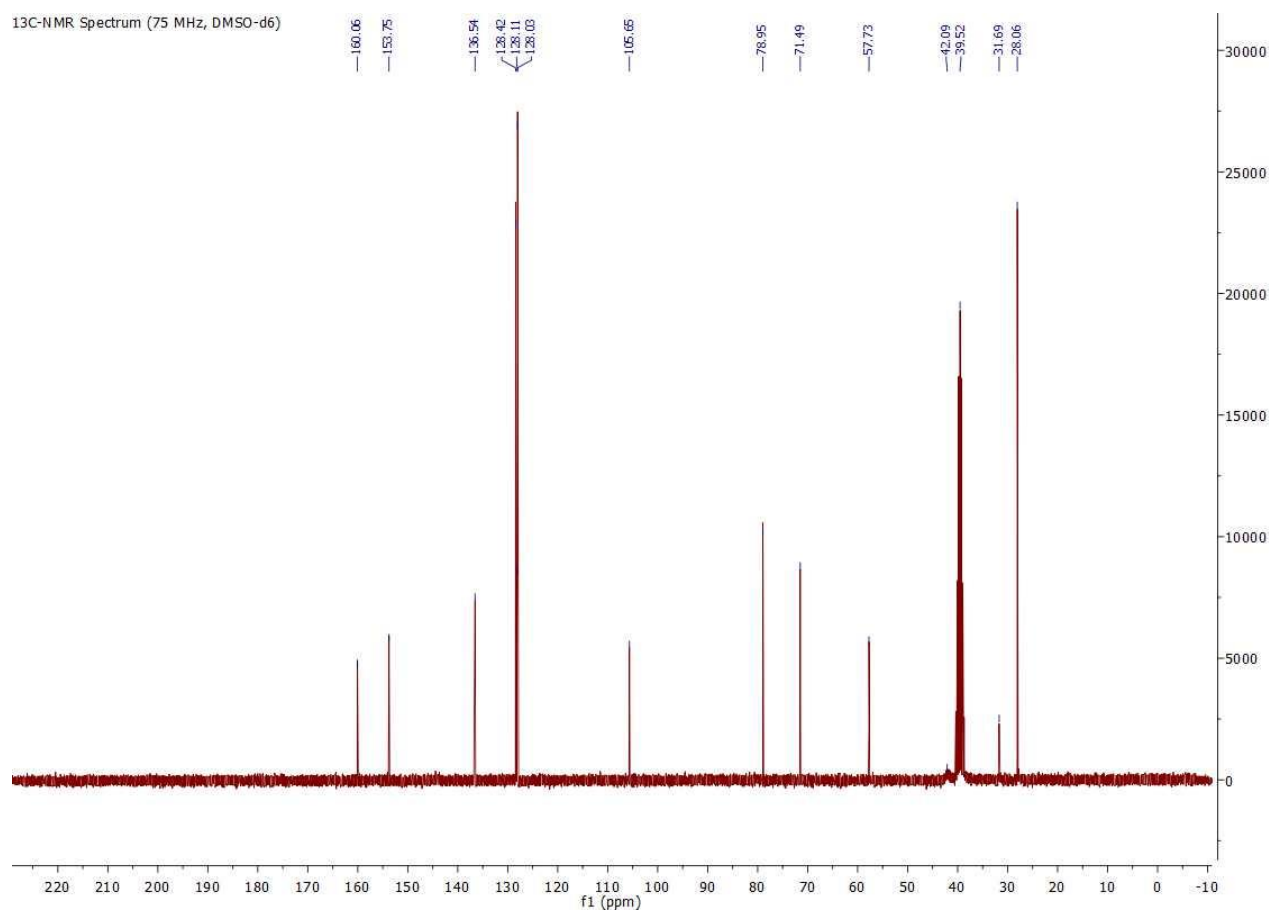
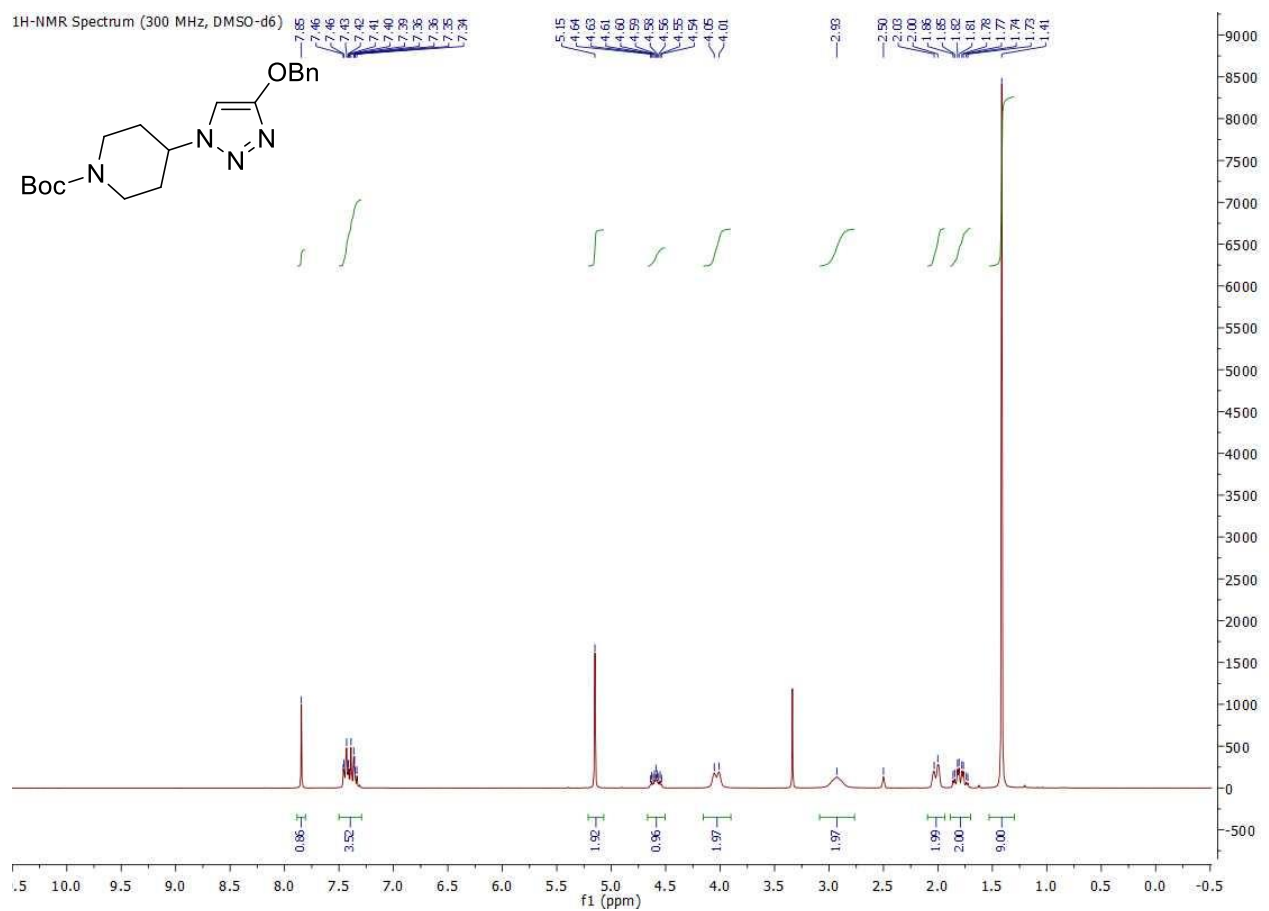


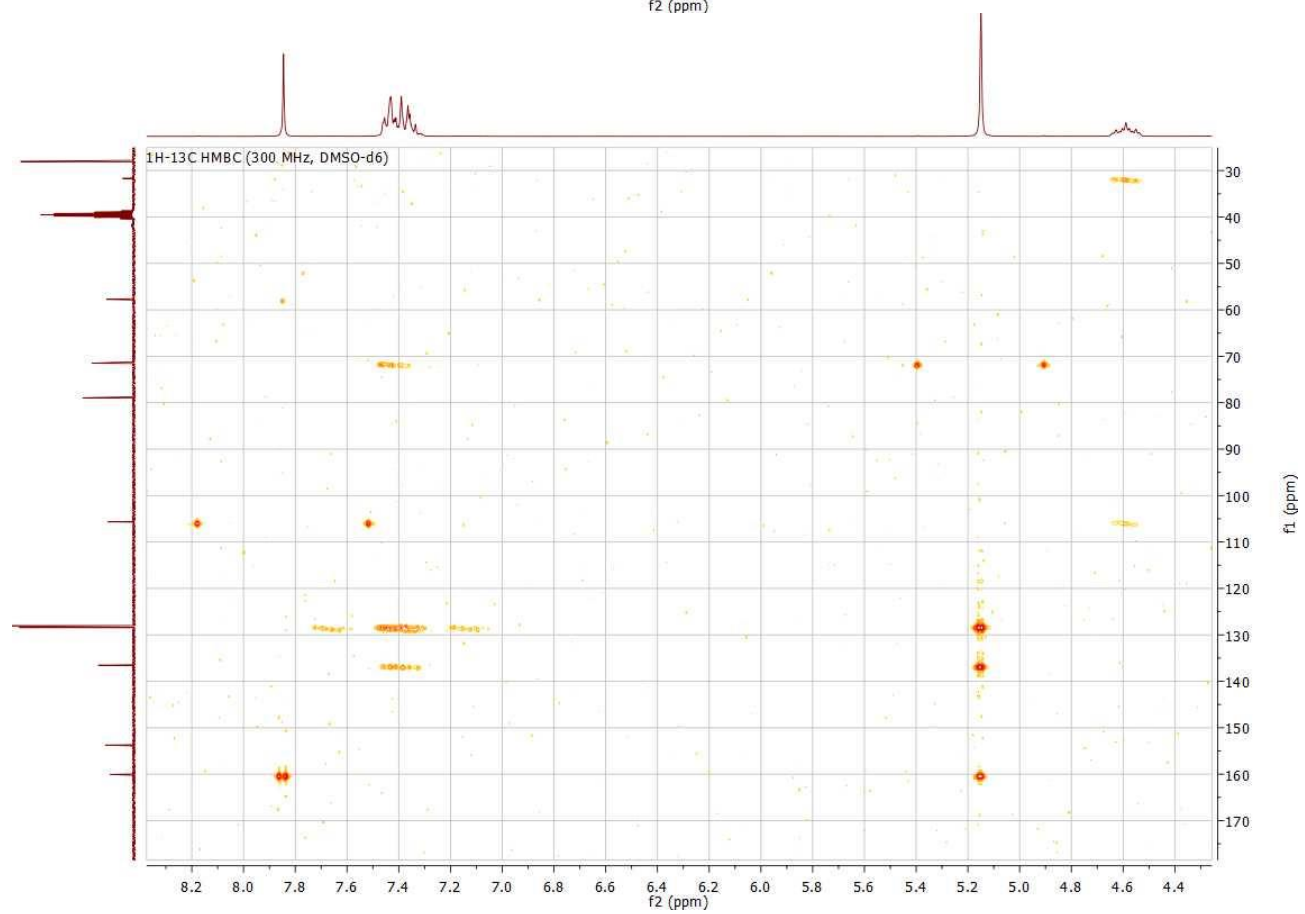
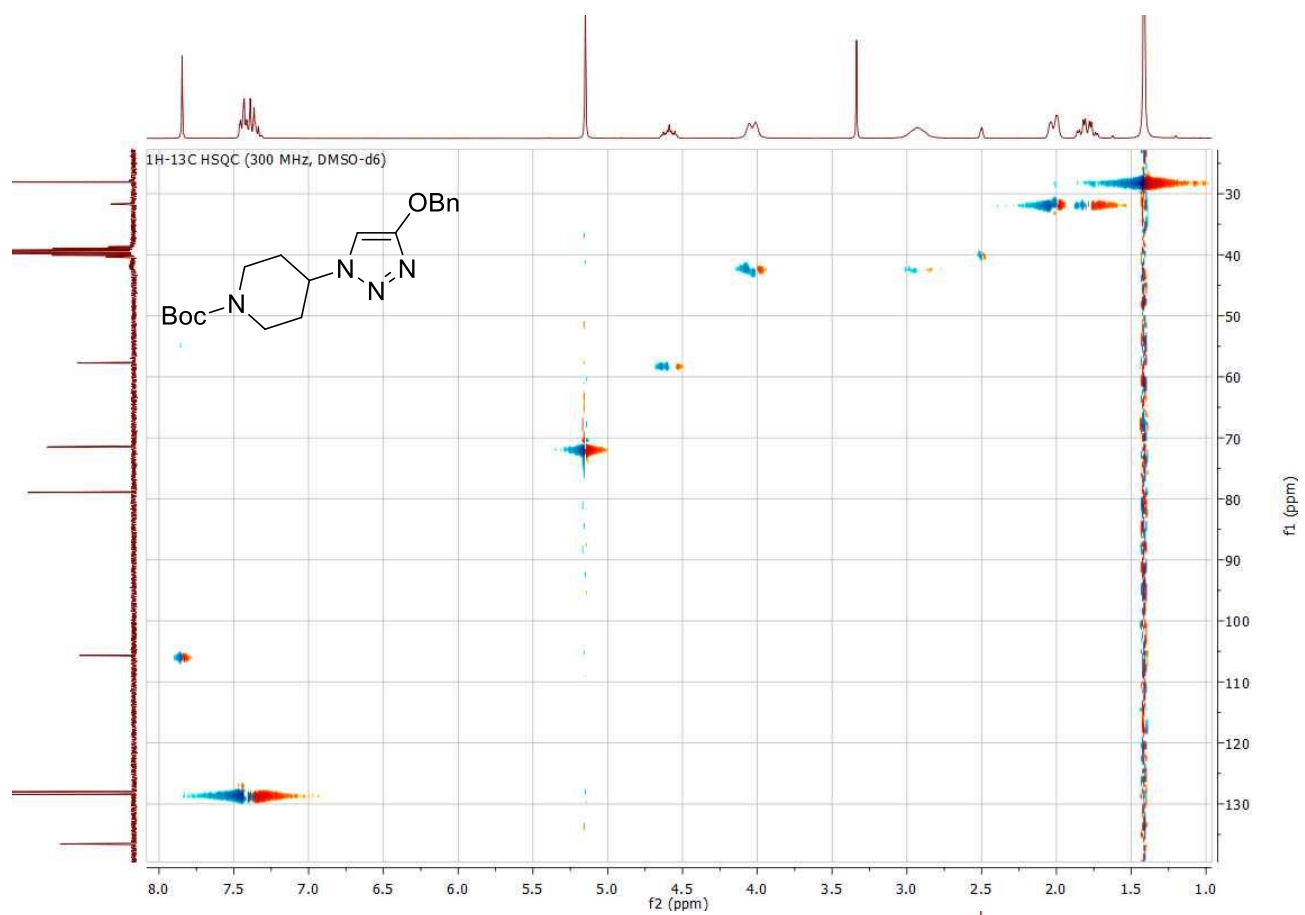
***tert*-Butyl 4-(4-(benzyloxy)-2*H*-1,2,3-triazol-2-yl)piperidine-1-carboxylate (2.23).**





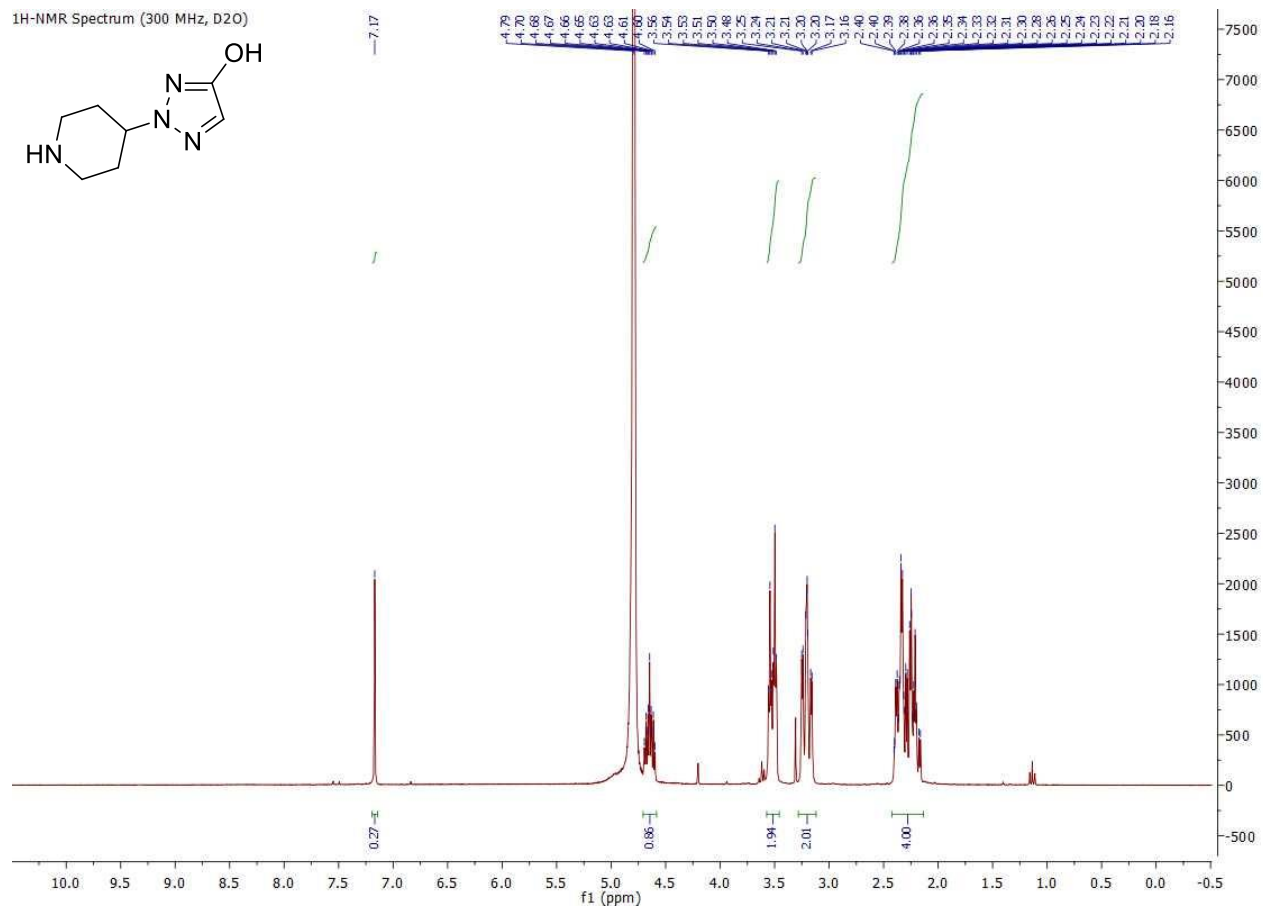
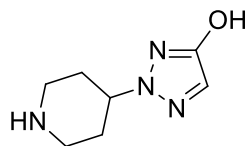
***tert*-Butyl 4-(4-(benzyloxy)-1*H*-1,2,3-triazol-1-yl)piperidine-1-carboxylate (2.22).**



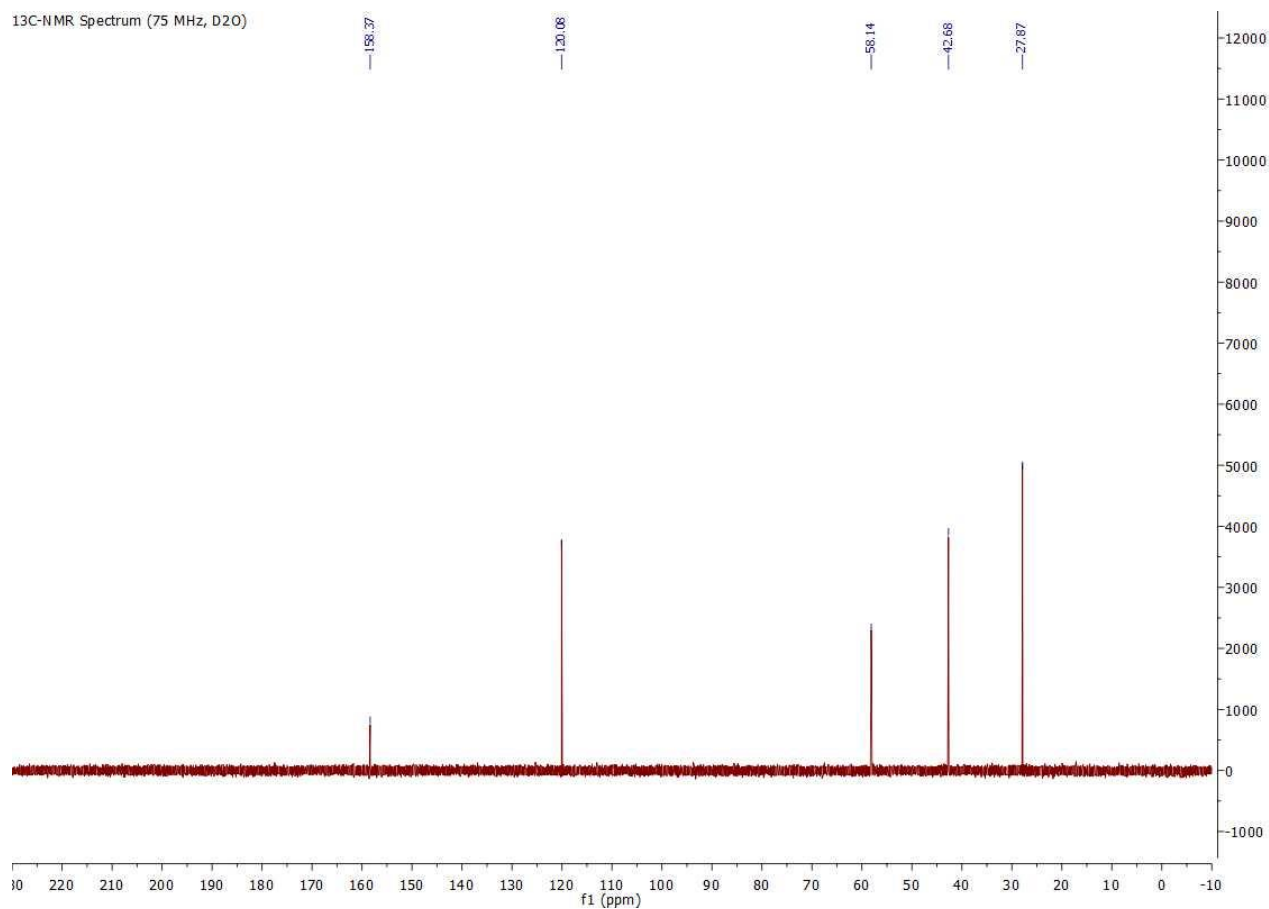


2-(piperidine-4-yl)-2H-1,2,3-triazol-4-ol hydrochloride (2.5a).

¹H-NMR Spectrum (300 MHz, D₂O)

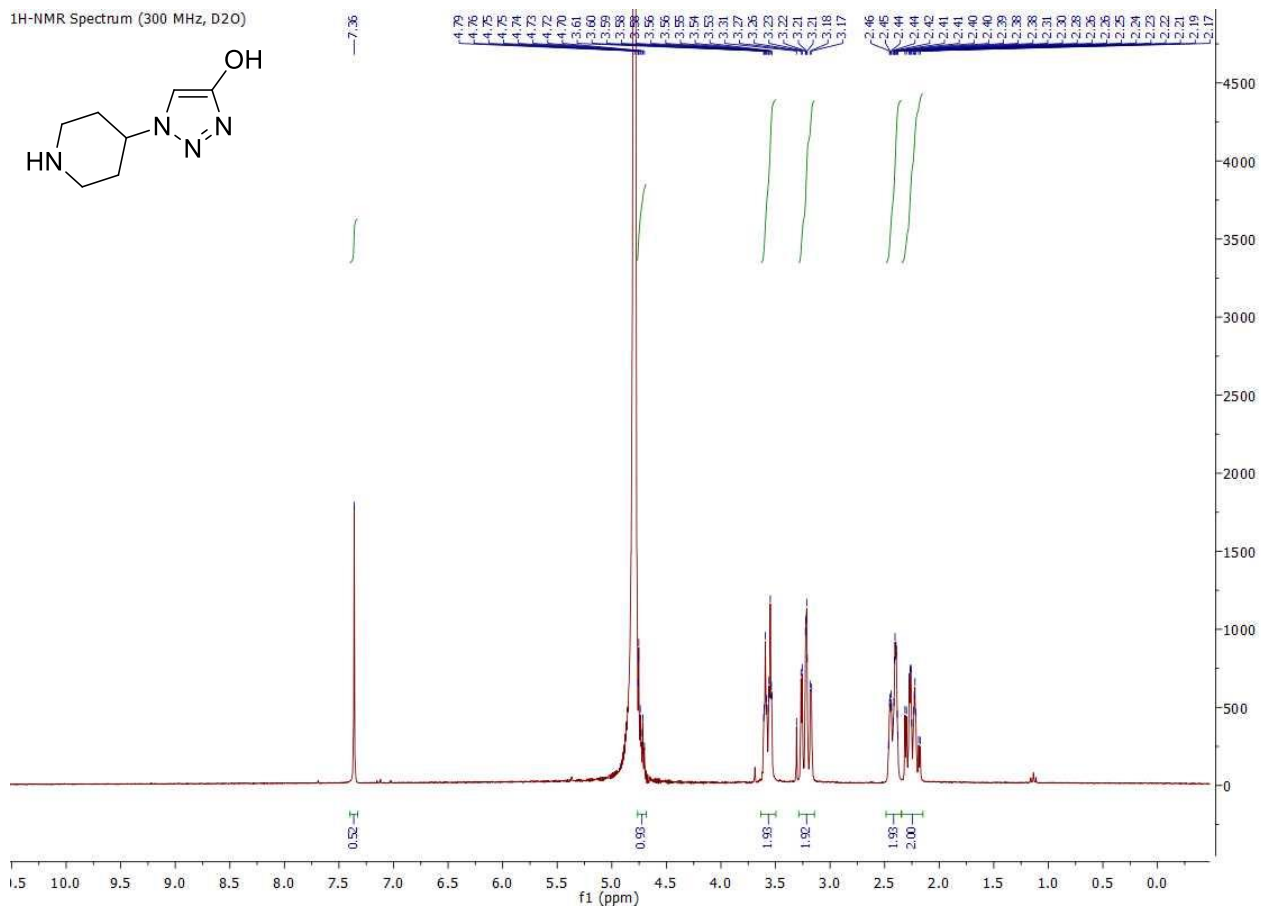
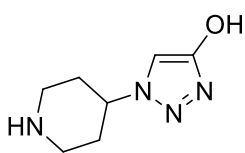


¹³C-NMR Spectrum (75 MHz, D₂O)

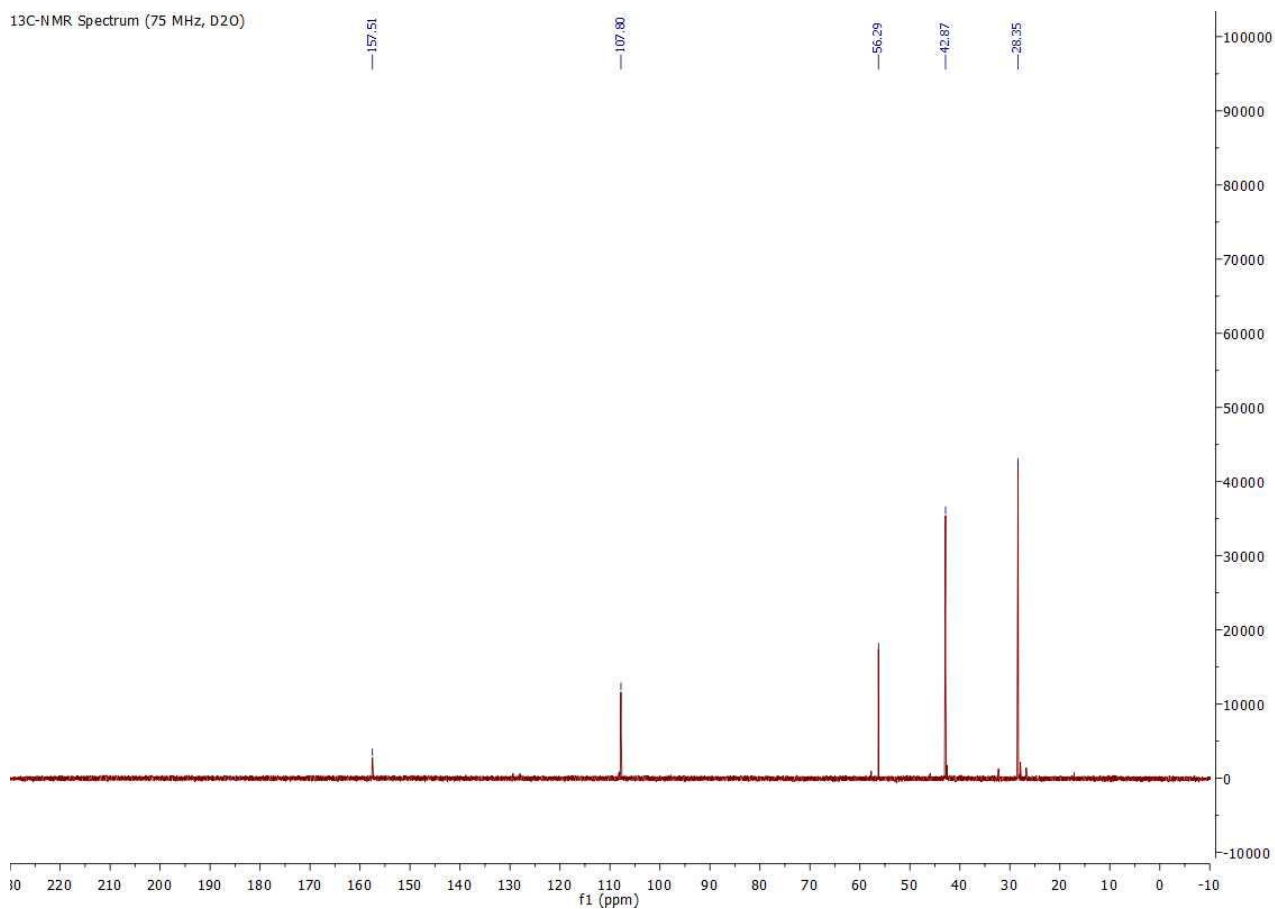


1-(piperidine-4-yl)-1H-1,2,3-triazol-4-ol hydrochloride (2.4a).

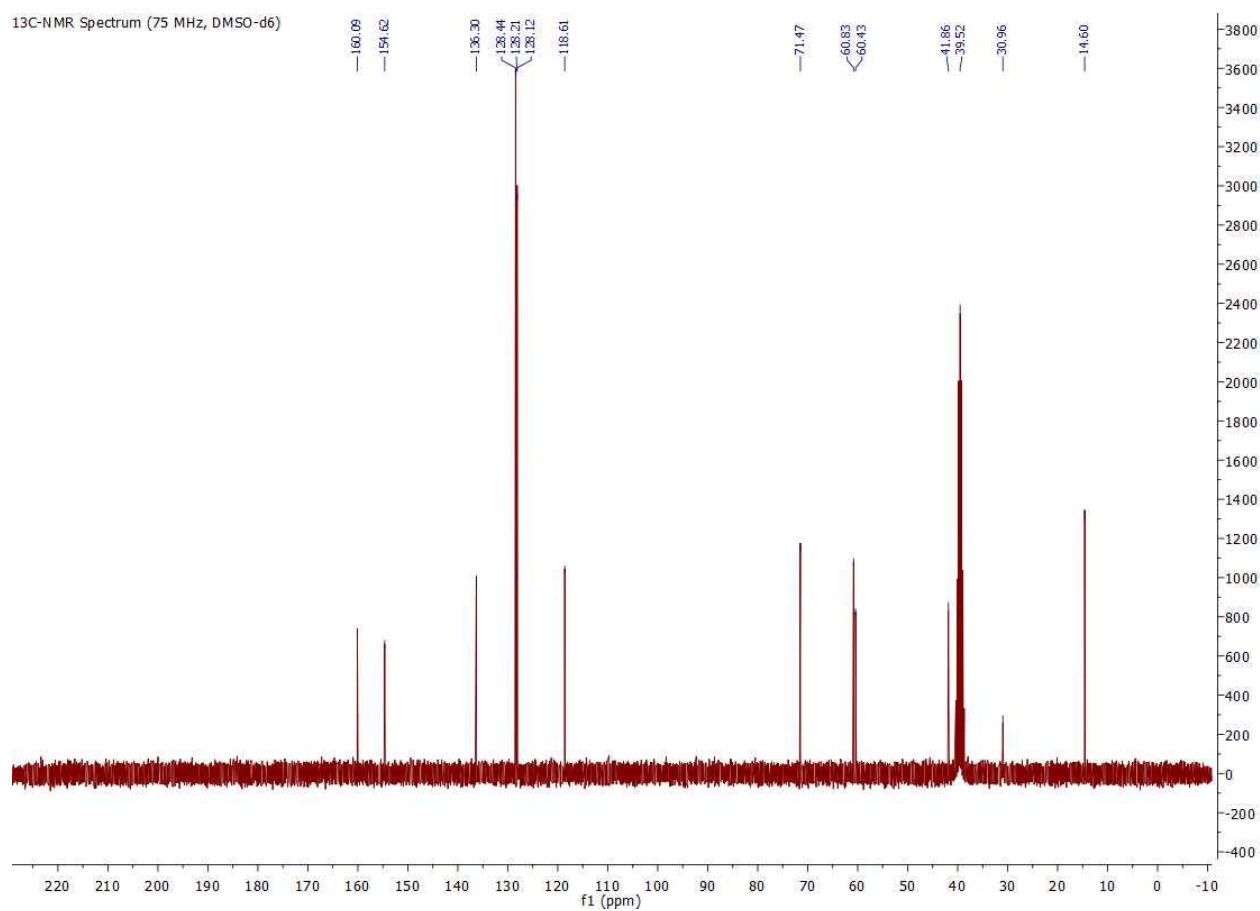
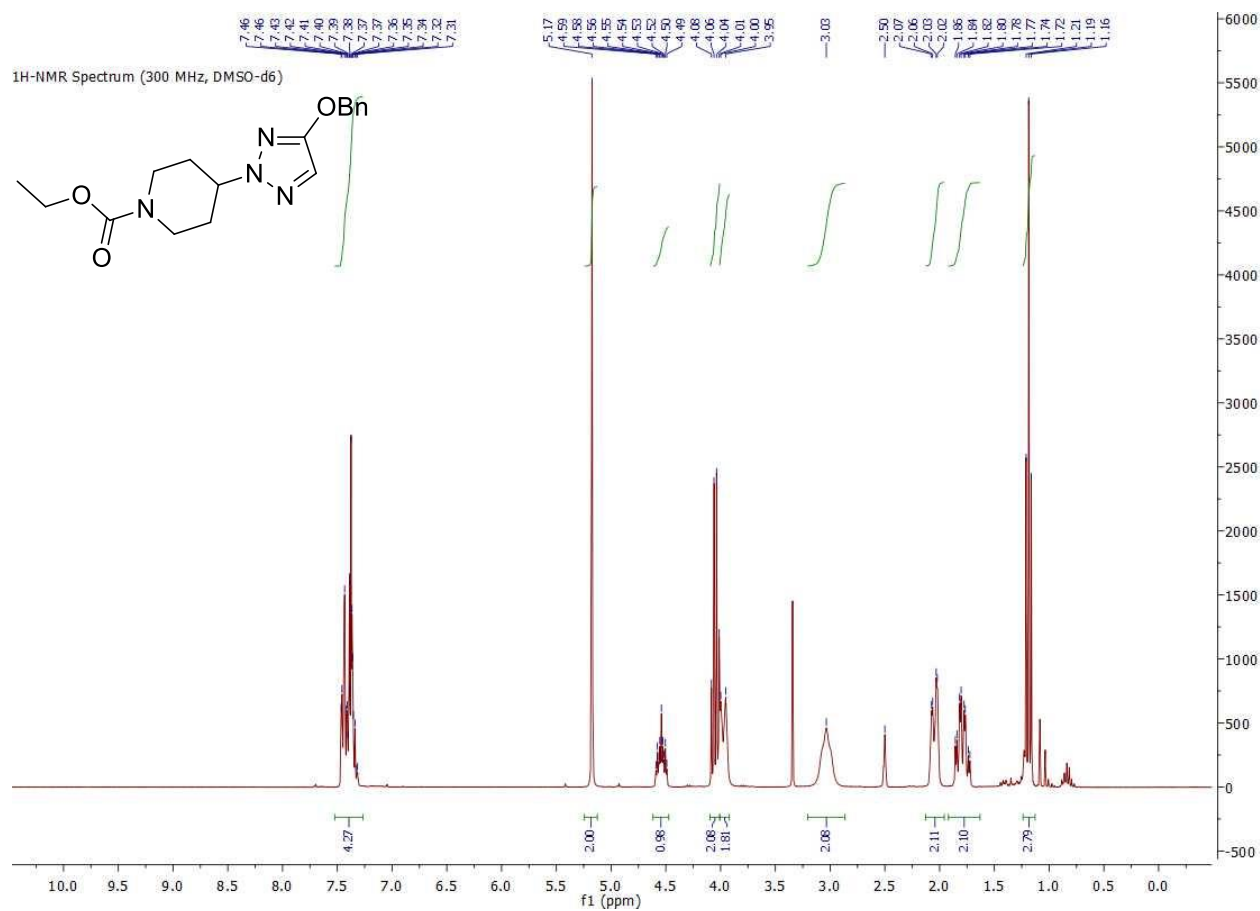
¹H-NMR Spectrum (300 MHz, D₂O)



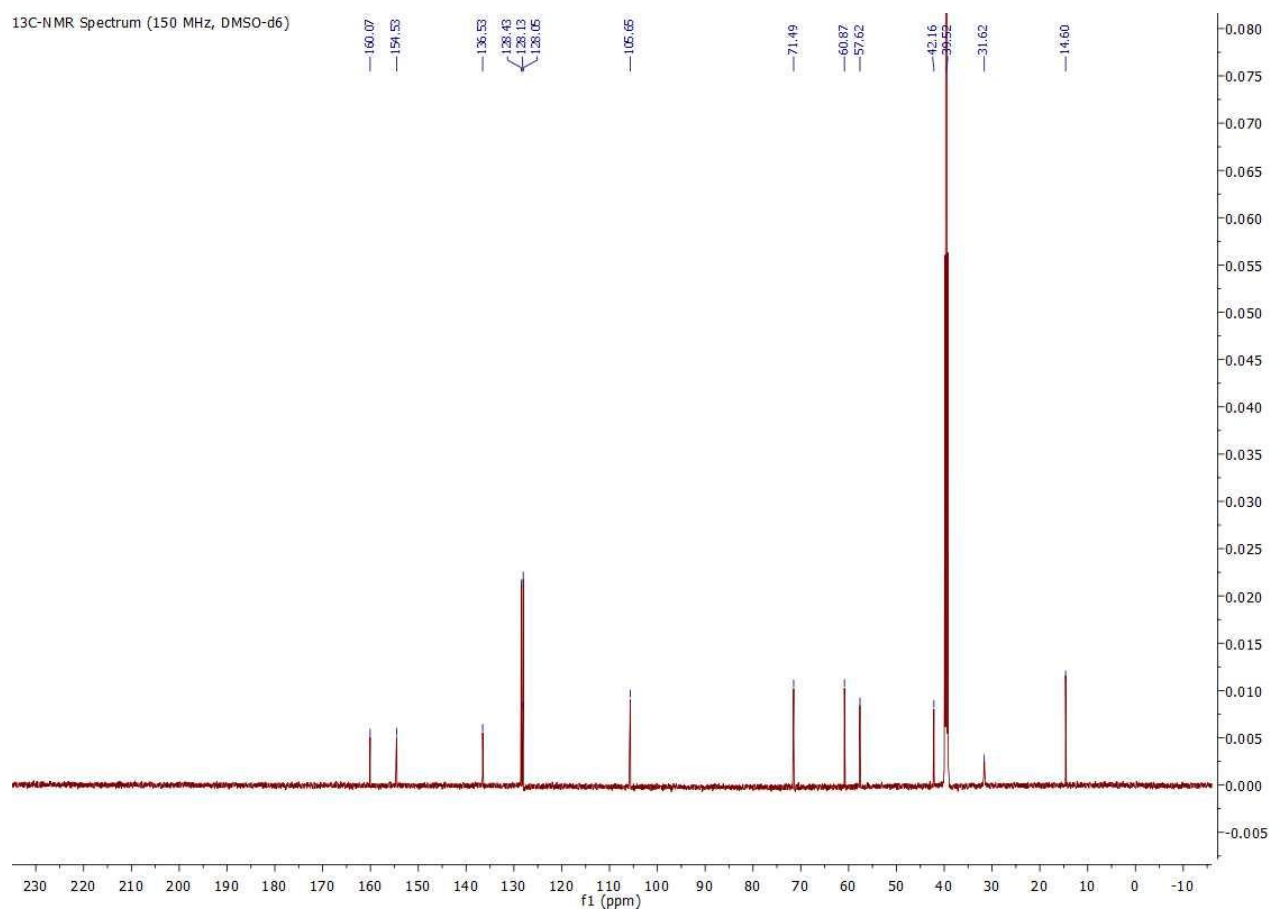
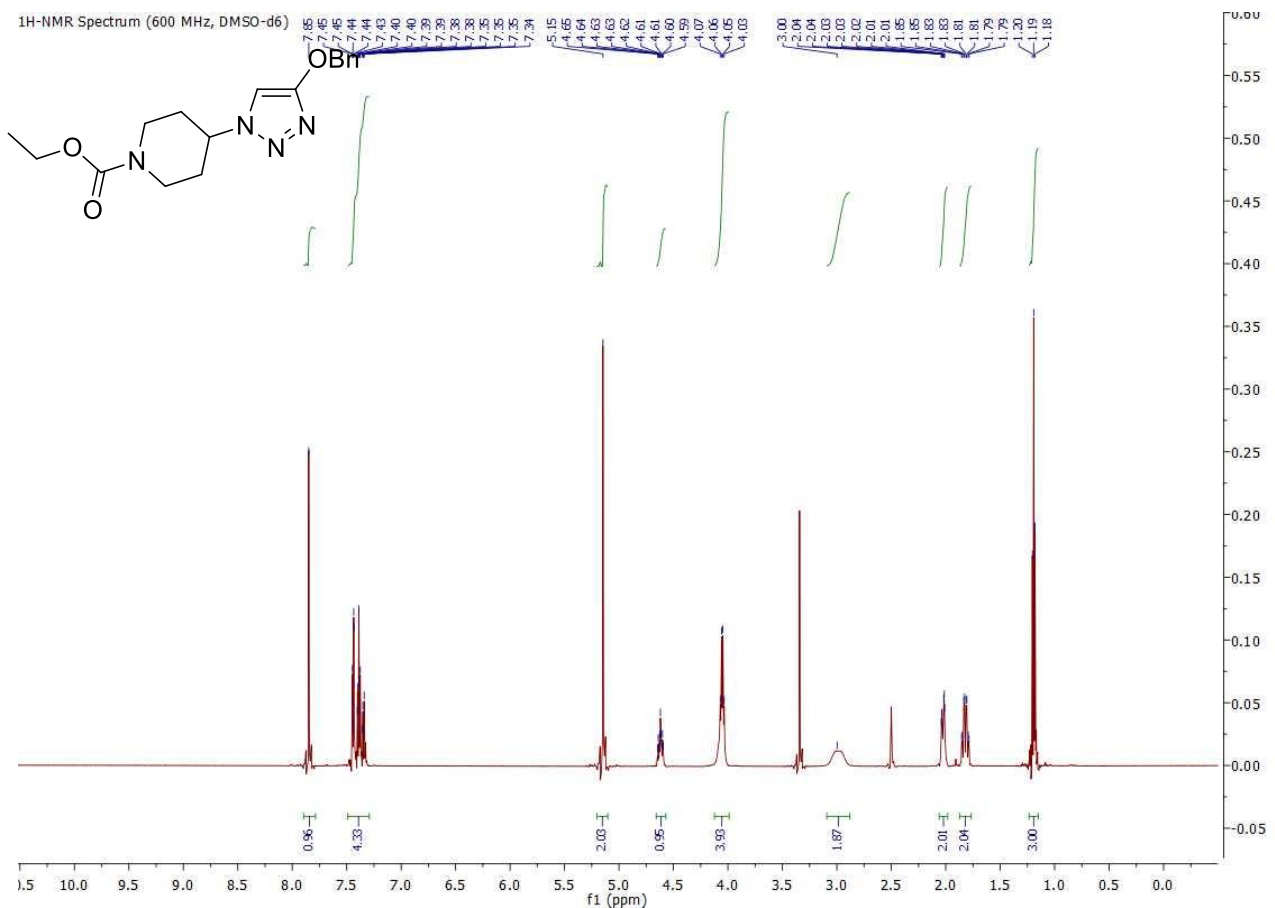
¹³C-NMR Spectrum (75 MHz, D₂O)



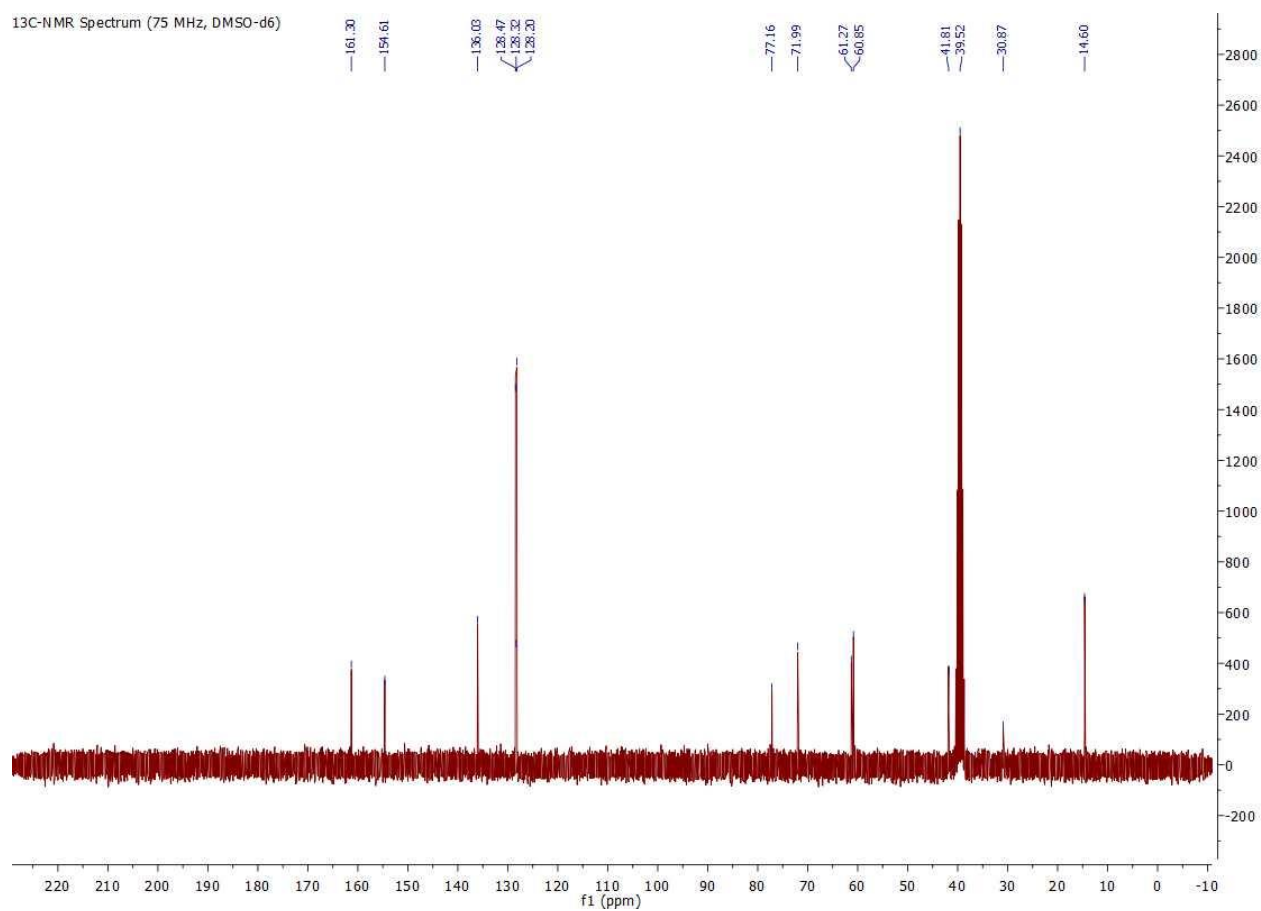
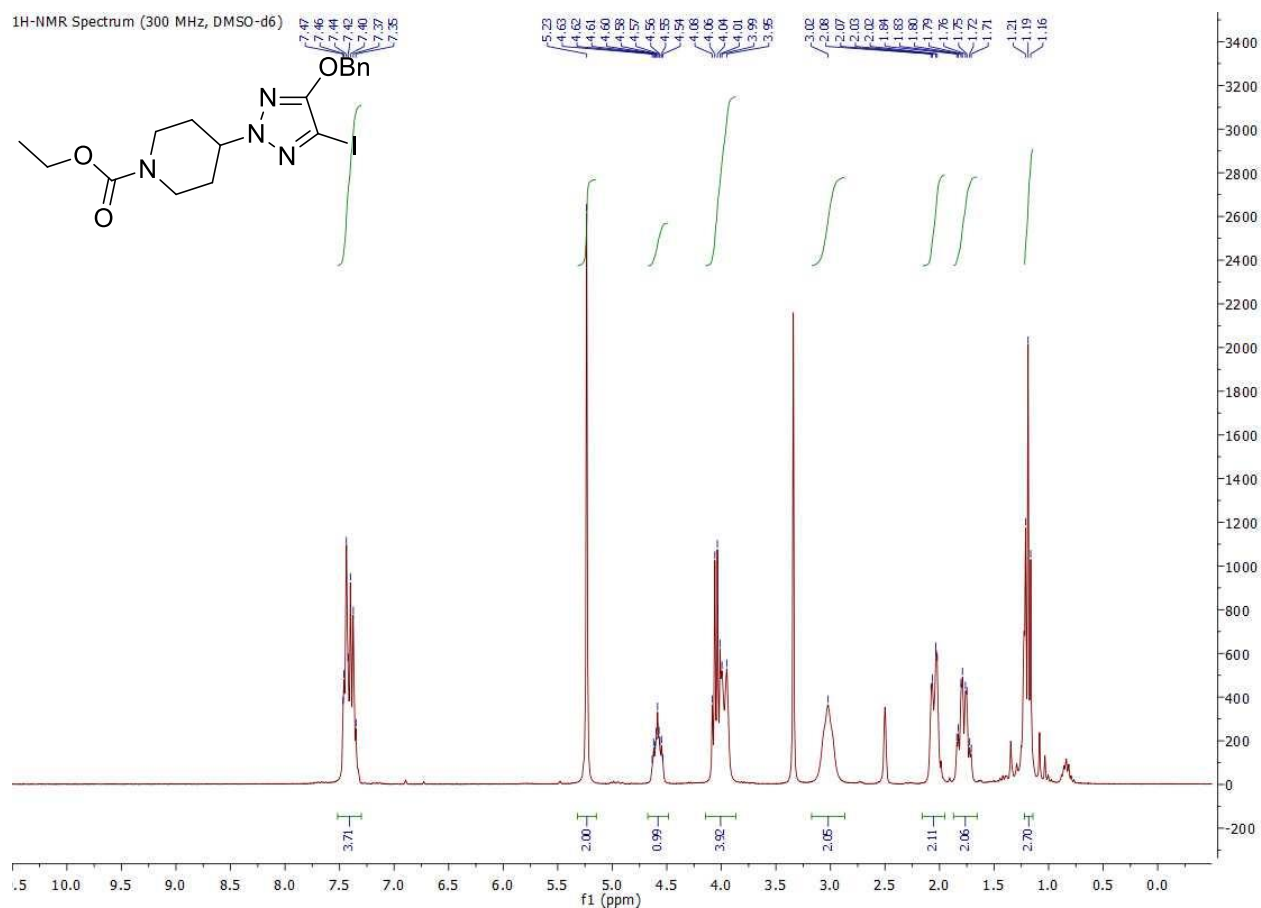
Ethyl 4-(4-(benzyloxy)-2H-1,2,3-triazol-2-yl)piperidine-1-carboxylate (2.26).



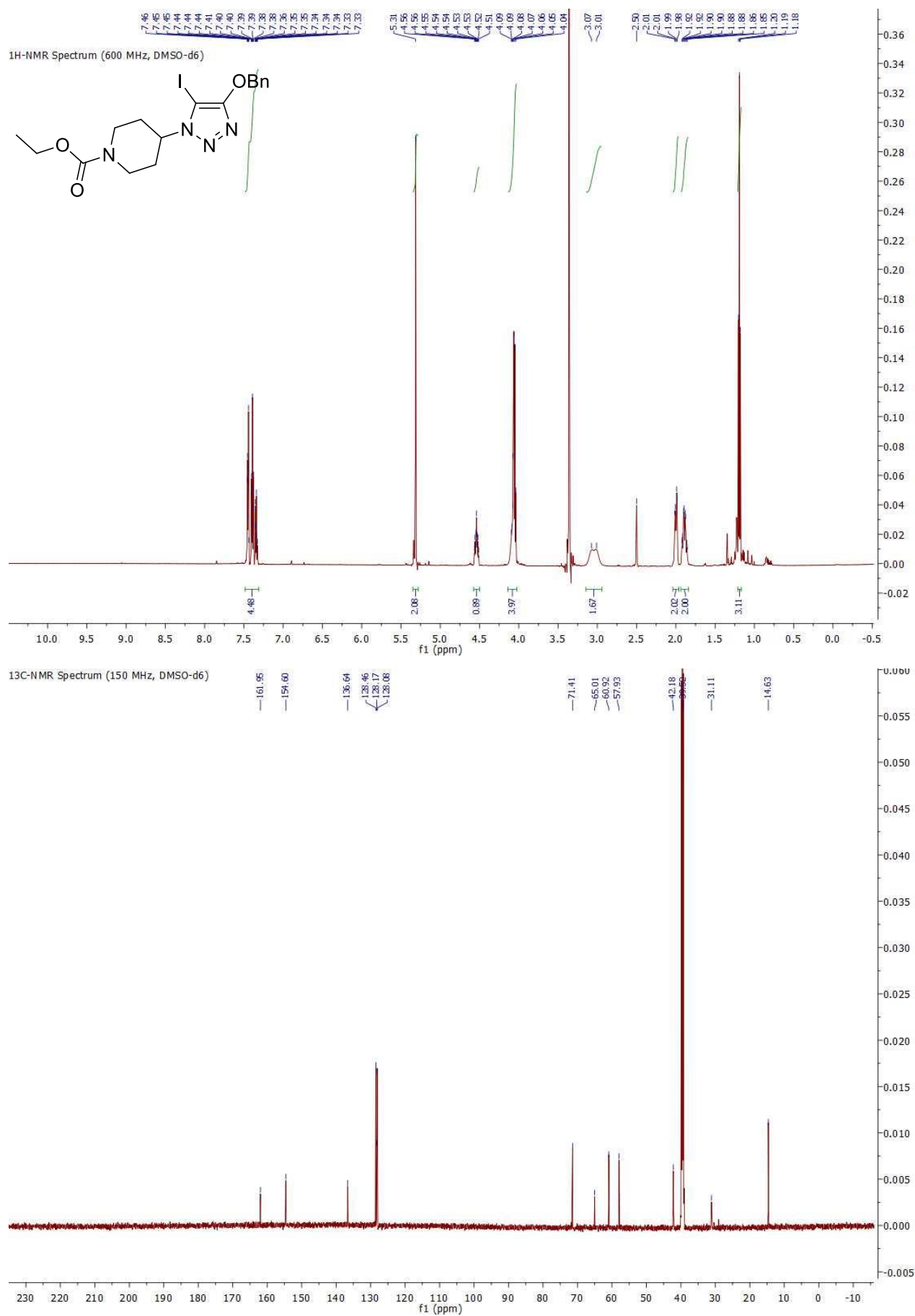
Ethyl 4-(4-(benzyloxy)-1H-1,2,3-triazol-1-yl)piperidine-1-carboxylate (2.25).



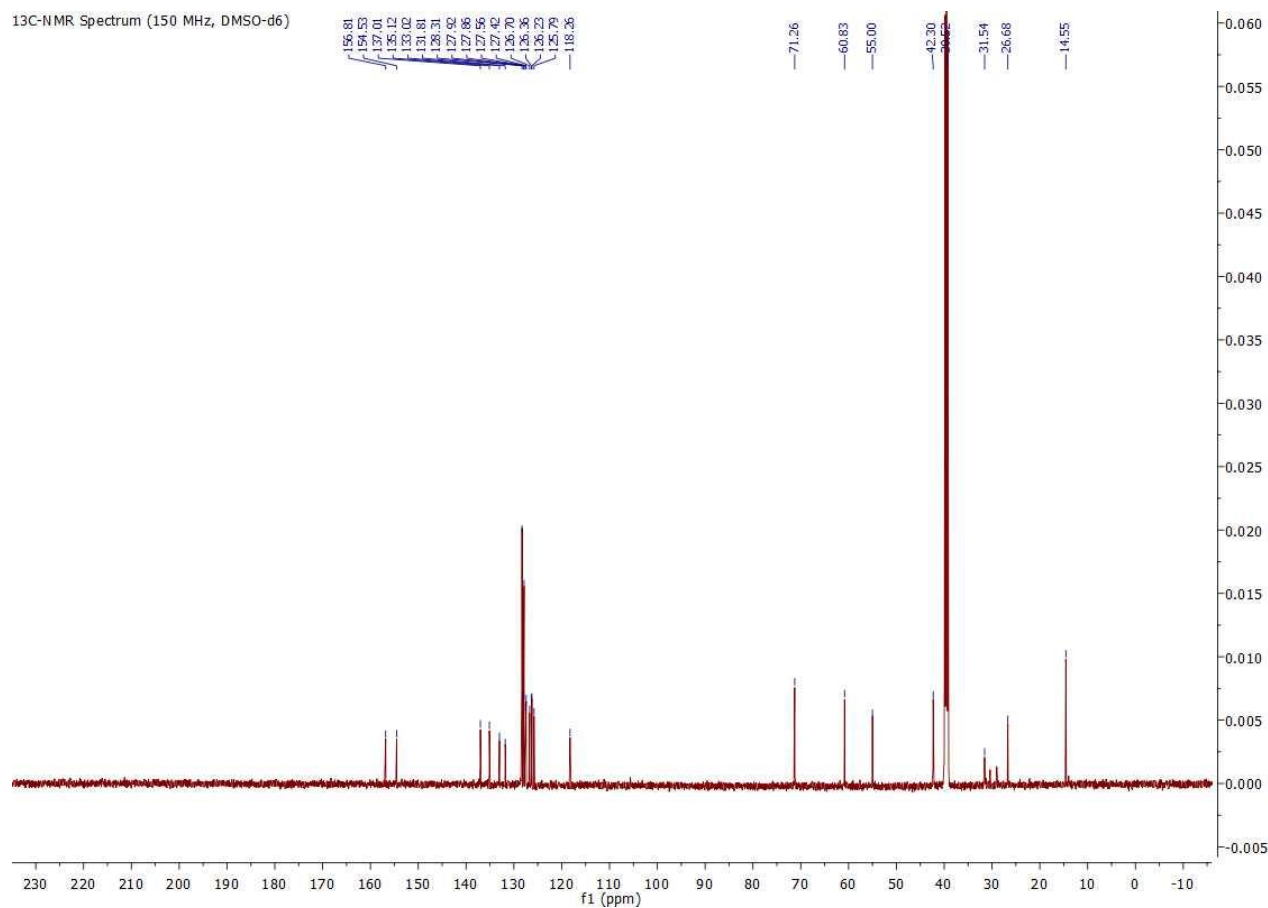
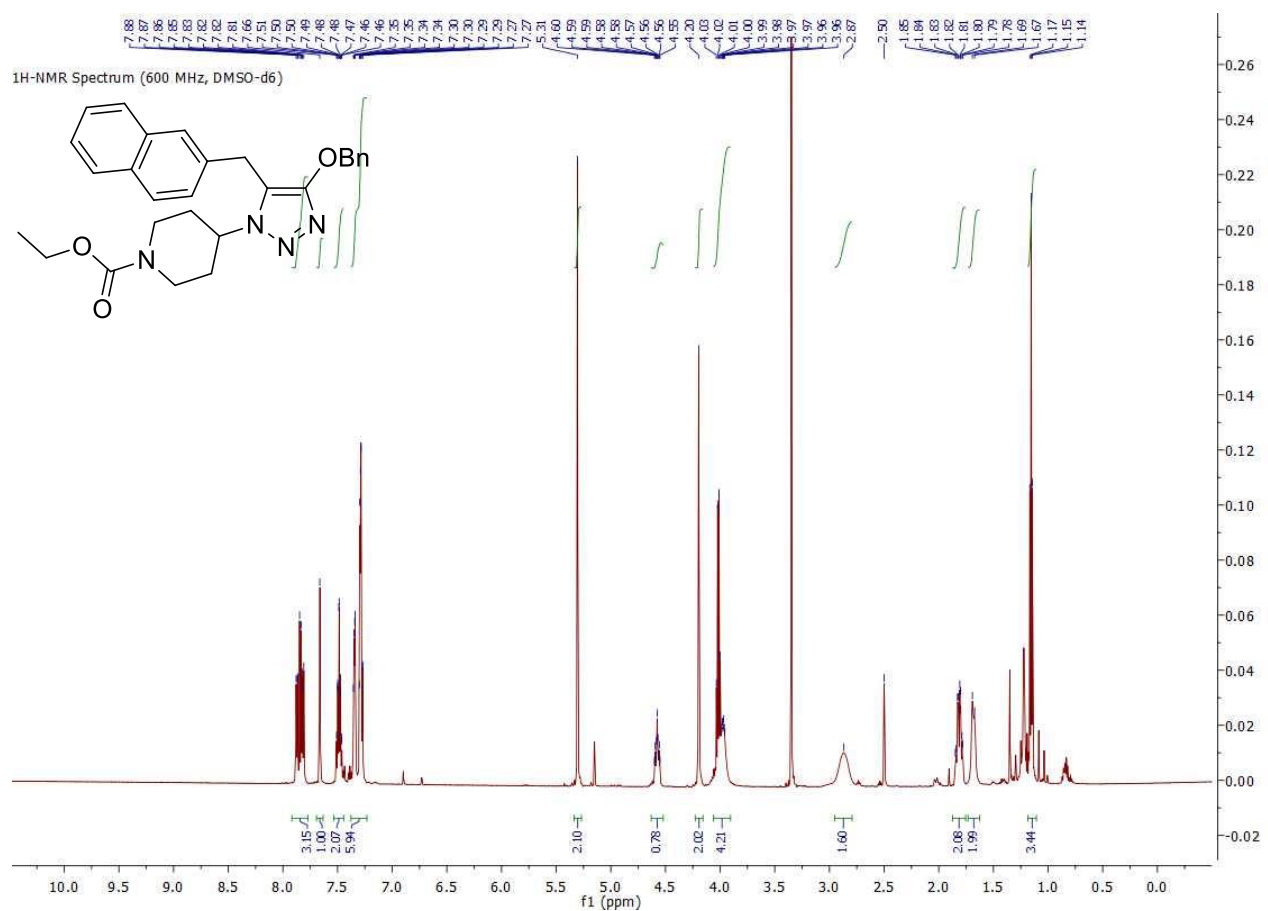
Ethyl 4-(4-(benzyloxy)-5-iodo-2H-1,2,3-triazol-2-yl)piperidine-1-carboxylate (2.28).



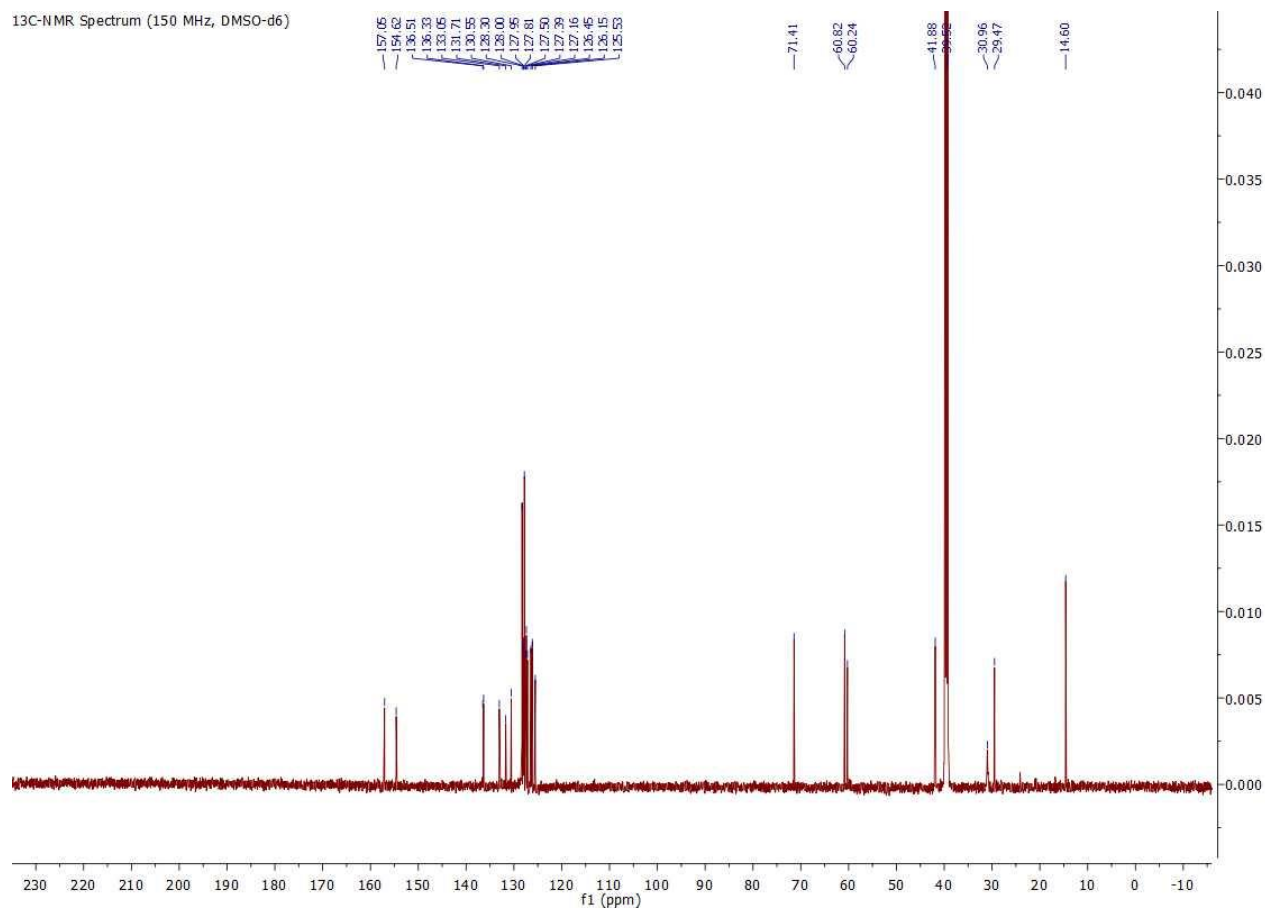
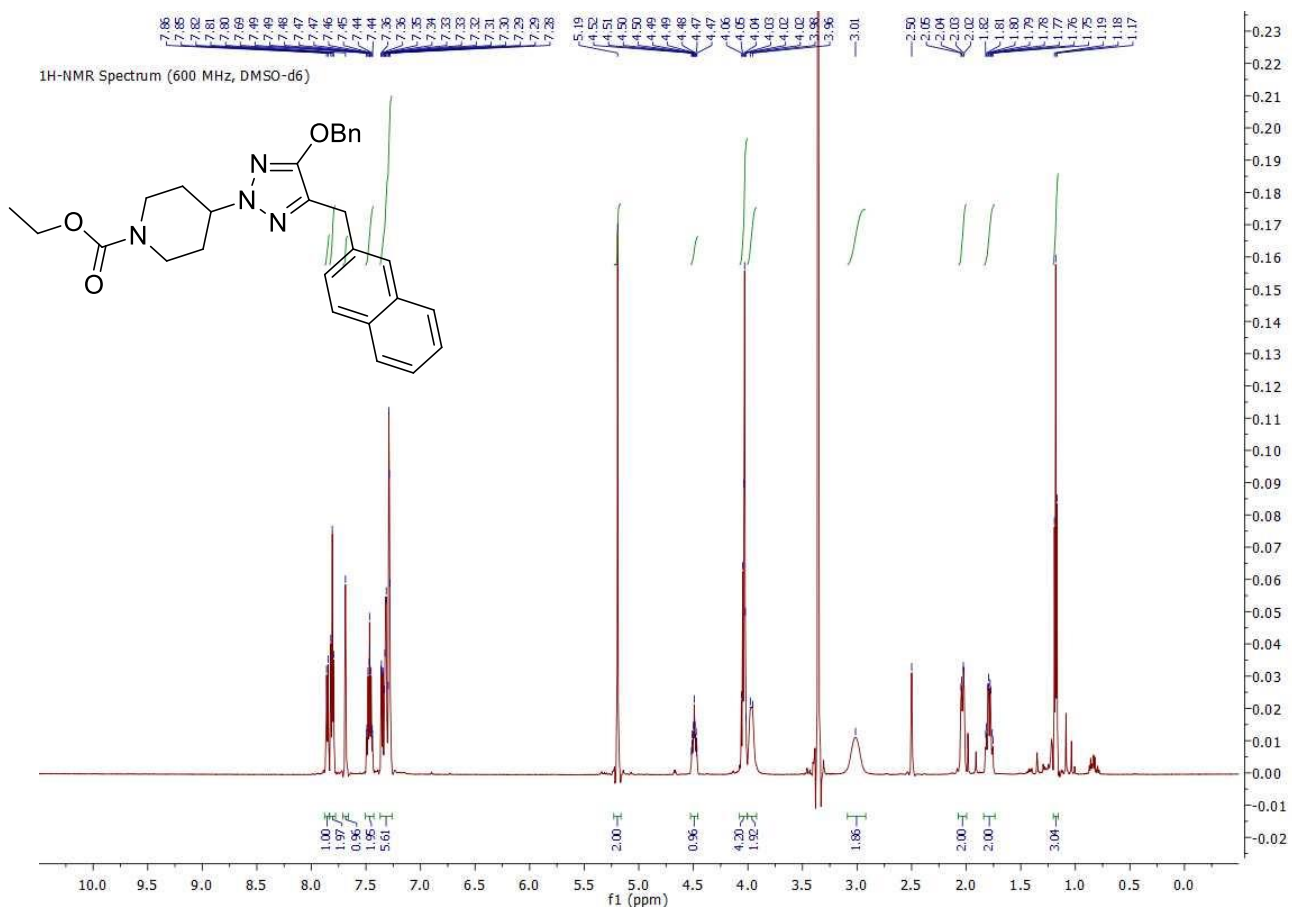
Ethyl 4-(4-(benzyloxy)-5-iodo-1H-1,2,3-triazol-1-yl)piperidine-1-carboxylate (2.27).



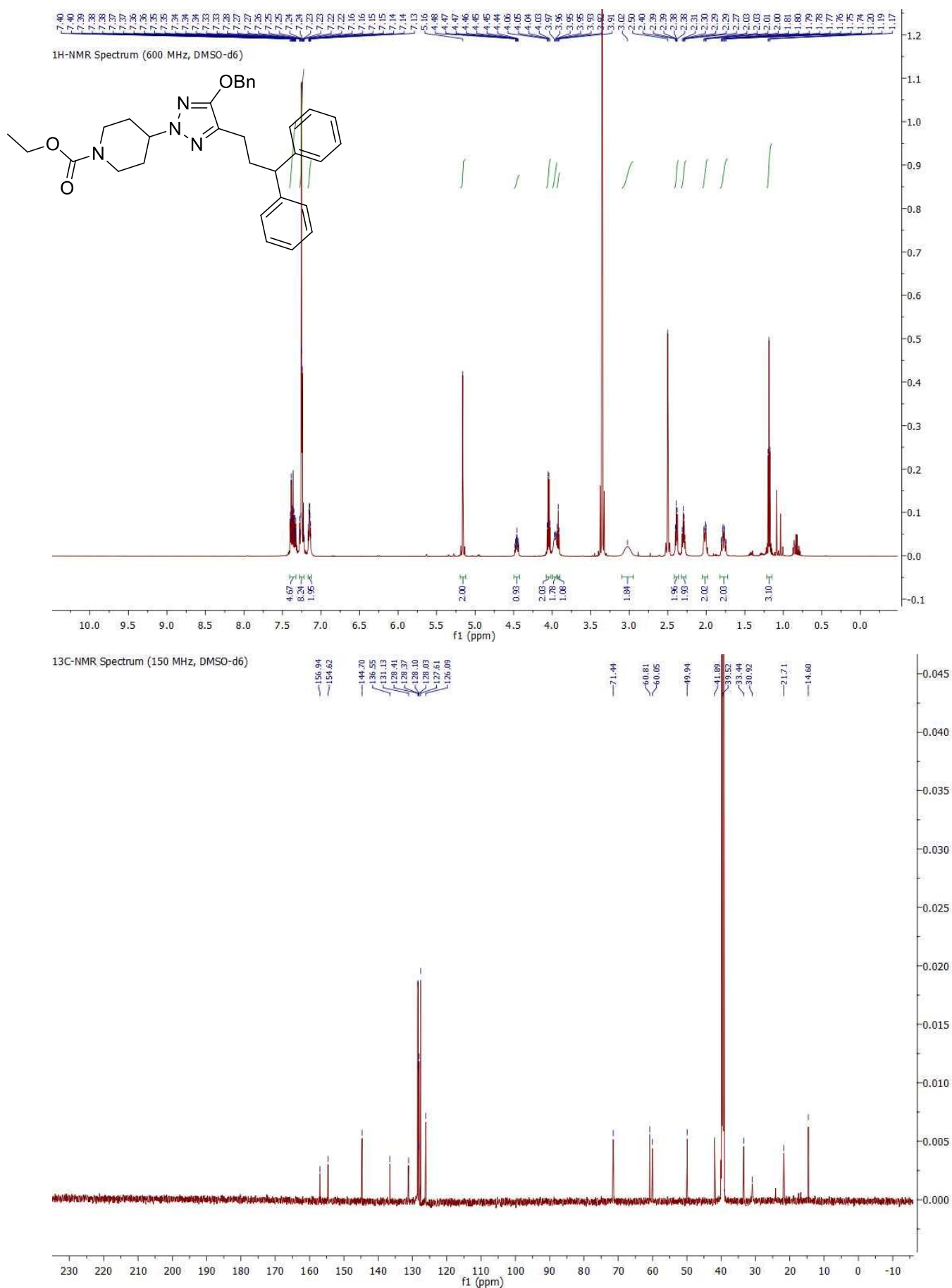
Ethyl 4-(4-(benzyloxy)-5-(naphthalen-2-ylmethyl)-1H-1,2,3-triazol-1-yl)piperidine-1-carboxylate (2.31b).



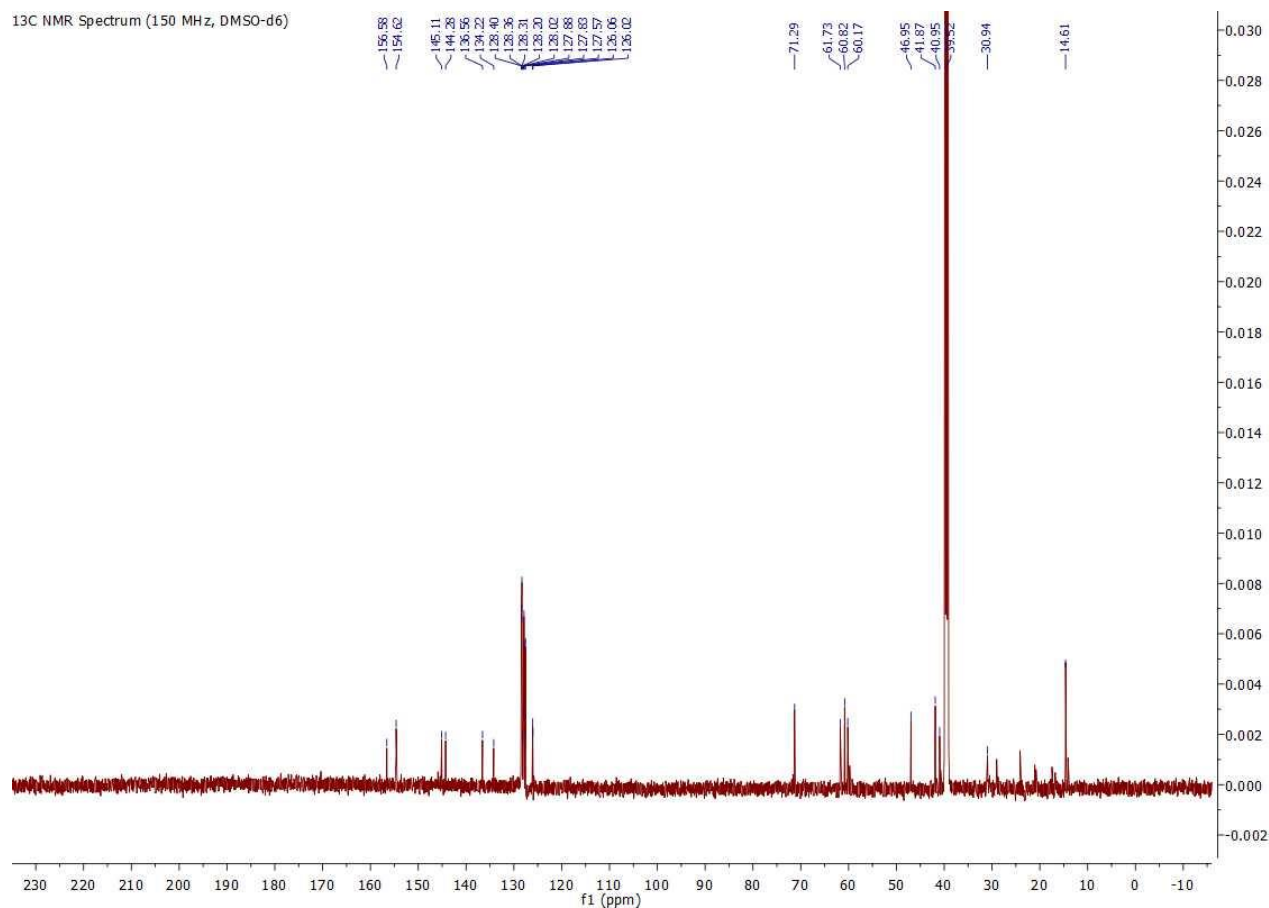
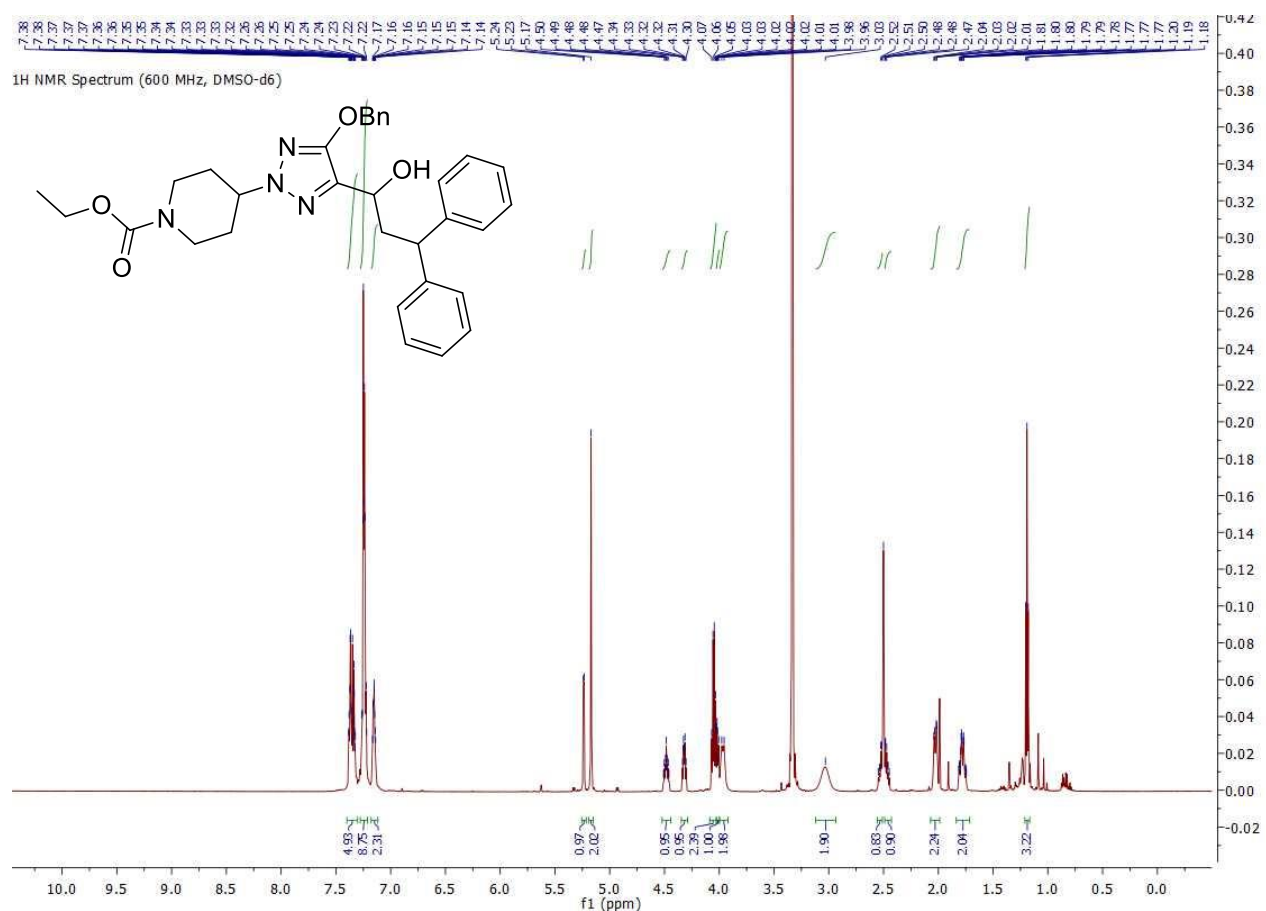
Ethyl 4-(4-(benzyloxy)-5-(naphthalen-2-ylmethyl)-2H-1,2,3-triazol-2-yl)piperidine-1-carboxylate (2.32b).



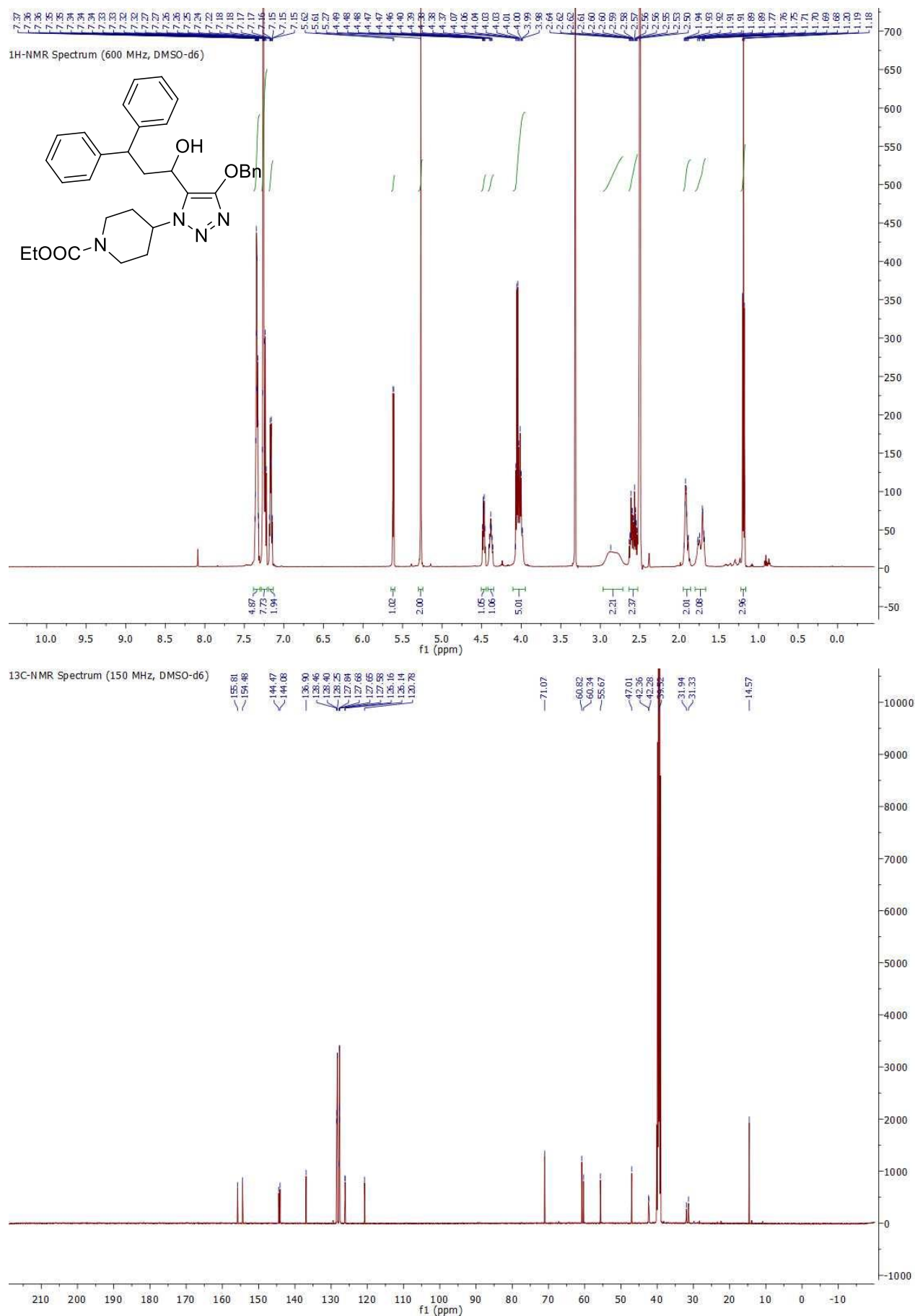
Ethyl 4-(4-(benzyloxy)-5-(3,3-diphenylpropyl)-2H-1,2,3-triazol-2-yl)piperidine-1-carboxylate (2.32c).



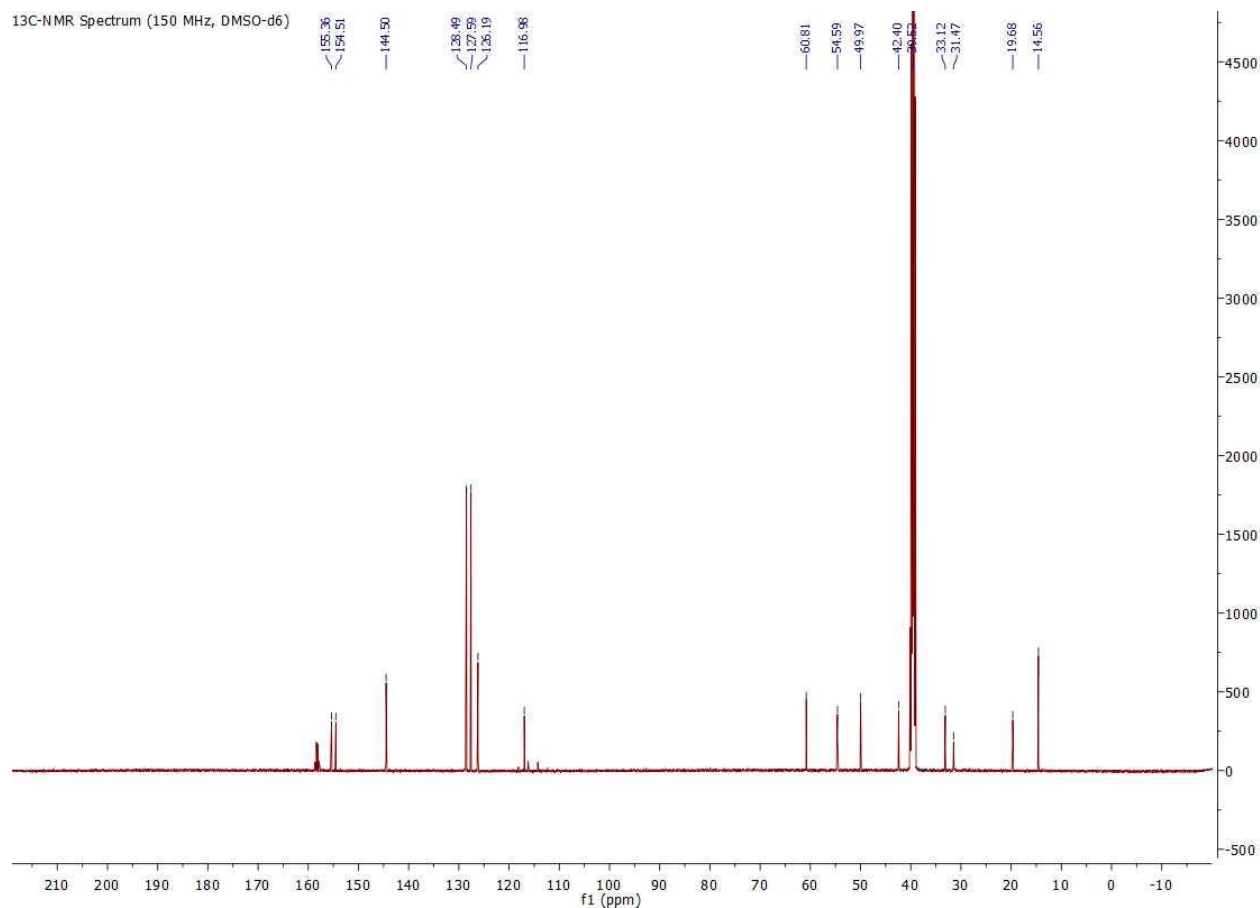
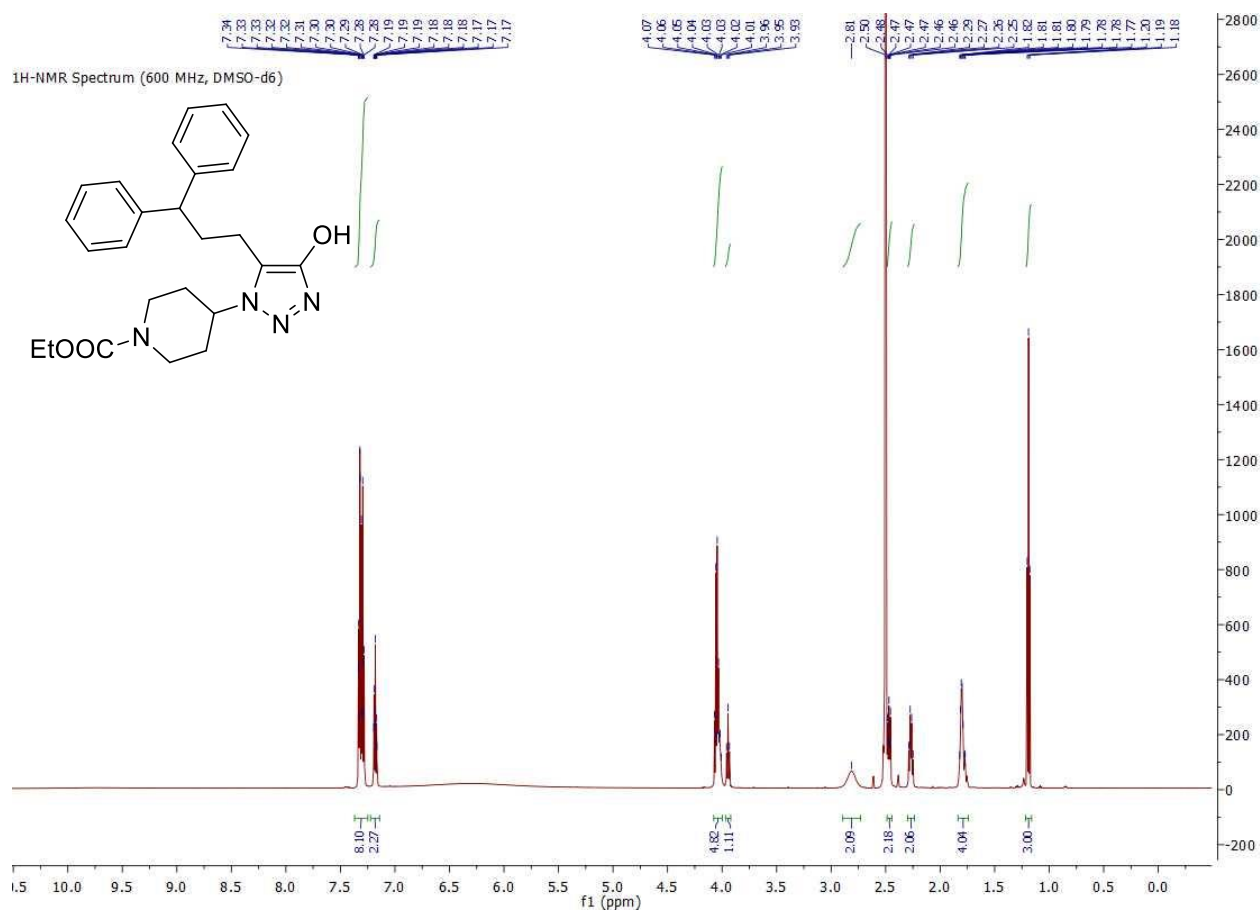
Ethyl 4-(4-(benzyloxy)-5-(1-hydroxy-3,3-diphenylpropyl)-2H-1,2,3-triazol-2-yl)piperidine-1-carboxylate (2.30c).



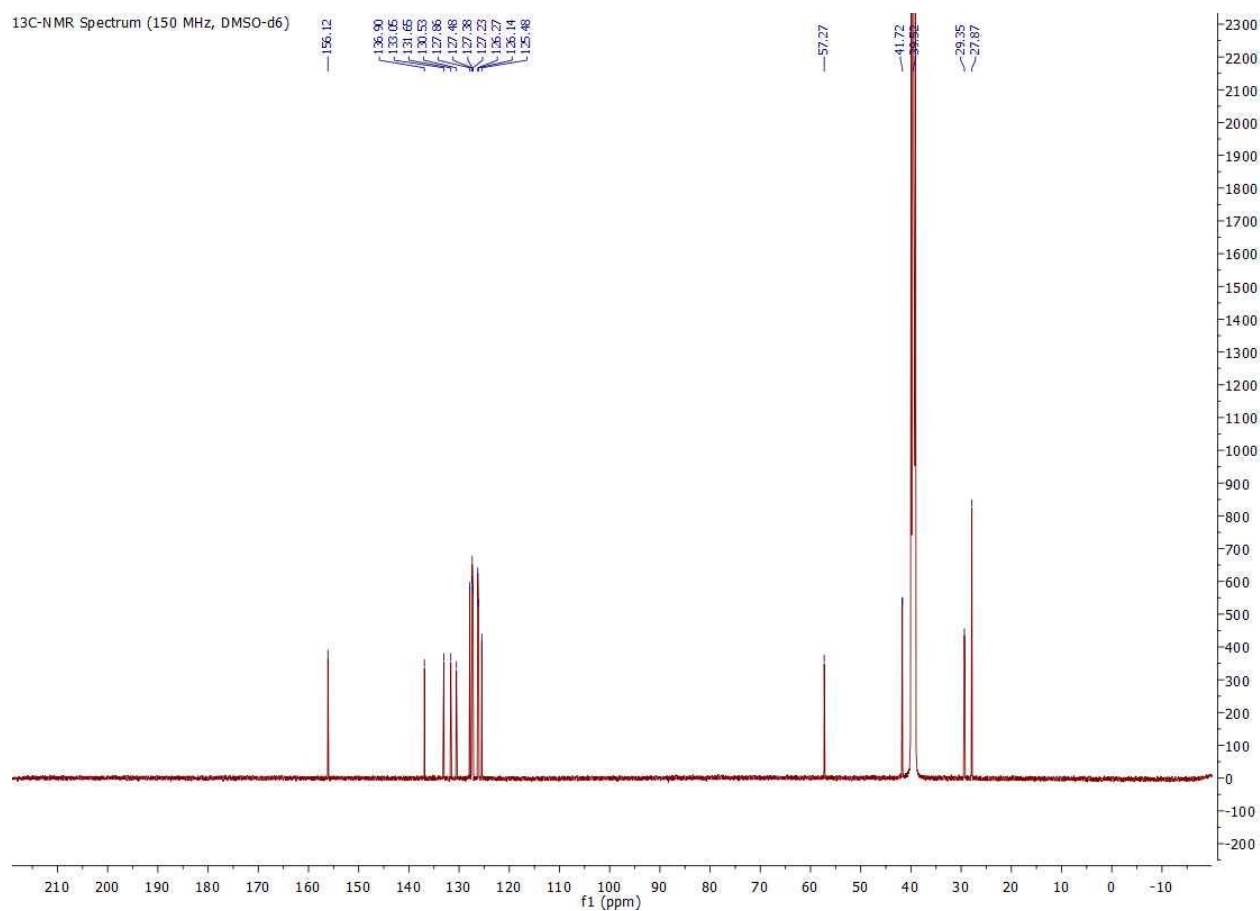
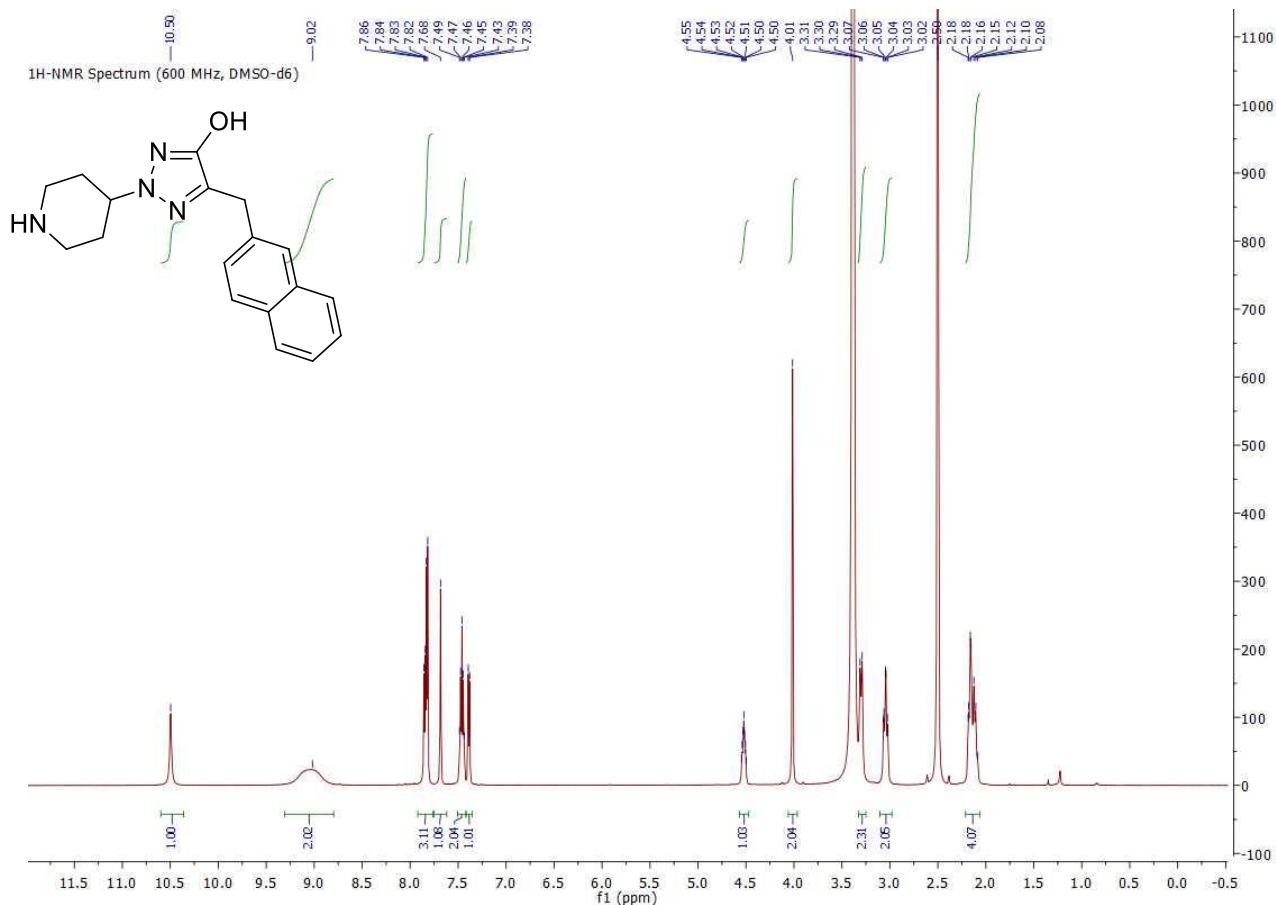
Ethyl 4-(4-(benzyloxy)-5-(1-hydroxy-3,3-diphenylpropyl)-1H-1,2,3-triazol-1-yl)piperidine-1-carboxylate (2.29c).



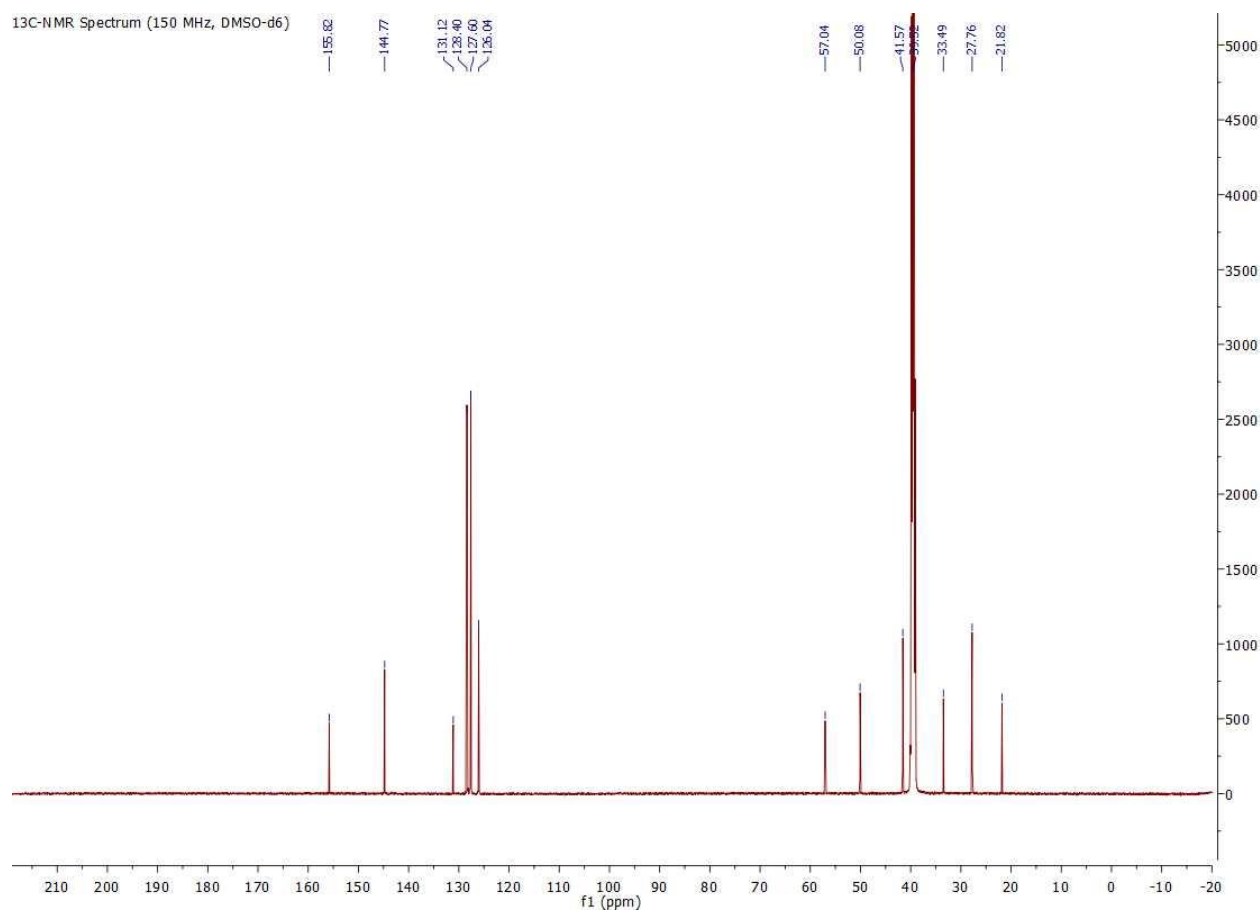
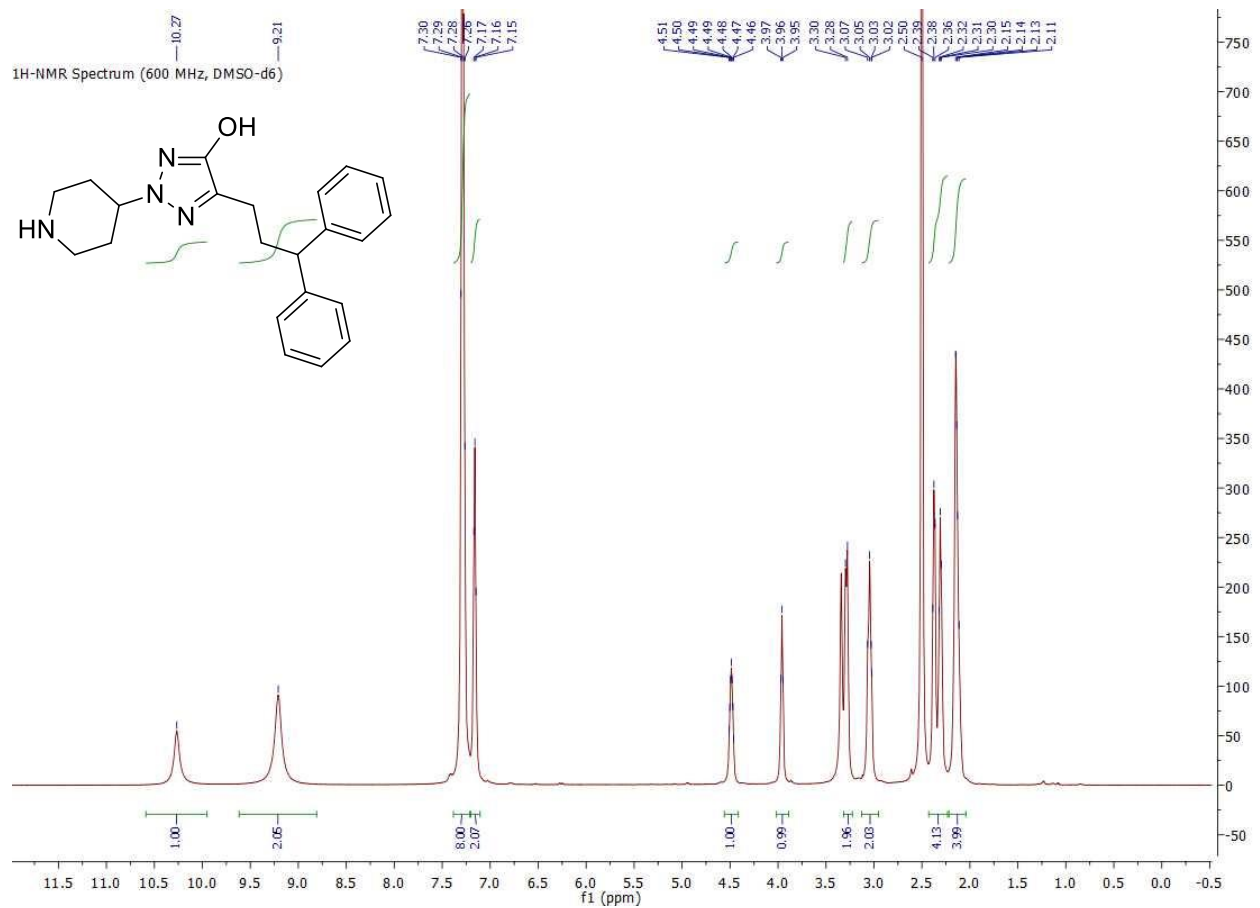
Ethyl 4-(5-(3,3-diphenylpropyl)-4-hydroxy-1H-1,2,3-triazol-1-yl)piperidine-1-carboxylate (2.35c).



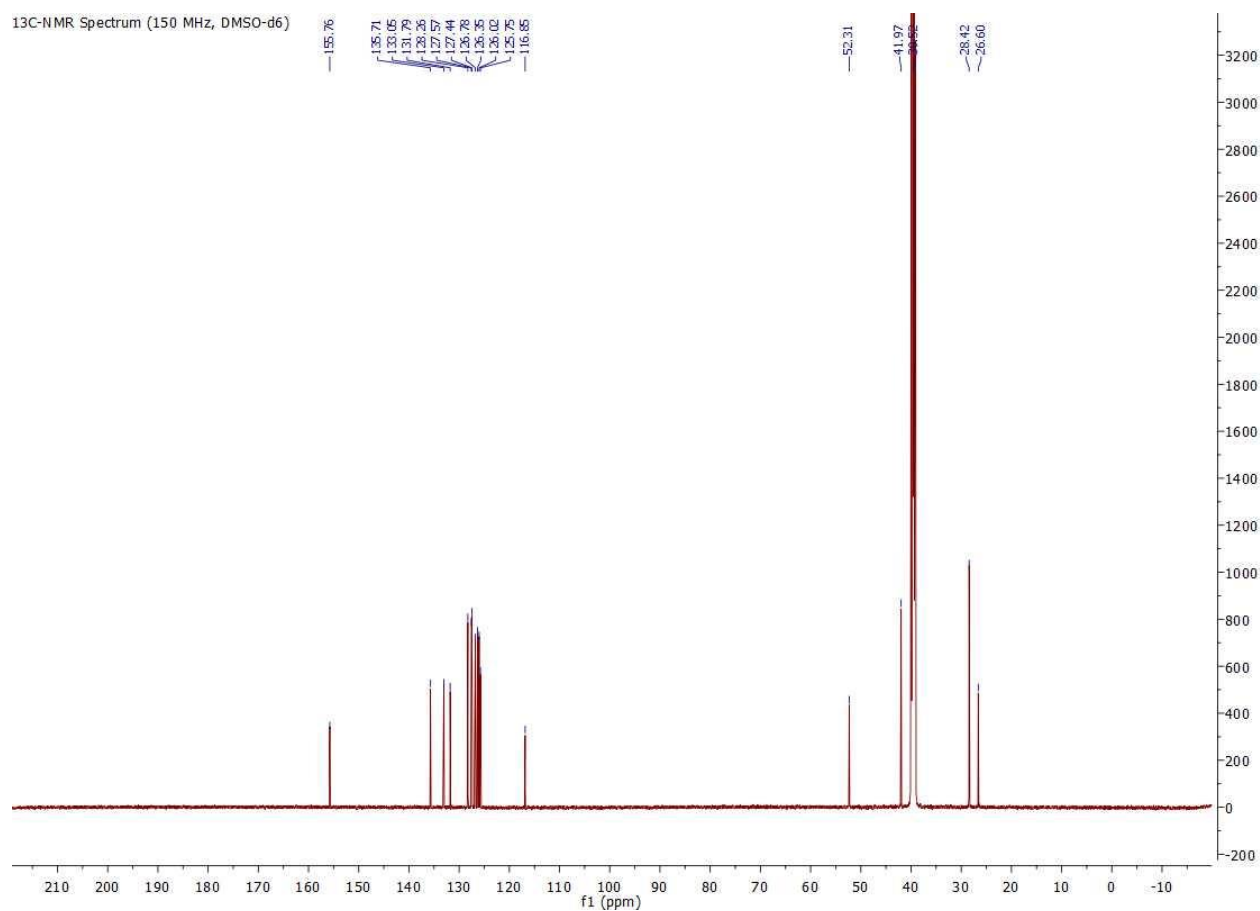
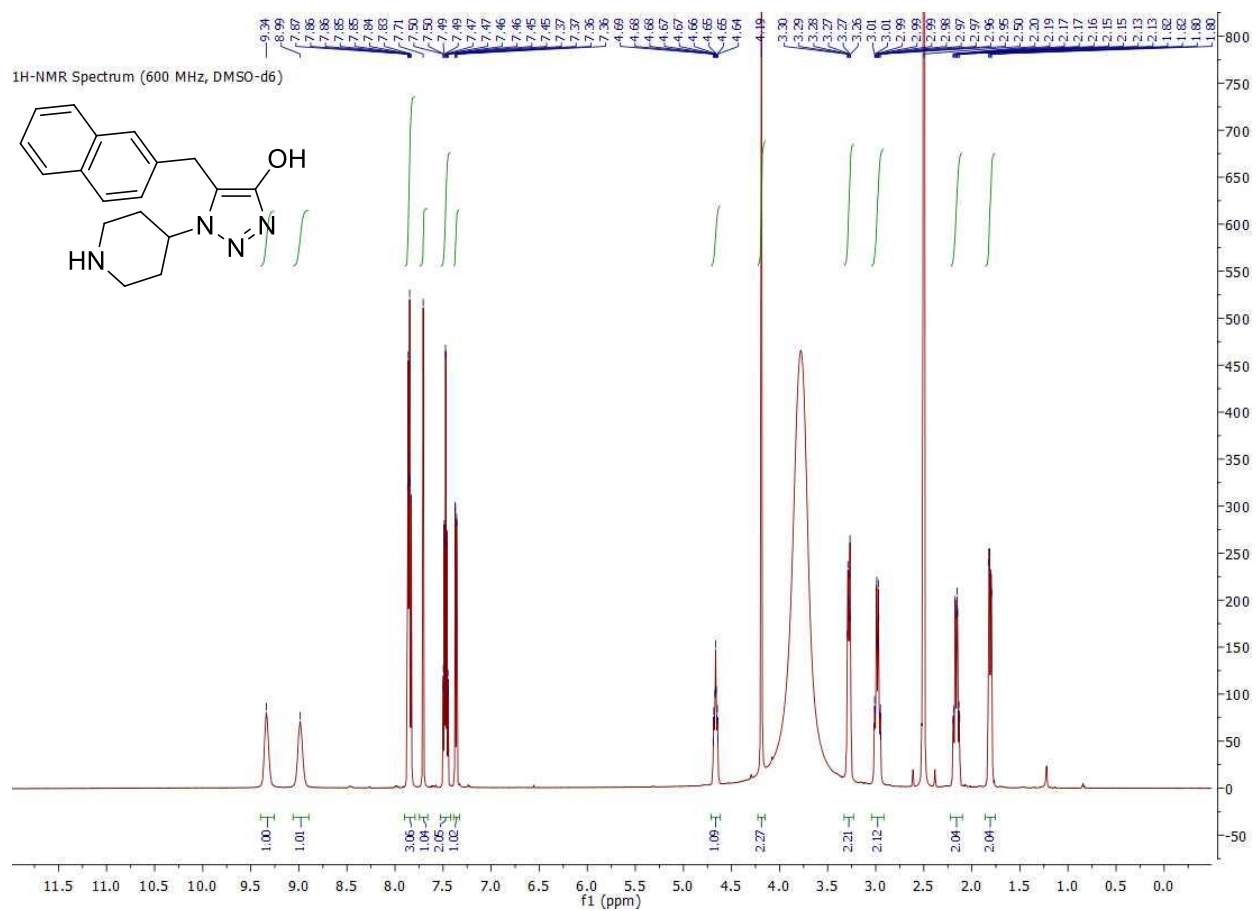
5-(naphthalen-2-ylmethyl)-2-(piperidin-4-yl)-2H-1,2,3-triazol-4-ol (2.5b).



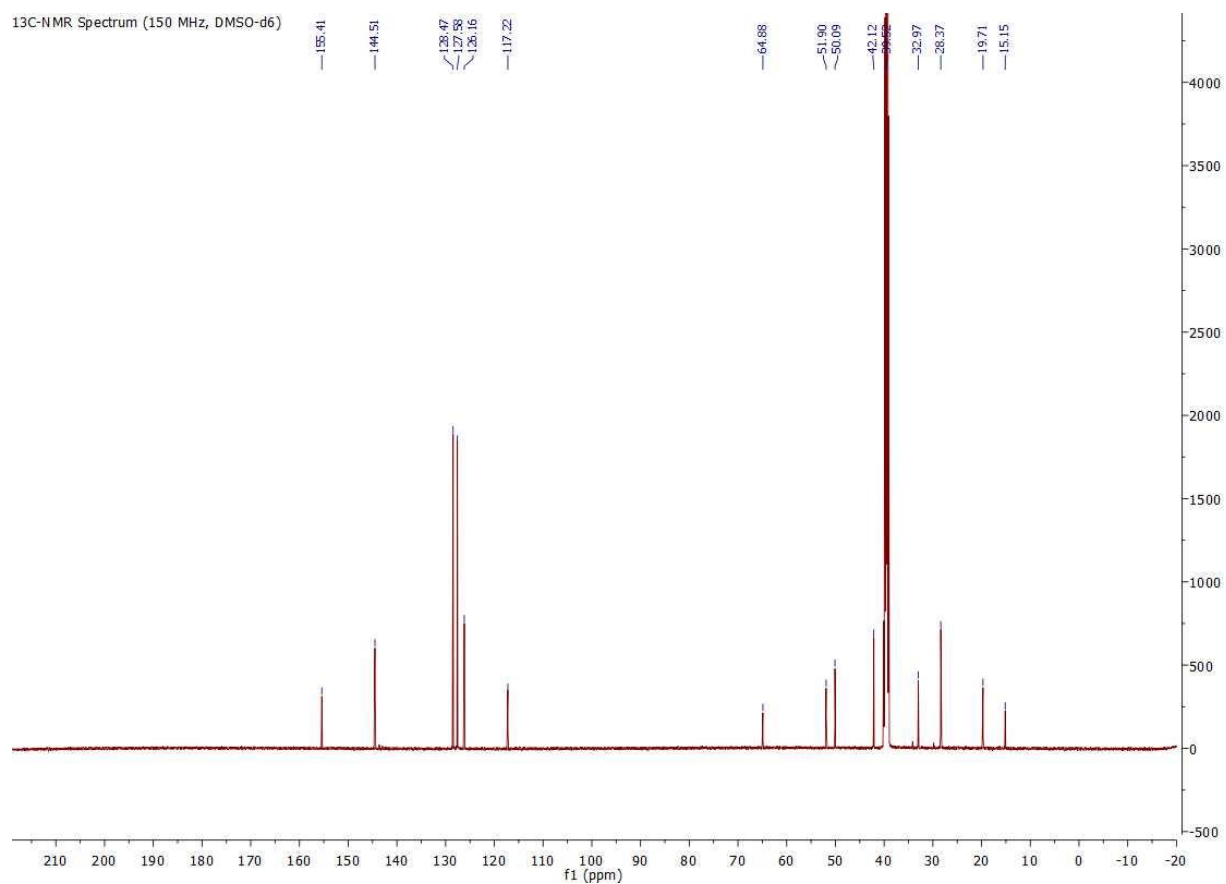
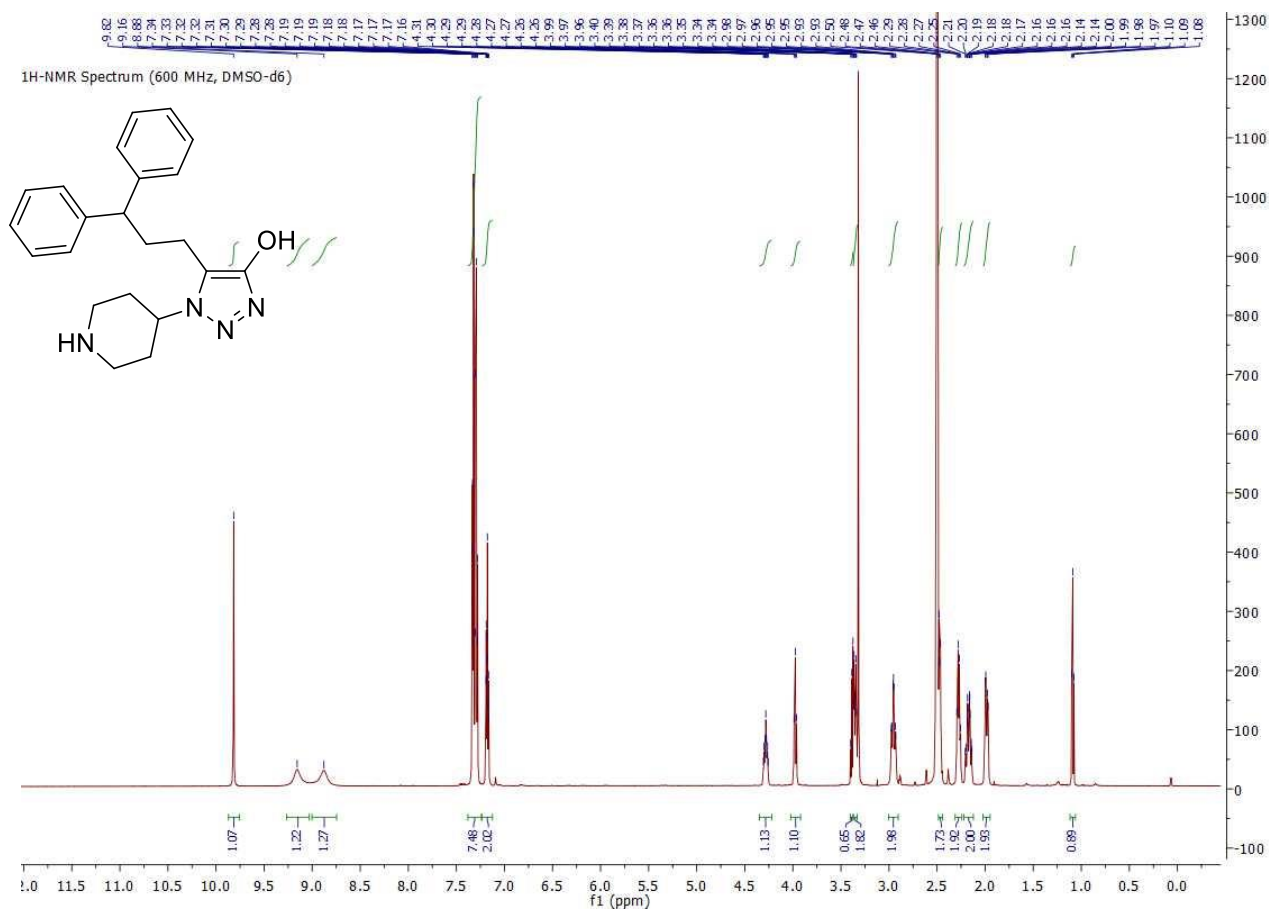
5-(3,3-diphenylpropyl)-2-(piperidin-4-yl)-2H-1,2,3-triazol-4-ol hydrochloride (2.5c).



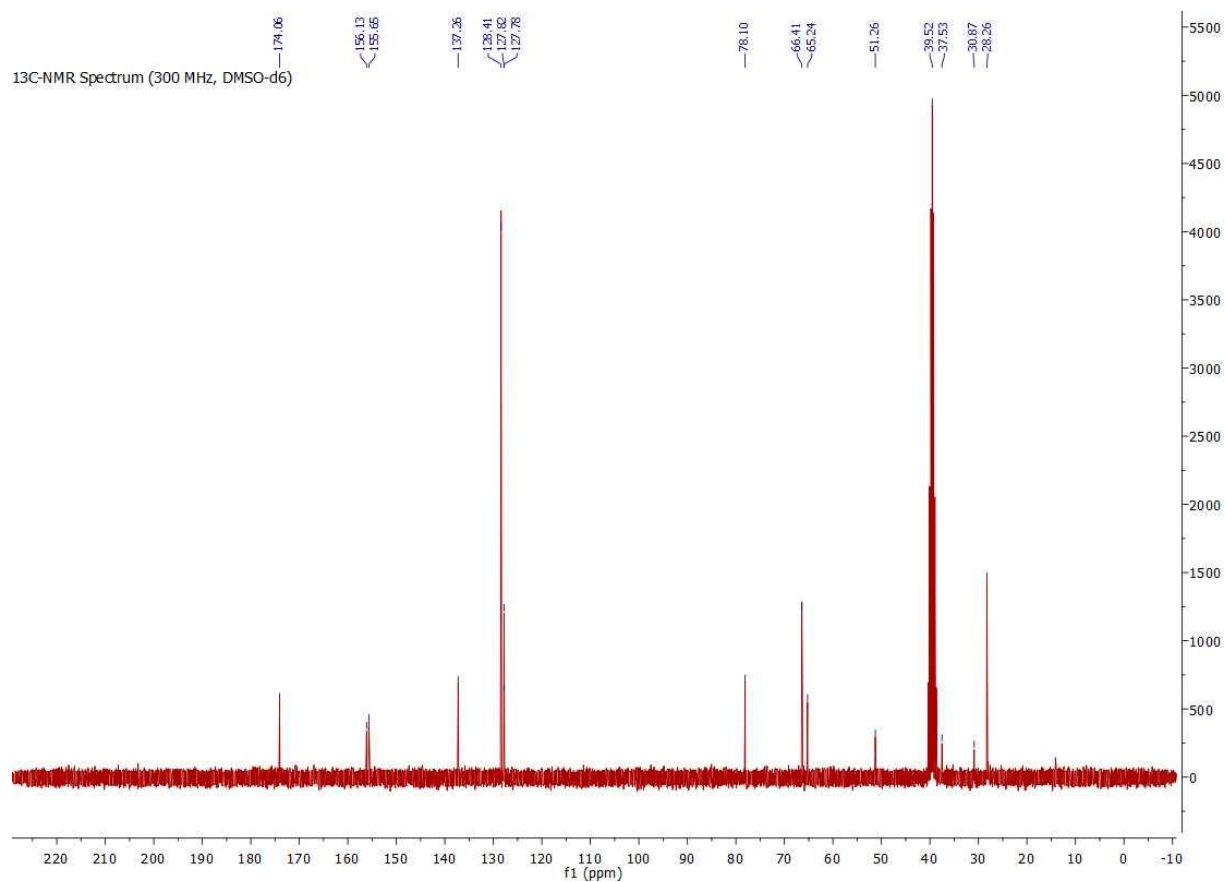
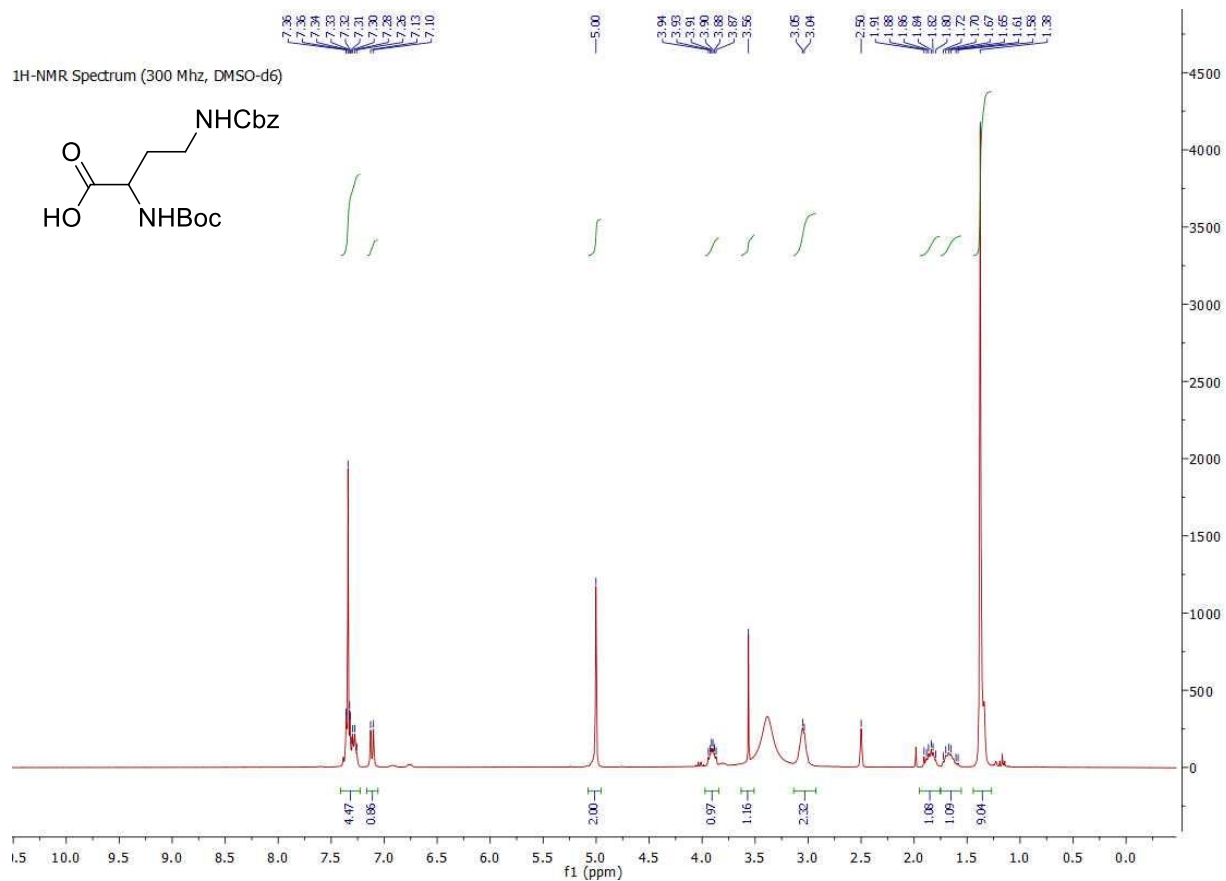
5-(naphthalen-2-ylmethyl)-1-(piperidin-4-yl)-1H-1,2,3-triazol-4-ol hydrochloride (2.4b).



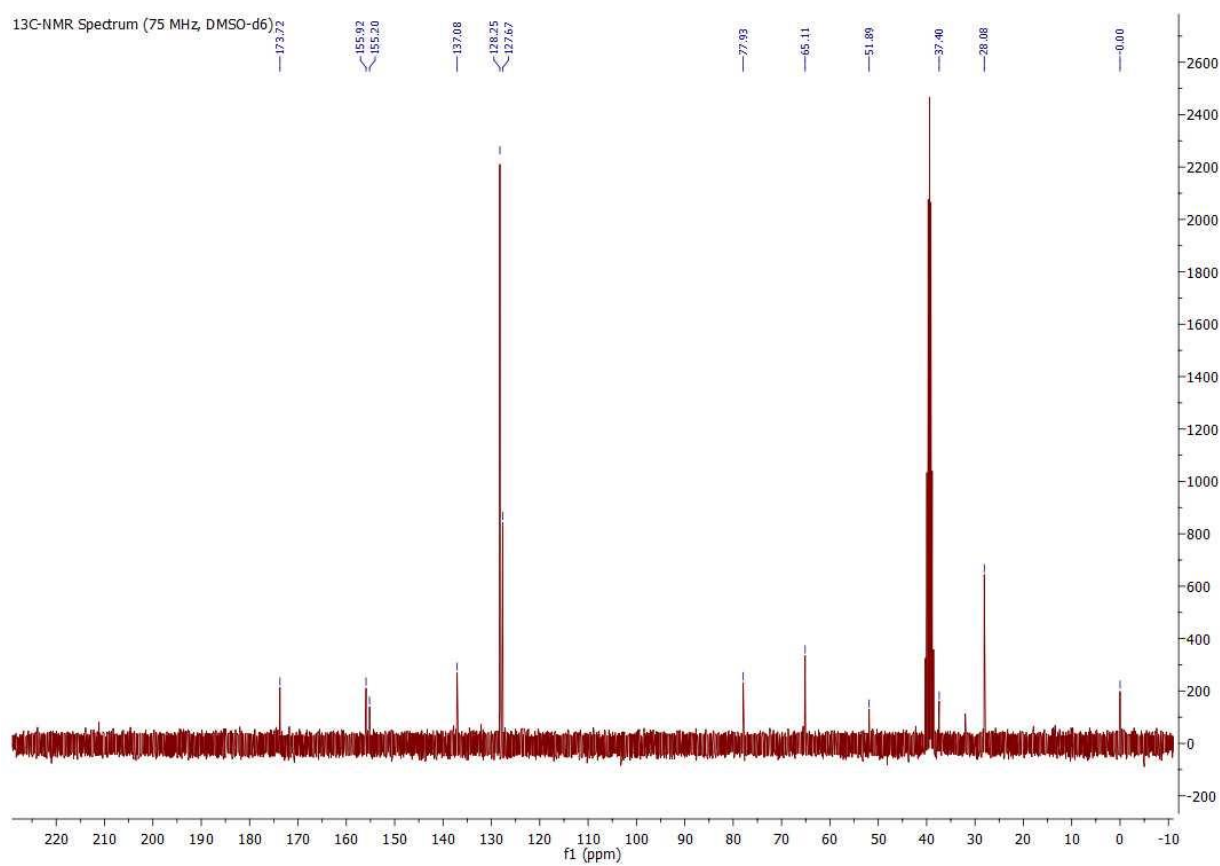
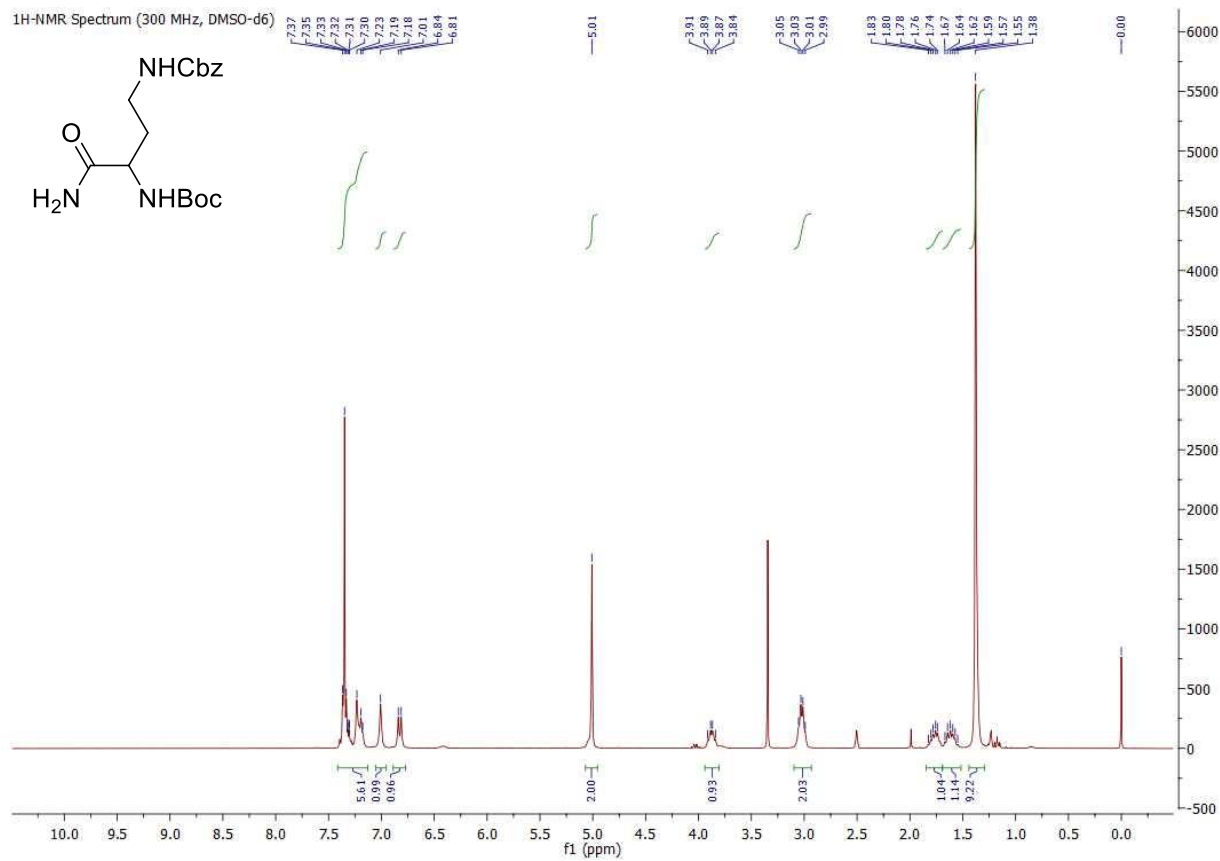
5-(3,3-diphenylpropyl)-1-(piperidin-4-yl)-1H-1,2,3-triazol-4-ol hydrochloride (2.4c).



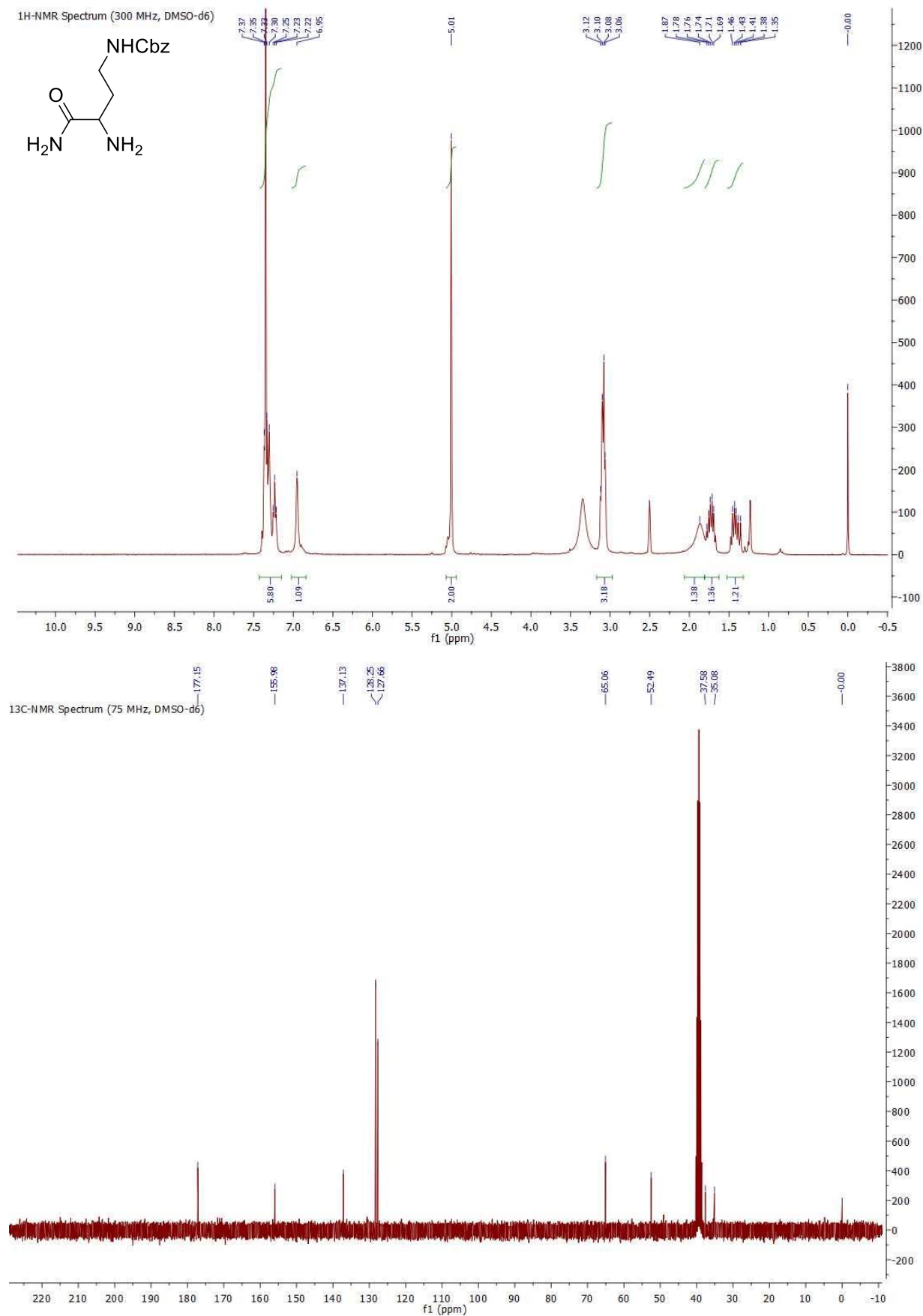
4-(((Benzyloxy)carbonyl)amino)-2-((tert-butoxycarbonyl)amino)butanoic acid (2.45).



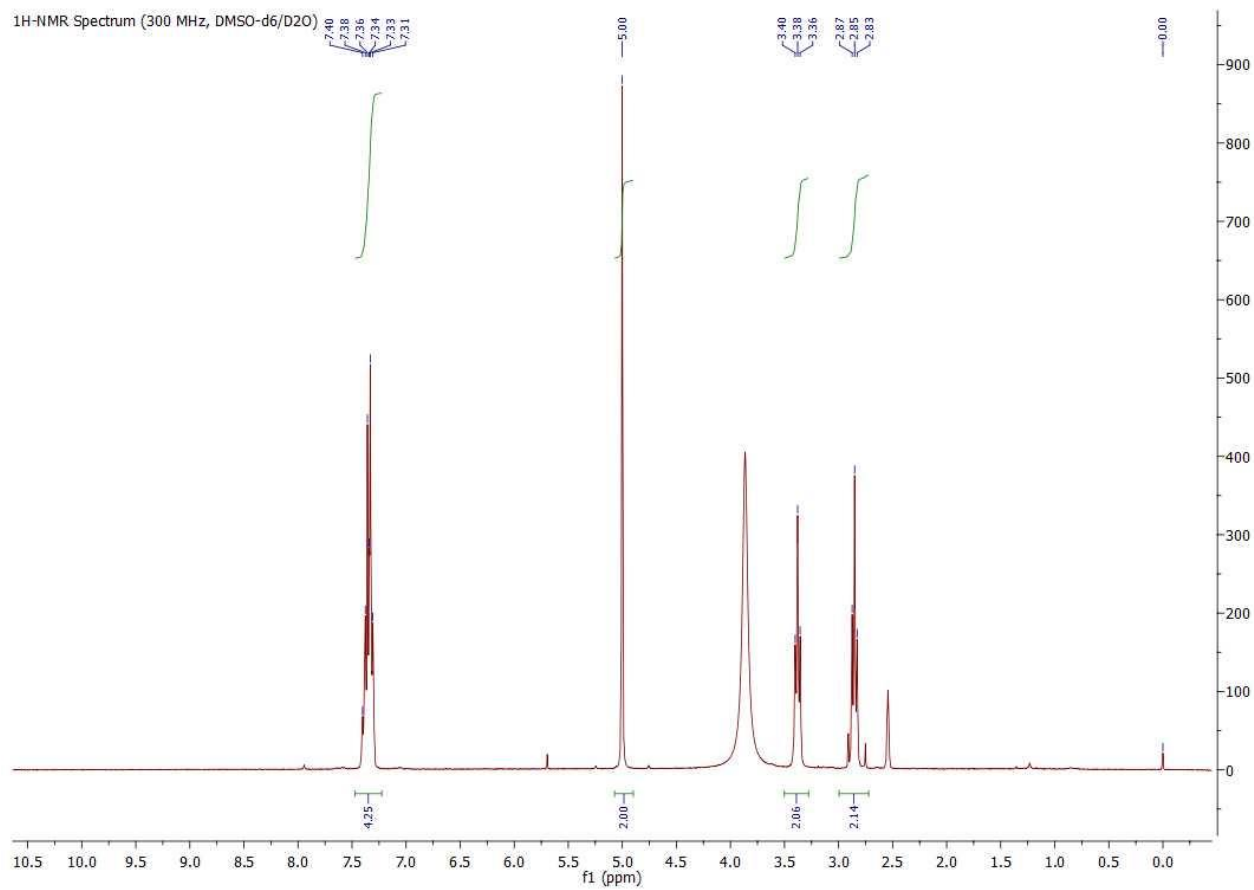
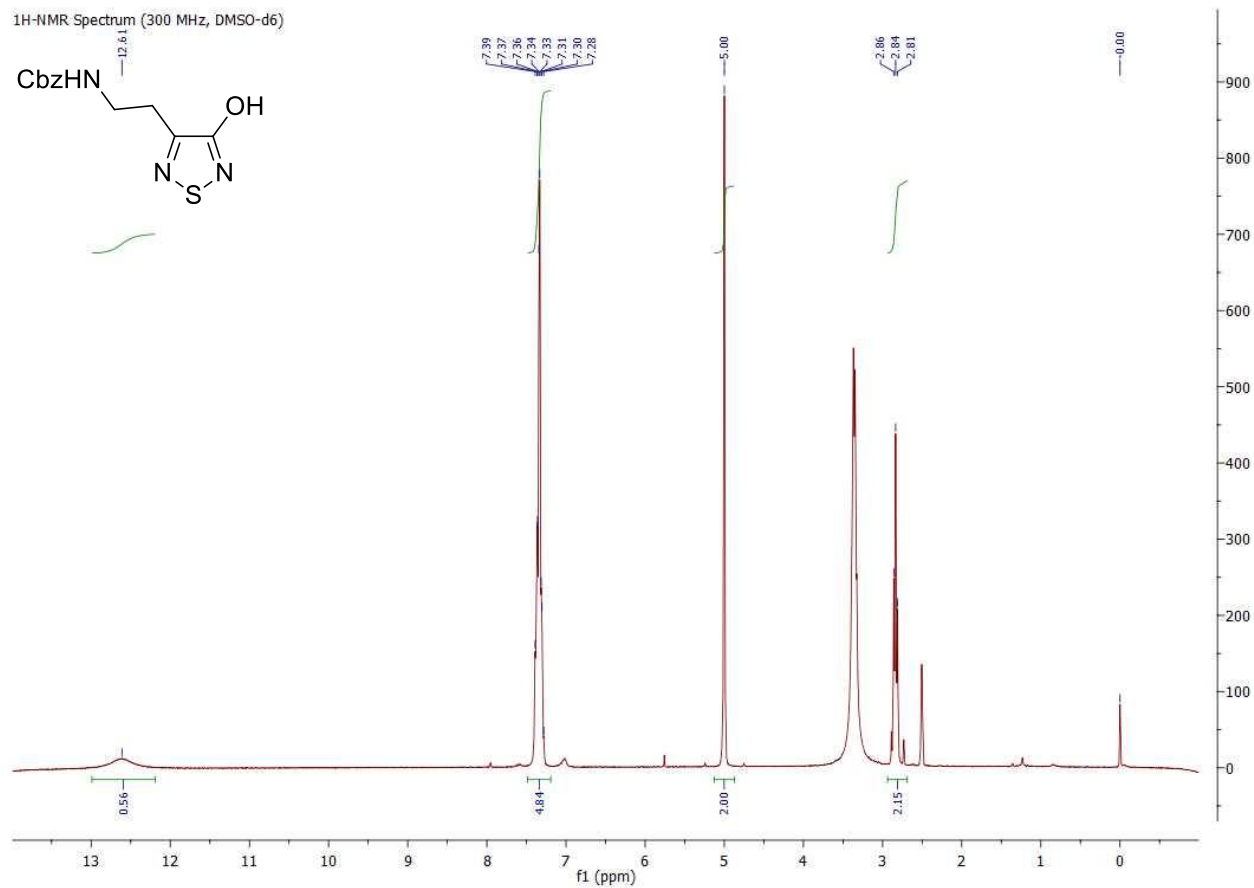
Benzyl *tert*-butyl(4-amino-4-oxobutane-1,3-diyl)dicarbamate (2.46).



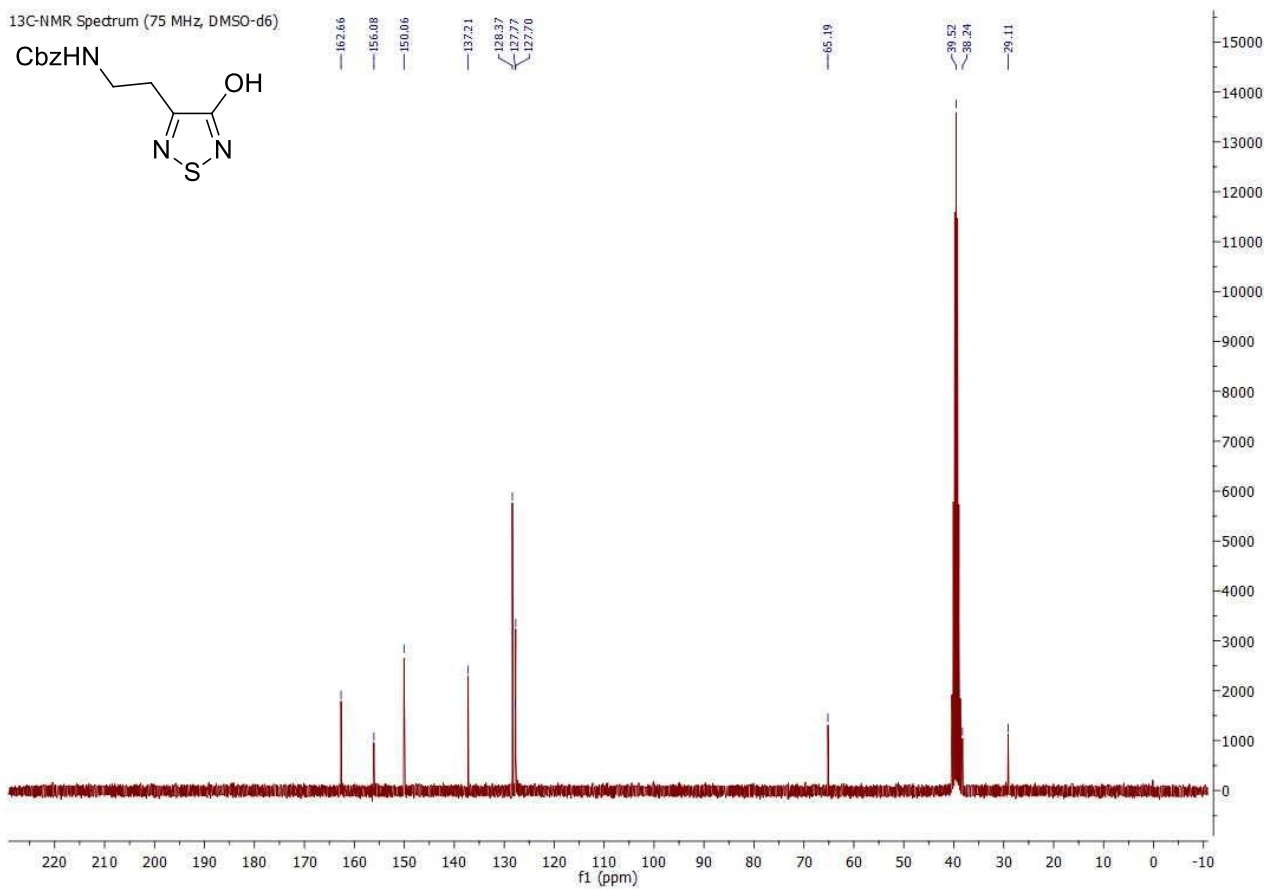
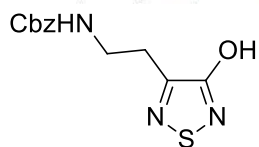
Benzyl (3,4-diamino-4-oxobutyl)carbamate (2.47).



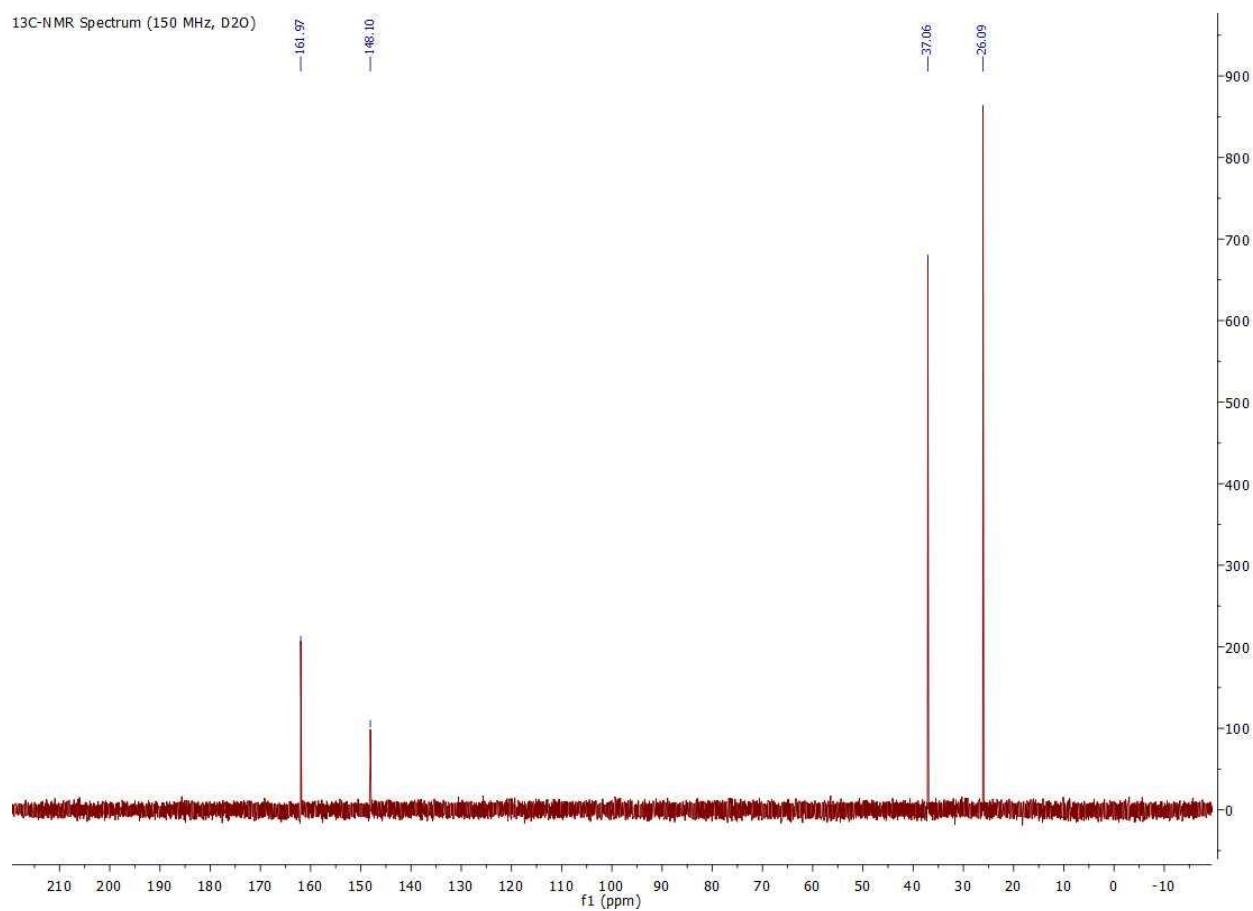
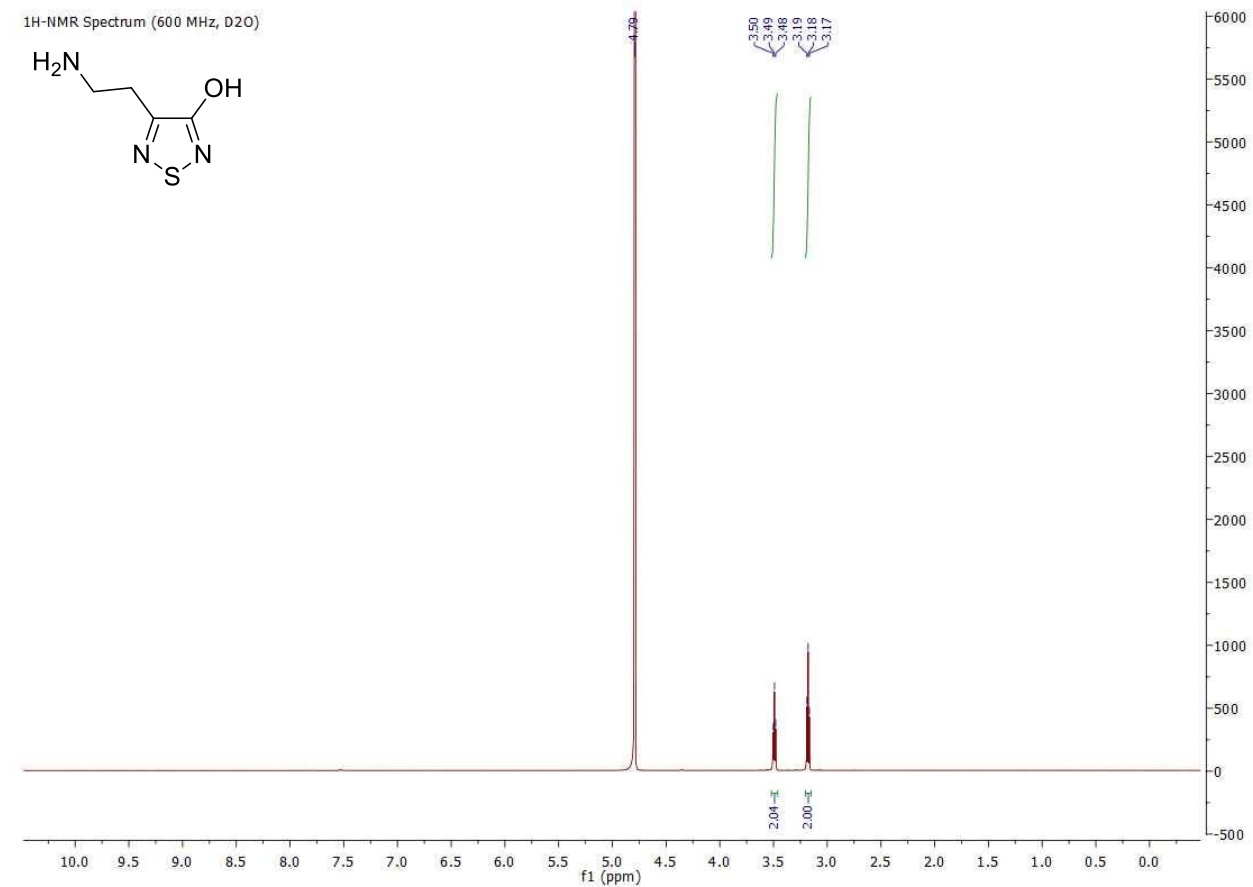
Benzyl (2-(4-hydroxy-1,2,5-thiadiazol-3-yl)ethyl)carbamate (2.48).



¹³C-NMR Spectrum (75 MHz, DMSO-d₆)

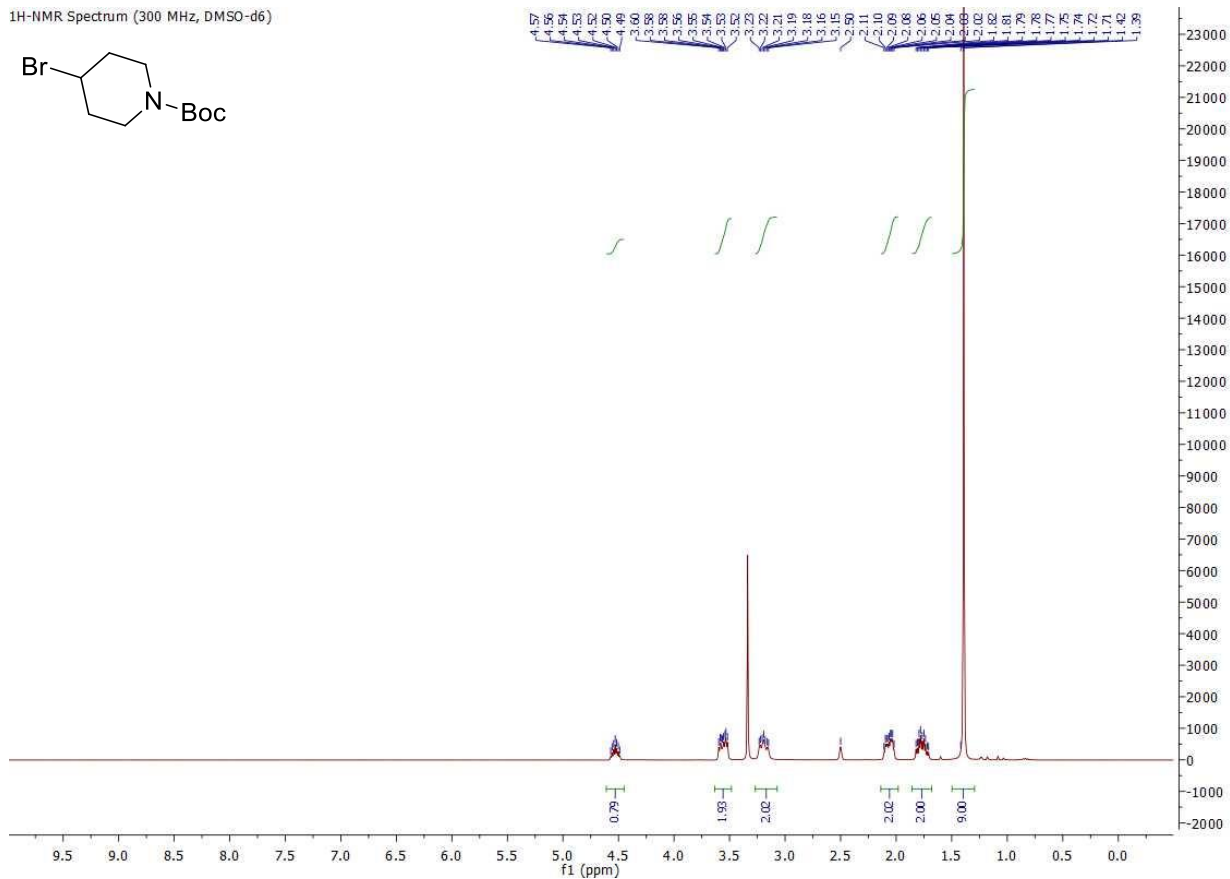
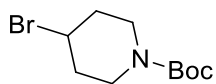


4-(2-aminoethyl)-1,2,5-thiadiazol-3-ol hydrochloride (2.2).

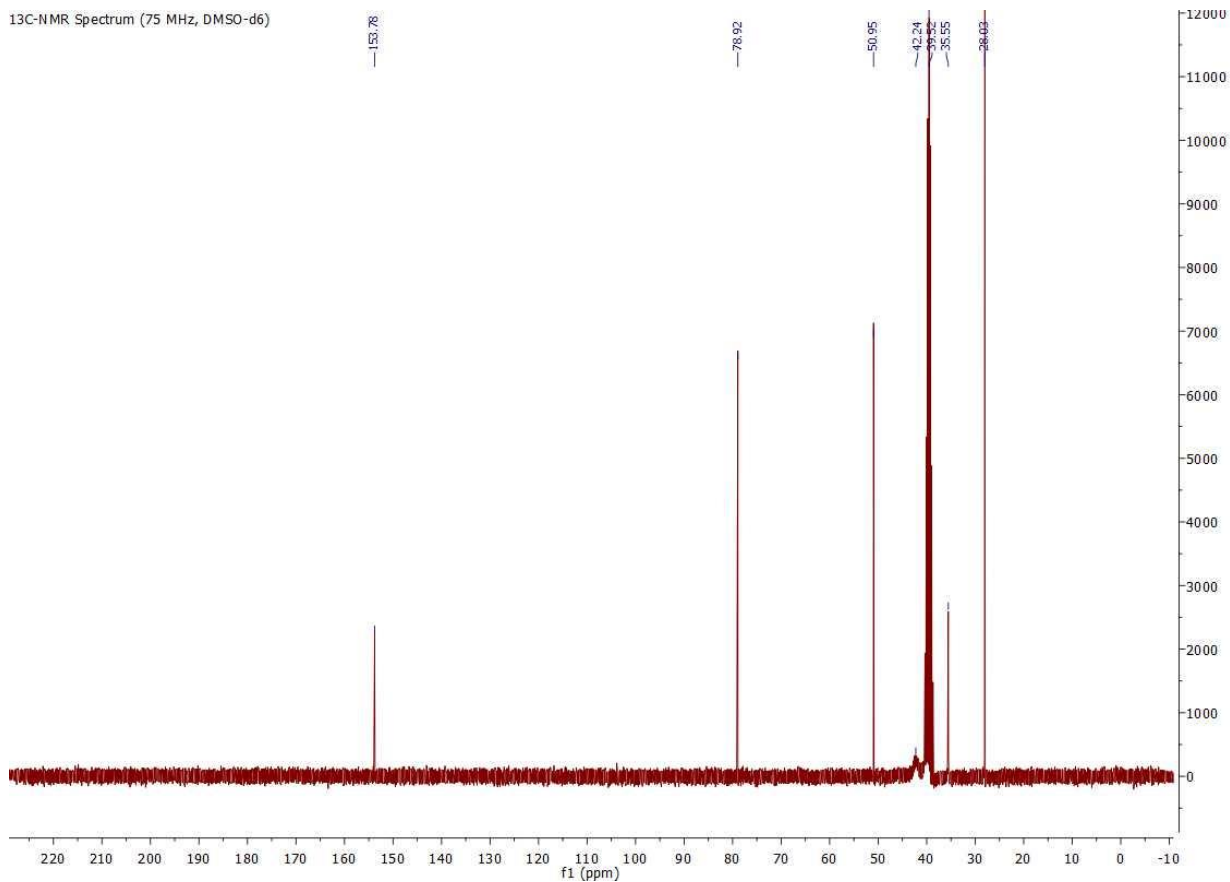


tert-Butyl 4-bromopiperidine-1-carboxylate (2.15).

¹H-NMR Spectrum (300 MHz, DMSO-d₆)

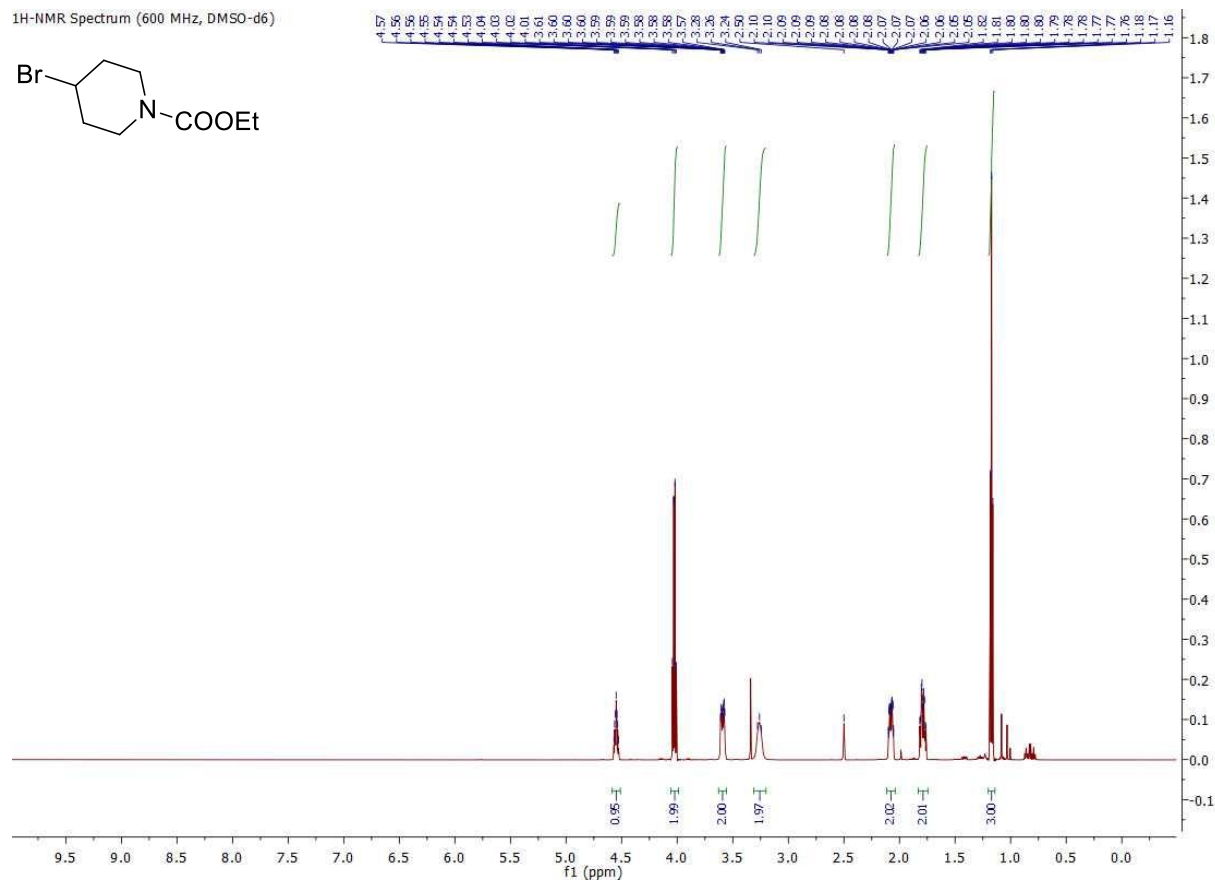
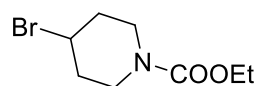


¹³C-NMR Spectrum (75 MHz, DMSO-d₆)

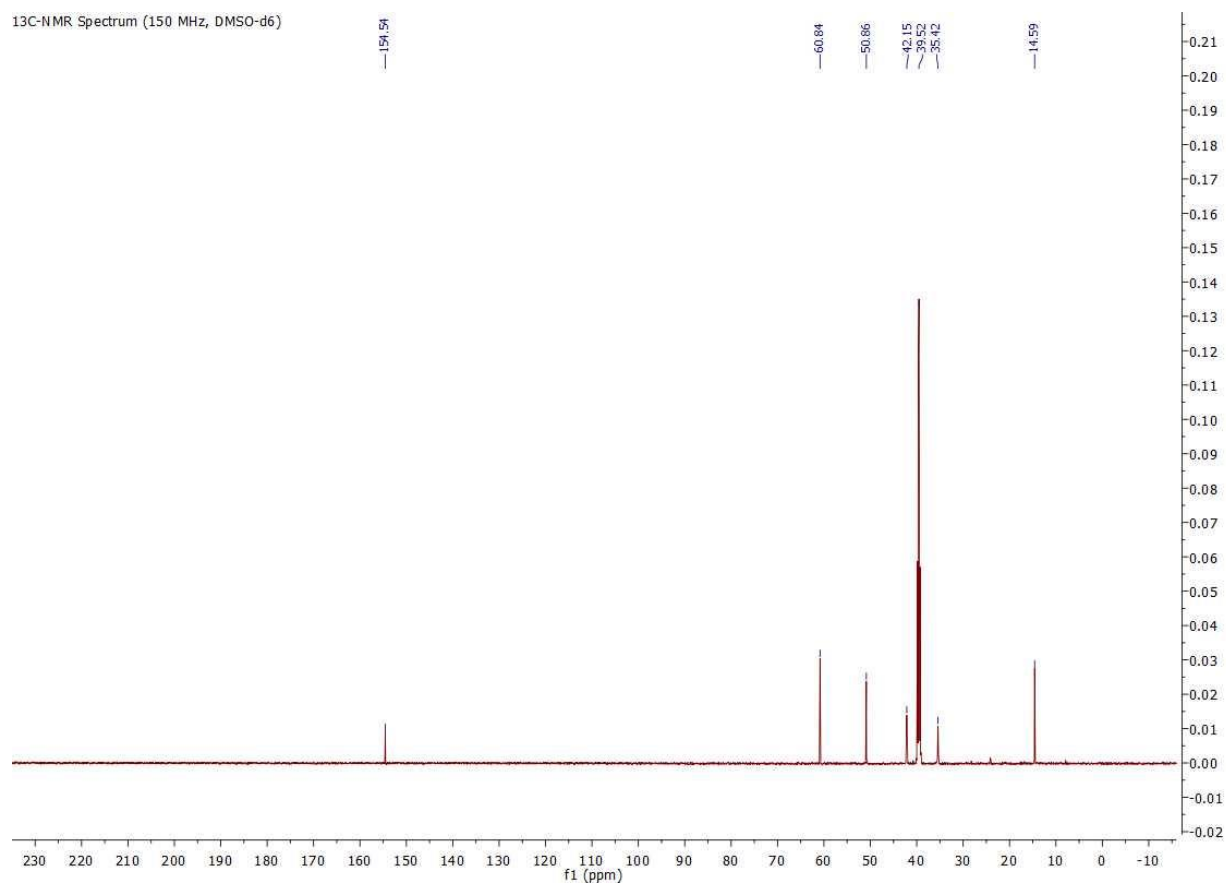


Ethyl 4-bromopiperidine-1-carboxylate (2.24).

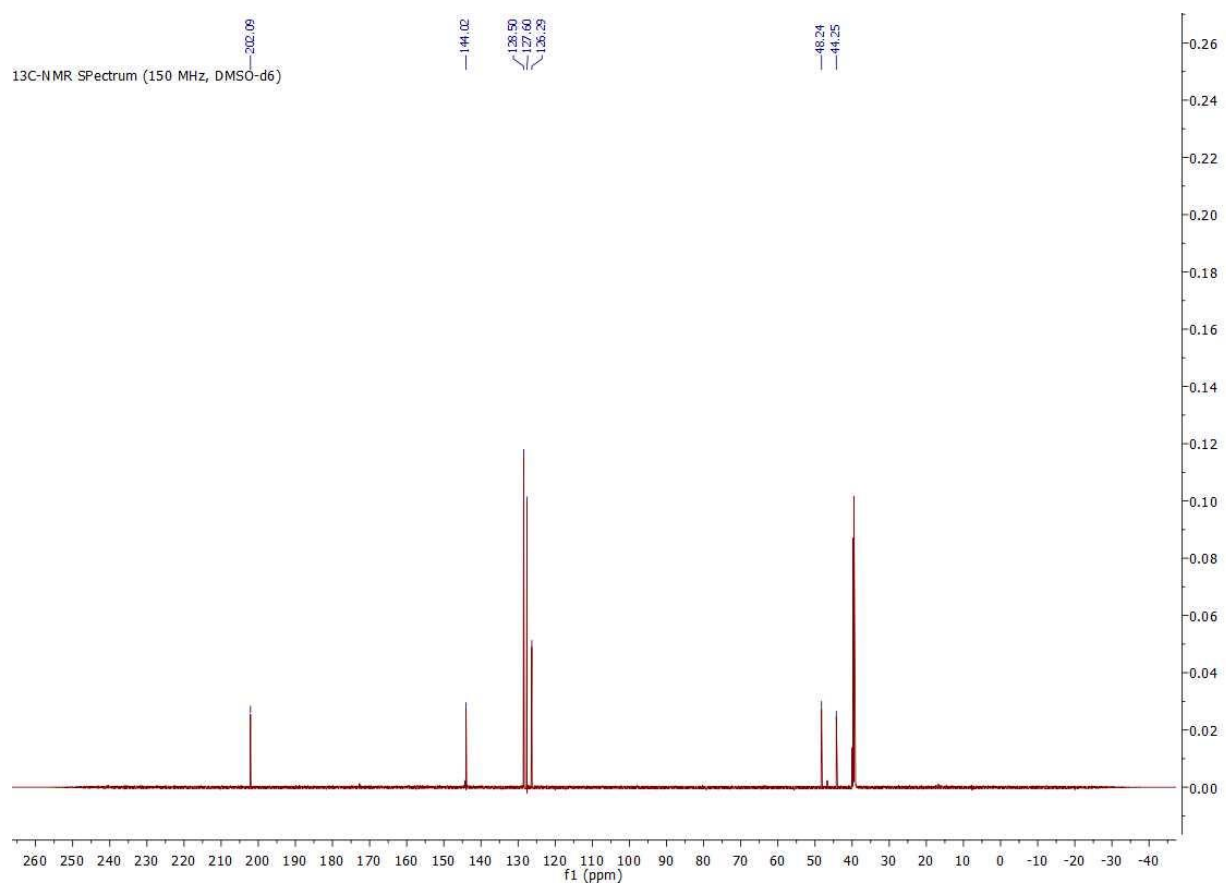
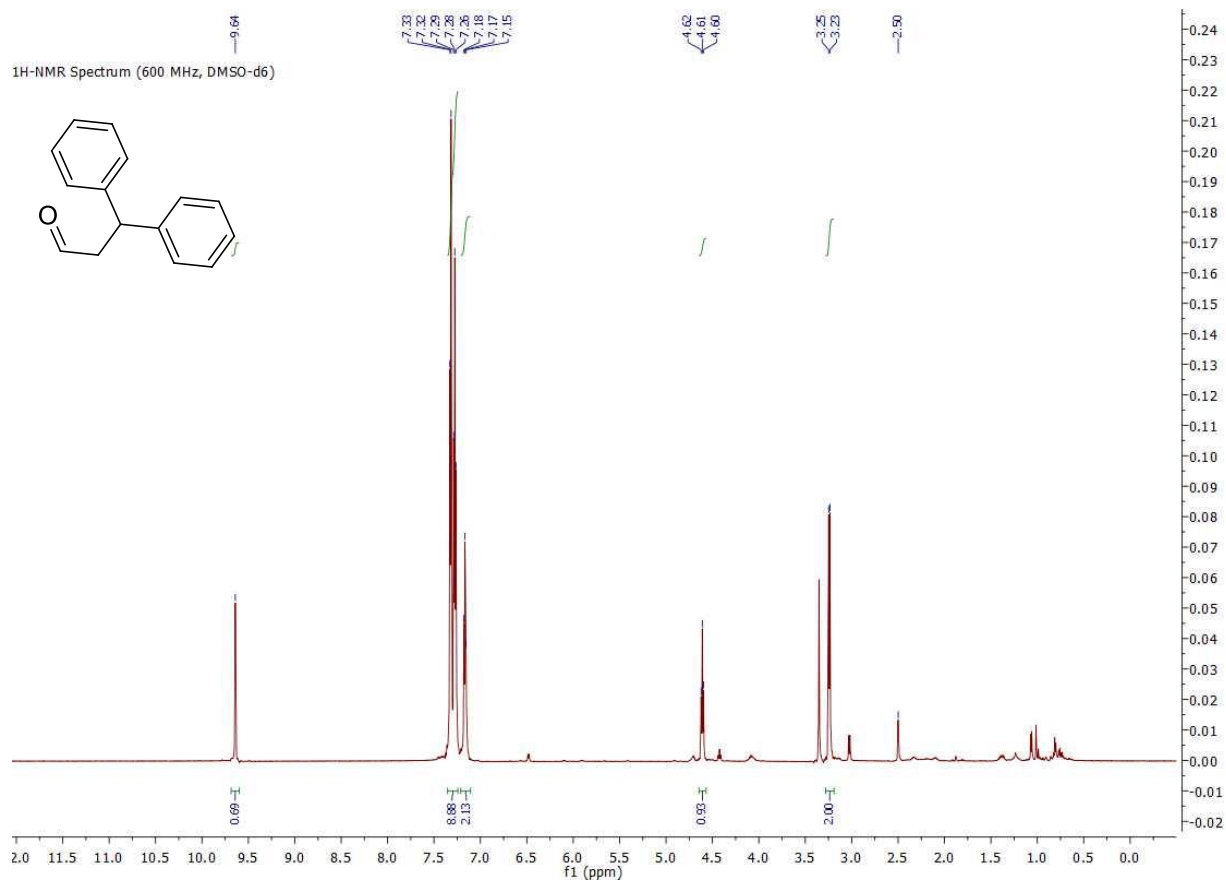
¹H-NMR Spectrum (600 MHz, DMSO-d₆)



¹³C-NMR Spectrum (150 MHz, DMSO-d₆)

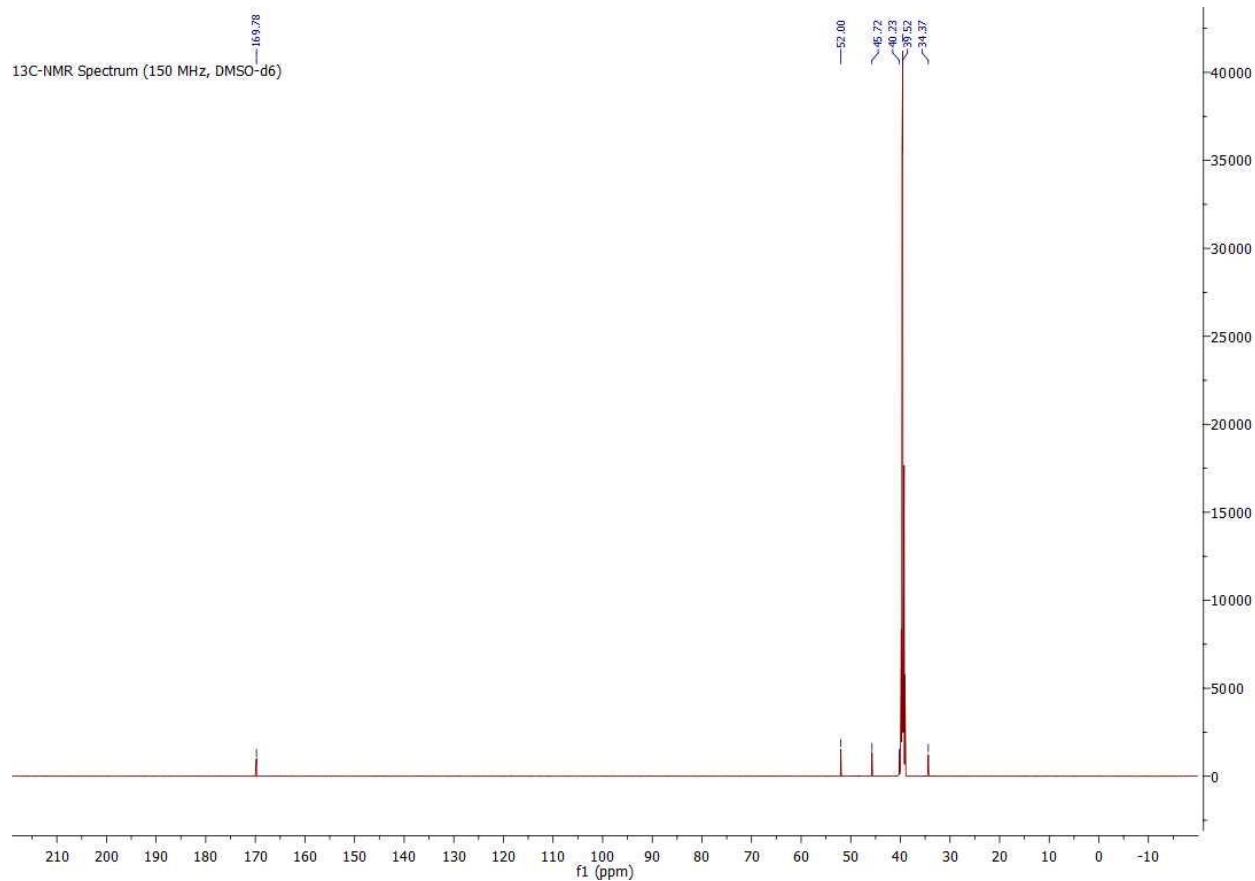
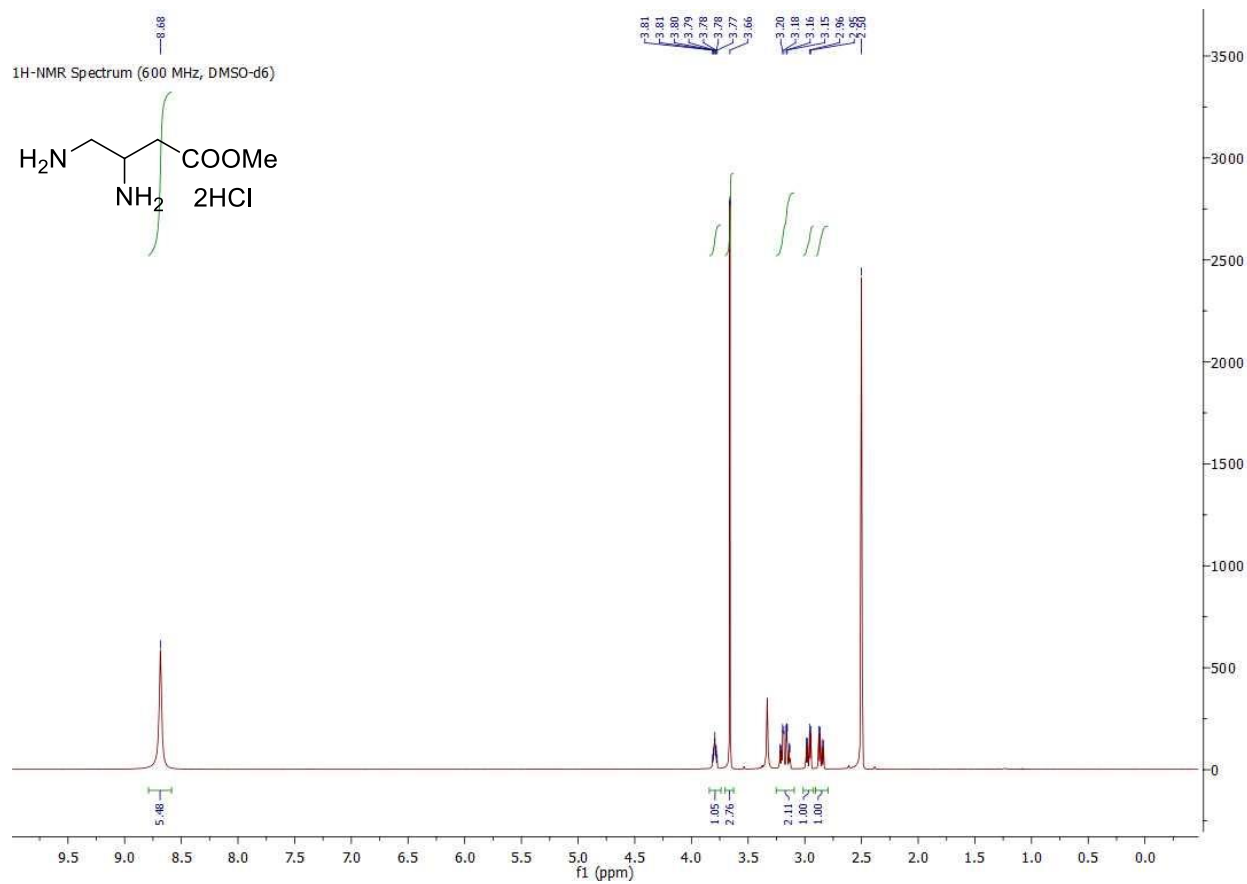


3,3-diphenylpropanal (2.33).

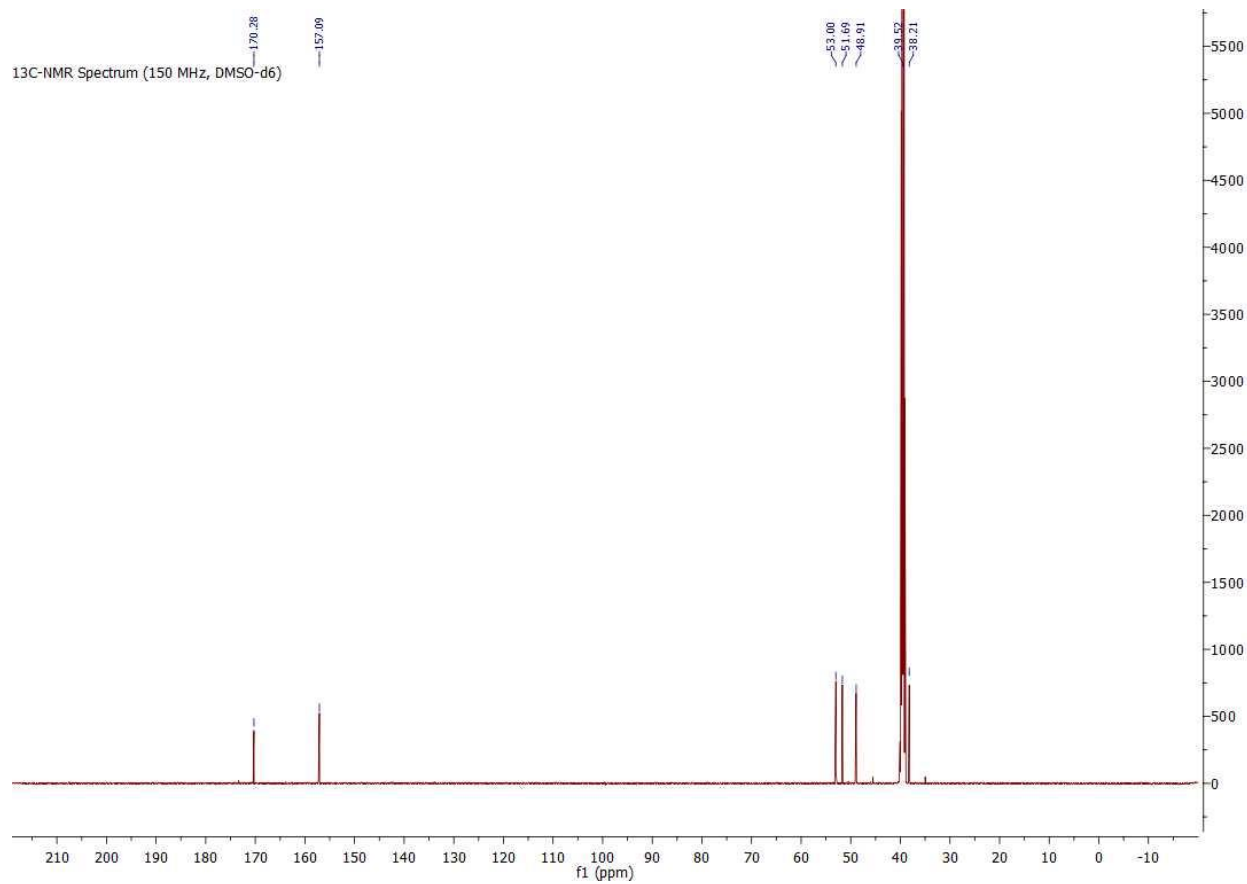
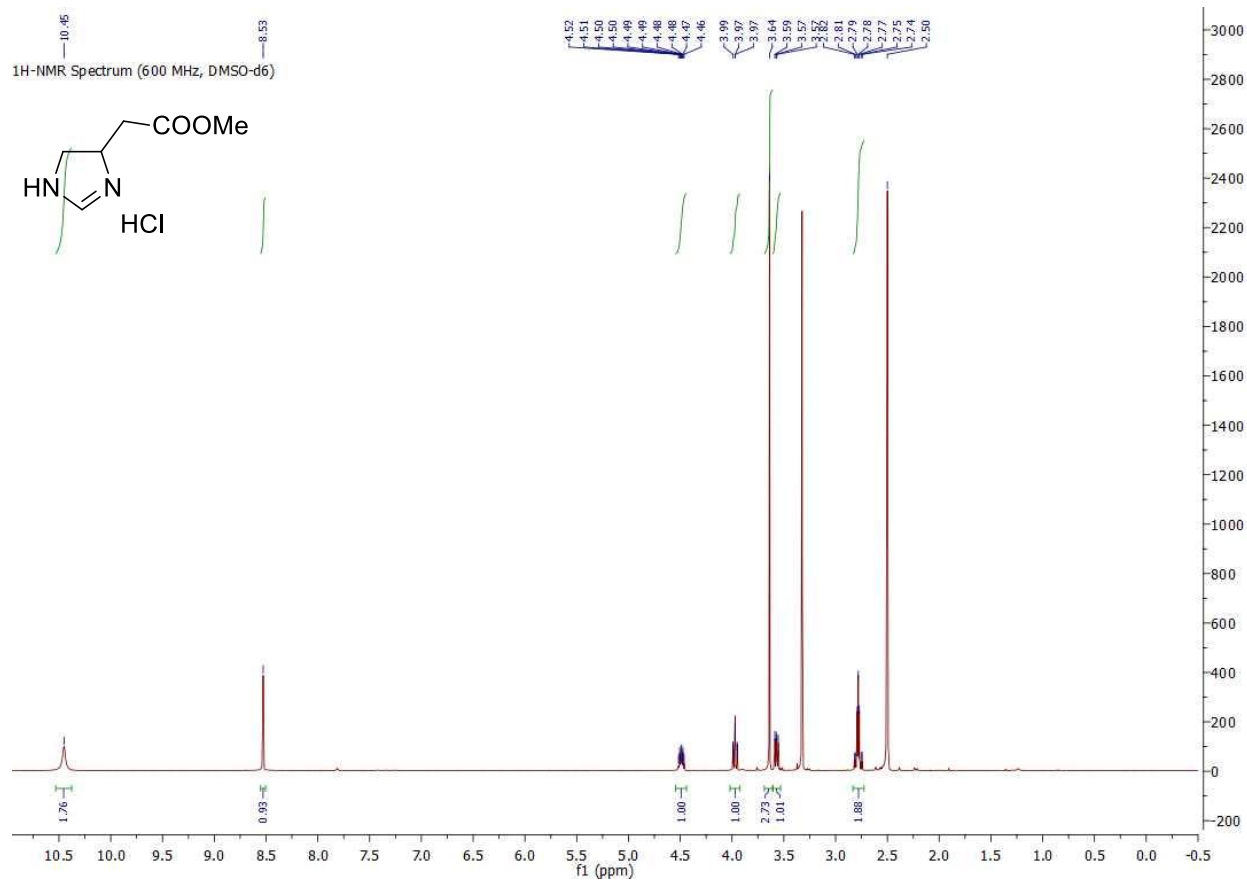


NMR analyses chapter 3

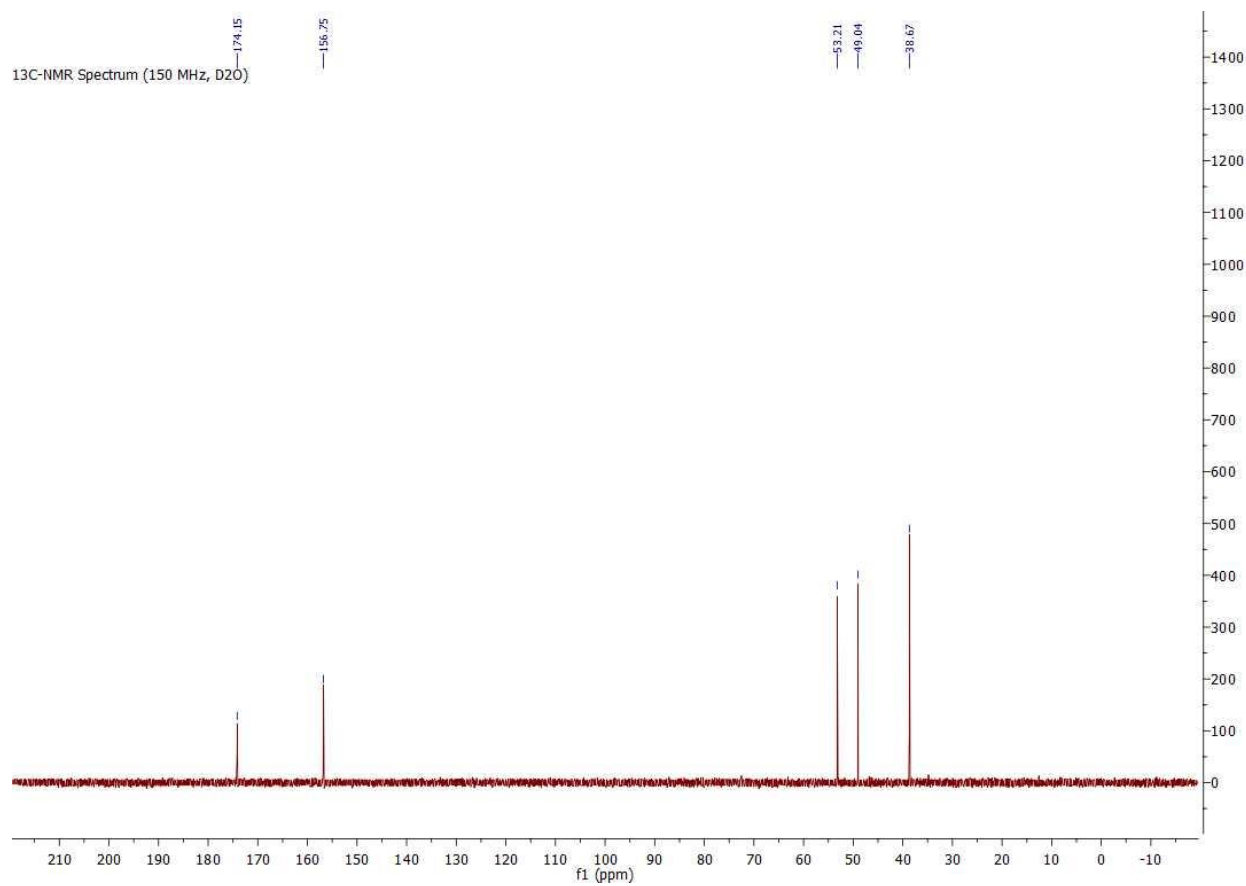
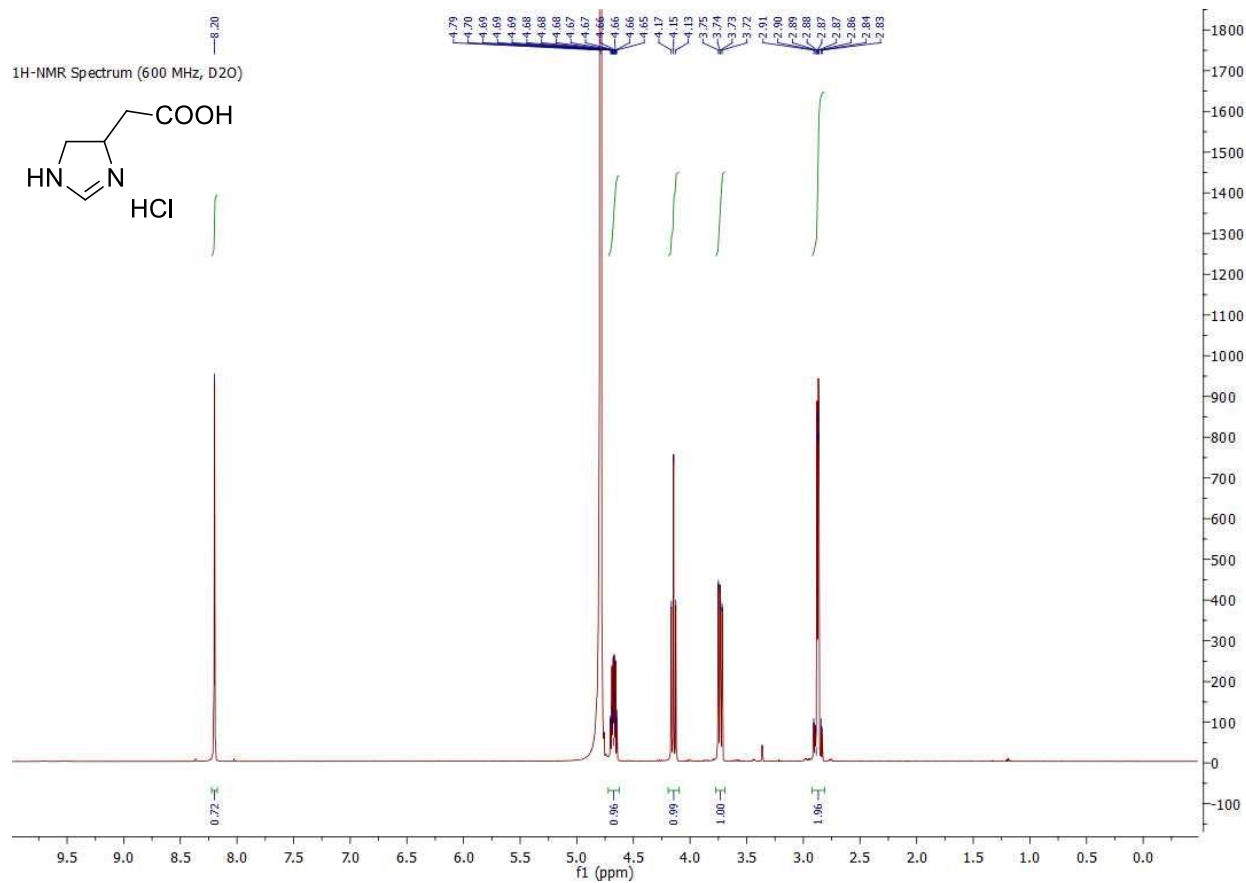
Methyl 3,4-diaminobutanoate dihydrochloride (3.12).



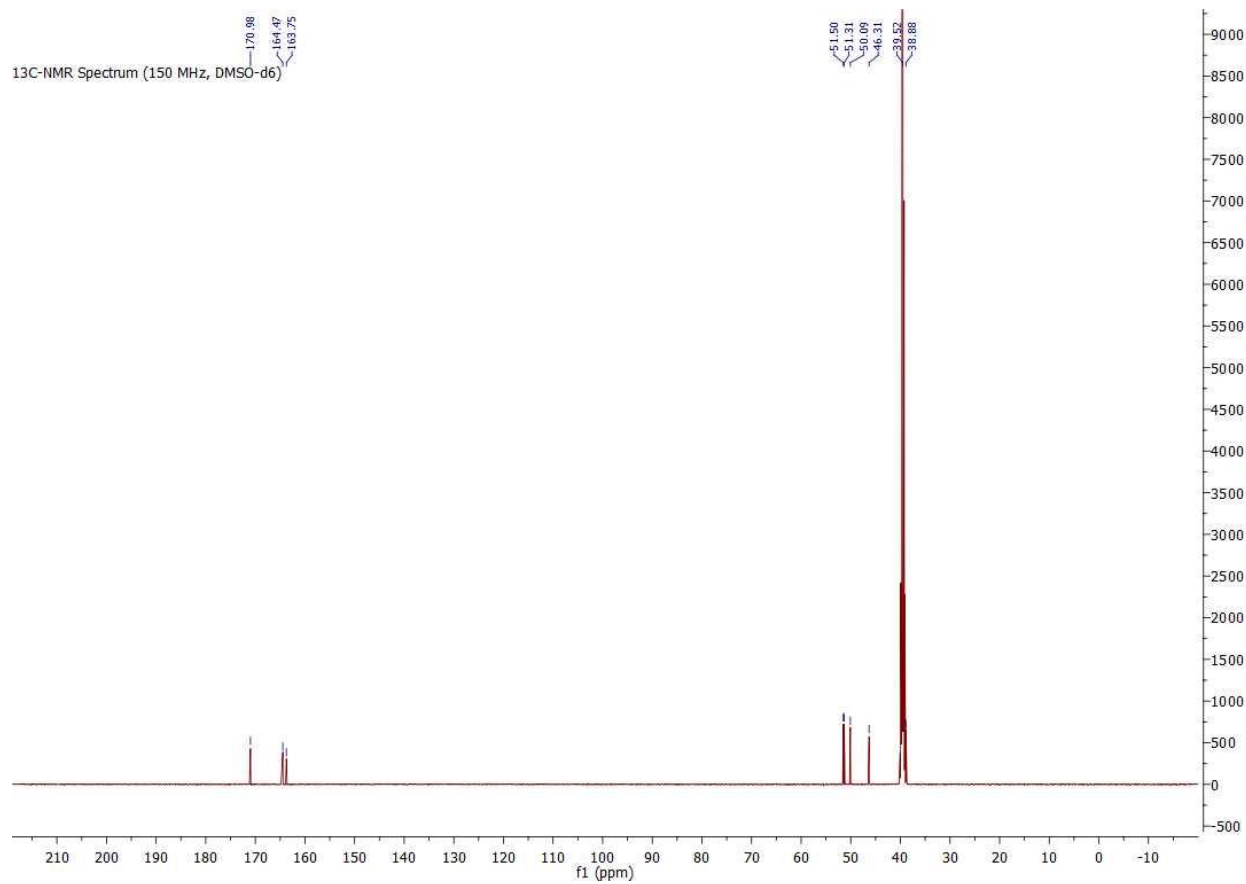
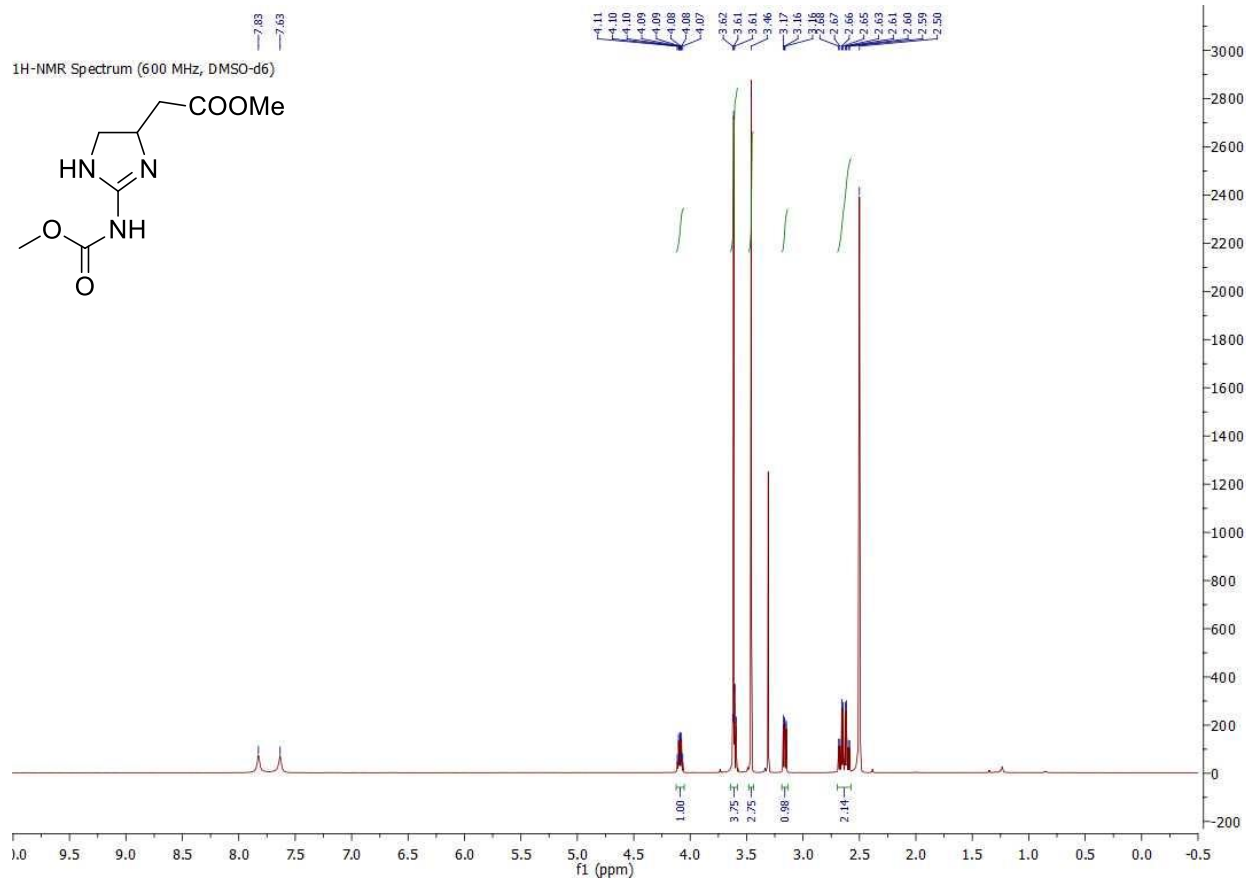
Methyl 2-(4,5-dihydro-1H-imidazol-4-yl)acetate hydrochloride (3.13).



2-(4,5-dihydro-1H-imidazol-4-yl)acetic acid hydrochloride (3.3).

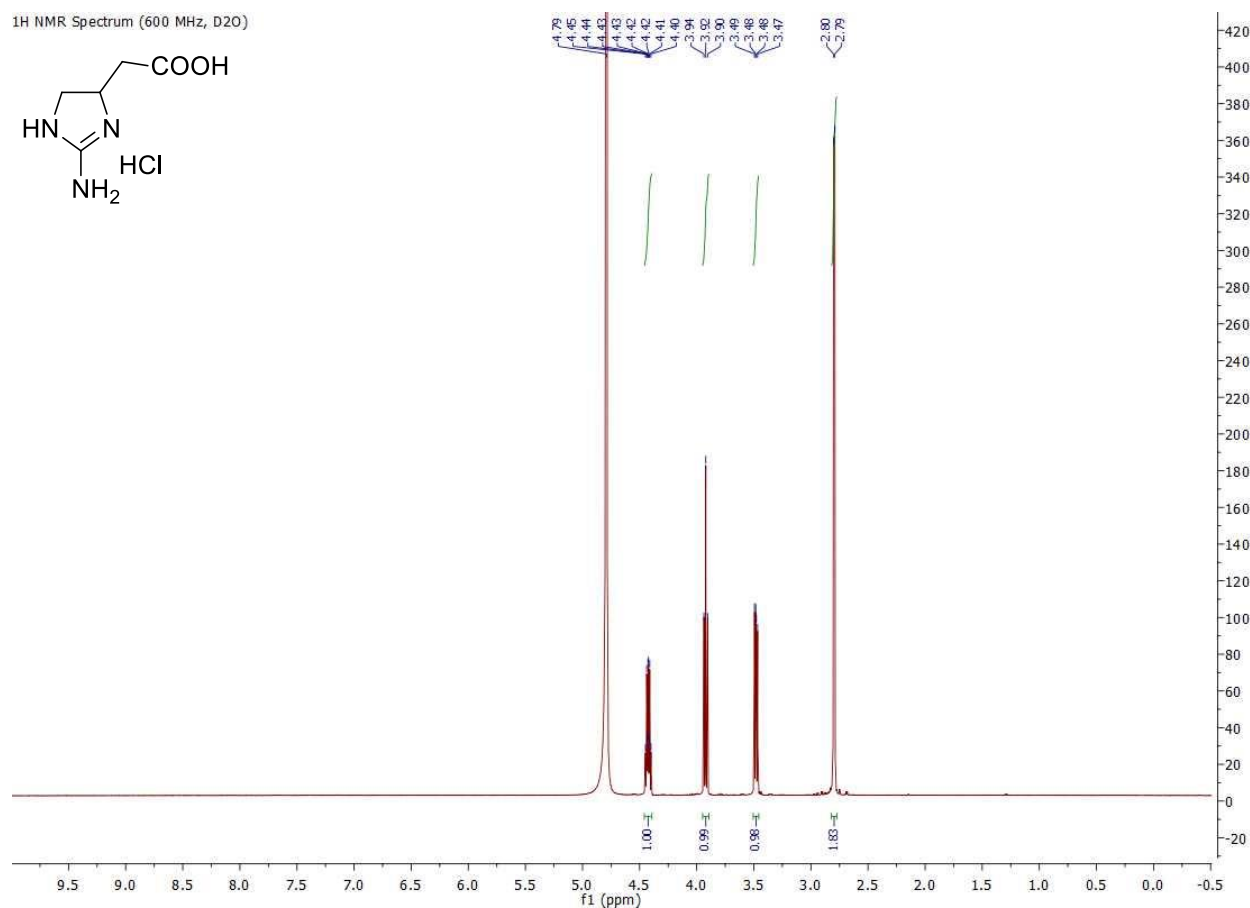
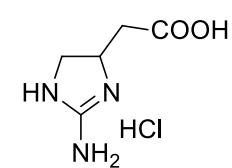


Methyl 2-(2-((methoxycarbonyl)amino)-4,5-dihydro-1H-imidazol-4-yl)acetate (3.28).

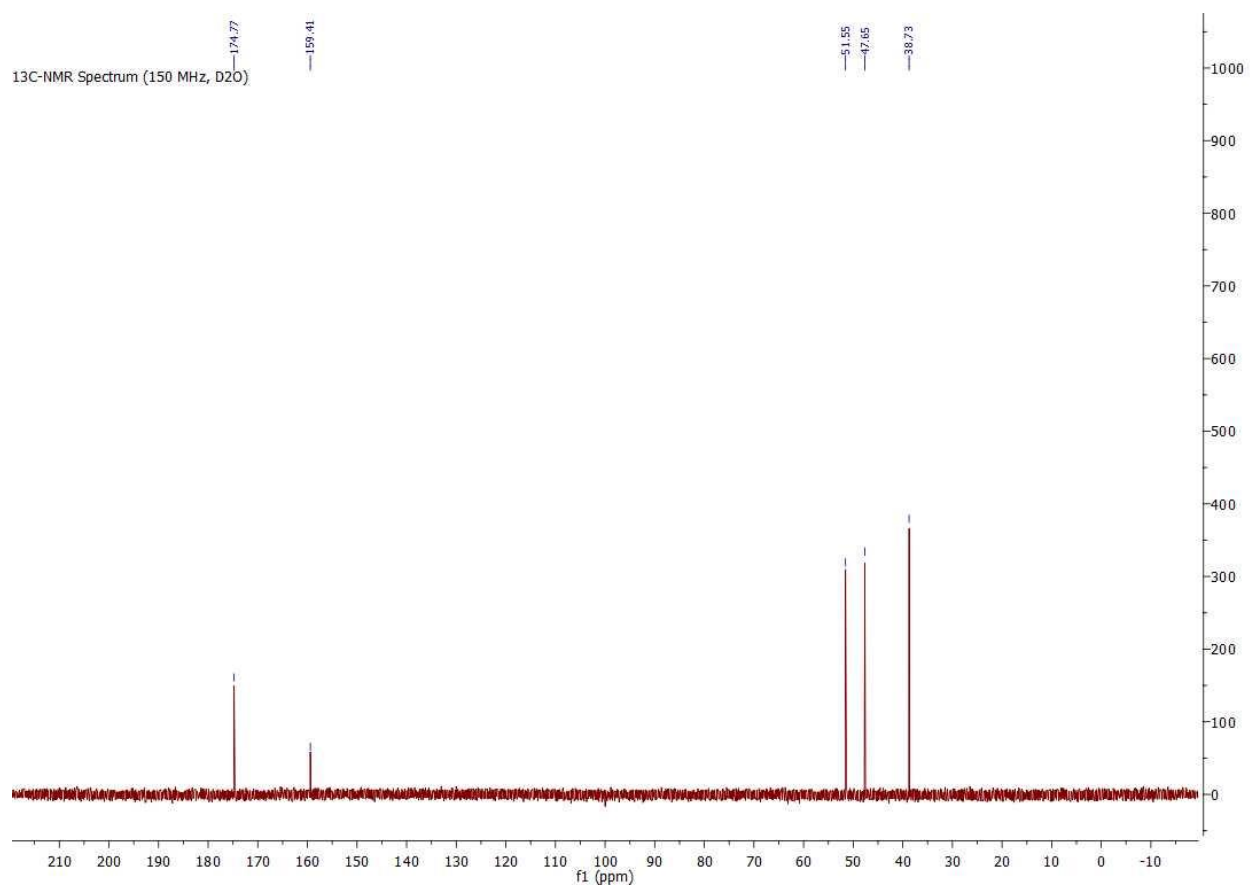


2-(2-amino-4,5-dihydro-1H-imidazol-4-yl)acetic acid hydrochloride (3.4).

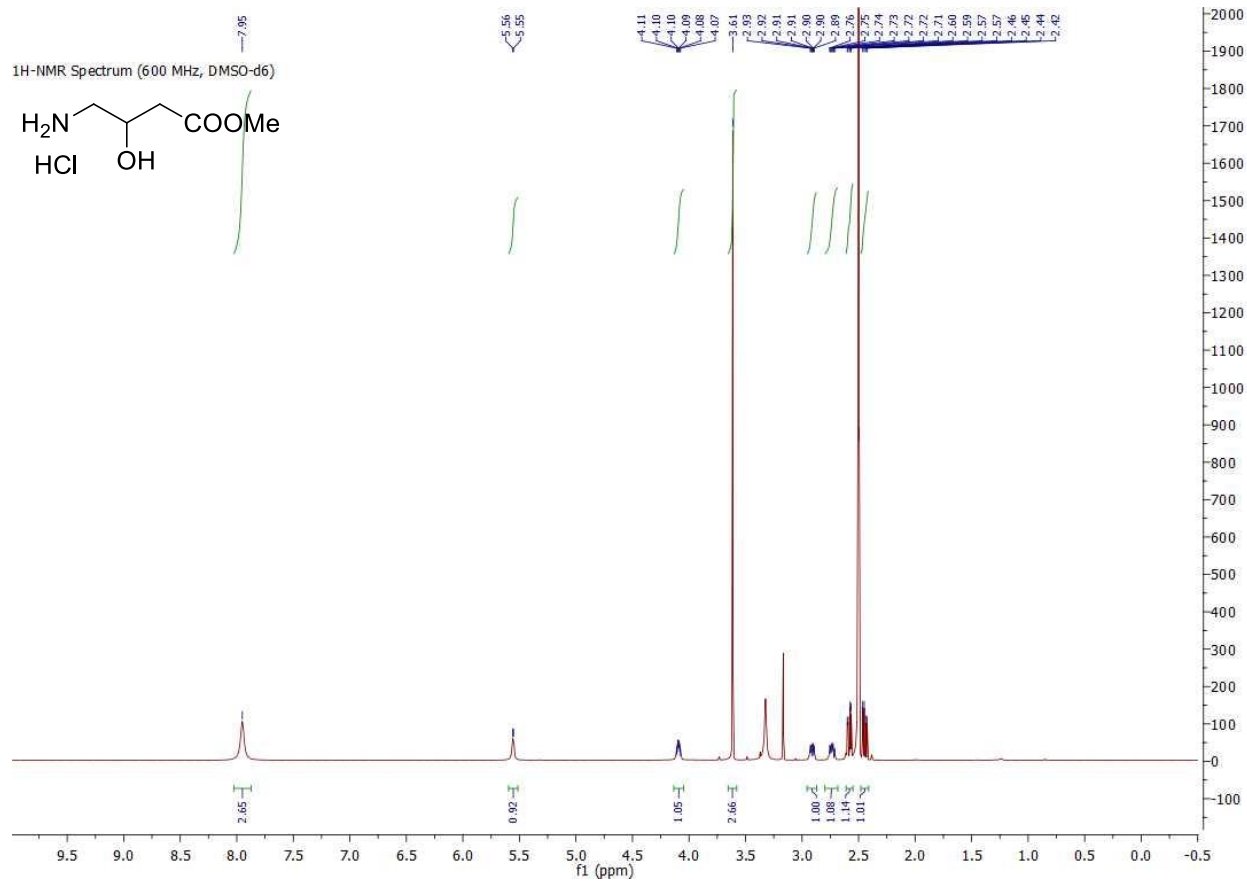
¹H NMR Spectrum (600 MHz, D₂O)



¹³C-NMR Spectrum (150 MHz, D₂O)

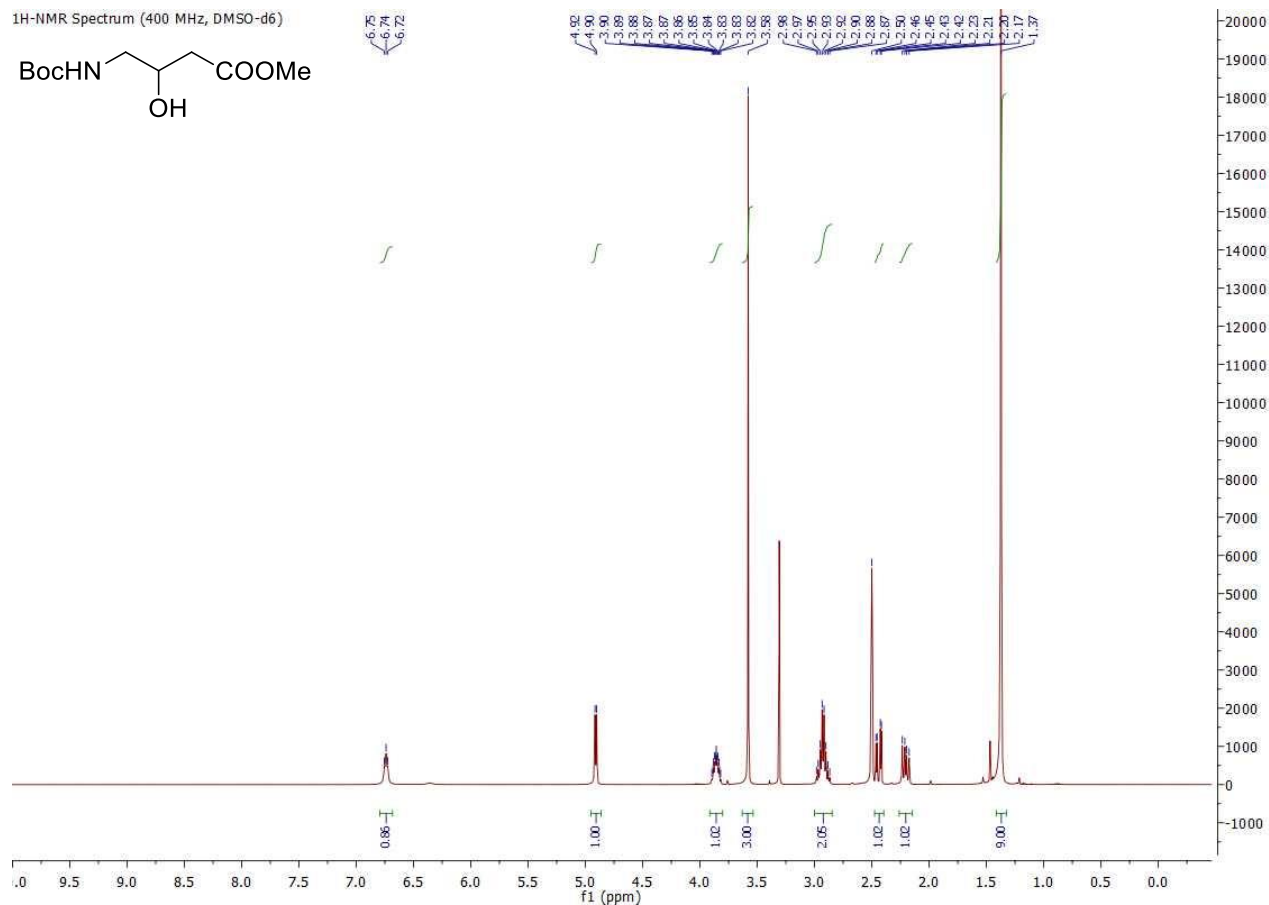
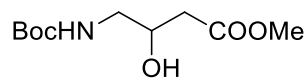


Methyl 4-amino-3-hydroxybutanoate hydrochloride (3.21).

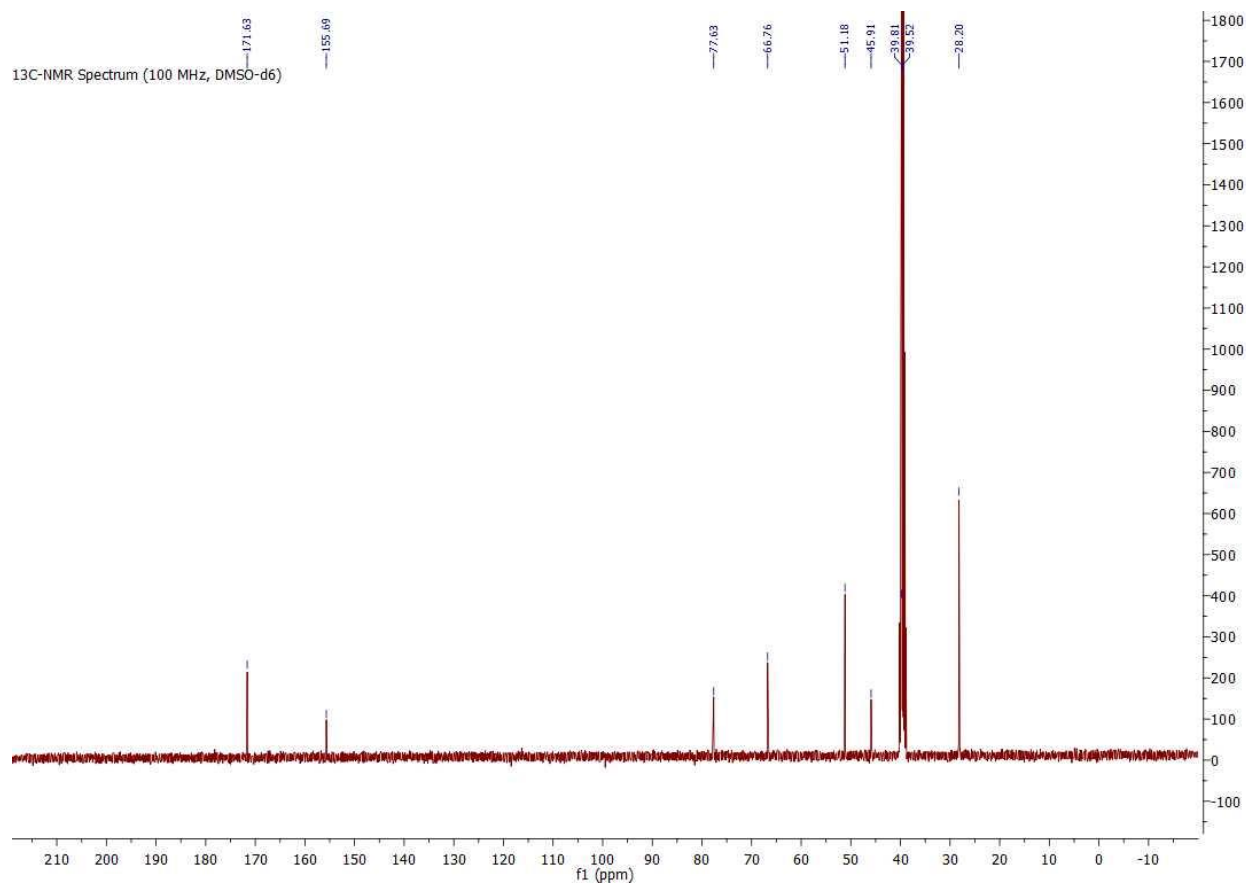


Methyl 4-((*tert*-butoxycarbonyl)amino)-3-hydroxybutanoate (3.22).

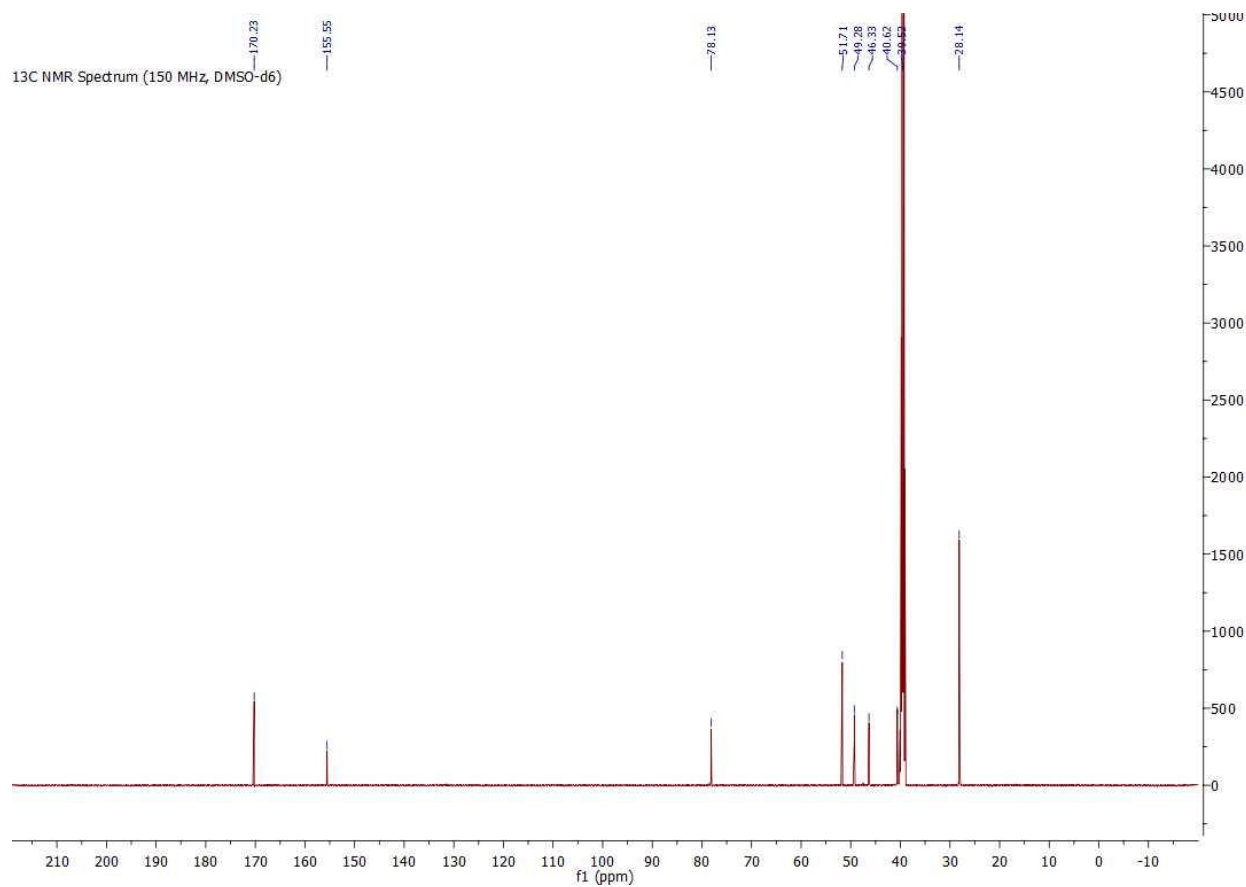
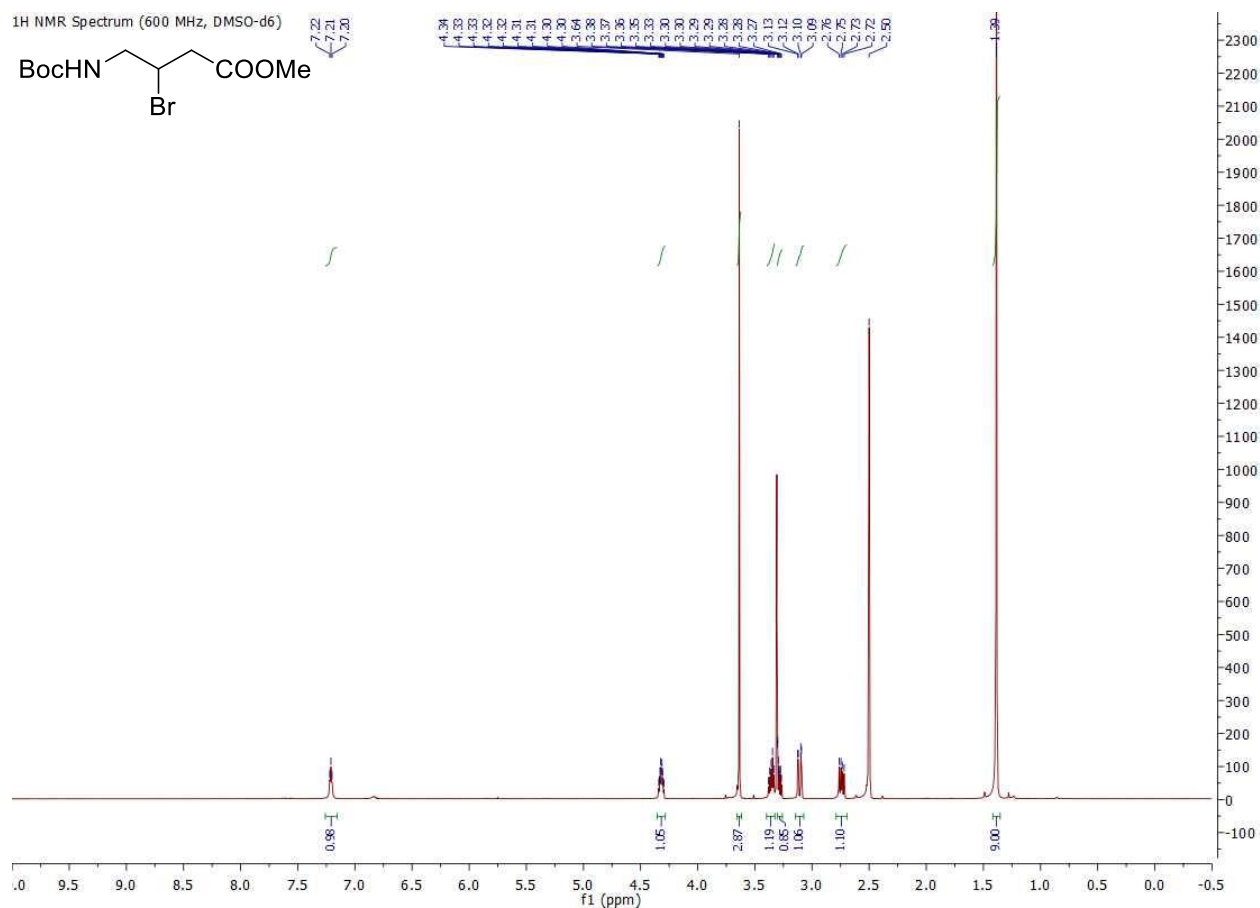
¹H-NMR Spectrum (400 MHz, DMSO-d₆)



¹³C-NMR Spectrum (100 MHz, DMSO-d₆)

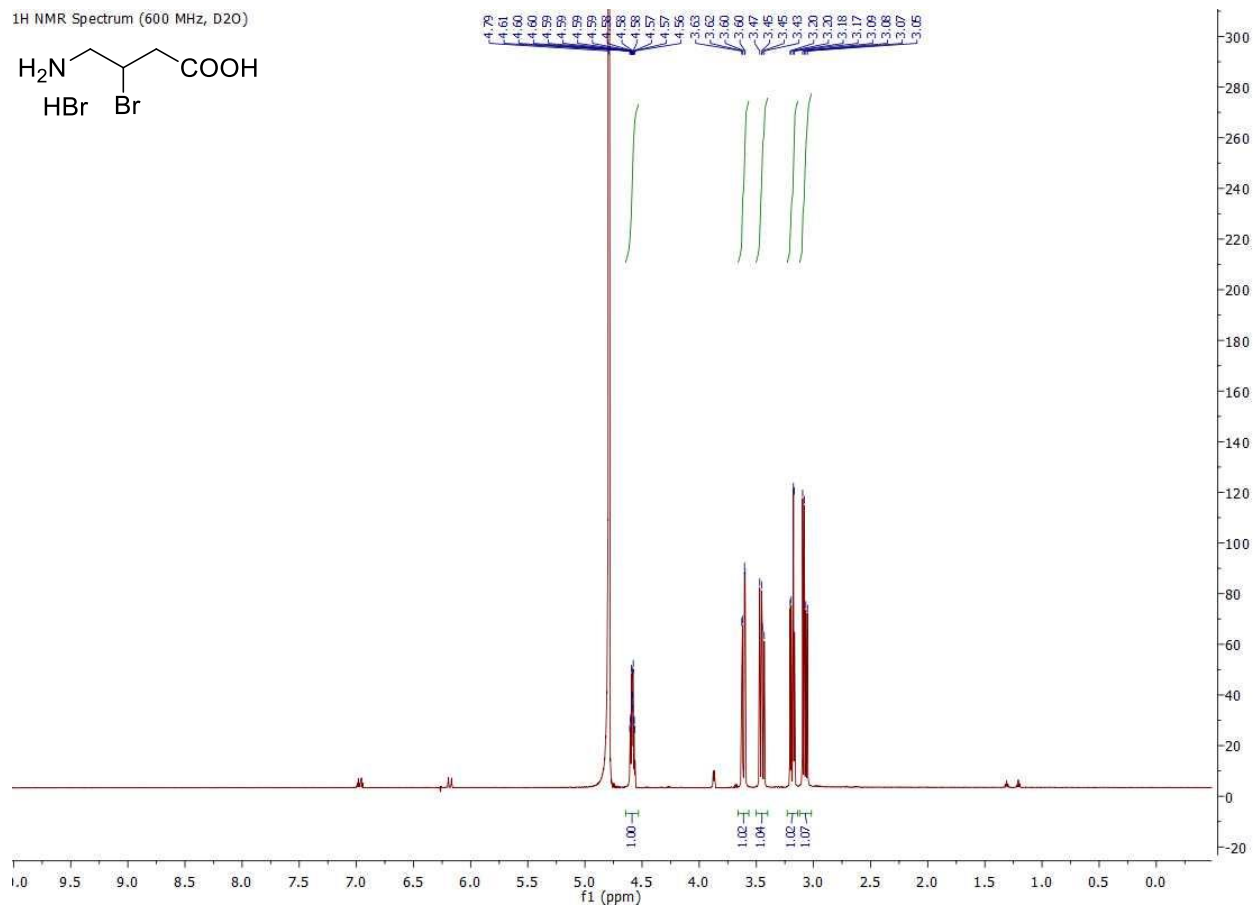
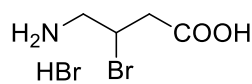


Methyl 3-bromo-4-((*tert*-butoxycarbonyl)amino)butanoate (3.23).

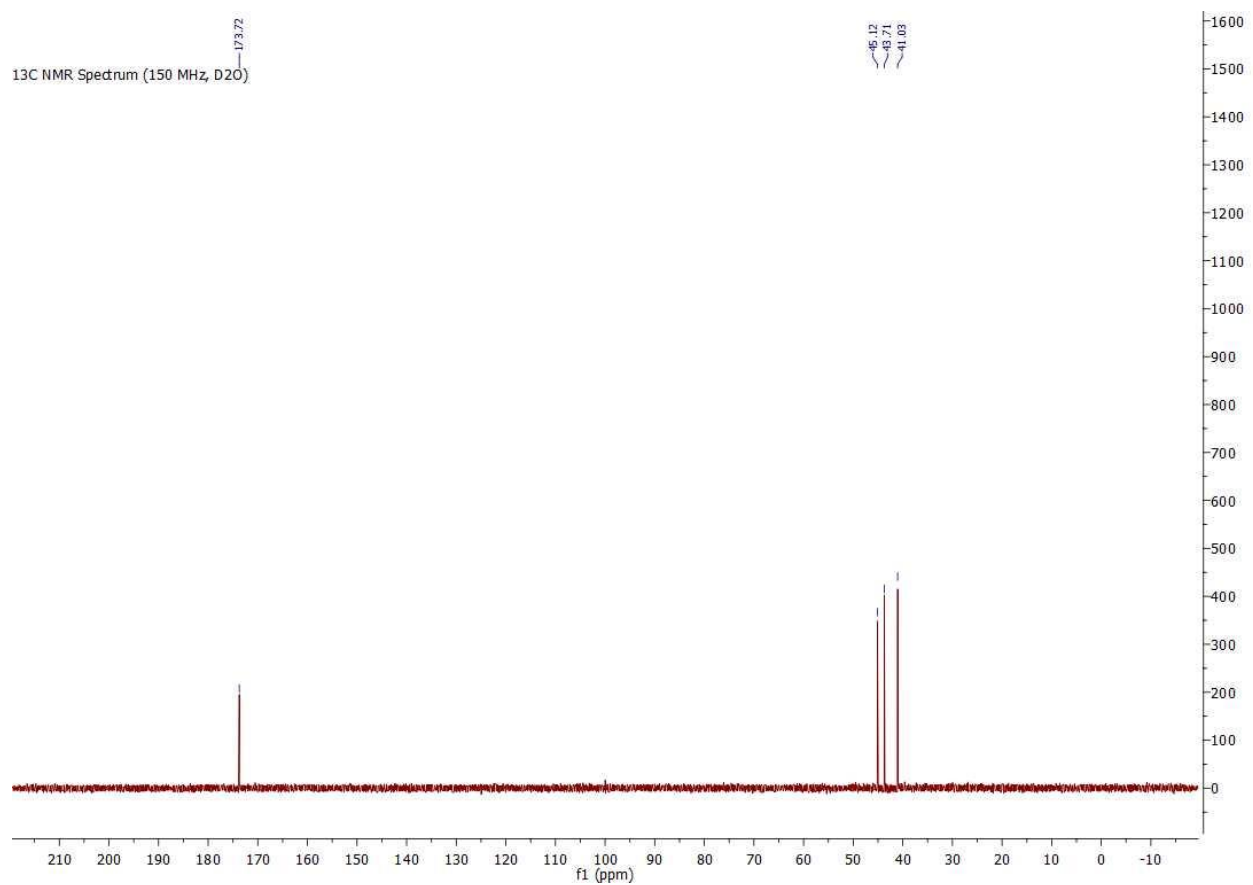


4-amino-3-bromobutanoic acid hydrobromide (3.24).

¹H NMR Spectrum (600 MHz, D₂O)

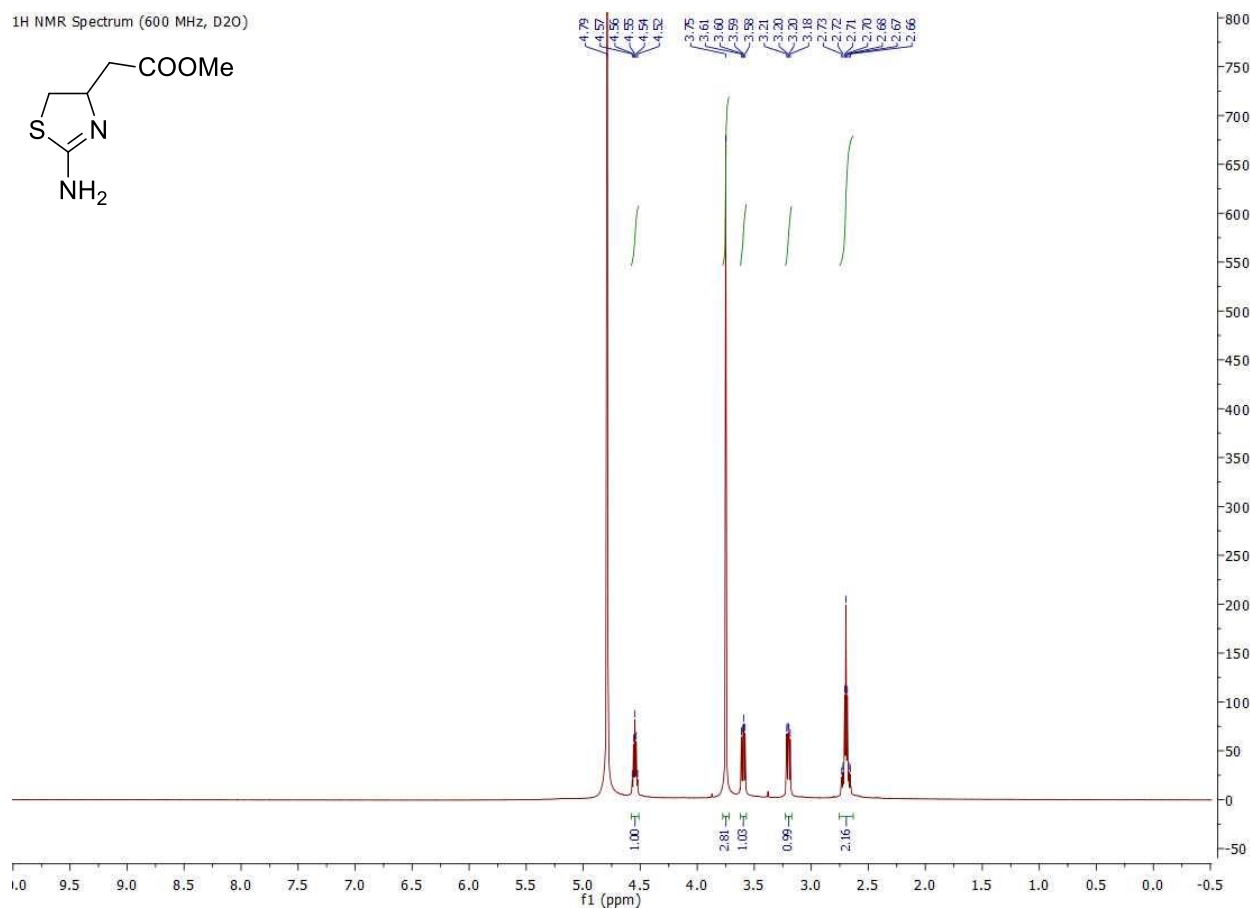
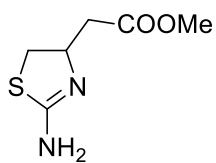


¹³C NMR Spectrum (150 MHz, D₂O)

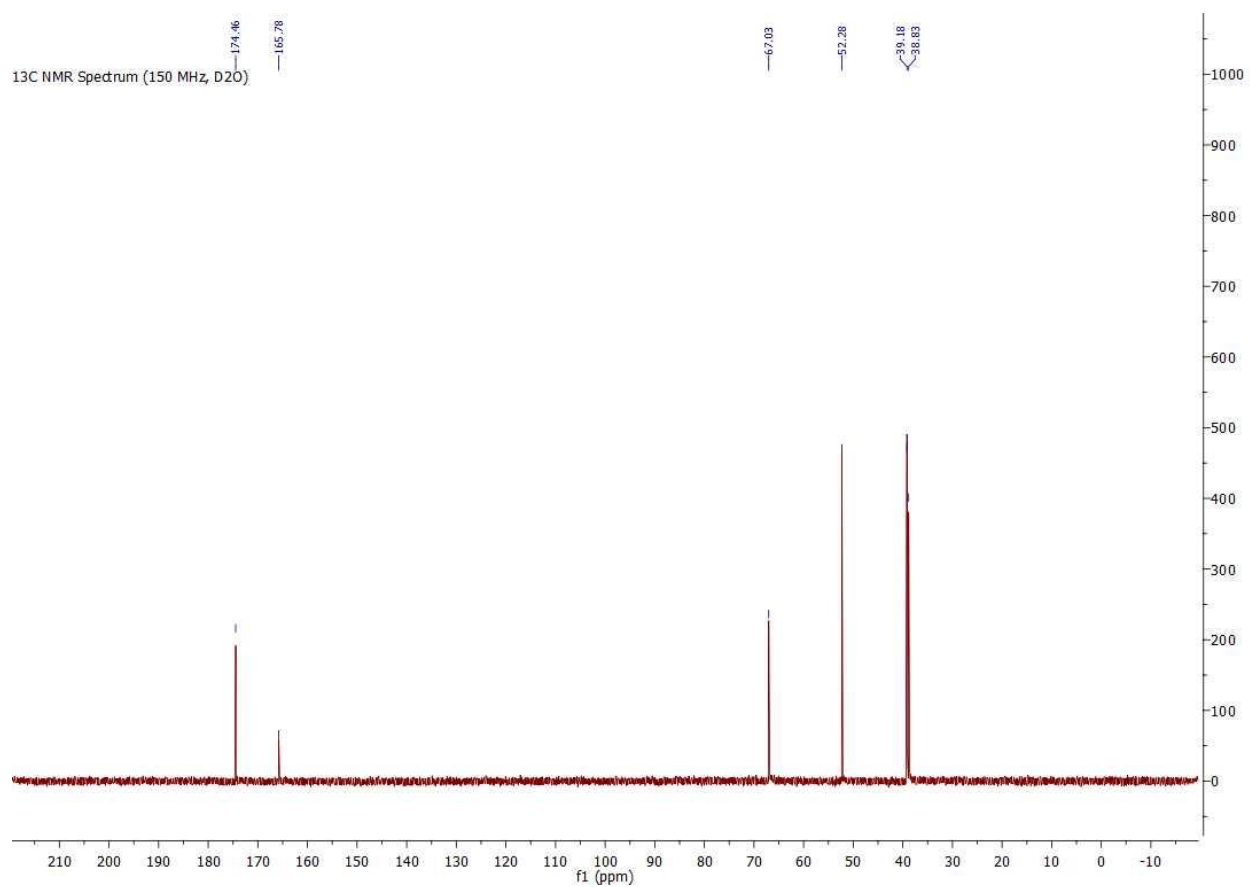


Methyl 2-(2-amino-4,5-dihydrothiazol-4-yl)acetate (3.15).

¹H NMR Spectrum (600 MHz, D₂O)

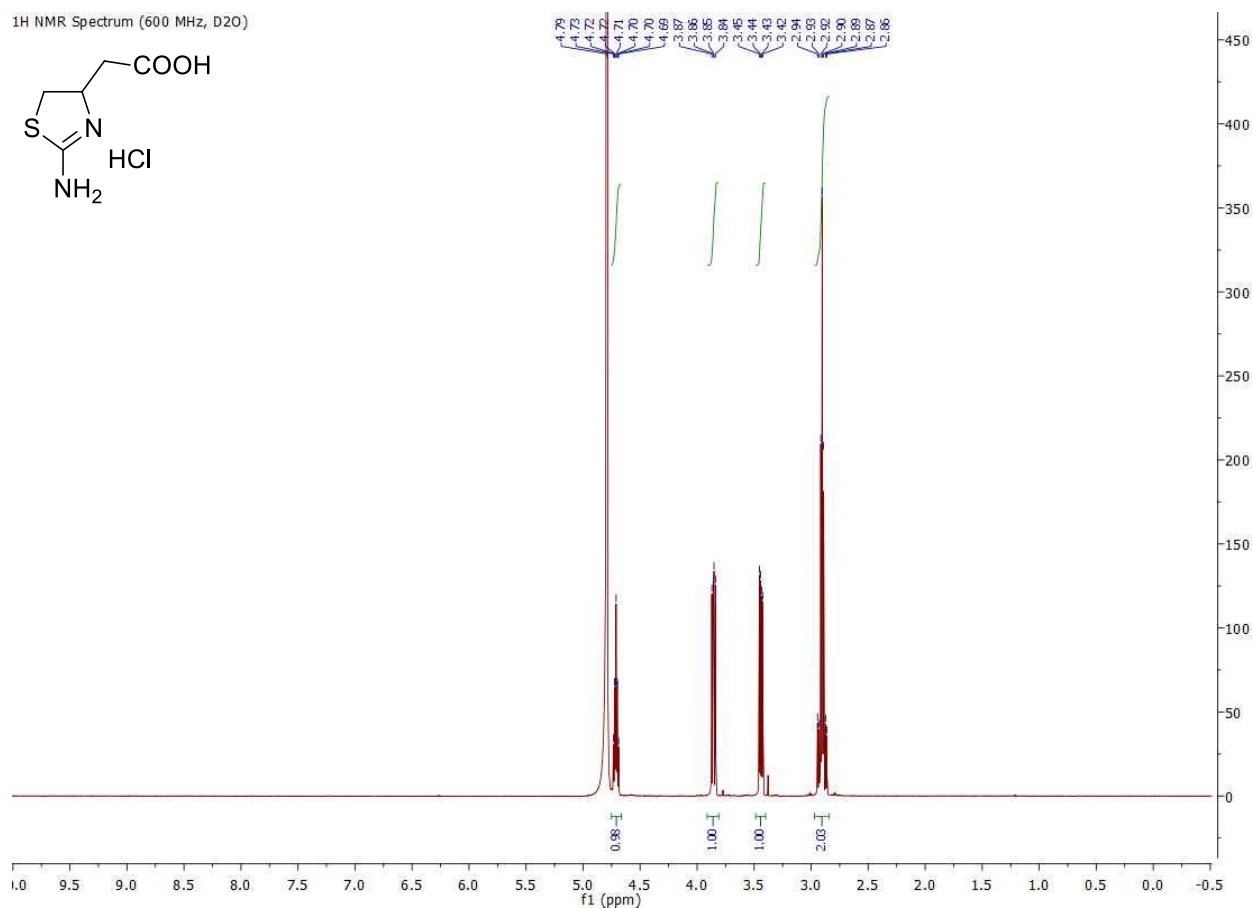
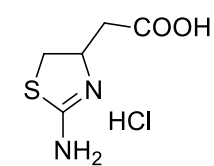


¹³C NMR Spectrum (150 MHz, D₂O)

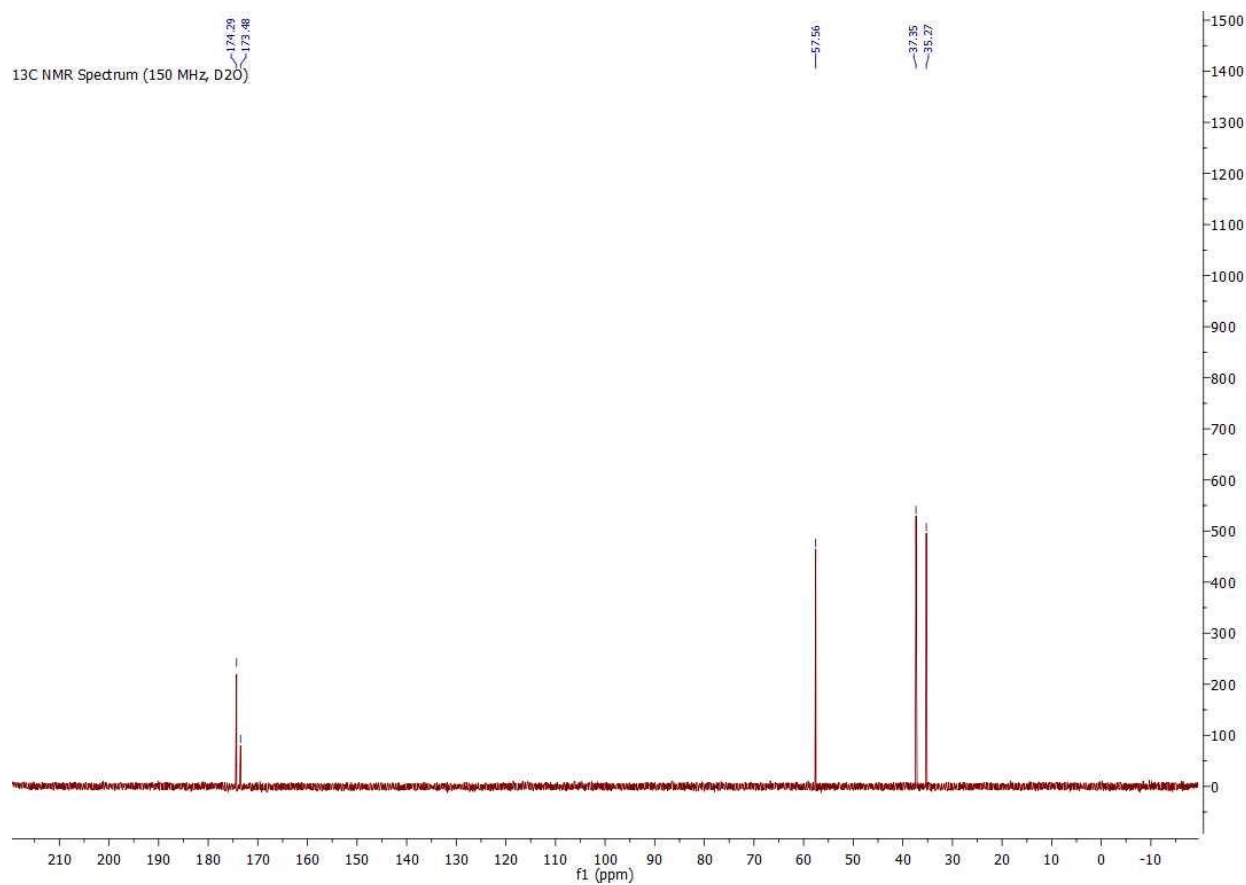


2-(2-amino-4,5-dihydrothiazol-4-yl)acetic acid hydrochloride (3.5)

¹H NMR Spectrum (600 MHz, D₂O)

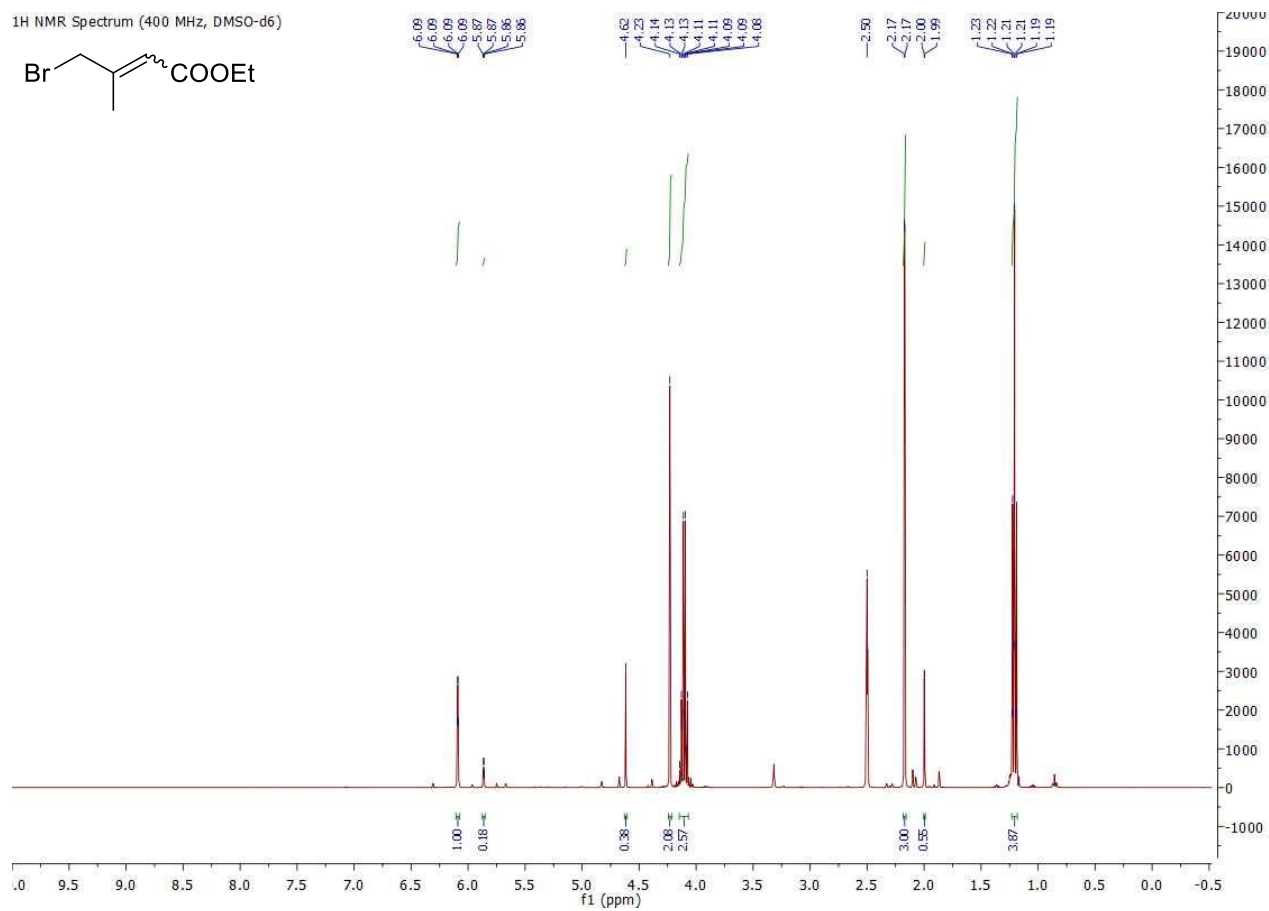


¹³C NMR Spectrum (150 MHz, D₂O)



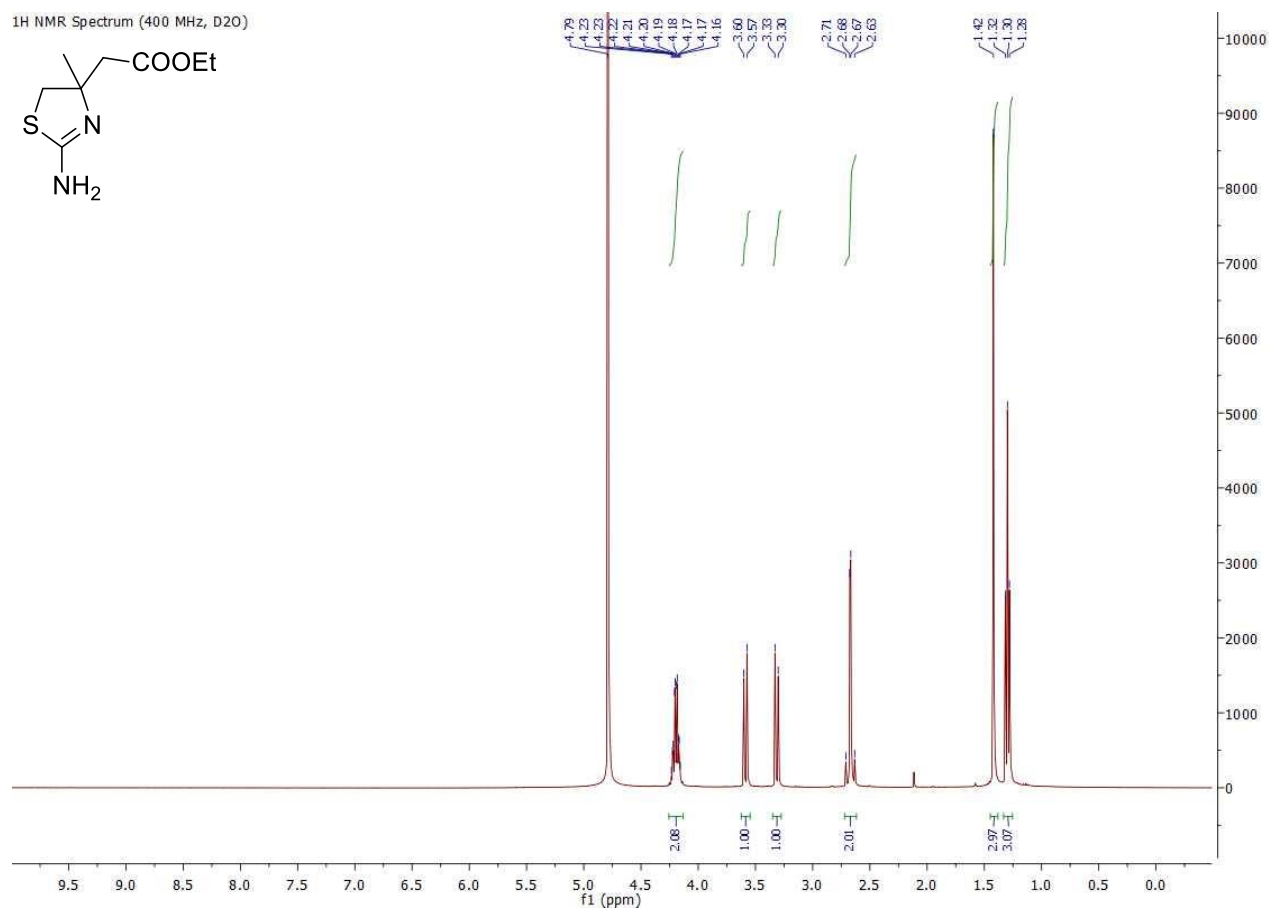
Ethyl 4-bromo-3-methylbut-2-enoate (3.36b).

¹H NMR Spectrum (400 MHz, DMSO-d₆)

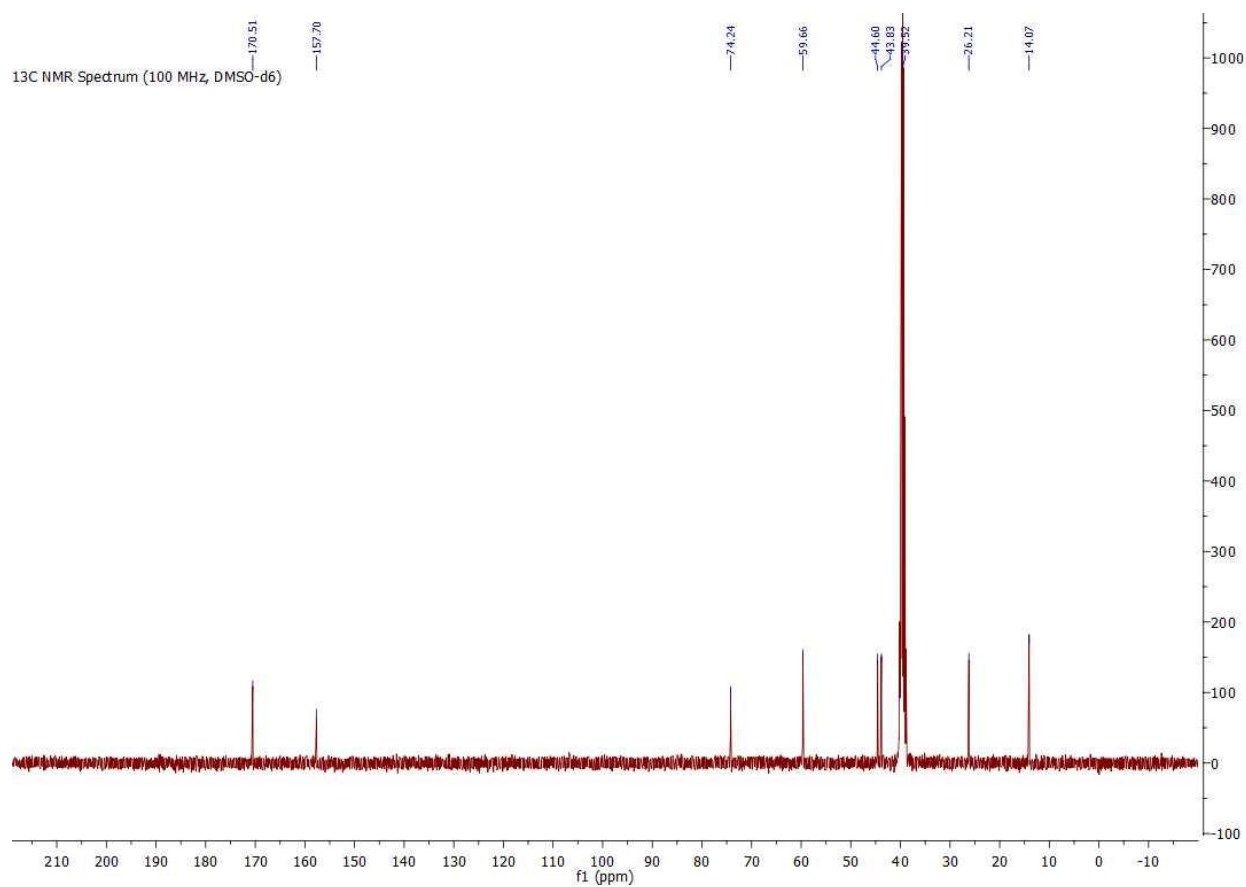


Ethyl 2-(2-amino-4-methyl-4,5-dihydrothiazol-4-yl)acetate (3.37b).

¹H NMR Spectrum (400 MHz, D₂O)

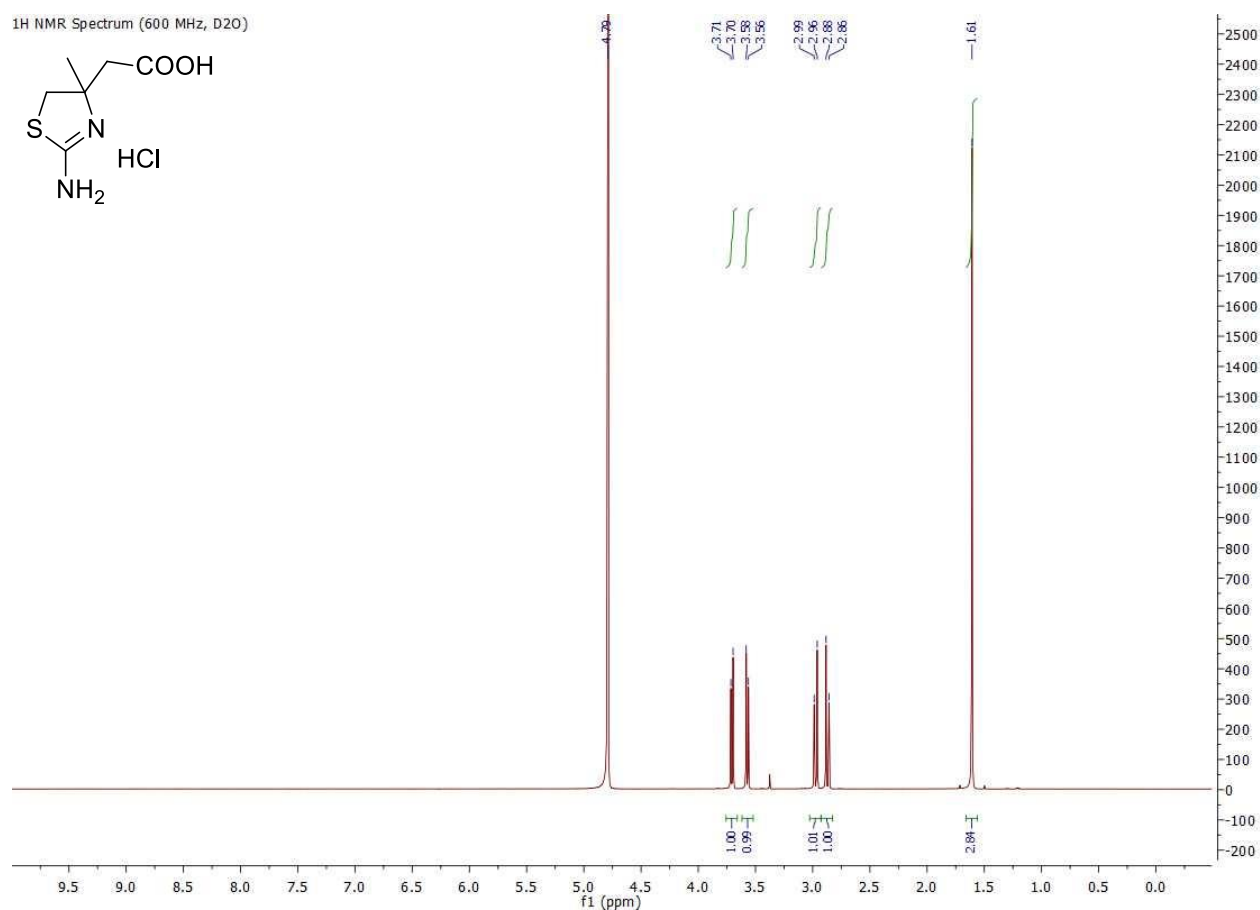
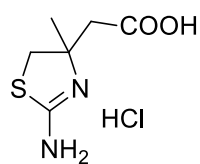


¹³C NMR Spectrum (100 MHz, DMSO-d₆)

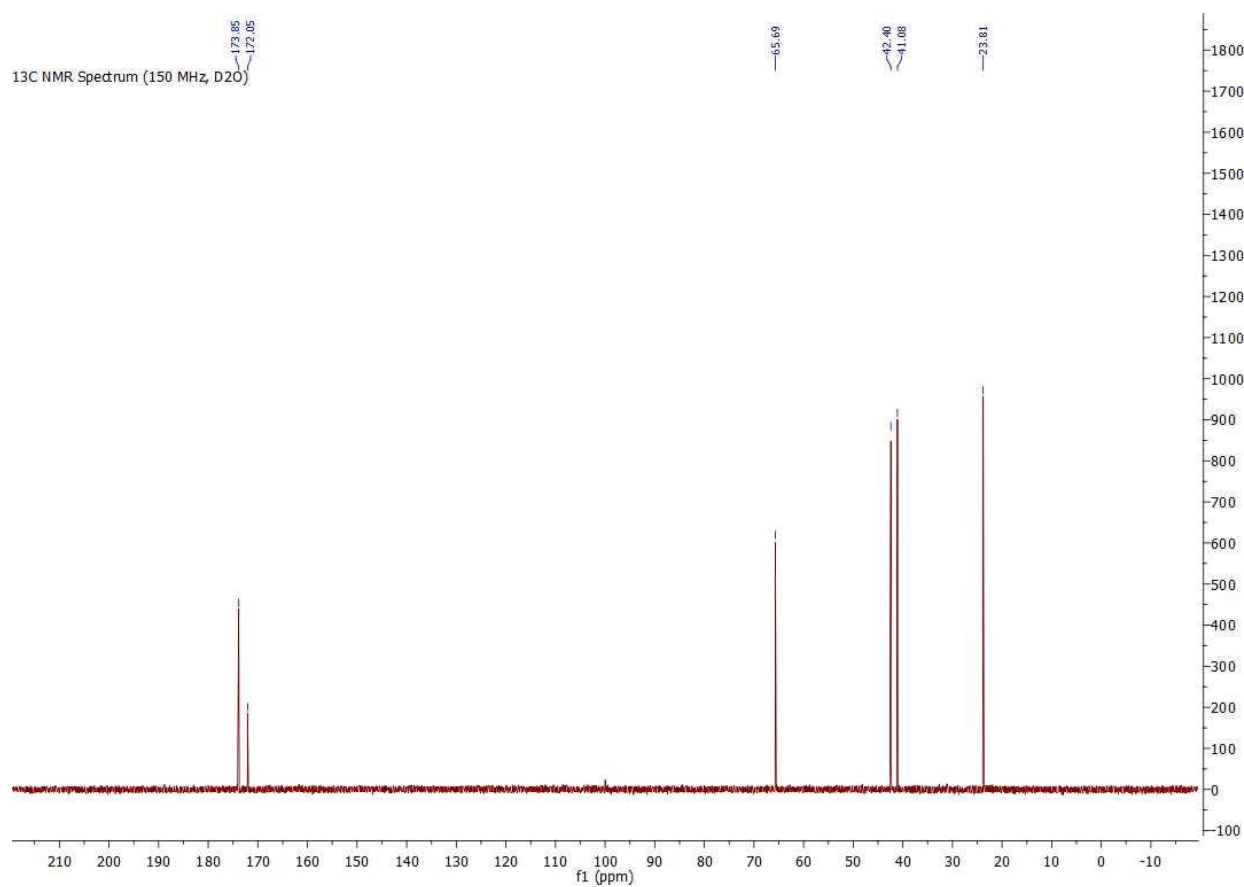


2-(2-amino-4-methyl-4,5-dihydrothiazol-4-yl)acetic acid hydrochloride (3.9).

¹H NMR Spectrum (600 MHz, D₂O)

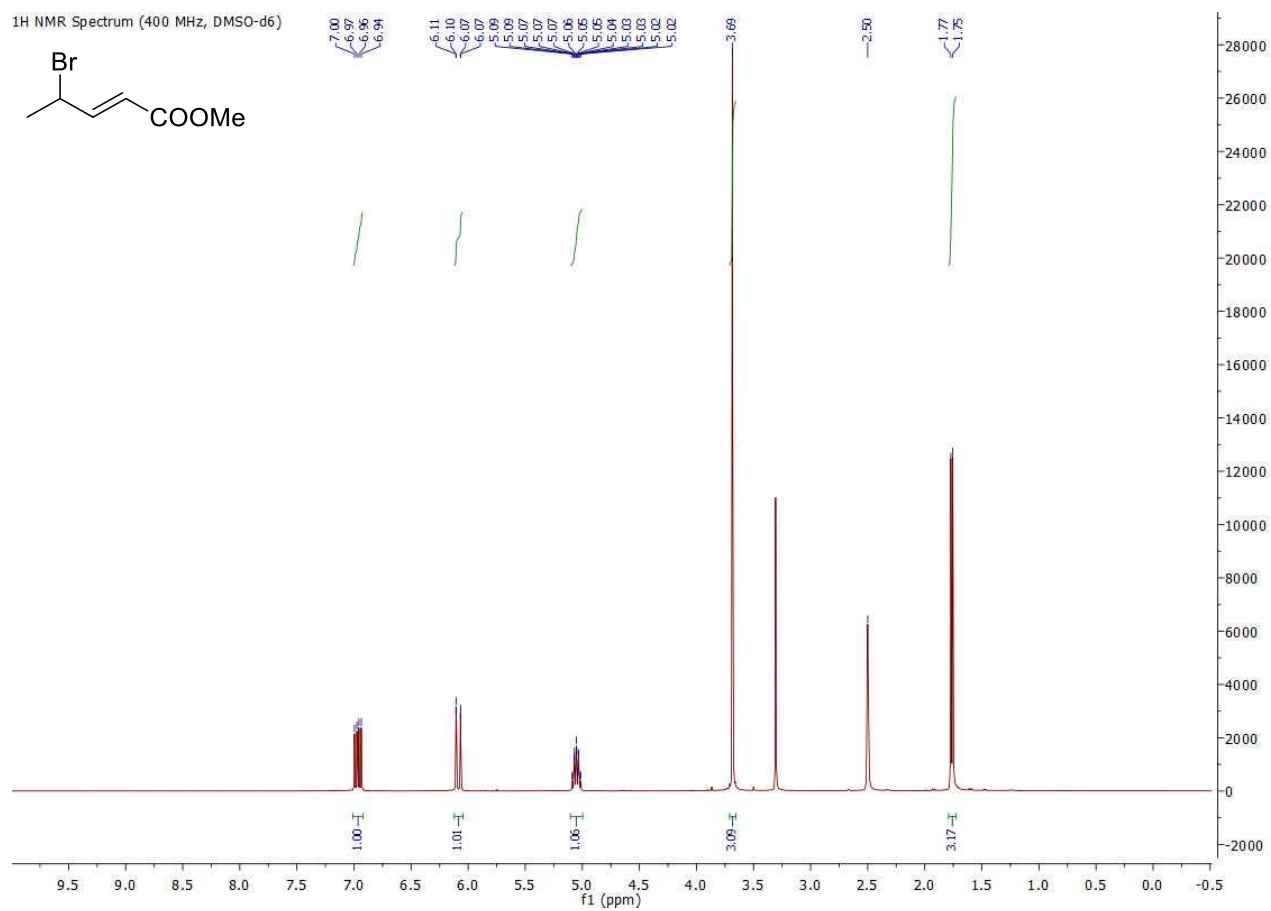


¹³C NMR Spectrum (150 MHz, D₂O)



(E)-methyl 4-bromopent-2-enoate (3.36a).

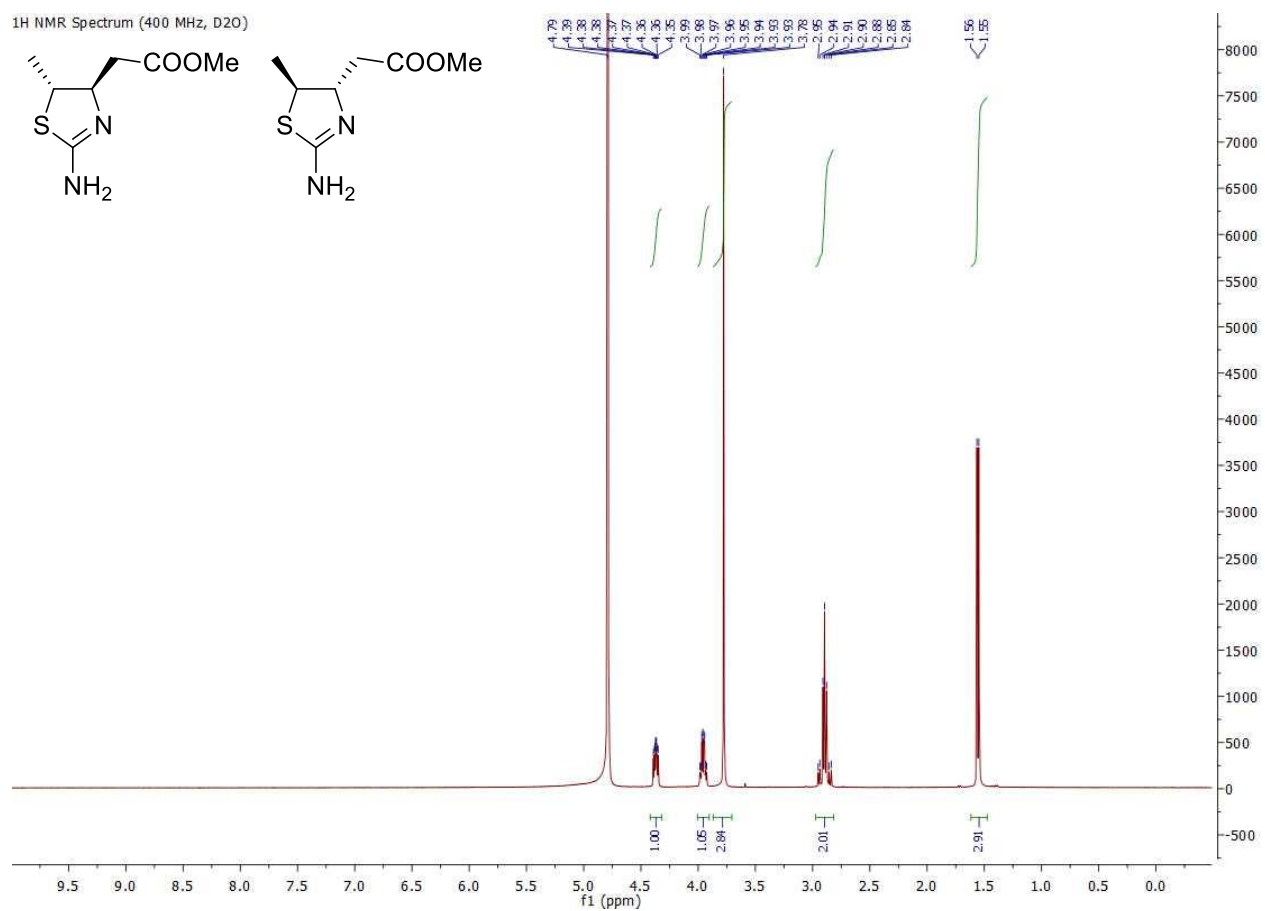
¹H NMR Spectrum (400 MHz, DMSO-d₆)



Methyl 2-((4*R**,5*R**)-2-amino-5-methyl-4,5-dihydrothiazol-4-yl)acetate trifluoroacetate (*trans*-3.37a).

2,2,2-

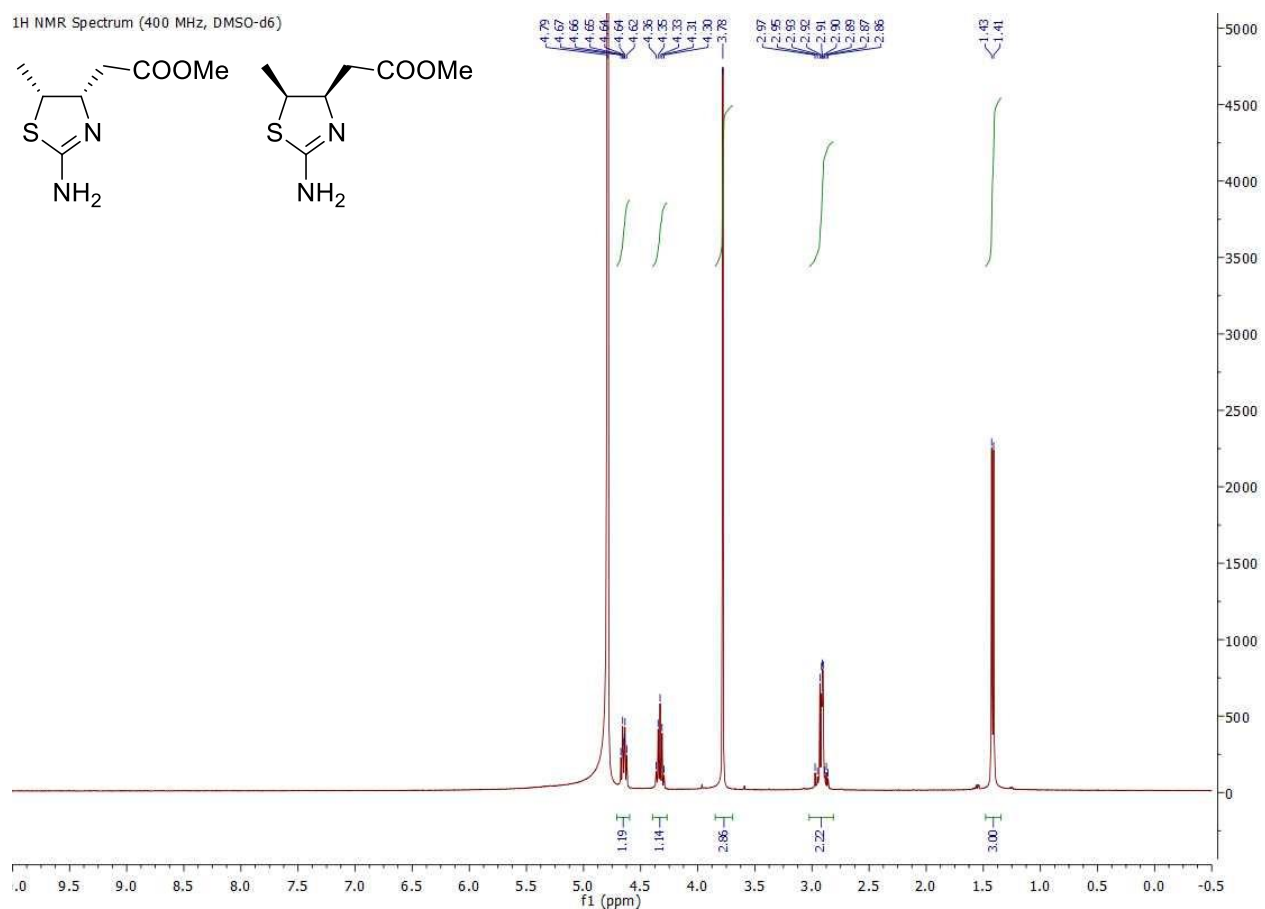
¹H NMR Spectrum (400 MHz, D₂O)



Methyl 2-((4*R**,5*S**)-2-amino-5-methyl-4,5-dihydrothiazol-4-yl)acetate trifluoroacetate (*cis*-3.37a).

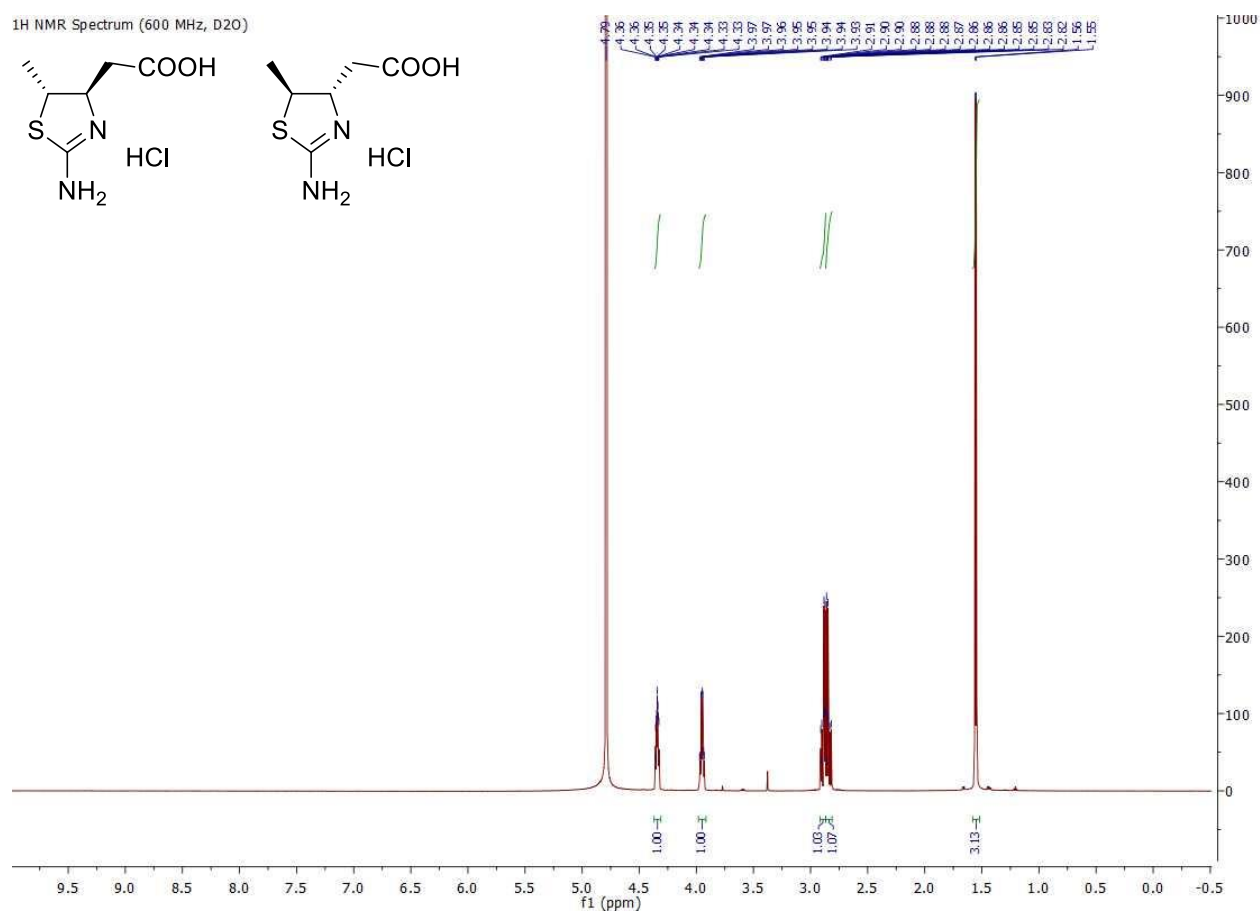
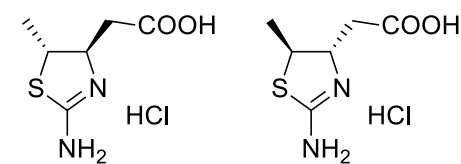
2,2,2-

¹H NMR Spectrum (400 MHz, DMSO-d₆)

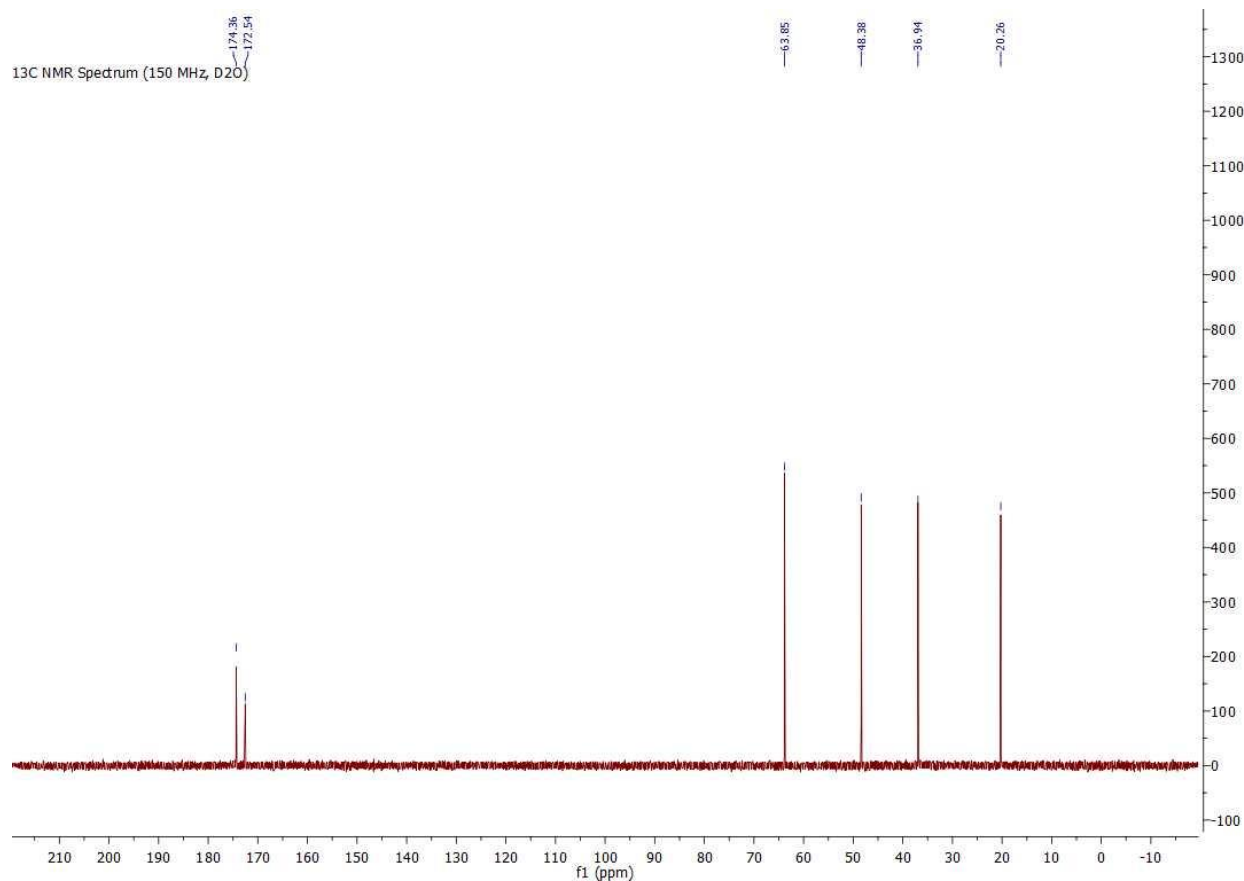


2-((4*R,5*R**)-2-amino-5-methyl-4,5-dihydrothiazol-4-yl)acetic acid hydrochloride (*trans*-3.8).**

¹H NMR Spectrum (600 MHz, D₂O)

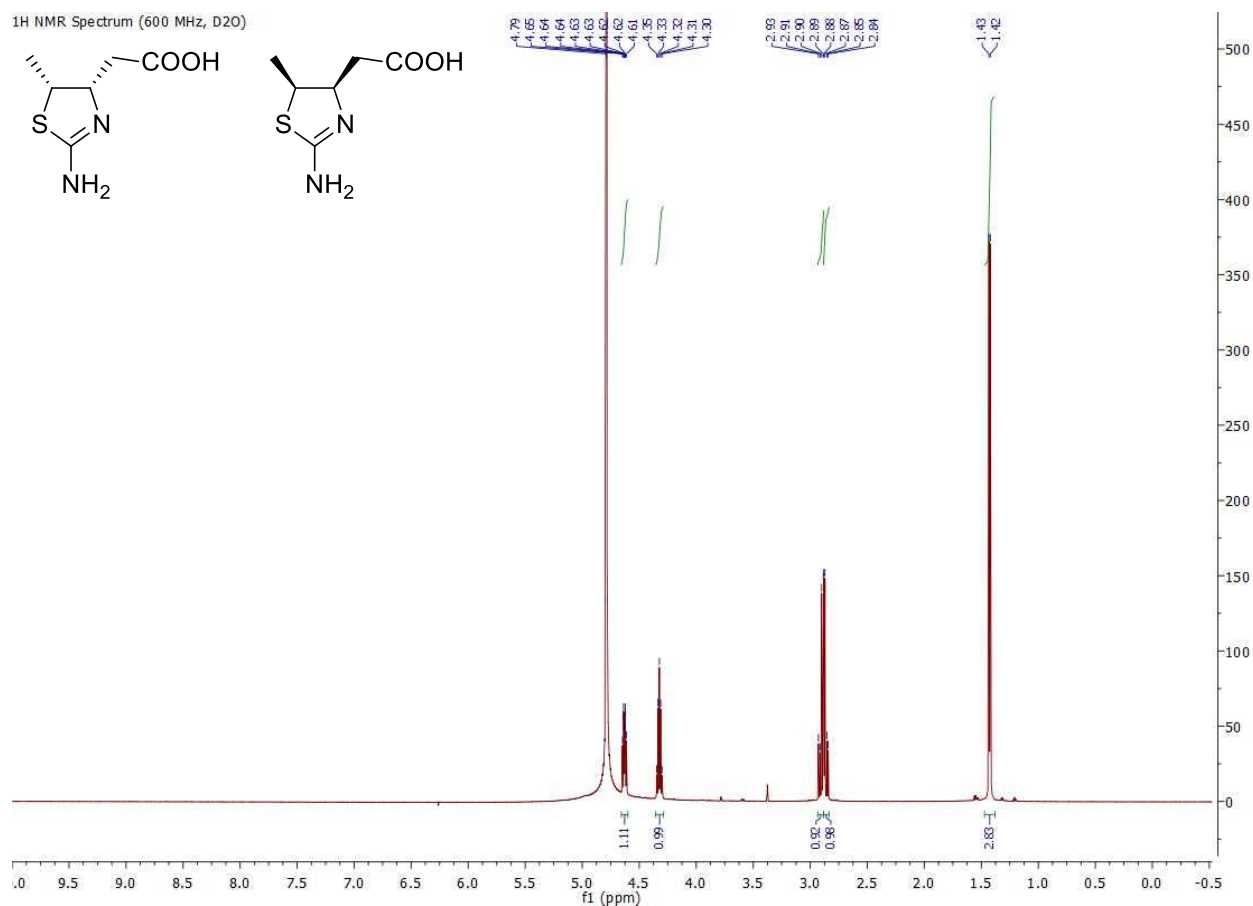


¹³C NMR Spectrum (150 MHz, D₂O)

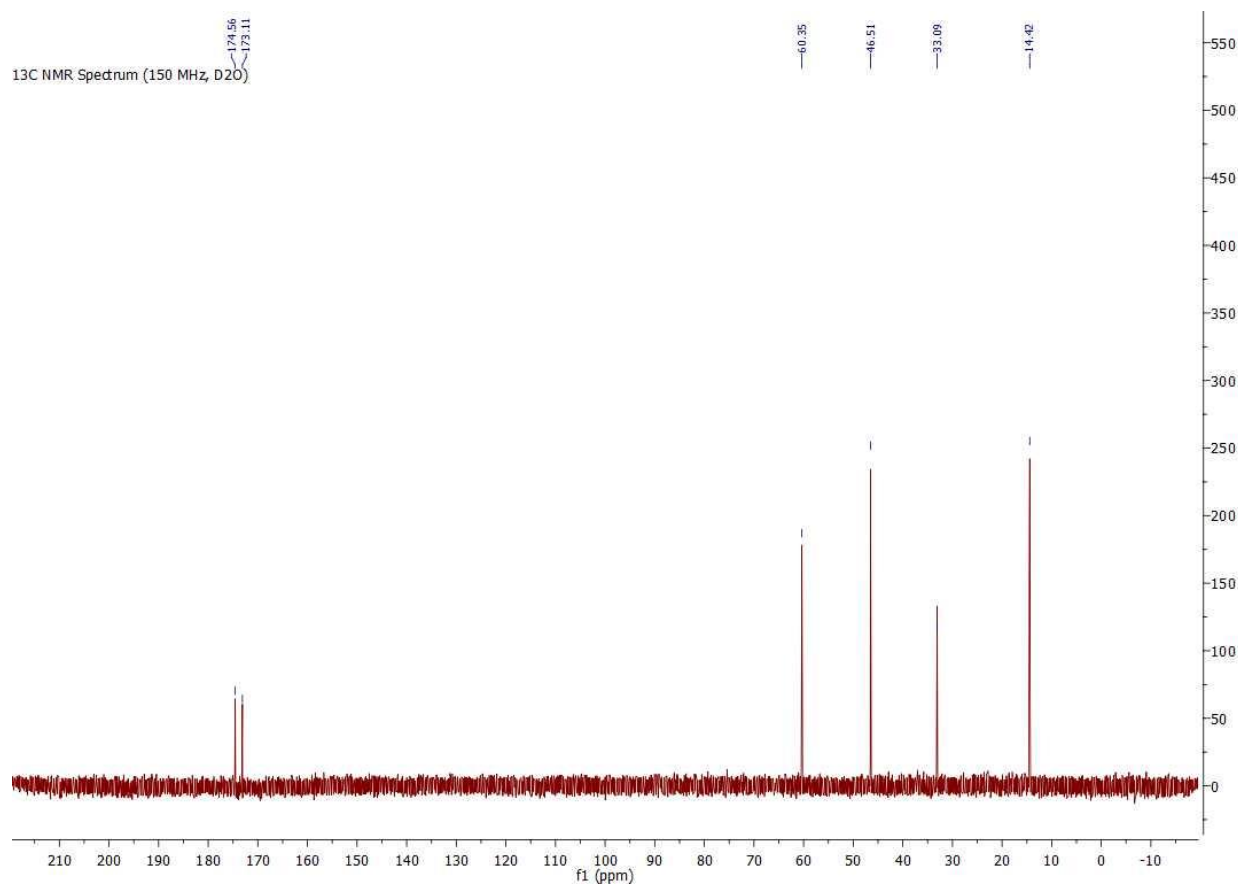


2-((4*R,5*S**)-2-amino-5-methyl-4,5-dihydrothiazol-4-yl)acetic acid hydrochloride (*cis*-3.8).**

¹H NMR Spectrum (600 MHz, D₂O)

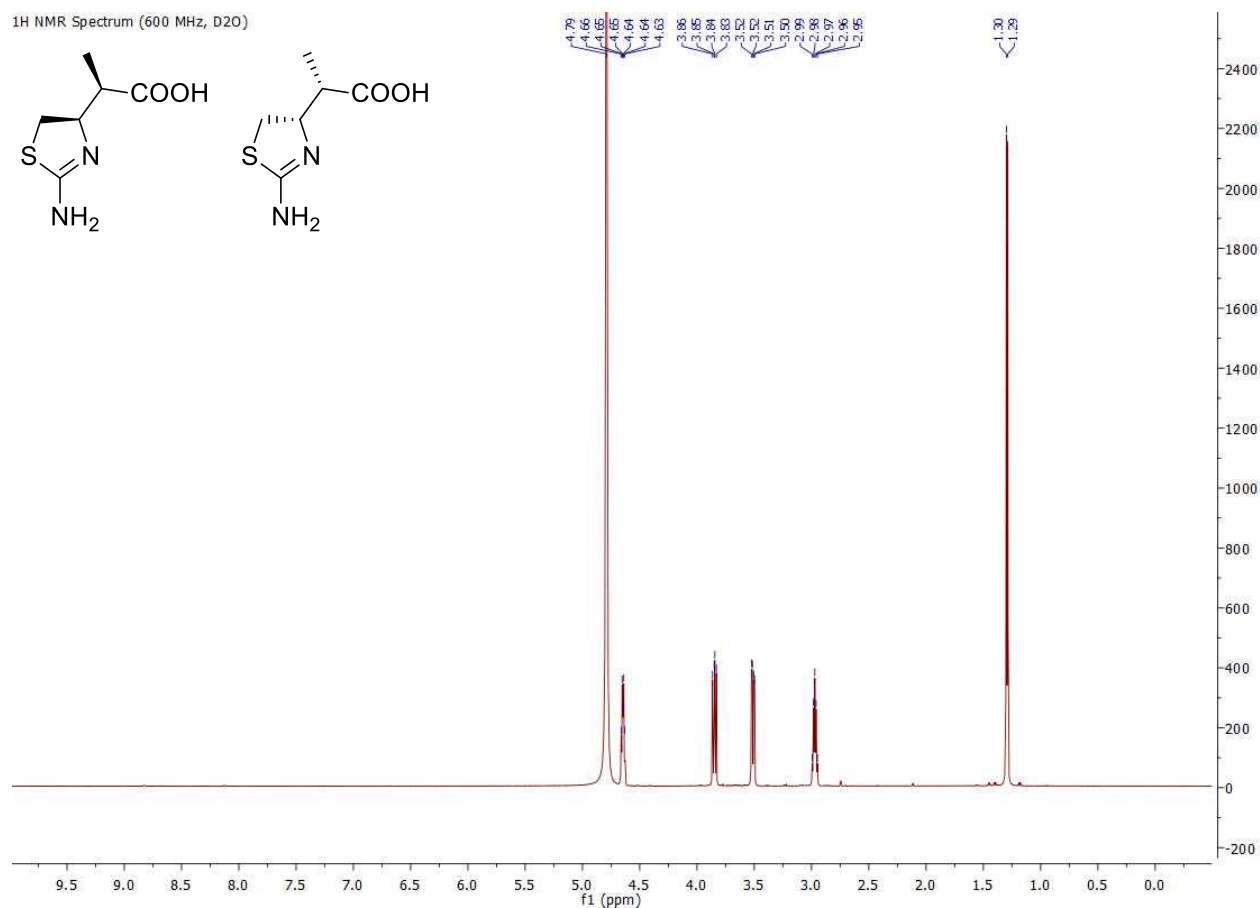


¹³C NMR Spectrum (150 MHz, D₂O)

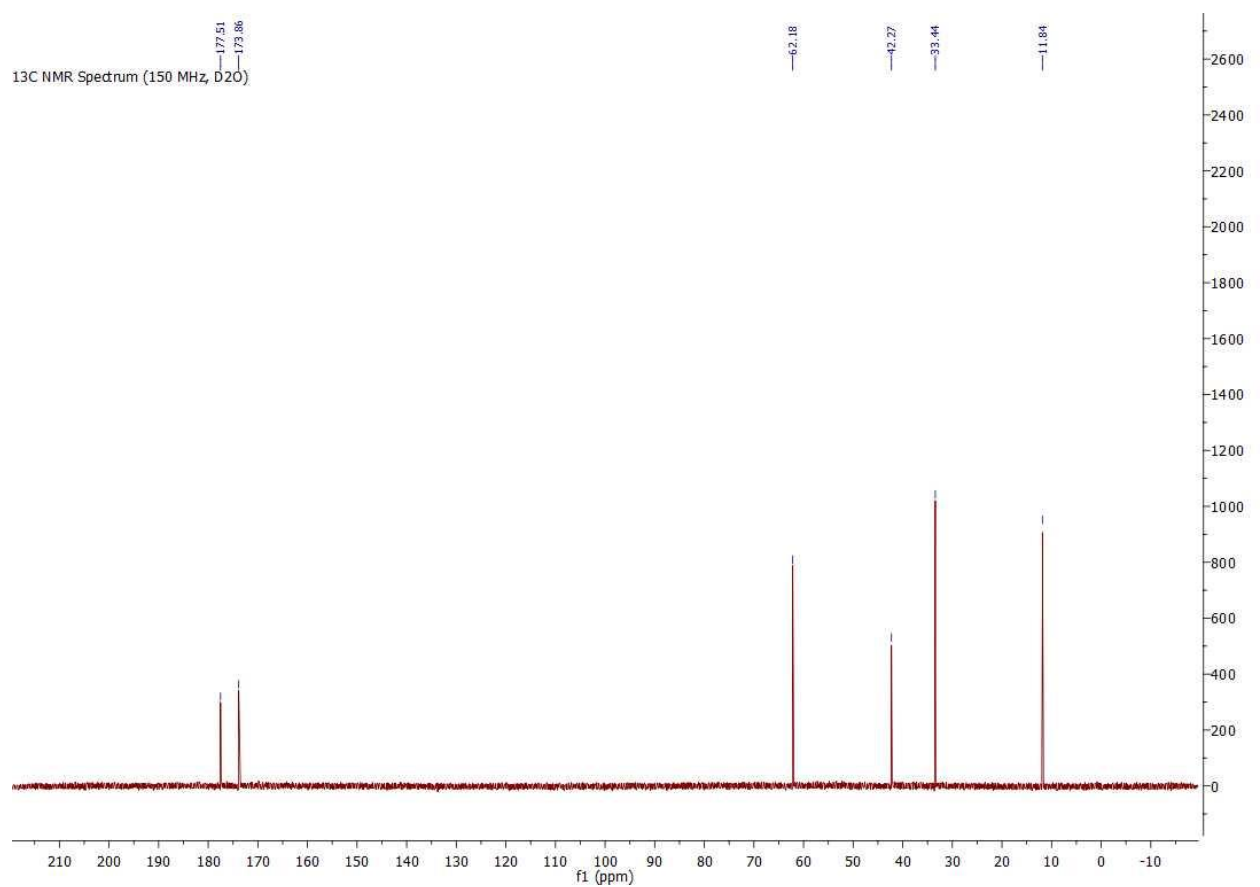


(R*)-2-((R*)-2-amino-4,5-dihydrothiazol-4-yl)propanoic acid hydrochloride (I-3.10).

¹H NMR Spectrum (600 MHz, D₂O)

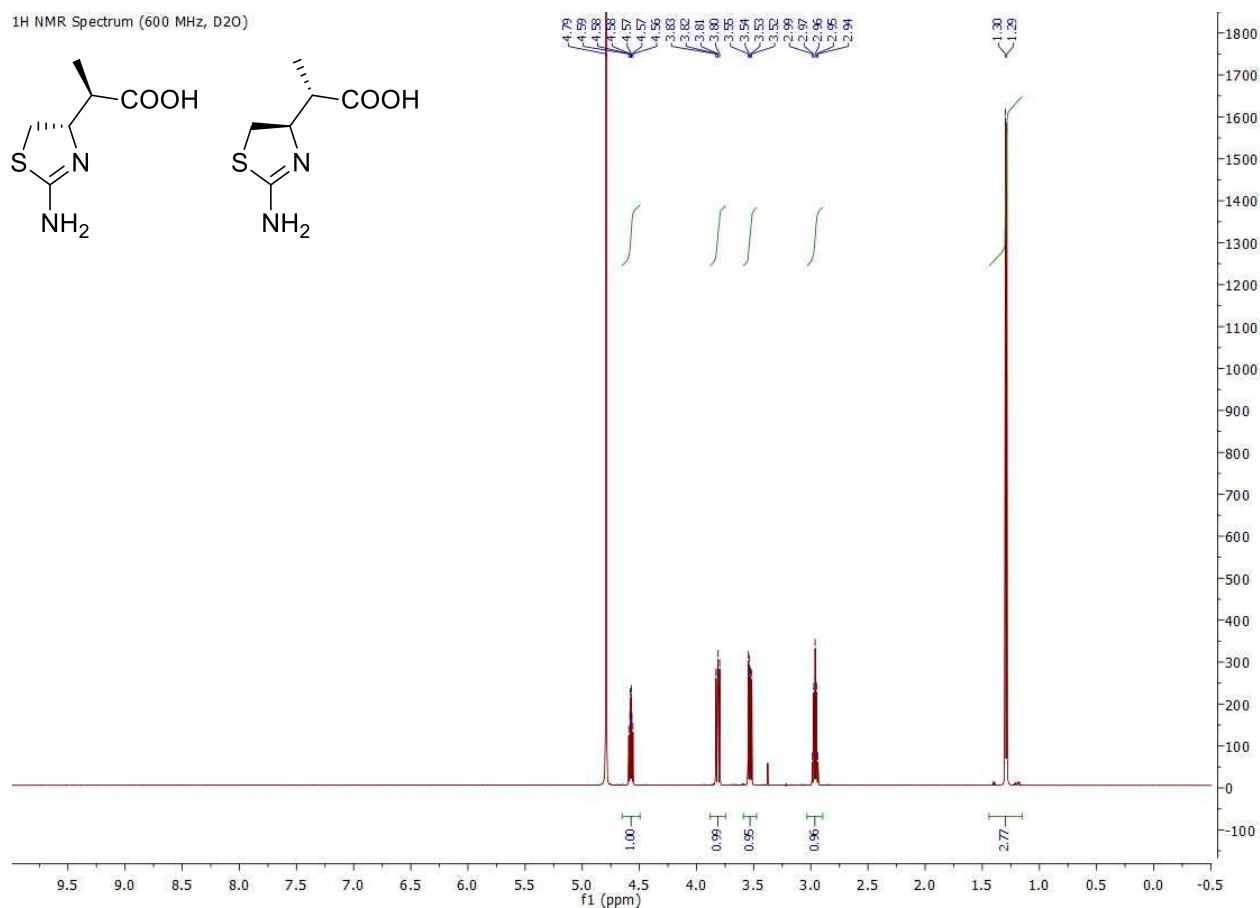
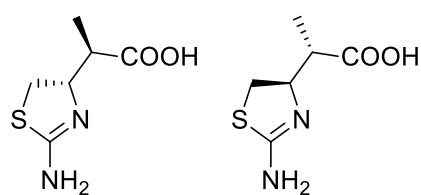


¹³C NMR Spectrum (150 MHz, D₂O)



(R*)-2-((S*)-2-amino-4,5-dihydrothiazol-4-yl)propanoic acid hydrochloride (u-3.10).

¹H NMR Spectrum (600 MHz, D₂O)



¹³C NMR Spectrum (150 MHz, D₂O)

